# Functionalized Prodrugs of a bacterial RNAP-Inhibitor

# &

# Bio-reversibly masked purinergic 2$^{nd}$ Messenger derivatives associated with Ca$^{2+}$ Signaling

**Dissertation**

to obtain the Scientific Doctoral Degree

by

**Alexandra Ruthenbeck**

presented to

the Department of Chemistry
of the Faculty of Sciences
at the University of Hamburg

**Hamburg 2018**

First Reviewer:        Prof. Dr. Chris Meier

Second Reviewer:       Prof. Dr. Dr. h.c. mult. Wittko Francke

Date of the disputation: 11.01.2019

Date of print approval: 14.01.2019

The present work was compiled in the group of Prof. Dr. Chris Meier at the Institute of Organic Chemistry in the Department of Chemistry at the University of Hamburg from November 2014 until October 2018.

*There is only one way to find out …*

*… always running for the thrill of it,*
*always pushing up the hill*
*searching for the thrill of it,*
*on and on*
*never looking down,*
*just in awe of what's in front.*

(from *'Walking on a Dream'* by Nick Littlemore, Jonathan T. Sloan, Luke J. Steele)

# Table of Contents

# Table of Contents

# Table of Contents

# Table of Contents

## List of Publications

Alexandra Ruthenbeck, Elisa Marangoni, Björn-Ph. Diercks, Aileen Krüger, Alexander Froese, Nadja I. Bork, Viacheslav O. Nikolaev, Andreas H. Guse and Chris Meier, Membrane-Permeable Octanoyloxybenzyl-Masked cNMPs As Novel Tools for Non-Invasive Cell Assays, *Molecules* **2018**, *23(11)*, 2960.

Björn-Philipp Diercks, René Werner, Paula Weidemüller, Frederik Czarniak, Lola Hernandez, Cari Lehmann, Annette Rosche, Aileen Krüger, Ulrike Kaufmann, Martin Vaeth, Antonio V. Failla, Bernd Zobiak, Farid I. Kandil, Daniel Schetelig, Alexandra Ruthenbeck, Chris Meier, Dmitri Lodygin, Alexander Flügel, Dejian Ren, Insa M. A. Wolf, Stefan Feske, and Andreas H. Guse, ORAI1, STIM1/2, and RYR1 shape subsecond Ca2+ microdomains upon T cell activation, *Science Signaling* **2018**, *11(561*), eaat0358.

A. Ruthenbeck, B.-Ph. Diercks, A. Krüger, V. O Nikolaev, A. H. Guse and C. Meier, Masked cNMPs as novel chemical tools for cell-based assays, poster presentation at the *XXIII International Round Table on Nucleosides, Nucleotides and Nucleic Acids (IRT)* **2018**, La Jolla, San Diego, CA, USA.

A. Ruthenbeck, W. A. M. Elgaher, J. Haupenthal, R. W. Hartmann and C. Meier, Bacterial RNAP Inhibitors: Synthesis and Evaluation of Prodrugs of Aryl-ureidothiophene-carboxylic acids, *ChemistrySelect* **2017**, *2*, 11899–11905.

A. Ruthenbeck and C. Meier, Functionalized and lipophilic Prodrugs of novel Inhibitors of the bacterial RNAP, poster presentation at the *International Congress on Antimicrobial Research* (ICAR) **2016**, Torremolinos, Málaga, Spain

## List of Abbreviations

| | |
|---|---|
| 2dADPR | 2'-deoxy ADPR |
| A | Adenosine |
| AB | Acyloxybenzyl |
| Ac | Acetyl |
| AC | Adenylyl cyclase |
| ADPR | Adenosine diphosphoribose |
| AN | Adenine nucleotide |
| AM | Acetoxymethyl |
| ATP | Adenosine triphosphate |
| AU | Absorption units |
| BnBr | Benzyl bromide |
| Bz | Benzoyl |
| cADPR | Cylic ADPR |
| CAS | Chromeazurol S |
| cAMP | 3',5'-Cyclic adenosine monophosphate |
| CD | Cluster of differentiation |
| cdAMP | 3',5'-Cyclic-2'-deoxyadenosine monophosphate |
| CFP | Cyan fluorescent protein |
| cGMP | 3',5'-Cyclic guanosine monophosphate |
| CNG | Cyclic nucleotide-gated |
| cNMP | cyclic nucleotide monophosphate |
| CNS | Central nervous system |
| cUMP | 3',5'-Cyclic uridine monophosphate |
| dA | 2'-Deoxyadenosine |

# List of Abbreviations

| | |
|---|---|
| DCC | *N,N'*-Dicyclohexylcarbodiimid |
| DCI | 4,5-Dicyanoimidazol |
| DIAD | Di*iso*propyl azodicarboxylate |
| DIPEA | *N,N'*-Di*iso*propylethylamine |
| DMAP | 4-Dimethylaminopyridine |
| DMF | *N,N'*-Dimethylformamide |
| DMSO | Dimethyl sulfoxide |
| DNA | Deoxyribonucleic acid |
| DPP | Diphenyl phosphine |
| EAE | Experimental autoimmune encephalomyelitis |
| Eq. | Equivalent |
| ESI | Electro spray ionization |
| ER | Endoplasmic reticulum |
| Fm | 9-Fluorenylmethyl |
| G | Guanosine |
| GDP | Guanosine diphosphate |
| GPCR | G protein couple receptor |
| GTP | Guanosine triphosphate |
| HPLC | High performance liquid chromatography |
| HMDS | 1,1,1,3,3,3-Hexamethyldisilazan |
| IP$_3$ | Inositol triphosphate |
| *i*Pr | *iso*-Propyl |
| LTP | Long-term potentiation |
| MALDI | Matrix assisted laser desorption ionization |
| MDR | Multi drug resistant/resistance |
| MeCN | Acetonitrile |

# List of Abbreviations

| | |
|---|---|
| MIC | Minimal inhibitory concentration |
| MOM | Methoxymethyl |
| Ms | Methanesulfonyl |
| MS | Mass spectrometry |
| *MS* | Multiple sclerosis |
| NA | Nicotinic acid |
| NAADP | Nicotinic acid adenine dinucleotide phosphate |
| NAD | Nicotinamide adenine dinucleotide |
| NAMN | Nicotinic acid mononucleotide |
| NAN | Nicotinic acid nucleoside |
| NADP | Nicotinamide adenine dinucleotide phosphate |
| NCS | *N*-Chlorosuccinimide |
| NDM-1 | New Delhi metallo-β-lactamase 1 |
| NMP | Nucleotide monophosphate |
| NP | Normal phase |
| OB | Octanoyloxybenzyl |
| OmpF/C | Outer membrane protein F/C |
| PA | Phosphor amidite |
| $PA_2$ | Phosphor diamidite |
| PARG | Poly(ADPR)glycohydrolase |
| PARP | Poly(ADPR)polymerase |
| PBS | Phosphate buffered saline |
| PG | Protecting group |
| PKA | Protein kinase A |
| PLE | Porcine liver esterase |
| POM | Pivaloyloxymethyl |

# List of Abbreviations

| | |
|---|---|
| RNA | Ribonucleic acid |
| RNAP | RNA polymerase |
| RP | Reversed phase |
| rt | Room temperature |
| RT | Retention time |
| RYR | Ryanodine receptors |
| TBA | Tetra-*n*-butylammonium |
| TBAI | Tetra-*n*-butylammonium iodide |
| TBS | *tert*-Butyldimethylsilyl |
| TBTU | 2-(1H-Benzotriazole-1-yl)-1,1,3,3-tetramethylaminium tetrafluoroborate |
| *t*Bu | *tert*-Butyl |
| TEA | Triethylamine |
| $T_{eff}$ | Effector T cells |
| Tf | Triflate |
| TFA | Trifluoroacetic acid |
| THF | Tetrahydrofuran |
| TIPDS | 1,1,3,3-Tetra*iso*propyldisiloxane-1,3-diyl |
| TLC | Thin layer chromatography |
| TMS | Trimethylsilyl |
| TPP | Triphenylphosphine |
| $T_{reg}$ | Regulatory T cells |
| TRP | Transient receptor protein |
| TRPM2 | TPR melastatin 2 |
| u | Units |
| UDP | Uridine diphosphate |
| UTP | Uridine triphosphate |

# List of Abbreviations

UV         Ultraviolet

WEF       World Economic Forum

YFP        Yellow fluorescent protein

# 1. Zusammenfassung

## 1.1. Funktionalisierte Prodrugs eines Inhibitors der bakteriellen RNAP

Die (multiple) Wirkstoffresistenz von Bakterien steigt stetig und hat sich zu einer der größten Bedrohung für Gesundheit, Nahrungsmittelsicherheit und Zusammenleben der globalen Gemeinschaften entwickelt. Zahlreiche bakterielle Infektionen führen zunehmend zu Komplikationen und die Risiken einer leichteren Verbreitung sowie Ansteckung, schwererer Krankheitsverläufe und höherer Sterblichkeit nehmen zu. Für die weitere erfolgreiche Behandlung bakterieller Infekte bedarf es daher dringend neuer Antibiotika, die neuartige Wirkorte und/oder neuartige Wirkungsweisen besitzen.

Die bakterielle DNA-abhängige RNA-Polymerase (RNAP) katalysiert die Transkription von DNA in RNA und ist dementsprechend essentiell beteiligt am Kernschritt der Genexpression. In der Entwicklung antibakterieller Wirkstoffe wird das Enzym bisher jedoch kaum berücksichtigt (s. Kapitel 3.).

Die Gruppe um R. HARTMANN initiierte ein Projekt zur Entwicklung neuartiger *small-molecule* Inhibitoren der RNAP und identifizierte Arylureidothiophencarbonsäuren als potentielle Wirkstoffkandidaten. Die Verbindungen zeigten wachstumsinhibierende Effekte gegenüber Gram-positiven Bakterien, waren jedoch inaktiv gegenüber Gram-negativen Stämmen. Als Gründe wurden eine mangelnde Akkumulation des Inhibitors im bakteriellen Zytoplasma sowie ein erhöhter Efflux durch entsprechende Pumpen in der bakteriellen Zellwand identifiziert. In diesem Zusammenhang ist die negative Ladung des Wirkstoffmoleküls als nachteilig sowie ursächlich einzuordnen.

Im Rahmen einer konsequenten Weiterentwicklung des potentiellen Wirkstoffes bietet sich eine Prodrugstrategie mit Maskierung der Carbonsäurefunktion an. In vorausgegangenen Arbeiten wurde dementsprechend bereits eine Reihe ladungsneutraler sowie positiv geladener Esterprodrugs synthetisiert und hinsichtlich ihrer chemischen Stabilität sowie enzymatischen Aktivierbarkeit untersucht. Die untersuchten Prodrugs wiesen ein gutes Hydrolyseprofil auf, indem sie eine zufriedenstellend hohe chemische Stabilität aufwiesen, während die enzymatische Freisetzung der Stammverbindung schnell stattfand.

Zusammenfassung

Im Rahmen dieser Arbeit wurden zwei Arylureidothiophencarbonsäuren mit Maskierungen versehen, die in der Lage sind, $Fe^{III}$ zu koordinieren. Hierbei sollten ausgewählte Linker eine leichtere enzymatische Freisetzung der Prodrugs gewährleisten. Die $Fe^{III}$-Affinität der Siderophor-artigen Prodrugs wurde mittels eines kompetitiven Assays evaluiert, und die antibakterielle Aktivität aller Prodrugs in Zusammenarbeit mit der Gruppe von R. HARTMANN (HIPS Saarbrücken) überprüft.

Vier verschiedene Siderophorprodrugs wurden erfolgreich synthetisiert, wobei eine TBAI-assistierte basische Veresterung sowie eine milde Debenzylierung mittels TMSI die Kernschritte darstellten. Diese Syntheseschritte gelangen grundsätzlich in zufriedenstellenden Ausbeuten zwischen 63 – 84%. Hierbei enthielten die Moleküle eine Catechol- oder Pyronmaske und unterschiedliche Linkergruppen.
Zur Bewertung der $Fe^{III}$-Koordinationseigenschaften wurde der kompetitive Chrome Azurol S (CAS) Assay verwendet. Hier zeigten die Catechol-basierten Prodrugs eine gute bis hohe Effizienz in der Komplexierung von $Fe^{III}$ mit $\Delta abs_{630}$ Werten um -0.51 mAU bis -0.63 mAU, welche im gleichen Bereich wie die der Referenzverbindung Vanchrobactin lagen. Das Pyron-basierte Prodrug hingegen koordinierte $Fe^{III}$ nur unzureichend ($\Delta abs_{630}$ = -0.34) (s. Kapitel 5.3. sowie 5.4.).

Die antibakteriellen Aktivitäten aller Prodrugs wurden gegen eine Auswahl Gram-positiver wie Gram-negativer Bakterien getestet. Hierbei zeigten die unter physiologischen Bedingungen positiv geladenen Prodrugs wachstumsinhibitorische Effekte.

Die geringe Polarität ladungsneutraler Prodrugs beeinträchtige vermutlich die antibakterielle Aktivität. In Bezug auf die Siderophorprodrugs wurde gefolgert, dass ihre Aktivierung durch bakterielle Esterasen nur unzureichend ablief. Weitere negative Aspekte könnten eine unzureichende Rezeptorinteraktion und/oder erhöhter Wirkstoffefflux darstellen. Die unter physiologischen Bedingungen positiv geladenen Cholinester-Prodrugs waren in der Lage, antibakterielle Effekte in Gram-negativen *E. coli* K12 Bakterien zu induzieren. Diese Beobachtung deutete darauf hin, dass die positive Ladung des Prodrugs hier vorteilhaft für den Wirkstoffinflux in die Bakterien war. Insgesamt stellen die erzielten Ergebnisse eine interessante sowie informative Grundlage für zukünftige Studien über neuartige Prodrugs ähnlicher Wirkstoffkandidaten dar.

### 1.2.  Bio-reversibel maskierte purinerge sekundäre Botenstoffderivate

Die Kommunikation von Zellen erstreckt sich über kurze wie lange Distanzen und oft muss eine Vielzahl von Nachrichten gleichzeitig empfangen, verarbeitet und/oder gesendet werden. Kommunikations- und Signalprozesse, die auf chemischen Signalen beruhen, implizieren immer die Erkennung dieser durch einen bestimmten Rezeptor. Diese Rezeptoren geben das extrazelluläre Signal weiter, indem sie sekundäre Botenstoffe mobilisieren. Das zentrale sekundäre Signal zur Verarbeitung solcher externen Stimuli stellt hierbei, zusammen mit Phosphat ($PO_4^-$), intrazelluläres $Ca^{2+}$ dar. Entsprechend ist das Kation substantiell in vielzählige und -fältige Prozesse involviert, etwa die Bewegung von Zellen, die Transkription von Genen oder die Exozytose. Die Modulierung intrazellulärer $Ca^{2+}$-Level wird dabei durch eine Reihe von Adeninnukleotiden, namentlich cAMP, (d)ADPR und NAADP, kontrolliert. Die Rezeptoren, mit denen diese Adeninnukleotide dazu interagieren, sind insbesondere assoziiert mit Prozessen, die in Verbindung mit Entzündungsreaktionen sowie der Regulation des Immunsystems stehen (s. Kapitel 6.).

Viele Details der genauen Involvierung von Adeninnukleotiden in das komplexe zelluläre Signalsystem sowie die physiologische wie pathologische Bedeutung ihres Beitrags zur $Ca^{2+}$ Mobilisierung sind heute noch nicht genau verstanden.

Zell-basierte Studien zu sekundären Botenstoffen gestalten sich hinsichtlich ihrer Durchführung generell schwierig. Die gewöhnlich verwendeten Einzelzell-präparativen Methoden bedürfen in der Regel einer zeitaufwändigen und sorgfältigen Vorbereitung und sind auf Grund ihres invasiven Charakters anfällig für Artefakte oder falsch-positive Ergebnisse. Die Entwicklung membran-permeabler, bio-reversibel modifizierter Derivate der sekundären Botenstoffe cAMP, (d)ADPR und NAADP stellt einen aussichtreichen Ansatz dar, um diese Nachteile und Limitierungen zu überwinden. Des Weiteren wäre eine Expansion hin zu Medium- und Hochdruchsatztestverfahren mit diesen Verbindungen möglich, und zellbasierte Assays würden grundsätzlich vereinfacht.

Eine etablierte bio-reversible Maskierung, insbesondere für Phosphate, stellt die Acyloxybenzyl- (AB) Gruppe dar. Diese wurde erfolgreich in Prodrugkonzepten für Mono-, Di- und Triphosphate antiviral aktiver Nukleosidanaloga eingesetzt. Es wurde experimentell bestätigt, dass die jeweiligen Prodrugs effizient durch zelluläre Membranen diffundierten und

das zugehörige Nukleotid selektiv innerhalb der Zelle durch enzymatische Aktivierung der Maskierungseinheiten freisetzten (s. Kapitel 6.).

Ziel dieser Arbeit war es, einen synthetischen Zugang zu AB-maskierten Derivaten von cNMPs, (d)ADPR und NAADP zu entwickeln. Für eine gezielte Einführung der AB-Maske boten sich totalsynthetische Ansätze bevorzugt an, und basierend auf der strukturellen Komplexität der Zielverbindungen wurden konvergente Syntheserouten entworfen.

Die Zielstruktur des membran-permeablen NAADP Derivates beinhaltete AB-Masken an der 2'-Phosphateinheit sowie der Carbonsäure der Nukleobase Nikotinsäure. Der entsprechende Adenosin-basierte Kupplungsbaustein wurde erfolgreich in vier Schritten synthetisiert, wobei ausgehend von Adenosin zunächst selektiv geschützt sowie in der 2'-Position phosphoryliert wurde, um anschließend zu deblockieren und ein zweites Mal in der 5'-Position zu phosphorylieren. Bezüglich des Kupplungspartners gelangen die Darstellung eines nukleobasenmodifizierten Nikotinsäurenukleosids sowie eines geschützten Nikotinsäurenukleotids. Eine Weiterverfolgung der entsprechenden Syntheserouten unter Entwicklung milder Deblockierungs- und Phosphorylierungsprotokolle gewährt dann den Zugang zu geeigneten Reaktionspartnern für den Adenosinbaustein. Die Darstellung verschiedenster Tri*PPP*ro-Verbindungen etwa gelang erfolgreich mittels einer Kupplung zweier Phosphate. Diese Strategie ließe sich potentiell auf die Synthese von NAADP-AB Derivaten übertragen. Vor diesem Hintergrund stellen die etablierten Syntheserouten eine wertvolle Basis für die weitere Entwicklung des Ansatzes zur Darstellung bio-reversibel maskierten NAADPs dar (s. Kapitel 8.1.).

Die AB-maskierten Derivate des ADPR und dADPR sollten die Maskierung an einem der Phosphate des Pyrophosphatrückgrats sowie an der anomeren Hydroxygruppe der Ribose tragen. Es wurde ein konvergenter Ansatz entwickelt, bei dem eine elektrophile $P^{III}$-Spezies und eine nucleophile $P^{V}$-Spezies die Kupplungskomponenten darstellten und H-Phosphonat-Chemie als Methodik gewählt wurde (s. Kapitel 8.2.).
Die benötigten Bausteine, ein nicht-symmetrisches H-Phosphonat sowie ein Nukleosidmonophosphat, wurden auf kurzen sowie flexiblen Routen, die einen adaptierbaren Austausch der einzelnen Komponenten zuließen, synthetisiert. Die im letzten Schritt vorgesehene Desilylierung gelang erfolgreich unter Verwendung von TEA · 3 HF in Acetonitril.

Zusammenfassung

Nächste Optimierungsschritte würden eine Verfeinerung der Desilylierungsbedingungen sowie des Reinigungsprotokolls beinhalten. Insgesamt stellt der entwickelte Syntheseansatz eine vielversprechende sowie weitestgehend etablierte Basis für die zukünftige adaptierbare Darstellung weiterer (d)ADPR-AB Derivate dar.

Maskierte cNMP Derivate wurden basierend auf einer kurzen sowie flexiblen Route, die ausgehend von eigenen Vorstudien zur Synthese nicht-symmetrischer Phosphoramidite entwickelt wurde, dargestellt. Die Synthesestrategie umfasste die Umsetzung eines ungeschützten Nukleosids mit einem Octanoyloxybenzyl- (OB)-modifizierten Phosphordiamidit (s. Kapitel 8.3.).

Fünf verschiedene maskierte cNMPs wurden erfolgreich synthetisiert und anschließend hinsichtlich ihrer Stabilität, Aktivierbarkeit und Performance in zellbasierten Assays untersucht. Diese Studien wurden in enger Zusammenarbeit mit den Gruppen um A. GUSE, V. NIKOLAEV und C. GEE (Universitätsklinikum Hamburg-Eppendorf) durchgeführt. Chemische wie enzymatische Hydrolysestudien bestätigten die zufriedenstellend hohe chemische Stabilität der OB-cNMPs über mehrere Stunden ($t_{\frac{1}{2}} \approx 8$ h) während die enzymatische Spaltung der OB-Maske signifikant schneller sowie selektiv das entsprechende cNMP Stammnukleosid lieferte. Basierend auf diesem Hydrolyseprofil sind Zellstudien über ausreichend lange Zeiträume und beispielsweise auch Präinkubationen mit den Verbindungen möglich (s. Kapitel 8.3.).

In Zell-Assays zeigten die OB-cNMPs eine hervorragende Membrangängigkeit. Des Weiteren wurden unmittelbar nach Inkubationsbeginn zelluläre Effekte gemessen, wie sie für die natürlichen, unmaskierten cNMPs erwartet würden. Diese Beobachtung lässt die Schlussfolgerung zu, dass die bio-reversible Maskierung, analog zum Enzymassay, sehr schnell gespalten und das jeweilige cNMP freigesetzt wurde. Folglich erfüllten die synthetisierten OB-cNMPs alle Kriterien, um als vielversprechende molekulare Werkzeuge für die Anwendung in neuartigen Assays zur detaillierteren Untersuchung cNMP-induzierter zellulärer Reaktionen bewertet zu werden.

## 2. Abstract

### 2.1. Functionalized Prodrugs of a bacterial RNAP-Inhibitor

The (multi-)drug resistance of microorganisms continues to develop and has evolved to one of the most concerning threats to global public health, food security and cohabitation of society. Numerous infections with bacteria become increasingly hard to treat, and the risks of spreading, contagion, prolonged illness and fatality are rising. Maintaining the ability to treat bacterial infections needs novel antibacterial agents that address innovative targets and/or possess alternative modes of action (see chapter 3.).

The bacterial DNA-dependent RNA-Polymerase (RNAP) catalyzes the transcription of DNA into RNA and thus is crucial for the most regulatory step within the expression of genes. However, the enzyme is rarely exploited in antibacterial therapy so far.
R. HARTMANN and co-workers initiated a project focusing on the development of novel small molecule inhibitors of the bacterial RNAP, and an aryl-ureidothiophene carboxylic acid was identified as such. Gram-positive strains showed susceptibility, but against Gram-negative strains, the compounds were not active. The observations were attributed to a lack of compound accumulation in the bacterial cytoplasm. Further, drug efflux and an inefficient passage of the outer membrane barrier added to this. Under physiological conditions, aryl-ureidothiophene carboxylic acids are negatively charged, which likely affects permeation into Gram-negative bacteria negatively.
A consequent further development features the elaboration of a prodrug strategy with masking of the impedimental carboxylate. In previous works, a range of charge-neutral ester-prodrugs as well as two derivatives bearing positively charged masking units were synthesized and demonstrated to successfully release the parent drug upon enzymatic activation while prodrugs possessed adequate chemical stability.

This thesis aimed at conjugating two aryl-ureidothiophene carboxylic acids with moieties that provide the capacity to coordinate $Fe^{III}$. In addition, spacer groups were introduced to facilitate enzymatic prodrug activation. The $Fe^{III}$-coordination of the siderophore-type prodrugs was evaluated in a competitive assay to yield relative affinities. The antibiotic activity

of all prodrugs, i.e. lipophilic, cationic and functionalized, was determined in collaboration with the group of R. HARTMANN (Helmholtz Institute for Pharmaceutical Research Saarland (HIPS), Saarbrücken).

In total, four different siderophore-type prodrugs bearing catecholate- and pyrone-masks as well as different linkages were successfully synthesized and obtained in high purity after the final coupling and deprotection. For these steps, a TBAI-aided basic esterification and mild debenzylation using TMSI were successfully developed and gave the respectively desired products in generally satisfying yields of 63 – 84%.

The Chrome azurol S (CAS) assay was applied to study the iron(III)-coordinating properties of siderophore-type prodrugs. All three catecholate-masked compounds achieved good to high efficiency in coordinating $Fe^{III}$ which was indicated by $\Delta abs_{630}$ values ranging from -0.51 mAU to -0.63 mAU. These values were in a similar range as those of the reference compound Vanchrobactin. The pyrone-based prodrug proved unsatisfactory in displacing the CAS ligand and a comparably low $\Delta abs_{630}$ value of -0.34 mAU was achieved (see chapters 5.3. and 5.4.).

The antibacterial activities of all prodrugs were determined against a variety of Gram-positive and negative bacterial strains, namely *B. subtilis*, *S. aureus* (Gram-positive) and *E. coli* K12, the outer membrane mutant *E. coli* D22, the efflux deficient mutant *E. coli* TolC and *P. aeruginosa* O1 (Gram-negative strains). Here, the under physiological conditions positively charged prodrugs showed growth-inhibitory effects.

The low polarity of charge-neutralized prodrugs might have impeded their growth inhibitory activity. Regarding the siderophore-type prodrugs, an inefficient pro-moiety-cleavage by bacterial esterases seemed detrimental. However, receptor recognition and/or drug efflux issues could be further contributing factors.

The positively charged choline ester prodrugs were able to restore antibacterial effects against the Gram-negative strain *E. coli* K12 in bacterial cell growth inhibition assays. The observation suggested that the cationic charge of the pro-moiety was beneficial for drug influx into Gram-negative bacteria here. These results constitute an interesting and informative basis for future investigations of novel prodrug concepts for drug candidates of a similar type (see chapter 5.4.).

## 2.2. Bio-reversibly masked purinergic 2nd Messenger derivatives associated with Ca2+ Signaling

Cells communicate over short as well as long distances, and often are confronted with a multitude of signals to receive, integrate and/or send simultaneously.

Communication and signaling processes that use chemical signals always imply the recognition of these by a certain receptor. These receptors forward the extracellular signal via the mobilization of 2nd messengers. Intracellular $Ca^{2+}$ constitutes, together with phosphate ($PO_4^{2-}$), the central secondary signal cells evolved to assimilate external stimuli. This implies a substantial involvement of $Ca^{2+}$ in aspects as diverse as cell motility, gene transcription or exocytosis, all examples of processes relevant e.g. in immune cell activation. A range of adenine nucleotides, namely cAMP, (d)ADPR and NAADP, show a joint engagement in the modulation of intracellular $Ca^{2+}$ concentrations. The receptors regulated by these nucleotides are particularly implicated in processes related to inflammation and regulation of the immune system.

However, many details of the precise involvement of adenine nucleotides in the complex cellular signaling system as well as the physiologic and pathologic value of their contribution to $Ca^{2+}$ mobilization are not understood yet.

Cell-based studies on 2nd messengers are generally difficult to perform since their application is carried out via single-cell preparative methods. These procedures require careful preparation and significant time in advance of each experiment. The invasive procedure further raises the potential for interfering artefacts or false-positives.

The development of efficient membrane-permeant, bio-reversibly protected derivatives of cAMP, ADPR and NAADP constitutes an approach to overcome the limitations of current setups. Further, an expansion of cell assays to medium- or high-throughput formats becomes possible and cell-based settings simplified in general.

An established bio-reversible protecting group, particularly for phosphates, is the acyloxybenzyl (AB) moiety. It was used successfully in prodrug approaches for mono-, di- and triphosphates of nucleoside analogues with antiviral activity. The respective prodrugs

were shown to efficiently diffuse across cell membranes and release the corresponding nucleotide intracellularly upon enzymatic activation (see chapter 6.).

This thesis aimed at developing synthetic access towards AB-masked derivatives of cNMPs, (d)ADPR and NAADP. Introduction of the AB-mask in a (site-) specific way and thus in total synthesis approaches was preferably considered. Based on the complexity of the dinucleotides in molecular structure, convergent synthesis routes with a final coupling step were designed.

The targeted structure of a membrane-permeant, bio-reversibly masked NAADP derivative was envisaged to carry AB-moieties at the 2'-phosphate and the carboxylic acid (see chapter 8.1). The according adenosine building block was synthesized successfully over four steps starting from adenosine, which was first protected selectively in the 6-, 3'- and 5'-positions. Successively, the 2'-phosphorylation was conducted using phosphoramidite chemistry, and was followed by 3',5'-desilylation. Lastly, the 5'-phosphorylation was carried out successfully using phosphoramidite chemistry again.

Regarding the counterpart, the syntheses of a carboxyl-modified nicotinic acid nucleoside and protected nicotinic acid nucleotide were achieved. Pursuing these approaches further, mild deprotection or phosphorylation protocols likely facilitate access to building blocks suitable for coupling reactions. The coupling of two phosphates for example is successfully used in the approach towards Tri*PPP*ro-compounds, where an activated masked pyrophosphate reagent is converted with a nucleoside monophosphate. Against this backdrop, the developed synthesis routes constitute a valuable basis for the further development of the total synthesis approaches towards AB-masked NAADP.

The AB-derivatives of ADPR and dADPR were planned to carry one AB-unit at one of the phosphates of the pyrophosphate backbone to mask the negative charges. A further AB-group occupied the anomeric hydroxy group of the ribose to convey additional lipophilicity (see chapter 8.2.)        .

A convergent approach was chosen, where an electrophilic $P^{III}$- and a nucleophilic $P^V$-phosphorous species constituted the coupling components, and H-phosphonate chemistry was identified as suitable coupling method. The required building blocks, a nucleoside monophosphate and a non-symmetric H-phosphonate, were prepared by convenient and

Abstract

flexible synthesis routes bearing the potential for interchange of components with regard to AB mask, nucleotide and riboside.

Desilylation of protected (d)ADPR-OB in the last step using TEA · 3 HF in acetonitrile gave the desired dADPR-OB derivative successfully for the first time. Fine-tuning of the desilylation and purification protocol would constitute the successive steps for this project. In summary, however, the developed approach constitutes a promising and to a large extent established basis for the adaptable future synthesis of AB-masked (d)ADPR-derivatives.

Masked derivatives of cNMPs were accessed following a short and flexible synthesis route deduced from own studies on non-symmetric phosphoramidites that included an unprotected nucleoside moiety. Here, phosphite by-products were repeatedly observed and concluded to result either from an intermolecular or an intramolecular substitution by a second nucleosidic hydroxy group. Hence, a synthesis involving different nucleosides and an OB-masked phosphordiamidite was developed (see chapter 8.3.).

Five different OB-cNMPs were prepared successfully and evaluated with regard to their stability and performance in cell-based settings. These investigations were carried out in close collaboration with A. GUSE, V. NIKOLAEV and C. GEE and their co-workers (University Medical Center Hamburg Eppendorf).

Hydrolysis studies, chemical and enzymatic, confirmed that the stability of the prepared OB-cNMPs was significantly higher than the rate of enzymatic activation. Further, the masked nucleotides proved to be satisfactory stable for application in cell-based assays as they allow for incubations even over several hours ($t_{\frac{1}{2}} \approx 8$ h). This would enable setups where direct effects could be measured as well as experiments that envisage e.g. a pre-incubation with the OB-cNMPs to load the respective nucleotides into cells prior to a successive stimulation of the cell.

The cell assays performed proved excellent membrane-permeability of the OB-cNMPs. Further, cellular effects similar to those of natural cNMPs were observed allowing the conclusion that the bio-reversible protection at the phosphate was removed efficiently. Hence, the synthesized OB-cNMPs fulfilled all requirements in terms of synthetic configurability of the approach, chemical stability and enzymatic activation to be valuable new tools for the use in and setup of novel cellular assays.

# Part I:

## Functionalized Prodrugs of a bacterial RNAP-Inhibitor

## 3.   Introduction and Background

The resistance of microorganisms to drugs they originally were susceptible to continues to develop. This topic has evolved to one of the most concerning threats to global public health, food security and cohabitation of society.[1–3] Numerous infections with fungi, viruses, parasites and in particular bacteria become increasingly hard to treat and control, and the risks of spreading, contagion, prolonged illness and fatality are rising.[4,5] In Europe and the United States for example, an estimated number of 25.000 and 23.000 people, respectively, are dying from infections with multidrug-resistant (MDR) bacteria per year, although high-quality medical treatment is accessible.[5,6] By now, the problem of antimicrobial resistance has reached a level so serious that it substantially endangers the achievements of modern medicine and provokes the scenario of a post-antibiotic era for the 21st century.[1,4,7,8] Consequently, the issue is perceived as a societal risk of high potential impact not only by scientist but also governments and international, (non)-governmental organizations (Fig. 01), and is tackled by various national as well as global initiatives and action plans.[2,4,6]
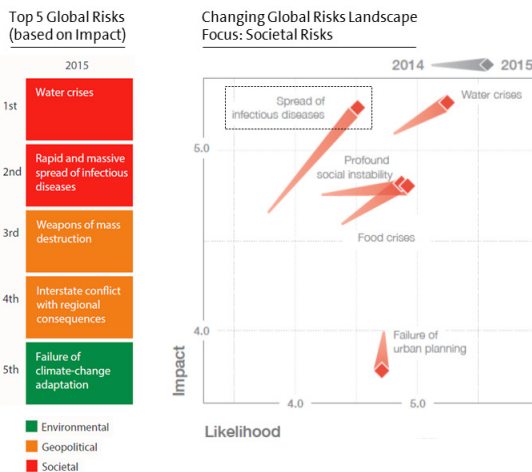


**Figure 01:** Extracts of the Global Risk Perception Survey 2015 issued by the WEF. Among all respondents, the risk of a rapid and massive spread of infectious diseases was in particular among societal risks underscored and rated second most impactful out of all global risks calling for action.[3]

DRUG VERSUS ANTIMICROBIAL RESISTANCE DEVELOPMENT

The development of antimicrobial resistance is a natural phenomenon and proceeded mil-
lennia prior to the modern antibiotic era. This was proven by samples of microorganisms
collected from ancient permafrost.[9,10] Their analysis and further studies on microorganisms
from soil showed that the antibiotic resistome, which constitutes the global collection of
all antibiotic resistance genes, is genetically diverse, ancient and widespread across the
environment and all its niches. Bacteria constitute one of the first forms of life that ap-
peared on Earth and managed to colonize virtually any habitat ever since. In this context,
countering selection pressure is a vivid expression of their adaptability. This aspect culmi-
nates in the development of drug resistances, when the focus is set on pathogenic spe-
cies.[11,12] Though the majority of bacteria are classified as harmless or even beneficial for
humans, some species cause severe infections with high morbidity and mortality.
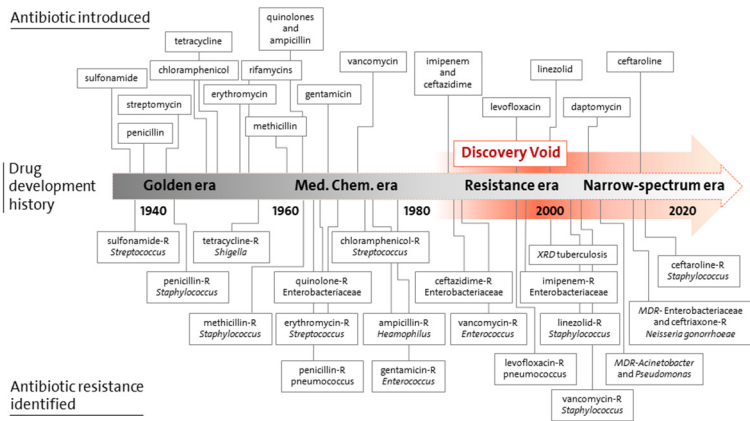


**Figure 02**: Time line of antibiotic drug discovery and development (selected examples). With the discovery of sulfonamide
and penicillin, the Golden era of drug discovery was initiated. Screenings of natural products for antibiotic activity yielded
the scaffolds research relies on until today. Significant improvement of pharmacologic aspects characterized the Medic-
inal Chemistry era. Upon this followed a period of lacking innovation while antimicrobial resistance increased massively.
Future approaches are forecasted to move on from target-based broad-spectrum to *in vivo* essential target screenings.
The focus is predicted to be set on disease-specific tailored, narrow-spectrum agents that decrease the pressure of re-
sistance evolution. Adapted from [9,13,14].

The ability to treat bacterial infections constitutes a remarkable accomplishment that was achieved not even a century ago (Fig. 02). At that time, the serendipitous discovery of penicillin (1929) and the development of Arsphenamine (1910) and sulfonamides (1932) as antibiotics, initiated the 'Golden Era' of antibacterial drug discovery and terminated the 'hegemony of infection' (Fig. 02).[9] From screenings of in particular soil-dwelling bacteria for metabolites that inhibit the growth of other microorganisms, scientists identified most of the natural scaffolds that until today build the foundation of the antibiotics in use. This approach, also termed the Waksman-platform, however reached its limits in the 1960s, since drug candidates frequently exhibited severe pharmacological and toxicological drawbacks.[15] The following era of 'Medicinal Chemistry' succeeded by innovative chemical derivatization of the natural antibiotic scaffolds and achieved huge improvements regarding drug application, dosage and expansion of the activity spectrum (Fig. 02). On the basis of these prospering eras, most antibiotics used today are somehow derived from naturally occurring antimicrobials. Additionally, the majority of compounds have pleiotropic and complex effects on the targeted bacterium as well as more than one cellular target. The most exploited targets include the protein biosynthesis at the ribosomes, the replication and transcription of DNA, and the bacterial cell wall synthesis (Fig. 03). [9,10]

The capacity to control infections paved the way for modern medicine and treatments like chemotherapy and invasive surgery. Childhood mortality was reduced drastically and live expectancy increased.[5] Still, the development of resistance to certain antibiotics proceeded parallel from the beginning of their use on and was first detected in hospitals, where they were mostly used (Fig. 02). Sulfonamide-resistant *Streptococcus pyogenes* for example were isolated in military hospitals in the 1930s already.[16] Similar, first resistances of *Staphylococcus aureus* against Penicillin were detected in civilian hospitals in London shortly after its introduction.[17] Resistance to multiple drugs, ranging from streptomycin over chloramphenicol and tetracycline to sulfonamides, was observed first in the 1960s for enteric bacteria like *Escherichia coli*, *Salmonella* and *Shigella*. Studies also elucidated that resistance genes could be transferred easily between *E. coli* and *Shigella*. However, the medical importance of this fact received few attention and genetic studies focused on the episomal factors for the moment.[7,18,19] The issue of emerging MDR was at that time

perceived as an oddity of little impact on health happening only in developing countries and being limited to *Enterobacteriaceae*. This common attitude changed when clinical isolates of *Haemophilus influenzae* and *Neisseria gonorrhoeae* with resistances to tetracycline as well as ampicillin and chloramphenicol, respectively, were identified in 1976/7. Moreover, the resistance genes were located on plasmids and further studies indicated the resistance acquisition to result from interspecies gene transfer with *E. coli* strains involved as well.[7,20,21]

In general, the emergence of resistance is the result of a selection process induced at the moment an antibiotic agent is presented to the bacterium. The ability to resist the agent can be intrinsic, due to inherent functional or structural characteristics, or it can be acquired from chromosomal mutation or inter-bacterial gene transfer (Fig. 03).[5,15] While susceptible bacteria are inhibited, resistant ones can propagate, spread and further amplify as well as extend their resistance factors to other organisms.[7]
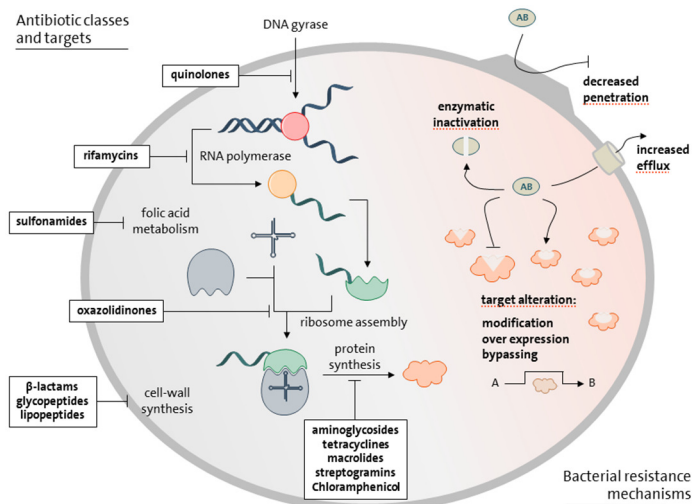


**Figure 03:** The antibiotic classes and targets most frequently exploited (left), and in contrast, the resistance mechanisms commonly observed to counteract these (right). Adapted from [15].

The increasing use and in parts misuse of antibiotics accelerates the development and frequency of resistance. Critical contributing factors are numerous: uncontrolled over-the-counter or street hawking availability of antibiotics, self-prescription and medication, missing knowledge on indication, use and contraindication, and application of low-potency/efficiency drugs of poor manufacture, to name a few. As well, poor urban infrastructure in combination with overpopulation, garbage- and waste water mismanagement, and stray animals promotes e.g. high levels of fecal pollution that puts together bacteria which otherwise rarely interact, thus enhancing chances for horizontal gen transfer. Even higher chances for an undetected but fast spread of resistance across bacteria are given in overcrowded but poorly equipped and staffed hospitals with only limited access to medical supply.[4,7,19]

These issues now are mainly attributed to developing countries but developed countries face severe confrontation with MDR bacteria as well. Pathogens of the ESKAPE group (including *Enterococcus, Staphylococcus, Klebsiella, Acinetobacter, Pseudomonas* and *Enterobacter*) constitute the main cause for nosocomial infections which are increasingly difficult to treat and are a serious risk especially to immunosuppressed patients. Reports on nosocomial *S. aureus* strains from the United States and United Kingdom state that 40 – 60% of these are methicillin and usually multidrug-resistant. Furthermore, the standard treatment using vancomycin is at risk since the proportion of vancomycin-resistance is steadily increasing.[7,22,23]

Another contribution to resistance propagation originates from migratory flows and growing human mobility as a result of globalization, as well as from migration of clinical pathogens into the community and back.[23–25]

This aspect is documented oppressively by the case of New Delhi metallo-β-lactamase (NDM)-mediated carbapenem resistance. The resistance-conferring gene *bla*NDM-1 was first found in *Enterobacteriaceae* isolates from Indian hospitals collected in 2006 and 2007. Further studies showed that the gene sequence was localized on plasmids of varying sizes that readily proved interspecies transferability *in vitro* and, in addition, encoded for an enzyme of a novel type of metallo-β-lactamase.[24] Ongoing studies strengthened the putative epidemiological link between resistance and geographic localization and lead to the identification of NDM-1-expressing strains in eleven more cities in India and Pakistan.[25] Even more

concerning, environmental studies from 2010 in the New Delhi area analyzing drinking and seepage water showed that in 14 out of 221 samples a range of $bla_{NDM-1}$ positive enteric bacteria could be grown. This indicated that NDM-mediated carbapenem resistant strains were not limited to hospitals but widespread in the community.[24,25] Shortly after and with increasing frequency, reports on NMD-positive tested bacteria samples were published from 40 more countries covering all continents except South America and Antarctica. Out of these, some possessed a known potential for epidemic or pandemic outbreaks as well.[24]

First *Enterobacteriaceae* but rapidly after, other Gram-negative strains like *P. aeruginosa*, *A. baumannii* and *K. pneumoniae* were identified carrying NDM-1 carbapenemase. The enzyme is part of a greater, versatile family of β-lactam-hydrolyzing enzymes being subdivided into metallo- and serine-enzymes regarding the hydrolysis mechanism. The clinically most relevant ones are integron-associated and thus spread rapidly as well as, by now, globally. They usually confer resistance to multiple drugs including most β-lactam antibiotics, fluoroquinolones and aminoglycosides, and appear in combination with further resistance mechanisms.[26] In the case of NDM-1-harbouring bacteria, the receptivity for antibiotic treatment was frequently limited to the so-called 'last resort antibiotics' Colistin and tigecyclin.[7,25]

These decade-long developments are accompanied by a discovery void of new antibiotic classes that spans from the 1960s until the 2000s (Fig. 02). In this period, no new class of antibiotics was identified, and instead improved versions of registered drug classes filled the product pipelines only. Despite significant improvements of infection treatment, society today experiences the consequences of this missing innovation in the shape of a profound crisis regarding e.g. the treatment of MDR Gram-negative bacterial infections.[9,14,15]

Maintaining the ability to treat bacterial infections therefor needs novel antibacterial agents that address innovative targets and/or possess alternative modes of action.

THE PURSUIT OF INNOVATION

Since the 1990s, high-tech drug discovery platforms like *High-Throughput Screening* and *Rational Drug Design* have been built up to push, in combination with genomics and combinatorial chemistry, the production of novel synthetic antibiotics. The cornerstone of this approach is that methods of genomics identify essential bacterial proteins that make up suitable targets for the screening or targeted design of novel inhibitors leading finally to new drugs.[15]

Such a venture is pursued e.g. for the case of bacterial DNA-dependent RNA-Polymerase (RNAP). The enzyme catalyzes the transcription of DNA into RNA and thus is crucial for the most regulatory step within the expression of genes. Accordingly, the enzyme is essential and, in addition, it is structurally highly conserved among a wide range of bacterial strains while it differs significantly from eukaryotic RNAP. Consequently, bacterial RNAP makes up a highly suitable target for drug development.[27,28]

However, thus far the enzyme is rarely exploited in antibacterial therapy. Members of the rifamycin family, a subclass of the ansamycins, are the only RNAP inhibitors of clinical relevance up until today. Rifamycin antibiotics were first isolated from *Amycolatopsis rifamycinica* in 1957 and introduced to the market in 1968. They display broad-spectrum activity based on their unique mode of action. It results from binding to a pocket deep within the RNAP β-subunit, and about 12 Å away from the active center cleft. There, they prevent the elongation of nascent RNA-strands by blocking the exit path so that RNA synthesis collapses.[28–30]

Rifamycins are effective against a broad range of Gram-positive as well as Gram-negative bacteria, and in particular used to treat infections with mycobacteria like *Mycobacterium tuberculosis* or *Mycobacterium leprae*. However, the acquisition of resistance to rifamycins by point mutation and subsequent exchange of amino acids at their binding site again illustrates the need for novel drugs.[31]

The bacterial RNAP has been studied extensively due to its central role in gene expression and the fact of being one of the few validated targets for broad-spectrum antibacterial activity. Thus, the structure of the flexible, multifunctional enzyme as well as the course of the catalytic cycle have been elucidated to a great extent.[32–34]

**Figure 04:** The naturally occurring α-pyrones Myxopyronin A (**1**) and Corallopyronin A (**2**) as well as the macrolactone Ripostatin A (**3**) exhibit antibiotic activity by means of inhibition of the bacterial RNAP by blocking the "switch region".

In complementation, further naturally occurring antimicrobial agents have been screened and studied with a focus set on inhibitors of the RNAP that exhibit alternative modes of action compared to rifamycin antibiotics. The identification of new binding sites and/or novel RNAP inhibitors was anticipated by this. [31,35]

ARNOLD and EBRIGHT described a promising new binding site, the RNAP "switch region", which they identified from characterization of the mode of action of three naturally occurring antibiotics: the two α-pyrones Myxopyronin A (**1**) and Corallopyronin A (**2**), and the macrolactone Ripostatin A (**3**, Fig. 04).[31,35–37] The compounds were isolated in the 1980s and 1990s already, and further found to display antibacterial effects based on RNAP inhibition. However, identification of the precise binding site and mechanism of action took until 2008. [35,36]

The α-pyrones **1** & **2** and macrolactone **3** bind to a region within the bacterial RNAP that mediates the conformational changes between the open and closed form of the enzyme. In the open state, DNA can be bound to or released from the active center cleft, which is located at the base of the two β subunits. The closed conformation enables DNA to be retained within the enzyme which is essential for transcription initiation and transcription elongation. The transition between both states involves a 30° swinging motion of the β' subunit around a hinge located at its base (Fig. 05). This hinge was termed "switch

region", and it undergoes frequent conformational changes. It was further found, that the "switch region" directly interacts with the phosphate backbone of DNA in the transcription-elongation state. This indicated that phosphate coordination is coupled to the closure of the clamp upon DNA binding.[31,35,37]

The compounds **1 – 3** are proposed to interact with RNAP at the "switch region" in conformations between partly to fully closed (Fig. 05). They prevent an opening of the β' clamp to load promotor DNA, and thus block transcription initiation. The interaction site consists of highly conserved residues and consequently, the compounds show broad spectrum activity. Since the site differs from binding sites of other RNAP inhibitors, cross resistances are unlikely to occur. In addition, the macrolactone and α-pyrones constitute structurally unrelated compound classes. This in combination with the predominantly hydrophobic architecture of the binding pocket provides evidence for a given druggability of the "switch region" by multiple chemotypes.[37]
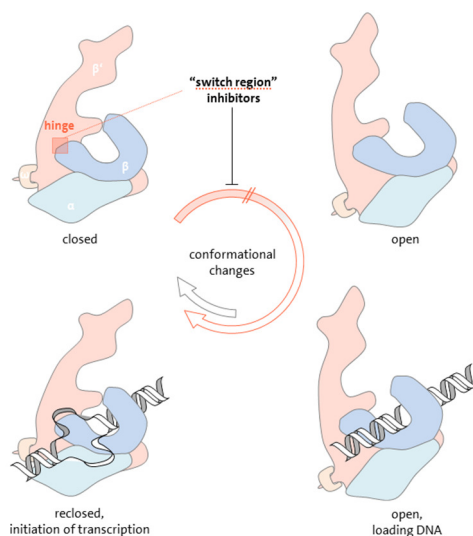


**Figure 05:** The "switch region" binders interfere with crucial conformational changes since they imped the active center cleft to open and load DNA. Consequently, the yblock transcription of DNA into RNA, and gene expression comes to a halt. Adapted from [35].

DEVELOPING A NEW RNAP-INHIBITOR

The properties attributed to the "switch region" contribute to a facilitation of *in silico* rational design and/or screening of new, optimized ligands.[31,37] On this basis, R. HARTMANN and co-workers initiated a project focusing on the development of novel small molecule inhibitors of the bacterial RNAP (Fig. 06).[38,39]

Following a pharmacophore-based virtual screening approach, including therein features of myxopyronins in combination with protein-derived "switch" region characteristics, an aryl-ureidothiophene carboxylic acid (**4**) was identified as a potent RNAP inhibitor (Fig. 06).[38,39] Docking experiments predicted that hit compound **4** would bind to the "switch region". The potential inhibitory activity against *E. coli* RNAP was confirmed in a functional *in vitro* assay (IC$_{50}$: 75 μM). The structure-based optimization of **4** included variation of residues at the aryl- and ureido-moiety, respectively, and an analogue design approach aiming at regio-isomers as well as hetero core derivatives (Fig. 06). Thus, efficacy was increased and a structurally optimized compound (**5**) validated to inhibit *E. coli* RNAP with an IC$_{50}$ of 22 μM. In the case of regio-isomeric derivative **6** similar results were obtained, which was explained by the almost identical spatial arrangement of fragments.[40]
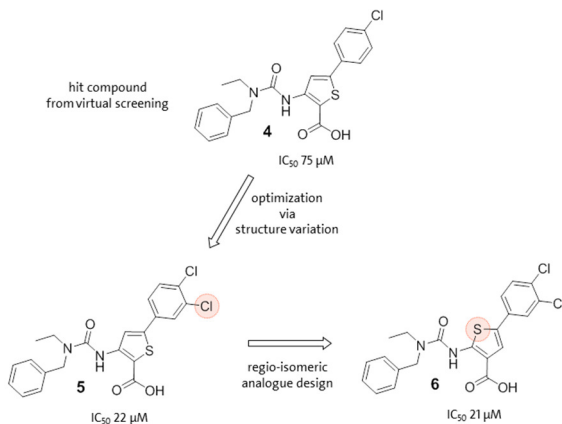


**Figure 06:** Hit compound (**4**) constituted the starting point for the development of optimized compounds with varied aryl residue (**5**) and rearranged substituents at the heterocyclic ring (**6**).

The antibacterial activity of aryl-ureidothiophene carboxylic acids was tested against two Gram-positive strains *(B. subtilis*, *S. aureus)* as well as two Gram-negative wild types (*E. coli* K12, *P. aeruginosa*) and one *E. coli* mutant (*E. coli* TolC).

Gram-positive strains showed susceptibility with MIC values of 8 – 11 µg/mL. The growth of an *E. coli* mutant deficient in the AcrAB-TolC efflux system was also affected (MIC: 11 µg/mL). This corresponded to observations made for many Gram-positive active compounds.[41,42] Yet, the data did not exclude that the observed growth reduction was a result of multi-target action since, untypically, almost no activity was lost from the enzyme to the whole-cell assay.

Against the Gram-negative wild-type strains, the compounds were not active (MIC > 25 µg/mL). These observations were suggested to result from a lack of compound accumulation in the bacterial cytoplasm. In further studies, drug efflux and an inefficient passage of the outer membrane barrier were identified to contribute to the ineffectiveness of the compounds.[38,40]
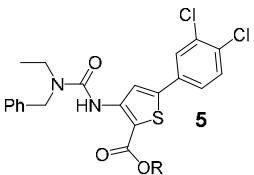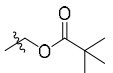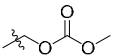
The RNAP inhibitors **5** and **6** are negatively charged under physiological conditions since they contain a carboxylic acid moiety (Fig. 06). This feature was determined to be beneficial regarding the RNAP inhibitory activity, and improved the solubility and hydrophilicity of the compounds. However, it was assumed that it affected the permeation into Gram-negative bacteria through general diffusion porins negatively at the same time. Mainly, the porin subfamilies OmpF and OmpC are associated with the passage of antibiotics through the bacterial outer membrane. Since these porins exhibit a slight preference for cations, the uptake of negatively charged compounds proceeds relatively slow.[43,44]

An extension of the efficacy spectrum of the RNAP inhibitors on Gram-negative bacteria appears desirable, especially against the backdrop of an urgent need for novel drugs against these pathogens. Here, a consequent further development features the elaboration of a prodrug strategy. The medicinal-chemical strategy of masking the impedimental carboxylate constitutes a common option to overcome pharmacokinetic deficiencies associated with poor intrabacterial accumulation.[45]

In particular, prodrug approaches that include polarity-reducing, enzyme-cleavable multipartite prodrug structures are commonly applied.[46] Pro-moieties that address active uptake mechanisms via bacterial transport systems constitute another promising yet sophisticated approach.

**Scheme 01:** Syntheses of prodrugs. *Reagents and conditions*: **i.** DIAD, TPP, *R*OH, DMF, rt, 4 h – 18 h, **6**: 99%, **7**: 93%, **8**: 27%; **ii.** TBTU, DIPEA, DMF, rt, 18 h, 68%; **iii.** TEA, halide reagent, DMF, rt → 40 °C, 18 h, **10**: 79%, **11**: 76%, **12**: 89%, **13**: 73%; **iv.** CH$_3$I, THF, rt, 20 h, 72%.

In previous works, a range of charge-neutral ester-prodrugs as well as two derivatives bearing positively charged masking units were synthesized (Scheme 01).[47] These were demonstrated to successfully release the parent drug upon enzymatic activation while possessing adequate chemical stability. Respective studies were performed by means of incubation assays followed by HPLC-analysis (Table 01). [47]

**Table 01:** Overview of the results of the stability determination assays.

| Prodrugs of | | Half-lives $t_{1/2}$ [h] calc. based on formation of the parent drug | | |
| --- | --- | --- | --- | --- |
| | | enzymatic activation (PLE) | chemical hydrolysis (PBS, 25 mM) | |
| | | *pH 8.7* | *pH 7.3* | *pH 8.7* |
| R = (acetyl spacer) | **10** | 2.6 | 124 | 3.2 |
| R = (pivaloyl spacer) | **11** | 2.1 | 14 | not performed |
| R = (methyl carbonate spacer) | **12** | 2.5 | 70 | 9.6 |
| R = (ethyl carbonate spacer) | **13** | 1.7 | 2.4 | not performed |
| R = Me | **6** | 4.5 | no significant release after 7 d of incubation | |
| R = Et | **7** | 3.1 | | |

Ester pro-moieties are generally activated by ubiquitous carboxyesterases. The implementation of spacer-groups facilitates this process as the cleavage site becomes easier to access. Upon enzymatic activation, the spacers applied here decompose spontaneously to release the parent drug (Fig. 07). The hydrolytic stability of the ester-groups needs to be sufficiently high to minimize extracellular decomposition by chemical cleavage of the ester bonds (Fig. 07).[45,46] Accordingly, a selection of prodrugs was studied with respect to enzymatic activation and chemical stability. Therefore, the prodrugs were incubated with PBS buffer (pH 7.3 (physiological pH mimic), 50 mM) as well as with pig liver esterase (PLE) as a model for carboxyesterase activation. The latter assay was performed in PBS at pH 8.7 (50 mM) since this approximates the optimum pH of the enzyme.[48,49] An additional chemical stability assay in PBS, pH 8.7 was performed for reference (Table 01).

In all cases, the parent drug was successfully released from the respective prodrug which was confirmed by HPLC analysis including co-injection experiments. The formation of further cleavage products was not detected in any case. These results confirmed that the parent drug is stable under physiological pH. Furthermore, the enzymatic reaction occurred exclusively at the ester and carbonate motif, respectively.

In case of the carbonate prodrugs **9** and **10**, the hydrolytic reaction proceeded via an intermediate species (Fig. 07). As expected, alkyl esters **7** and **8** showed in both assays the highest chemical stabilities (Table 01). Acyloxymethyl esters (**5**, **6**) and carbonate prodrugs (**9**, **10**) showed similar half-lives of about 2 – 3 h for enzymatic activation. The determined chemical stabilities of prodrugs **5**, **6**, **9** and **10** differed but were generally higher than the half-lives for the enzymatic reaction. In general, the enzymatic cleavage of all masks proceeded relatively fast and importantly, faster than the chemical decomposition (Table 01).
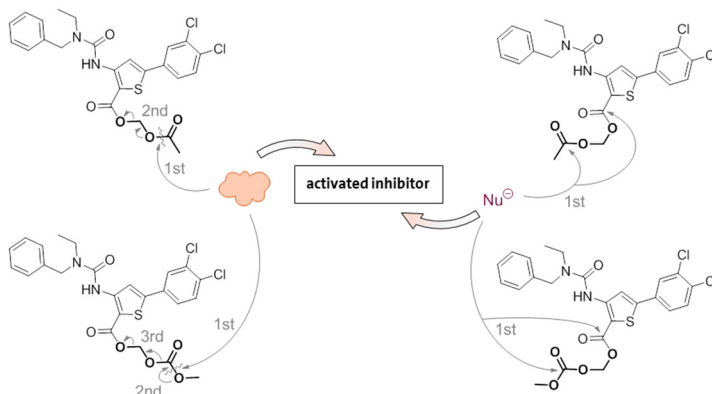


**Figure 07:** Mechanisms of enzymatic activation (left) versus chemical hydrolysis pathway (right).

When comparing enzymatic activation of the esters **7** and **8** to the oxymethyl- and carboxymethyl-linked prodrugs (**5**, **6**, **9** & **10**), the half-lives indicated that the more distal esters possessed favorable substrate properties towards the esterase, as expected.[47]

A conjugation of the RNAP-inhibitor with molecular entities that address active uptake mechanisms is of great interest to further expand the set of different prodrugs. The exploitation of siderophore-based iron uptake mechanisms constitutes one approach here.[9]

Typical siderophore ligands

Catecholate      Hydroxamate      Polycarboxylate

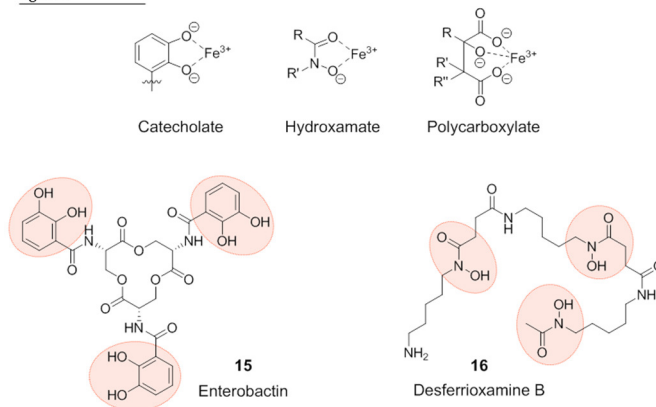**15**
Enterobactin

**16**
Desferrioxamine B

**Figure 08:** Ligands typically found in siderophores are catecholate, hydroxamate and polycarboxylate. These moieties are integrated into a variety of structures ranging from cyclic ones like Enterobactin (**15**) to linear compounds like Desferrioxamine B (**16**).

Upon iron depletion, bacteria activate a pathway for the production of siderophores and expression of respective membrane receptors while the bacterial host – the infected organism – commonly uses iron withholding as an important defence mechanism. Most relevant in this context are iron binding, trafficking and recycling through the proteins transferrin and lactoferrin, and storage by ferritin. Bacteria can only survive under such conditions if they are able to secrete siderophores with iron(III)-affinities high enough to successfully compete for the iron bound to the host proteins. The aspect that bacteria, through the siderophores they secrete, purposefully target $Fe^{III}$ results from an efficient selectivity: along with the kinetically inert $Co^{III}$, $Fe^{III}$ is the only trivalent metal ion occurring in biological matrices. In contrast, divalent cations are formed by a broader range of biologically important metals.[50,51]

A high affinity-ligand for $Fe^{III}$ ideally comprises highly charged oxygens as donor atoms integrated into a structure that allows for an octahedral arrangement.

Within siderophores, the three groups most frequently found are the bidentate catecholate, hydroxamate and α-hydroxycarboxylate or citrate-based polycarboxylate residues (Fig. 08). Apart from these recurrent structural features, siderophores constitute a highly diverse group of compounds ranging from cyclic (**15**) to linear (**16**) and mono- to

multinuclear complexes that contain a mixture of coordinating ligands and amino acids forming the backbone (Fig. 08).[50,52–54] Accordingly, respective transporters recognize the coordination sphere around $Fe^{III}$ and structural features of the ligands rather than the molecular entity. Hence, board structural variation of compounds is possible and tolerated. This aspect constitutes the central fundament of siderophore-drug conjugate approaches, which are designed to exploit siderophore receptors for subsequent intracellular drug delivery. The existence of naturally occurring sideromycins, i.e. conjugates between siderophores and antibiotics that are produced by certain bacteria against competing microorganisms, underlines the applicability of this concept further.[50,52–54]

# 4. Aim of the Work

Addressing bacterial uptake mechanisms to promote an active transport across the bacterial cell wall and plasma membrane constitutes a promising approach to overcome this major limiting factor of a compound's antibacterial activity. This is in particular important for antibiotic agents against Gram-negative bacteria.

Bacteria essentially rely on iron and ensure the supply with it by secretion of siderophores, a very heterogeneous class of compounds exhibiting a high affinity for iron(III). The uptake of $Fe^{III}$-loaded siderophores proceeds via different, but rather unspecific membrane receptors. Thus, the conjugation of a potential drug that suffers from low penetration of the bacterial envelope with a siderophore-type motif is expected to induce an active uptake, and thus increase its efficacy and expand its activity spectrum.

In addition, enzyme-cleavable masks and/or linking moieties are integrated to ensure a fast activation of prodrugs upon entry into the bacterial cell.



**Scheme 02:** General approach towards siderophore-type prodrugs of the RNAP-inhibitors **5** and **6**.

For the bacterial RNAP inhibitors **5** and **6** it has been proposed that low intracellular accumulation impeded their antibacterial effect. Prodrugs of **5** and **6** designed for active uptake have not been synthesized neither studied so far. Therefore, this thesis aimed at conjugating both compounds with moieties that provide the capacity to coordinate $Fe^{III}$. The introduction of spacer groups was envisaged to facilitate enzymatic prodrug activation, as found earlier in the context of charge-neutral ester prodrugs.

Regarding synthetic aspects, this implied a site-specific modification of the mask with linker and/or drug that leaves the $Fe^{III}$-coordinating functionalities unaffected. Hence, the development of a suitable protecting group/release strategy was demanded which at the same time considered the lability of the envisaged ester and carbonate linkages.

Apart from prodrug synthesis, the $Fe^{III}$-coordination of the siderophore-type prodrugs was to evaluate in a competitive assay to yield relative affinities.
Finally, the antibiotic activity of all prodrugs, i.e. lipophilic, cationic and functionalized, was to determine in collaboration with the group of R. HARTMANN (Helmholtz Institute for Pharmaceutical Research Saarland (HIPS), Saarbrücken).

## 5. Results and Discussion

Several examples for natural and/or synthetic siderophore-conjugated antibiotics were reported, and some demonstrated to beneficially affect the effectiveness of the drug. In 2012, JI and MILLER described the synthesis of Desferrioxamine B-ciprofloxacin conjugates.[55] The siderophore part (Desferrioxamine B) was connected to the fluoroquinolone (ciprofloxacin) via a biochemically labile linker that lactonized spontaneously upon esterase/phosphatase activation, and thus released the drug. Despite the fact that a naturally occurring hydroxamate-siderophore was incorporated, the inhibitory activities of the conjugates were either weaker than that of the parent drug or completely lost. This was explained by inefficient recognition through siderophore transporters as well as an insufficient release of the drug.[55]

Similar outcomes were reported for conjugates of 2,3-dihydroxyphenol-type siderophores with antibiotics like norfloxacin and aminopenicillins. For these cases, iIt was shown that the siderophore-drug conjugates generally displayed an antibacterial effect, but this effect was weaker than that of the parent compound. Reasons stated were vague and attributed to insufficient receptor recognition/transportation and/or drug release. [56,57]

In contrast, BROWN *et al.* were able to synthesize a range of structurally diverse pyridone-conjugated monobactams that exhibit a balanced profile of antibacterial activity against several clinically relevant strains.[58] A part of their work focused on the uptake mechanisms of their compounds. Studies on *P. aeruginosa* strain PAO1 pointed to two siderophore transporters, PiuA and PirA, as transporting enzymes which was further underpinned by control experiments with PiuA and PirA-deficient strains. The authors thus hypothesized, that the pyridone moiety efficiently mimicked the catechol motif and consequently induced a receptor interaction/recognition.[58] A related publication on C4-modified monobactams by ARNOULD *et al.* pointed in a similar direction. They described an improvement of antibacterial activity for respective conjugates with 3,4-dihydroxyphenol moieties as siderophore-mimics.[59] These findings were further substantiated by a publication of CURTIS *et al.* who performed a study on catechol-substituted cephalosporins and observed broad susceptibility of E. *coli* K12 *in vitro*.[60] These results encouraged the study of 3,4-dihydroxy-phenol- and pyridone-moieties as siderophore mimicking masks. However, a potential

drawback and noteworthy objection is that the described successful siderophore-drug conjugates were members of the β-lactam family. For these, the bactericidal potential relies on an interference with the bacterial cell wall synthesis. The target thus is located in the outer shell of bacteria whereas the RNAP-inhibitors have to pass cell wall, inner membrane and periplasmic spaces in-between to reach their target in the cytoplasm. In contrast, the mentioned aminopenicillins target bacterial cell walls as well, but lost activity when they were conjugated with three 2,3-dihydroxyphenol moieties in total.[57] Thus, it was reasoned that the beneficial effect on antibacterial activities originated at least in parts from the pyridone- and 3,4-dihydroxyphenol-moieties and their recognition by siderophore transporters. Therefore, these motifs were chosen as masking units for the synthesis of siderophore prodrugs of compounds **5** and **6**.

## 5.1.   Catecholate-type masks

Catecholates exhibit the highest coordination constants for iron(III) in comparison to polycarboxylates and hydroxamates and were included successfully in synthetic siderophores before. Hence, this study aimed at the investigation of multipartite masks containing this structural feature attached to RNAP inhibitors **5** and **6**.[54,61,62] Linker lengths were varied and catecholates with different side chain functionalities were studied.

Starting from carboxylic acid **17**, the corresponding alcohol was synthesized to either directly esterify carboxylic acids **5** and **6,** or further convert to the carbonate-linked mask building block (Scheme 03, left). For both paths, a protecting group (PG) strategy that allowed for regioselective modification was necessary. Analogously, a suitable strategy to block the phenolic hydroxy functions while leaving access to the carboxylic acid was required to conduct the acylation of **17** to the corresponding chloromethyl carboxylate mask-building block (Scheme 03, right).
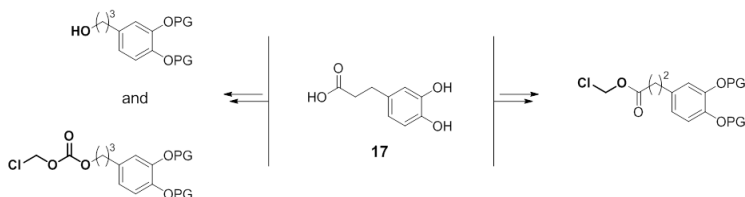
**Scheme 03:** General synthesis paths to access the reactive mask building blocks required for the conversion with carboxylic acids **5** and **6**. The starting material for catecholate-type siderophore-masks constituted 3,4-dihydroxyphenylpropionic acid (**17**).

The motifs connecting drug and pro-moiety are particularly sensitive towards basic and/or nucleophilic conditions. Based on this aspect and the demands mentioned before, benzyl PGs were considered. Common hydrogenolytic debenzlyation, however, was ruled out due to the high degree of aromatic rings in the molecular system and the potential risk of undirected hydrogenolysis.

Rather, the possibility to cleave benzyl ethers using Lewis acids under anhydrous conditions at low temperature was envisaged for the release of the final prodrugs. This procedure additionally was reported to proceed with sufficient chemoeselectivity.[63]

### 5.1.1.   Synthesis of dibenzyloxyphenyl carboxylic acids and alcohols
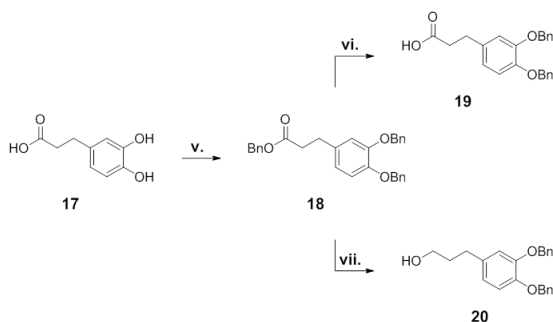


**Scheme 04:** Synthesis routes towards the oxyphenyl-benzylated carboxylic acid and alcohol. **v.** 4.5 eq. $K_2CO_3$, 6 eq. BnBr, MeCN + 4% water, 95 °C, 20 h, 93%; **vi.** 2 eq. KOH, THF/water 1:1, rt to 50 °C, 5 h, 82%; **vii.** 3 eq. $BH_3 \cdot THF$, THF, 0 °C to rt, 20 h, 91%.

The per-benzylation of the starting material 3,4-dihydroxyphenylpropionic acid **17** proceeded smoothly with benzyl bromide and potassium carbonate as base. The addition of 4% water to the solvent acetonitrile was found to increase the conversion, likely due to a better dissolution of base and starting material.[64] Upon column chromatography, product **18** was isolated in satisfying yields of up to 83% and as colorless to yellowish wax (Scheme 04). Subsequent cleavage of the benzyl ester was performed under aqueous conditions with potassium hydroxide as base and generated the corresponding carboxylic acid

**19** in 82% yield (Scheme 04). Synthesis of the corresponding alcohol **20** was carried out by reduction of **18** with the borane-THF complex between 0 °C and room temperature over 20 h.[65]

Again, the reaction proceeded almost quantitatively and the desired product was obtained in high yields of around 90% (Scheme 04).

In summary, all reactions of this sequence went smoothly and could further be performed easily in multi-gram scales. Since conversions were excellent for each step, purification methods like column chromatography were feasible for multi-gram batches as well, thus providing fast access to the partially protected mask building blocks.

### 5.1.2. Synthesis of the chloromethyl carbonate and the carboxylate building blocks

Earlier studies had shown that the RNAP inhibitor **5** was easily converted into its esters using halogenated reagents such as chloromethyl(alkyl) carbonates under triethylamine basic conditions.[47] Therefore, similar reagents were prepared from the siderophore-type mask precursors to take advantage of the established reaction.

Carboxylic acid **19** was converted with chloromethyl chlorosulfate in a biphasic mixture of dichloromethane and water under basic conditions.[66] Tetra-*n*-butylammonium hydro-gensulfate was added as phase transfer catalyst assuring a thorough mixing and hence a better conversion (Scheme 05). Upon conversion of the starting materials, the colorless cloudy mixture turned clear and the desired product **21** was isolated from the organic layer in quantitative yield.

The synthesis of the carbonate-linked mask building block **22** was achieved by converting the respective alcohol with chloromethyl chloroformate in the presence of pyridine as hy-drochloride scavenger (Scheme 05).[66] The synthesis again went along with excellent yields of over 95%. Further, the isolation of the desired product succeeded in high purity after only an aqueous work up as confirmed by NMR analysis.

Concluding these steps, both linker-bearing mask building blocks were accessed by overall convenient synthesis sequences that went along with high yields and further allowed up-scaling.
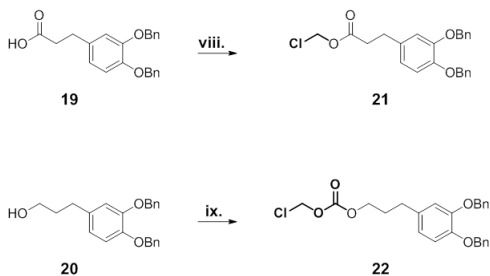


**Scheme 05:** Conditions for the chloromethyl acylation and carboxylation of siderophore-type mask precursors. **viii.** 1.1 eq. chloromethyl chlorosulfate, 4 eq. NaHCO$_3$, 0.1 eq. (nBu)$_4$NHSO$_4$, dichloromethane/water 1:1, rt, 30 min, quant.; **ix.** 1.1 eq. chloromethyl chloroformate, 2.5 eq. pyridine, dichloromethane, 0 °C to rt, 18 h, 96%.

Based on throughout high conversions, purification steps were as well handy to perform, even in multi-gram batches. Having accessed the benzyl-protected chloromethyl carbonate **22** and chloromethyl carboxylate **21** building blocks, their applicability in coupling reactions with the potential drugs **5** and **6** was studied.

## 5.2.     Pyrone- and pyridone type masks

Syntheses of pyrone- and pyridone-masks were designed based on the publications by BROWN *et al.* and MITTON-FRY *et al.* and started from Kojic acid **23** (Scheme 06).[58,67] The anticipated linking structures were kept consistent with the previous set of prodrugs which contained oxymethyl acylates and oxymethyl carbonates (Scheme 06).[47] Benzyl-protection of hydroxy groups was envisaged again for the regioselective introduction of these linkers.
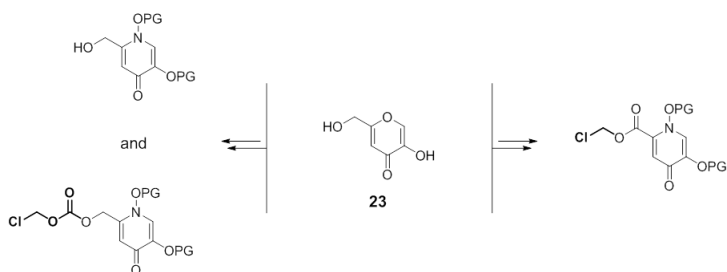
**Scheme 06:** Starting from Kojic acid **23**, the synthesis of the reactive pyridone mask building blocks was designed including the exchange of the hetero atom and functionalization of the side chain.

### 5.2.1. Synthesis of the benzyl protected pyridone

The key intermediate, 5-benzyloxy-2-hydroxymethyl-*N*-benzyloxy pyridine-4-on **25**, was accessed by 1.) benzyl-protection of the 5-hydroxy function, 2.) exchange of the ring-oxygen against the *N*-hydroxy motif and 3.) benzyl protection of the newly introduced OH-group. The procedures were adapted from BROWN *et al.*, but required in parts optimization.[58]

The benzyl-protection of the phenolic hydroxy-function of starting material **23** proceeded smoothly with benzyl bromide and sodium hydroxide (Scheme 07). Isolation of the product was performed either by precipitation induced via addition of 1 M hydrochloric acid to the reaction mixture or column chromatography. In contrast to the reported procedure[58], where precipitation of the product was carried out at room temperature and stopped after 20 min, this study found that complete precipitation of **24** required a minimum of 60 min of stirring at 0 °C. Otherwise, yields were significantly lower than described

The dibenzylated *N*-hydroxy pyridone **25** was first synthesized as described by BROWN *et al.* in a two step-reaction (Scheme 07, upper reaction pathway).[58] For this, 5-*O*-benzylated Kojic acid **23** was suspended in ethanol/water 1:7 and converted with hydroxylamine hydrochloride in the presence of sodium acetate trihydrate over 24 h at 60 °C. Then, ethanol was evaporated and the precipitating *N*-hydroxy pyridone **25a** collected by filtration. The solid was washed, dried and in a next step dissolved in DMSO and converted to **25** using benzyl bromide and potassium carbonate as base. The reported combined yields for these

two steps were 39%[58]. This yield was not reached in this study by following the reported procedures. Crucial points were 1.) an incomplete conversion of the starting material **24**, which could be overcome and led to completion by increasing both, reaction temperature and time, and 2.) an insufficient precipitation of **25a** even under cooling. Thus, despite a smooth subsequent benzlyation, combined yields did not exceed 23%. Based on these findings, the reaction protocol was modified to a *one pot* strategy that circumvents the inefficient isolation of **25a**.

Inspired by a related protocol described by BROWN *et al.*, *N*-methyl-2-pyrrolidone was employed as solvent and potassium carbonate used as base in both reaction steps (Scheme 07, lower reaction pathway).[58] The substitution of the ring-oxygen by hydroxylamine was carried out at 75 °C for 24 h, which was followed by the addition of benzyl bromide and additional potassium carbonate as well as further stirring under the same conditions as before. Upon final column chromatography, pyridone **25** was isolated in 56% yield.
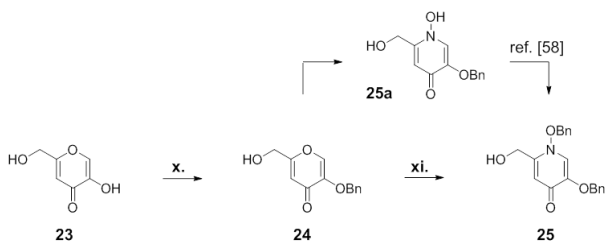


**Scheme 07:** Synthesis of 5-benzyloxy-2-hydroxymethyl-*N*-benzyloxy pyridine-4-on **25**. **x.** 1.1-1.5 eq. 1 M NaOH, 3 eq. BnBr, methanol, 100 °C, 24 h-48 h, 83%; **xi.** *one pot* a) 3-5 eq. $K_2CO_3$, 3-5 eq. $NH_2OH*HCl$, 75 °C, 24 h, b) 1.5 eq. BnBr, 1.8 eq. $K_2CO_3$, *N*-Methyl-2-pyrrolidone, 75 °C, 24 h, 56%.

The *one pot*-protocol thus constituted not only a more convenient approach towards the mask building block **25**, but was also more efficient.

Having mask precursor **25** in hands, the introduction of the carbonate linker succeeded. Further, procedures for the oxidation of the benzylic alcohol to the corresponding carboxylic acid were studied to then introduce the acyloxymethyl-linker.

### 5.2.2. Oxidation and linker modification of the 2-hydroxymethylene group
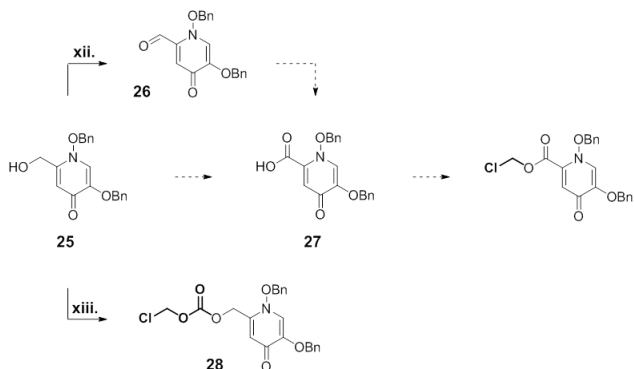


**Scheme 08:** Synthesis routes towards the chloromethyl acylate and chloromethyl carbonate building blocks of the pyridone mask. **xii.** 1.3 eq. Dess-Martin-Periodan, dichloromethane, rt, 3 h, 65%; **xiii.** 1.1 eq. chloromethyl chloroformate, 2.5 eq. pyridine, dichloromethane, 0 °C for 30 min, then rt, 22 h, 35%.

In contrast to the results reported by BROWN *et al.* and presented in earlier related works by BRICKNER and co-workers[68], oxidation of the primary alcohol of pyridone **25** to the corresponding carboxylic acid **27**, both as single- or multistep procedures, led to either significant side or decomposition reactions. Moreover, protocols for the isolation and purification of the product could not be retraced (Scheme 08).

Attempts to directly oxidize alcohol **25** to the corresponding carboxylic acid **27** adapted from BRICKNER and colleagues[68] using sodium dichromate were not successful, and only starting material was recovered (Scheme 08, middle).

Stepwise approaches synthesizing first the aldehyde **26** were carried out under Parikh-Doering (DMSO, $SO_3 \cdot py$, TEA) and Dess-Martin (Dess-Martin periodan) conditions (Scheme 08, upper path). The former again went along with insufficient conversion whereas the latter successfully yielded aldehyde **26**. Thus, the compound was isolated in good yields after column chromatography. Further oxidation of aldehyde **26** was performed under Pinnick oxidation ($NaClO_2$, $NaHPO_4$, MeCN/*t*BuOH/2-methyl-2-butene) conditions as reported by BROWN *et al.* A conversion of the starting material basically was observed. However, the usual work up consisting of acidification of the aqueous phase and extraction of the protonated carboxylic acid from the reaction mixture was not feasible,

probably due to the high polarity of compound **27**. BROWN *et al.* alternatively concentrated to dryness, re-slurried the remaining solids several times with dichloromethane/methanol and combined the organic phases to isolate carboxylic acid **27**.[58] Following this procedure, no pure product was obtained and, additionally, the generated crude yields were low.

Attempts of purification via column chromatography, normal or reversed phase, were neither successful. The use of additives to the solvent, like acetic acid to disrupt strong interactions with the stationary phase, also had no impact. Spectra of the crude product, in particular ESI-mass analysis, hinted towards the decomposition of carboxylic acid **27** under acidic conditions. In particular, a loss of the carboxylic acid function was observed which could result from decarboxylation.

Apart from decomposition, the formation of by-products exceeding the molecular weight of **27** was concluded from the respective spectra. One cause potentially laid within the α,β-unsaturated structure of the pyridone. Being a Michael acceptor, the pyridone itself could act as a scavenger of the hypochlorous acid formed during the reaction and thus a variety of side reactions could be initiated.

Consequently, the isolation of pure carboxylic acid **27**, although being reported in the literature, was not successful. Additionally, the compound exposed a significant lability towards acidic pH values and nucleophiles whilst synthesis and/or attempts of purification. Further investigations on e.g. optimization of reaction protocols or introduction of linking structures hence were ruled out at this point. Instead, the chemical properties of **27** raised severe doubts regarding its efficiency as a masking unit for prodrugs with an intracellular target requiring a certain chemical stability.

The synthesis of the chloromethyl carbonate modified mask building block **28** was successful (Scheme 08, lower path). For this, alcohol **25** was converted with chloromethyl chloroformate in the presence of pyridine as hydrochloride scavenger and compound **28** was isolated in 35% yield. This building block was applied successively in the esterification reactions with RNAP inhibitor **5**.
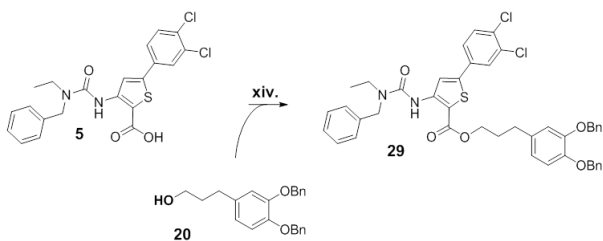
### 5.3. Syntheses of the siderophore-type prodrugs
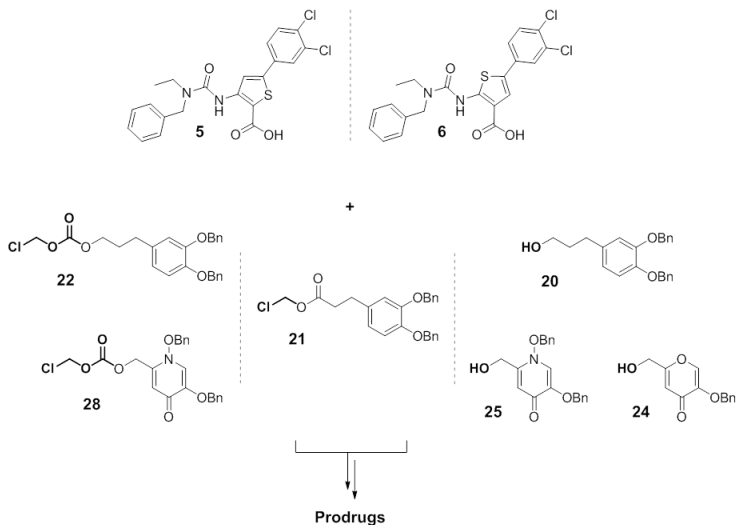


**Scheme 09:** Overview of building blocks to be converted with the RNAP inhibitors **5** and **6**.

The synthesized building blocks (**21 – 22**, **24**, **25**, **28**) consisting of the benzyl-protected masks and the respective halogenated linkers, were anticipated to react efficiently with the carboxylate function of RNAP inhibitors **5** and **6** under similar conditions as used previously for the first set of prodrugs. In addition, siderophore-type prodrugs containing no linker were synthesized in analogy to the first prodrug set as well (Scheme 09).

### 5.3.1. Synthesis of benzyl-protected siderophore-type ester prodrugs

The ester prodrug representatives of the first set of compounds, the methyl and ethyl esters **6** and **7**, were prepared using Mitsunobu (TPP, DIAD) conditions. Since excellent conversions and yields underlined the feasibility of this approach, the respective reaction conditions were transferred to the siderophore-type masks here.

**Scheme 10:** Synthesis of the benzyl-protected siderophore-type ester prodrug **29** under Mitsunobu esterification conditions: **xiv.** 4.5 eq. alcohol **20**, 6 eq. DIAD, 6 eq. TPP, DMF, 40 °C, 18 h, 63%.

Accordingly, carboxylic acid **5** was converted with alcohol **20** in the presence of di*iso*propyl azodicarboxylate (DIAD) and triphenylphosphine (TPP) in DMF (Scheme 10). The desired prodrug precursor **29** was purified by column chromatography and obtained in a yield of 63%.

In contrast to the smooth reaction of **5** with the catecholate-mask building block **20**, the reaction with the benzylated pyrone and pyridone building blocks **24** and **25** did not lead to the formation of the desired esters (Scheme 11). Instead and surprisingly, the β-lactam-type condensation product **9** was isolated from the reaction mixtures in 90% and 23% yield, respectively. This reaction outcome, the formation of **9**, had been observed previously, but only under Steglich-esterification conditions. In this case, the carboxylate is activated to-wards nucleophilic attack from conversion with *N,N'*-dicyclo-hexylcarbodiimid (DCC) and 4-dimethylaminopyridine (DMAP) as a catalyst to an *N*-acylpyridinium ion. This activated compound then is attacked by the alcohol to form the desired ester.[69] Since a secondary amine is adjacent to the carboxylic acid in compounds **5** and **6**, an intramolecular ring clos-ing reaction through attack of the amine on the electrophilic carbonyl carbon constituted a side reaction to expect. However, this being the exclusive reaction that proceeded under the described conditions was surprising, in particular since the respective alcohols were employed as co-solvents.

Based on these findings, the Mitsunobu reaction had been investigated and was, until this point, successfully employed for the synthesis of several esters of **5**.
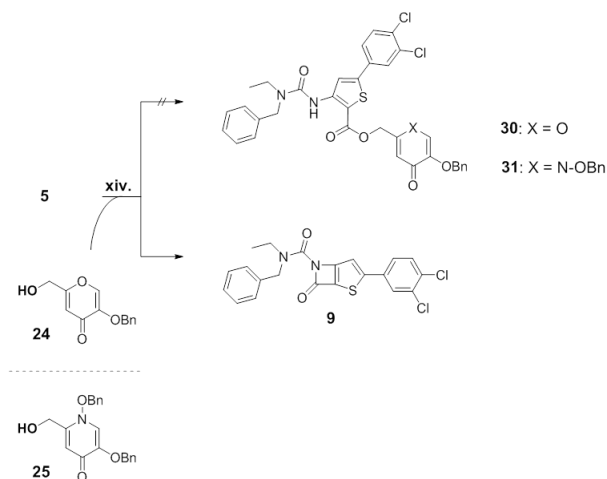
**Scheme 11:** Outcome of the Mitsunobu esterification reactions performed with pyrone **24** and pyridone **25**: **xiv.** 3-4.5 eq. alcohols **24** & **25**, 3-6 eq. DIAD, 3-6 eq. TPP, DMF, 40 °C, 18 h, 90% & 23% of **9**.

In contrast to the Steglich esterification, the ester formation here relies on an attack of the carboxylate at the *O*-adjacent carbon of an alcohol-triphenyl phosphonium ion. Therefore, the adduct formation between alcohol and triphenyl phosphine and the basicity of the carboxylate are the relevant parameters for the product formation to achieve good conversions.[70–72]

Given that the esterification method successfully allowed the synthesis of several esters before, it was concluded that the reactivity of the carboxylate of **5** was sufficiently high. Consequently, the formation of the alcohol triphenyl phosphonium ion of **24** and **25** was deduced to be hampered. Precise reasons could not be identified but a possible explanation might be a misdirected coordination of TPP on the pyrone-/pyridone-carbonyl oxygen.

Against this drawback, the strategy was once more changed to a reaction protocol where the carboxylic acid **5** was esterified under basic conditions (TEA) with halogenated reagents, as had been successfully used for the syntheses of prodrugs **10 – 13**. A transfer of this approach to alcohols **24** and **25** required the conversion of these into more reactive derivatives, e.g. the corresponding mesylates or even alkyl halides. Alcohol **20** was included

in this study to test the feasibility of the approach. For this compound, no complications with regard to unwanted side- or decomposition reactions had been observed before. Hence, the hydroxy function of alcohols **20**, **24** and **25** were converted into better leaving groups next (Scheme 12).
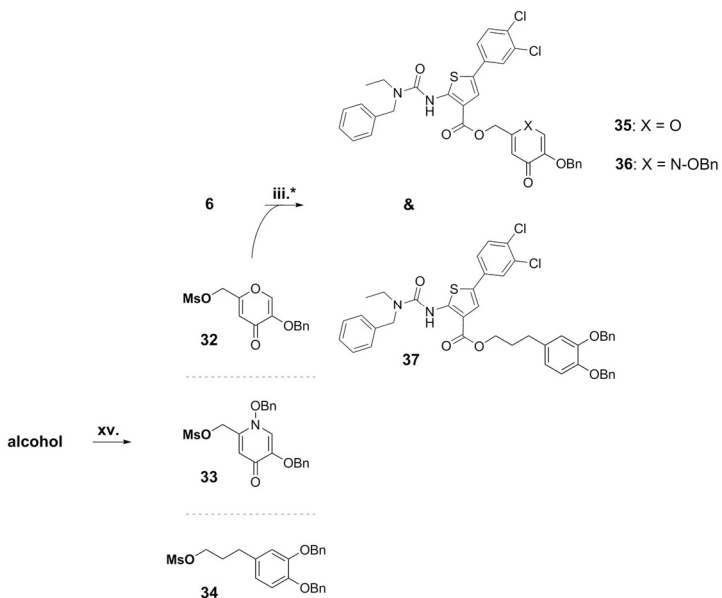


**Scheme 12:** Two step route towards the siderophore-type carboxylic acid esters aligned with the reaction conditions previously used in the synthesis of prodrugs **10 – 13**: **iii.*** 1.8 eq. TEA, 1.9-3.5 eq. OMs reagents **20a**, **24a** & **25a**, DMF, 40 °C, 18 h, **35**: 77%, **36**: –, **37**: 67%; **xv.** 1.3 eq. MsCl, 1.3 eq. TEA, dichloromethane, 0 °C to rt, 2 h , **32**: 80%, **33**: [19%], **34**: 76%.

The reaction with methanesulfonyl chloride (MsCl) in the presence of TEA proceeded smoothly and alcohols **20** and **24** were converted quantitatively, as shown by TLC monitoring. An aqueous work up sufficed for the purification of the respective products **34** and **32** (Scheme 12). In contrast, the same reaction performed with pyridone **25** featured a multitude of side and/or decomposition reactions to unknown species (observed by TLC monitoring). The outcome was surprising, since this type of reaction had been described by BROWN *et al.* as feasible and high-yielding.[58]

In line with the observed poor reaction progress, mesylate **33** was only isolated in a low yield of 19% and could not be isolated in high purity. Attempted column chromatographic purification of **33** failed so that the product mixture obtained after the aqueous work up was used in the following reaction with carboxylic acid **6**.

Carboxylic acid **6** was treated with mesylates **32**, **33** and **34** in the presence of TEA in DMF at 40 °C for 18 h following the successful protocol for starting material **5** (Scheme 12). Upon completed conversion, the solvent was evaporated and the crude product purified by normal phase (NP) column chromatography. The benzyl-protected prodrug precursors **35** and **37** were isolated successfully with good yields of 67% and 77%, respectively. An additional benefit of the protocol was the more convenient purification of the reaction mixtures since the product only had to be separated from traces of excess reagent. In contrast, the purification of crude mixtures from Mitsunobu-esterification reactions was tedious and yield-limiting as the respective reagents revealed a tendency to co-elute with the product.

In case of the reaction of **6** with pyridone mesylate **33**, the observed conversion only was low, despite the fact that a larger excess of reagent had been used (Scheme 12). Upon evaporation of the solvent after 18 h, the attempted isolation of product **36** from the crude mixture by column chromatography failed (no product was isolated). Presumably, **36** decomposed on the slightly acidic silica gel. Another attempt to purify the crude reaction mixture via size-exclusion chromatography on a Sephadex LH 20 stationary phase with dichloromethane as eluent was neither successful. Thus, a synthesis of **36** was discontinued here.
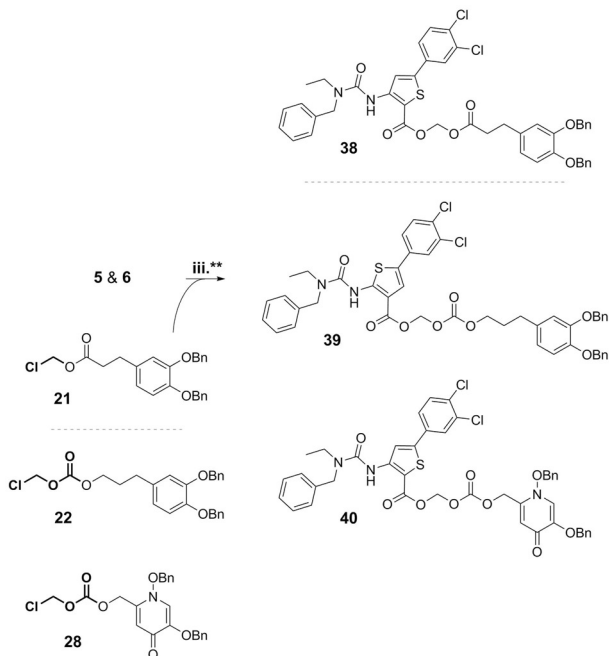
### 5.3.2. Synthesis of benzyl-protected siderophore-type acyloxymethyl and carboxyloxymethyl ester prodrugs

The reaction conditions established for prodrugs **10** – **13** were transferred on the synthesis of the respective siderophore-type prodrug precursors **38** – **40** (Scheme 13). Accordingly, carboxylic acids **5** and **6** were converted with the halide reagents in the presence of TEA in DMF at 40 °C. The addition of TBAI to achieve a Finkelstein-like reaction further was found to be beneficial for product formation. Following this procedure, the catecholate-based

prodrug precursors **38** and **39** were obtained in good to high yields of 84% and 65%, respectively (Scheme 13).

For pyridone motif-containing compound **40**, the yield was significantly lower with only 37%. Probably, the reaction efficiency was decreased since amounts of reagent and base, and in particular catalyst were lowered (Scheme 13) in acknowledgement of the previously observed general sensitivity of pyridone-derived reagents. Additional loss of product while column chromatography constituted a further potential reason since lability towards silica gel had been observed before.



**Scheme 13:** Synthesis of the benzyl-protected siderophore-type prodrug precursor bearing acyloxymethyl- and carboxy-loxymethyl-linkers: **iii.\*\*** 1.3-1.8 eq. TEA, 1.2-1.9 eq. halide reagents **21**, **22** & **28**, 0.1-0.5 eq. TBAI, DMF, 40 °C, 18 h, **38**: 84%, **39**: 65%, **40**: 37%.

In total, five different siderophore-type prodrug precursors (**35**, **37** – **40**) were successfully synthesized. Three (**37** – **39**) contained a catecholate-derived masking unit and included variation in type and length of the linkage to the drugs **5** and **6**, respectively. Two (**35**, **40**) were derived from derivatives of Kojic acid and featured variation in linkage to the drug molecule and in the hetero atom.

In the following, the prodrug precursors were studied with respect to an efficient and selective cleavage of the phenolic *O*-benzyl protection groups to generate the uoprotected prodrugs.

### 5.3.3.    Synthesis of unprotected siderophore-type prodrugs

When setting up the synthesis route towards siderophore-type prodrugs, benzyl ethers were chosen as PGs for the phenolic hydroxy functions as they can be removed under anhydrous, Lewis-acidic conditions. This was a valuable option since the implemented linkers feature an intrinsic lability towards (strong) Brønsted acids and bases as well as nucleophiles, which for example ruled out the use of many other ether PGs (MOM, *t*Bu, Allyl), ester PGs (Ac, Bz) or bis-protecting acetals or ketals.[63]

The option of hydrogenolytic debenzylation using standard conditions ($H_2$ and Pd(C) as a catalyst) was avoided due to possible side-reactions with the aromatic structures of carboxylic acids **5** and **6**. However, a more directed variant in terms of adjusting equivalents uses cyclohexene as a hydrogen source, and was taken into consideration for debenzylation of prodrug precursor **40** in particular.

As Lewis acids, boron trichloride and boron tribromide were studied following a deprotection procedure described by Brown *et al.* for the pyridone-conjugates they prepared.[58] Further, two milder variants making use of trimethylsilyl bromide (TMSBr) and trimethylsilyl iodide (TMSI), respectively, were investigated. In these cases, the phenolic benzyl ethers are replaced transiently by trimethylsilyl groups. These are cleaved successively by the addition of a protic solvent like methanol or water to release the desired product. Lastly, a pivotal aspect of the debenzylation step was the development of a suitable work up and purification protocol that took the lability of the prodrugs into account.

### 5.3.3.1. Development of the reaction protocol for debenzylation

Prior to performing the debenzylation reactions with the prodrug precursors (**35**, **37 – 40**), a model system was used to test and optimize synthesis protocols. The focus was set on the different linkers used to connect pro-moiety and drug since these constituted the most labile part within the prodrugs. Accordingly, respective benzoic acid ester conjugates were synthesized and subsequently treated with the Lewis acids mentioned above (Scheme 14).
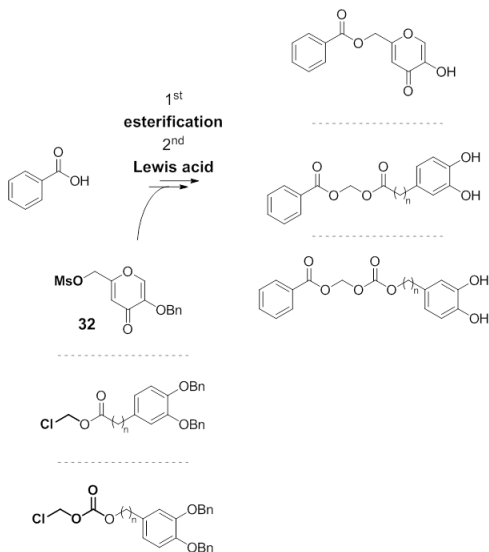


**Scheme 14:** Modell system for the development of a debenzylation protocol using benzoic acid as drug mimic: synthesized were the pyrone ester and the acyloxymethyl- and carboxyloxymethyl-linked catechol ester. These were finally treated with the Lewis-acids $BCl_3$, $BBr_3$, TMSBr or TMSI.

Debenzylation reactions with $BCl_3$ or $BBr_3$ were carried out at -78 °C in anhydrous dichloromethane using two equivalents of the respective reagent. As substrate served the carboxyloxymethyl-linked catechol ester. This conjugate model was expected to be the most sensitive one, and the underlying hypothesis was that conditions tolerated by this compound would be applicable also for the other prodrug types. The reaction was monitored by TLC. In the case of $BCl_3$, TLC indicated the formation of a single product which was assumed to be the deprotected derivative. In contrast, mainly decomposition was observed when $BBr_3$

was used. The reaction was terminated in both cases by addition of sodium hydrogen carbonate solution (aq./sat.) in order to cleave the intermediately formed boron-oxygen complex via hydrolysis and simultaneously neutralize the formally released hydrogen chloride or bromide. Upon extraction of the aqueous solution with dichloromethane and concentration of the organic layer, TLC control of the $BCl_3$-promoted reaction again indicated the formation of one reaction product and largely the absence of starting material or decomposition products.

Parallel to this, the applicability of TMSI and TMSBr as debenzylation agents was investigated. The model acyloxymethyl- and carboxyloxymethyl-linked benzoic acid esters were dissolved in dichloromethane and the resulting solutions cooled to -30 °C. Two to five equivalents of the TMS halide were added and the reaction stirred under further cooling. Since at these low temperatures only very little conversion was observed, the reaction mixtures were allowed to slowly warm up to 0 °C. This process was closely monitored by TLC. In case of TMSI, full conversion of the starting material was observed upon reaching 0 °C. For the bromine reagent, conversion was slower and did not reach completion even at room temperature.

The debenzylation mechanism for the TMS halides relies on a transient replacement of the benzyl ethers by trimethylsilyl ethers with the benzyl halide being formed as a byproduct. Accordingly, the formation of compounds with higher $R_f$ values was observed during reaction by TLC. As no products with lower $R_f$ values compared to the starting material were detected, the formation of decomposition products was excluded.

The reaction was terminated by the addition of sodium hydrogen carbonate solution (aq./sat.), and the biphasic mixture extracted with dichloromethane to obtain the crude product. This was studied further by $^1$H-NMR spectroscopy. The respective signals, in particular those assigned to the linker, supported the conclusion that de-*O*-benzylation with TMSI in the presence of a carbonate or ester was feasible. Summarizing these preliminary studies, $BCl_3$ and TMSI appeared to be suitable debenzylation agents.

Encouraged by these results, the first-mentioned conditions (2 eq. $BCl_3$, $CH_2Cl_2$, -78 °C, 45 min) were transferred on an oxymethyl(ethyl)carbonate-linked catechol ester of **5**. TLC monitoring of the reaction indicated the formation of a new, more polar compound but

also two minor by-products. Upon termination of the reaction by addition of a mixture of methanol/water/NaHCO$_3$ solution (aq./sat.), the extracted and concentrated crude residue was analyzed by NMR spectroscopy. Product-characteristic signals were observed and pointed to its successful formation.

However, in following reactions it was not possible to circumvent or lower the formation of the mentioned by-products. In addition, the debenzylation reaction could be hardly controlled based on the reactive character of the reagent. In a couple of cases this led to substantial decomposition- and byproduct formation.

The protocol making use of TMSI (5 eq., CH$_2$Cl$_2$, -30 °C to rt, 3 h to 5 h) was transferred to the oxymethyl(ethyl)carbonate-linked catechol ester of **5** as well. In a first attempt, the reaction mixture was allowed to warm up to rt upon addition of TMSI at -30 °C. This led to a partial cleavage of the pro-moiety and thus, the formation of **5**. In successive experiments the reaction temperature therefore was raised only up to 0 °C which enabled a smooth and selective cleavage of benzyl ethers while decomposition reactions were attenuated. TLC monitoring of the reaction showed this, and further revealed the cleavage process to proceed stepwise. Mass analysis of the reaction composites separated by TLC was used for further confirmation. Here, the observed m/z values were successfully assigned to the mono-benzylated intermediate as well as the desired product.

Thus, the debenzylation protocol using TMSI met the requirements and restrictions stipulated by the chemical properties of the different variants of catecholate and pyrone prodrugs (**35**, **37 – 39**) best.

Regarding prodrug precursor **40**, it was observed frequently in previous studies, that derivatives and conjugates of the pyridone exhibited a particular sensitivity and/or reactivity under (anhydrous) acidic conditions (see e.g. oxidation & mesylation of **25**). Therefore, the hydrogenolytic cleavage of the phenolic *O*-benzyl PGs with cyclohexene (10 eq.) in ethanol under Pd(C) catalysis was studied for this compound (Scheme 15). The reaction seemingly proceeded only slowly so that catalyst was added twice after 24 h and 48 h. After 72 h of stirring at 40 °C, no more starting material was detected and the reaction terminated by removal of the catalyst. The red-brownish filtrate was concentrated. The crude residue was analyzed by NMR spectroscopy, but unfortunately, no product-specific signals were

observed. Hence, it was concluded that substantial decomposition of prodrug precursor **40** occurred during the reaction.

At this point, the pyridone-motif and respective prodrugs were abandoned due to their incompatible chemical properties, which were found to significantly deviate from reports. The synthesis of a pyridone prodrug was not pursued further.

### 5.3.3.2.         Development of the purification protocol

In the debenzylation reaction models with benzoic acid, the reactions were quenched by the addition of sodium hydrogen carbonate solution (aq./sat.) and the reaction mixtures extracted with dichloromethane. Upon concentration of the organic layer, the crude residue was purified by column chromatography.

This procedure however was not applicable to the siderophore-type prodrugs as the extraction step led to significant loss of product. Consequently, the reaction mixture was concentrated to dryness after quenching. To avoid an increase of pH from concentrating the sodium hydrogen carbonate solution, the reaction quenching method also was altered: instead of sodium hydrogen carbonate solution (aq./sat.) phosphate buffer (1 M, pH 7) was added to hydrolyze the transiently formed silyl ethers. The solvent was removed subsequently and the crude residue subjected to chromatographic purification.

NP column chromatography failed as no product eluted from the respective column. It was assumed, that the phenolic hydroxy functions interacted too strongly with the silica gel so that the prodrug stuck on the stationary phase. Based on this observation, size-exclusion chromatography was investigated using Sephadex LH 20 as a stationary phase and dichloromethane as eluent. In case of the model siderophore-type benzoic acid esters, this purification method was successfully implemented and the respective compound obtained in good purity. However, the purification method was not successful for the siderophore-type prodrugs of **5** and **6**, as again no product eluted from the column. An alternative approach using neutral $Al_2O_3$ was neither successful.

Purification of the siderophore-type prodrugs finally was achieved by automated reversed phase chromatography on a $C_{18}$-modified silica phase with an acetonitrile gradient in

water. The applied conditions (5% – 100% acetonitrile in 20 min, 6 mL/min flow rate, standard 6 g RP C$_{18}$ column) enabled a thorough separation from salts and traces of starting material so that the final products were obtained in high purity (Fig. 09).

Following this procedure, largely complete conversions of the benzyl protected prodrug precursors **37 – 39** to the desired products were reached and the targeted siderophore-type prodrugs **42 – 44** obtained in good yields of 66 – 77% (Scheme 15).

Only in case of the pyrone prodrug precursor **35**, the reaction proceeded significantly slower. The reaction mix was allowed to warm up to rt to increase conversion. Once decomposition products were observed via TLC-monitoring, the reaction was quenched and the pyrone siderophore-type prodrug **41** isolated and purified as described for compounds **42 – 44**. Prodrug **41** was obtained in a yield of only 39% due to the incomplete debenzylation and partial decomposition of **35** (Scheme 15).

In total, four different siderophore-type prodrugs (**41 – 44**) of drugs **5** and **6** were successfully synthesized and obtained in high purity via a final reversed phase chromatography step (Scheme 15 & Fig. 09). These include three catecholate-masked compounds (**42 – 44**) that comprise different linkages to the respective drugs **5** and **6**. The fourth compound (**41**) is conjugated with a pyrone moiety via an ester bond.

Having these different prodrugs in hands, the evaluation of their iron(III)-coordination capacity and determination of their antibacterial activity succeeded.
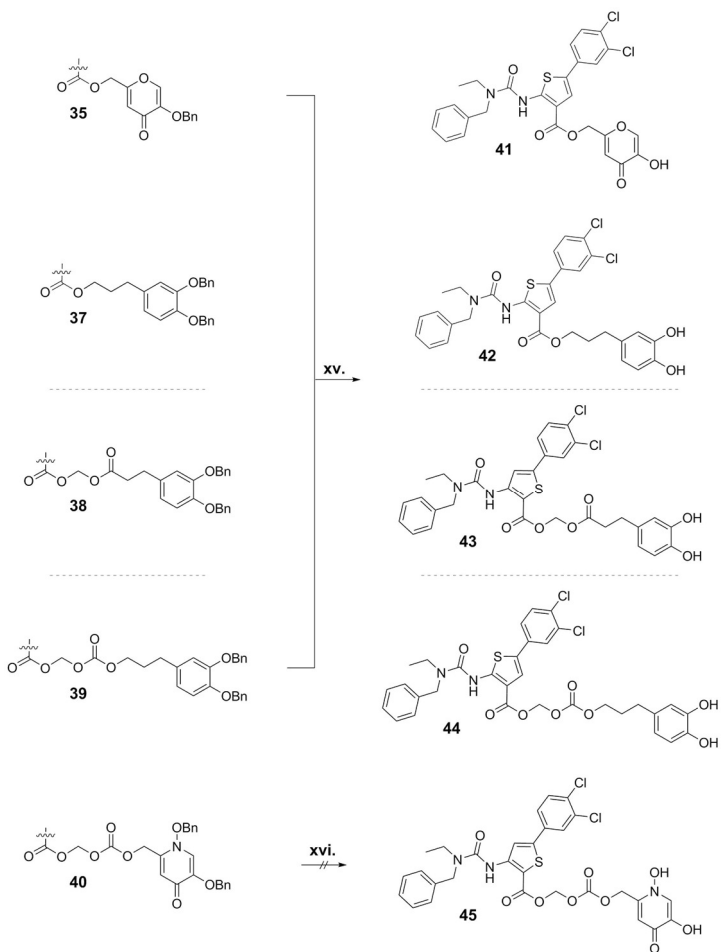
**Scheme 15:** Overview of the successfully synthesized siderophore-type prodrugs: **xv.** first: 5 eq. TMSI, dichloromethane, -30 °C to 0 C, 3 h to 18 h, second: 1 M phosphate buffer (pH 7), third: RP chromatography (water/MeCN 5%-100%, 20min, 6 mL/min, standard 6 g RP C$_{18}$ column ) **41**: 39%, **42**: 73%, **43**: 77%, **44**: 66%. Conditions for the attempted hydrogenolytic cleavage of benzyl ethers: **xvi.** 10 eq. cyclohexene, Pd(C), rt to 40 °C, 72 h.
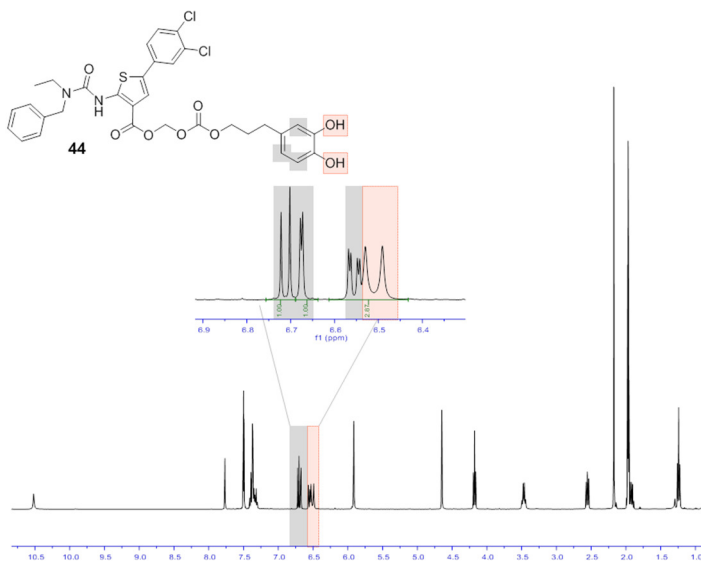
**Figure 09:** $^1$H-NMR spectrum (MeCN-d$_3$, 600 MHz. 25 °C, shifts δ in [ppm]) of siderophore-type prodrug **44**. Highlighted in red are the signals of the phenolic OH-protons. Highlighted in grey are the signals of the aromatic protons of the catechol-mask. Characteristic proton-shifts of the drug are the N*H* signal at 10.5 ppm and the aromatic signals between 7.0 – 8.0 ppm which belong to the *N*-benzyl group, the 5-dichloro aryl motif and the thiophene core. At ca. 5.9 ppm, the protons of the oxymethylene group resonate and at 4.6 ppm, the two *N*-benzylic protons. Following in the direction of higher field, the signals for protons of the linker side chain and *N*-ethylene group are found.

## 5.4. Evaluation of siderophore-type prodrugs

The synthesized prodrugs were designed to act as iron(III)-coordinating compounds that, in the Fe$^{III}$-loaded state, address bacterial siderophore receptors which subsequently promote their transport into bacteria. Once inside, the pro-moiety was envisaged to be cleaved by carboxylesterases. The implementation of linking structures was reported and in earlier studies found to facilitate the enzymatic hydrolysis (see chapter 4). On the other hand, the prodrugs waiving a linker were expected to exhibit a higher activation barrier and thus a higher hydrolytic stability which is advantageous for example for prodrug stability in medium.[45,46] Accordingly, these different aspects were evaluated.

### 5.4.1.    Study of the iron(III) coordination capacity

The Chrome azurol S (CAS) assay reported by SCHWYN and NEILANDS was applied to study the iron(III)-coordinating properties of prodrugs **41 – 44**.[73] This assay is based on a competitive exchange of the $Fe^{III}$-coordinating ligands. Initially, $Fe^{III}$ and CAS form a deep blue complex. If a potent siderophore is added to the solution, it dispels the CAS-ligand which is accompanied by a color change from blue to red/orange. This can be followed by UV/Vis spectroscopy. The observed decrease in absorbance at 630 nm is analyzed, particularly in relation to the negative (no compound) control (Fig. 10).

An advantage of the assay is that it directly indicates the coordinating efficiency of a given compound. Also, the identification of siderophores is not restricted to a certain molecular structure, as is it the case for assays that use reporter systems tailored for a certain functionality like catecholates or hydroxamates.[73]
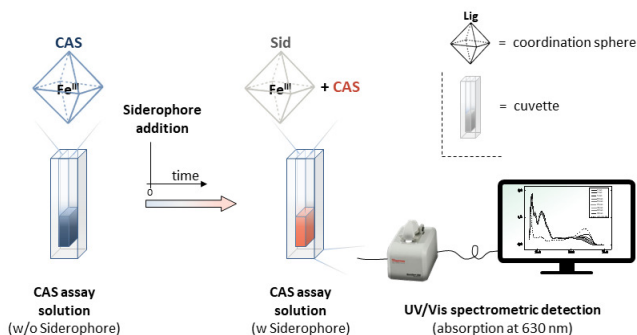


**Figure 10:** Setup of the CAS assay. The blank solution has a deep blue color and shows an absorption maximum at 630 nm in the UV/Vis spectrum. The assay is started with the addition of the potential siderophore (Sid) at t0. Displacement of the CAS ligand by the siderophore can be followed as a decrease in absorbance and a change of color from blue to orange/red (= free CAS).

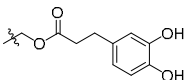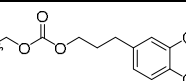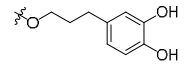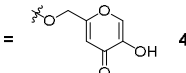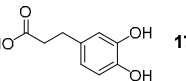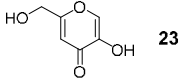The assay was performed for all siderophore-type prodrugs (**41 – 44**).

For this purpose, 150 µM stock solutions (in DMSO/water) were prepared and subsequently mixed with the CAS solution. The aliquots of CAS and prodrug were adjusted in a way that the substrates competed in a 1:1 ratio (each 135 µM final concentration) for $Fe^{III}$

(13.5 µM final concentration). Starting directly after mixing, the absorption intensity at 630 nm was measured repeatedly until equilibrium between substrate and CAS ligand was reached (indicated by a constant value).

In case of a potent siderophore, the absorption at 630 nm would decrease rapidly until a distinct minimal absorption. This would correspond to an efficient replacement of the CAS ligand (Fig. 10). A stable siderophore-$Fe^{III}$ complex would be indicated by a steady minimal absorption whereas instable complexes were aligned by ongoing competition for coordination sites which would correspond to values oscillating around an average minimum.

**Table 02:** Overview of the results from the CAS assay based $Fe^{III}$ affinity determination.

| Prodrug of **5** | $\Delta abs_{630}$ in [mAU] |
|---|---|
| R =  **43** | -0.63 |
| Prodrugs of **6** | |
| R =  **44** | -0.54 |
| R =  **42** | -0.51 |
| R =  **41** | -0.34 |
| Reference compounds: | |
|  **17** | -0.67 |
|  **23** | -0,06 |
| Vanchrobactin[56] | -0.63 |

The obtained minimal absorption values were compared to the negative control (w/o sample) and the difference between these values, $\Delta abs_{630}$, calculated to estimate the efficacy of $Fe^{III}$-coordination. For this purpose, the catecholate **17**, the pyrone **23** and the natural monocatecholate siderophore Vanchrobactin constituted further reference and positive controls, respectively (Table 2).[56,74]

Prodrug **43** was found to coordinate $Fe^{III}$ most efficiently (Table 02). Within minutes, a significant decrease in absorbance at 630 nm was detected and within approximately one hour, a constant low-intensity absorption was reached. The difference in absorbance compared to the negative control, $\Delta abs_{630}$, was -0.63 mAU for siderophore-type prodrug **43**. From these results, it was concluded that prodrug **43** showed not only a high affinity for $Fe^{III}$ but also formed a stable complex with the metal ion, and that this complex governed the equilibrium in the competitive CAS assay (Figure 11).

Compound **44** as well accomplished a fast displacement of the CAS ligand and achieved equilibrium within a similar time-range as prodrug **43**. In contrast to the acyloxymethyl linked ester **43**, carboxyloxymethyl linked compound **44** was slightly less efficient with regard to $Fe^{III}$-coordination, as demonstrated by the higher $\Delta abs_{630}$ value of -0.54 mAU (Table 2). This concluded, prodrug **44** showed a comparable affinity to $Fe^{III}$ (fast ligand displacement). Yet, the complex formed was minimal less stable than in case of **43**. However, it governed the equilibrium over CAS as indicated by the $\Delta abs_{630}$ value and the observed steady state of complexation at low absorption intensity.

In the case of prodrug **42**, the ligand exchange took significantly longer which indicated a lower affinity for $Fe^{III}$ in comparison to **43** and **44**. Nevertheless, the $\Delta abs_{630}$ value was still within the range of the two related compounds (-0.51 mAU) indicating the formation of a stable complex with the equilibrium on the prodrug site (Table 2).
The $\Delta abs_{630}$ values for prodrugs **42 – 44** were compared to the mask precursor **17**. For this compound, a $\Delta abs_{630}$ value of -0.67 mAU was determined by the CAS assay. The value approximated the results obtained for prodrugs **42 – 44**, which thus allowed the conclusion that the masking unit principally governed to the coordination of $Fe^{III}$.
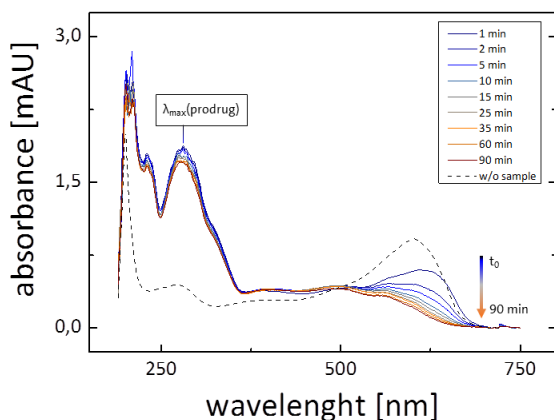
**Figure 11:** UV-Vis spectra of the CAS assay performed with siderophore-type prodrug **43**. Measurements were carried out with increasing periods of time after addition of the prodrug to the CAS solution and the Δ[abs(630 nm)] calculated against the negative control (dashed trace).

For the parent compounds, $Fe^{III}$-coordination could not be determined since these repeatedly precipitated from the CAS solution, even when lowering concentrations. This however allowed the conclusion that the parent compounds did not act as $Fe^{III}$-coordinating agents, which regardless was expected based on their molecular structure.

The iron(III)-coordination efficiency further was compared to the natural monocatecholate siderophore Vanchrobactin.[56,74] In particular compound **43** was found to possess a comparably high $Fe^{III}$-affinity. Nonetheless, the catecholate-type prodrugs **42** and **44** displayed a competitive $Fe^{III}$-affinity as well (Table 2).
These results substantiated, that the approach chosen indeed could compete with natural siderophores to exploit bacterial iron-uptake system.

In contrast to the catecholate-masked prodrugs **42 – 44**, the pyrone-based prodrug **41** proved unsatisfactory regarding the displacement of the CAS ligand which was expressed by a comparably low $\Delta abs_{630}$ value of -0.34 mAU (Table 2). Further, the rather long time span afforded to reach this value, indicated a relatively low affinity for $Fe^{III}$. An interesting observation in this case was that pyrone **23,** which here constituted the reference compound to evaluate the influence of the masking unit on $Fe^{III}$-coordination, showed even less affinity for $Fe^{III}$ than prodrug **41**. The compound achieved almost no

displacement of the CAS ligand which is expressed by the low $\Delta abs_{630}$ value of -0.06 mAU (Table 2). Therefore, a certain contribution of the drug-part of compound **41** to $Fe^{III}$-coordination was assumed in this case.

These aspects ruled out prodrug **41** as a potential siderophore prodrug.

Regardless, the encouraging results obtained for the catecholate-based siderophore-type prodrugs **42 – 44**, motivated the further investigation of their antibacterial activity and, in this context, their activation by bacterial esterases.

### 5.4.2. Investigation of the activation by bacterial esterases and the antibacterial activity of siderophore-type prodrugs 41 – 44

The first set of prodrugs (**6 – 14**) had been evaluated regarding chemical stability under physiological conditions and activation by esterases, as described in chapter 4 in more detail. It was found that, in general, the enzymatic cleavage of all masks proceeded relatively fast (approx. mean 3 h) and importantly, faster than the chemical decomposition (approx. mean 70 h). This fulfilled an important criterion for the prodrug concept. The chemical stabilities of the different prodrug classes (alkyl-, acyloxymethyl- and carboxyloxymethyl-ester) were presumed to be similarly high for the corresponding siderophore-type prodrugs (**41 – 44**).

In cooperation with the group of R. HARTMANN, incubation experiments in *E. coli* cell homogenate were performed with the prodrugs **41 – 44** to investigate their enzymatic activation. The general esterase activity in the crude bacterial protein mixture was evaluated by an exemplary hydrolysis study where α-naphthyl acetate was converted to α-naphthol (measured via fluorescence detection at 330 nm and 471 nm). This model reaction usually was completed within 20 – 30 minutes (incubation at 37 °C, concentrations of α-naphthyl acetate between 0.2 – 20 µM).

Solutions of the siderophore-type prodrugs **41 – 44** (20 µM in DMSO) were incubated with *E. coli* homogenate at 37 °C (0 min to maximum 5 h, each time-point constituted a single, individual experiment). The enzymatic reactions were stopped through the addition of acetonitrile. Ethyl acetate was added to extract remaining prodrug and formed drug, respectively.

In order to quantify the amount of released drug, an HPLC-MS/MS based set up was employed and a structurally to **5/6** related compound used as internal standard. Further, calibration curves were calculated for quantification of released parent compounds with the lowest calibrator at 200 nm.

Surprisingly, free drug contents did not exceed 5% relative to the applied prodrug for all incubation periods. These results were unexpected, since the cleavage of the structurally related prodrugs **5 – 10** proceeded readily in the PLE mediated hydrolysis (previous studies). It could be assumed that the siderophore-type prodrugs were less suitable substrates, in particular for bacterial esterases. However, since cell homogenates in general are complex mixtures of proteins and enzymes, lipids and nucleotides, co-precipitation during sample work-up and thus low substrate recovery might have impaired the analysis. Besides, alternative protein binding of the released drug or the siderophore-type prodrugs (both proved quite lipophilic) could have impacted the anticipated enzymatic reaction and recovery, which further would have led to the described observation of seemingly low activation efficiency.

In parallel, the antibacterial activities of the siderophore-type compounds **41 – 44** and the first set of prodrugs were determined against a variety of Gram-positive and negative bacterial strains, namely *B. subtilis*, *S. aureus* (Gram-positive) and *E. coli* K12, the outer membrane mutant *E. coli* D22, the efflux deficient mutant *E. coli* TolC and *P. aeruginosa* O1 (Gram-negative strains). Except for the choline (-analog) esters **8** and **14**, no significant growth inhibition was determined (MIC > 50 µM).

Interestingly, compounds **8** and **14** showed a concentration dependent growth inhibition of *E. coli* K12 (with 22 % and 36 % growth inhibition at 50 µM for **8** and **14**, respectively, compared to no compound control), while the parent drug **5** was inactive. These observations indicated that a cationic charge, as hypothesized, was indeed a beneficial feature for these compounds to enhance e.g. the porin-mediated influx into Gram-negative bacteria.

A MIC determination assay setup adapted from Ji *et al.* using iron-depleted as well as iron-enriched media was employed to investigate the influence of $Fe^{III}$-concentration on the activity of siderophore-type prodrugs **42 – 44** by challenging specifically their active

transport into bacterial cells.[57] However and surprisingly, these variations led to no significant differences in activity.

The results pointed to a lack of diffusion across the outer and/or cytoplasmic membrane and/or drug efflux, regarding in particular the first set of prodrugs which mainly featured charge-neutralized esters.

In case of the siderophore-type prodrugs, an inefficient activation inside the bacterial cell is presumed to limit activity. Another aspect to be considered could be the insufficient recognition by siderophore transporters presented by the selected bacteria. In this context, it is known, that bacteria express siderophore transporters differently and that these further exhibit e.g. specific preferences for certain functionalities.[52,53,75,76] In contrast, general siderophore transporters show a broader substrate tolerance. However, these were found to be included in enzyme complexes containing efflux pumps. This supposedly ensures an efficient recycling of siderophores since the Fe$^{III}$-loaded siderophore is transported only into the periplasmic space. There, the metal ion is released and the siderophore directly excreted into the extracellular surrounding again.[50,53,61,77–79] Such a process would hamper any antibacterial effect for respective prodrugs as well.

Summarizing the evaluation of the siderophore-type prodrugs in particular and the antibacterial activity determination for all prodrugs, the respective compounds basically featured promising characteristics.

Hydrolysis studies at physiological pH in PBS confirmed good chemical stabilities for the charge-neutralized dipartite and tripartite prodrugs **10 – 13**. Enzymatic hydrolyses with PLE showed an efficient activation of the prodrugs aligned by the exclusive release of parent compound **5** in all cases. Especially the linker connected prodrugs **10 – 13** were activated rapidly (expressed by their short half-lives), as was hypothesized.

The Fe$^{III}$-coordination properties of the siderophore-type prodrugs **41 – 44** were evaluated with the competitive CAS assay. Here, all three catecholate-masked compounds achieved good to high efficiency in coordinating Fe$^{III}$ which was indicated by $\Delta abs_{630}$ values ranging from -0.51 mAU to -0.63 mAU. These values were in a similar range as those of the reference compounds Vanchrobactin and carboxylic acid **17**.

However, only two prodrugs (**8** & **14**) showed growth-inhibitory effects when studied in whole-cell assays.

The low polarity of the charge-neutralized prodrugs might have impeded activity of compounds **10 – 13** in bacterial cell growth inhibition assays. A balanced and low polarity as found in these compounds likely deferred the passage through general diffusion porins similar to the case observed for negatively charged compounds.[43]

With respect to the siderophore-type prodrugs **42 – 44**, the lack of antibacterial activity in conjunction with the results from the activation studies in *E. coli* cell lysate suggested that an inefficient pro-moiety-cleavage by bacterial esterases was a detrimental factor. However, receptor recognition and/or drug efflux issues also could be contributing factors.

The exploitation of siderophore uptake mechanisms in prodrug strategies in general is promising since the approach addresses bacterial cells only.[61] Yet, it is as well sophisticated. In this study, an efficient coordination of Fe[III] by the catecholate-masked prodrugs did not suffice since the prodrugs then lacked successive aspects, ranging from receptor recognition over directed transport to successful drug-release. Therefore, further investigation of e.g. molecular mechanisms of siderophore recognition and uptake in the context of artificial siderophores in particular would contribute to a better understanding of such prodrugs. Here, the substrate tolerance of siderophore receptors would constitute a central element as well as the direction of transport (periplasmic space vs cytosol).

The choline ester prodrugs **8** and **14** in contrast were able to restore the antibacterial effects of drug **5** against the Gram-negative strain *E. coli* K12 in bacterial cell growth inhibition assays. The observation suggested the cationic charge of the pro-moiety to be beneficial for drug influx into Gram-negative bacteria in this case. This result may be an interesting aspect for investigations of novel prodrug concepts for drug candidates of a similar type.

**Part II:**

**Bio-reversibly masked purinergic 2$^{nd}$ Messenger derivatives associated with Ca$^{2+}$ Signaling**

## 6.   Introduction and Background

Cells live in community, independent of their occurrence as single-celled organisms or within a multicellular structure. The association of cells to groups usually goes along with a certain functional differentiation to specialized subsystems. This comportment enables multicellular organisms to better use livelihood opportunities and adapt to environmental factors. Yet, a division of tasks between different subsystems requires a balanced and guided cooperation. In this context, the ability to receive and process information from the environment is a substantial factor for survival, development and prosperity of a cell in its community. Consequently, cell communication constitutes a prerequisite for all living organisms.[80–82]

Communication, in a more sociologic context, is defined as a tool for the exchange of information between two parties, the sender and the receiver, which concomitantly possesses an aspect of mutual monitoring and control.[83] This implicates, that the medium carrying the information, e.g. a verbal message, features more than one dimension and not only a neutral, informative element. Consequently, a message commonly includes more issues, like an appeal to the receiver, an indication on the relationship between sender and receiver, and/or a certain self-revelation of the sender.[83]

These seemingly sociologic aspects can be transferred surprisingly sound on cells engaged in a multicellular organization or organism. In inflammatory processes for example, a damaged or stressed cell sends distinctive signals that convey not only the neutral information about its poor condition, but also comprise an appeal to cells of the immune system. Accordingly, these receive and process this appeal to then become activated and drawn towards the signaling cell for clearance from the organism. Between this, extracellularly receiving a message and intracellularly forwarding and processing a message, it inevitably requires a linking element. This central feature of effective cell-communication is implemented by the very broad and diverse group of cellular receptors.[80–82]

The exemplary stated inflammatory process as a response to a harmful stimulus is accompanied by a multitude of biochemical reactions in general. In this context, cell-communication plays a fundamental role as it is the tool to mediate and regulate the protective actions

of the immune system against the stimulus. In other cases, the communication between endogenous cells and immune system becomes misled which results in disordered and often auto-destructive reactions of the immune system against the own organism. This phenomenon is called autoimmune disorder and expressed by a vast number of pathologies.[80,81,84,85]

A detailed understanding of the immune system, its activation and its interaction with the organism is essential, i.e. for ultimately interfering with such pathological auto-destructive activation patterns. For both aspects, the intercellular communicative processes as well as the intracellular signaling cascades are relevant and go hand in hand. Substantial progress to broaden our understanding of the immune system and its components was achieved, but many further aspects, particularly in the context of pathology, remain elusive still. The transmission and amplification of an extracellular signal by intracellular signaling cascades constitutes such an aspect. In the context of inflammation and immune regulation, two signaling systems and their link to the extracellular reception of cell-communicative signals, are particularly important but not fully understood to date: adenine nucleotide signaling and calcium ($Ca^{2+}$) signaling.[85–88]

The following section thus outlines first general aspects of cell-communication to then combine these with selected examples that illustrate the central role of purine nucleotides in the context of inflammation and their relation to calcium signaling.

WAYS TO SEND A MESSAGE

Cells communicate over short as well as long distances, and often are confronted with a multitude of signals to receive, integrate and/or send simultaneously. These processes however proceed according to a general principle. The signaling cell produces and excretes a certain signal to transmit a precise piece of information. This is received and processed by those cells that present a signal-specific receptor. In the majority of cases, the respective signal is conveyed in the form of molecular structures, e.g. smaller compounds like nucleoside/-tides, amino acids, small peptides and lipids, or more complex molecules like proteins.[80,81]

Despite the general pattern, cells organized in highly developed organisms evolved differ-ent pathways of signal-transmission that vary e.g. in purpose, duration and/or distance to cover. In the case of *endocrine signaling* for example, hormones are released into the bloodstream from respective glands and distributed over the whole body over time (Fig. 12). This process enables the long distance-transmittance of a certain signal. In con-trast to this, *paracrine signaling* is restricted to the closer environment of a cell (Fig. 12). This signaling mechanism becomes particularly effective in inflammation and wound heal-ing processes. Conjugated with *autocrine signaling*, an additional, self-stimulating effect on the signaling cell is observed (Fig. 12).[80,81] These three forms of cell-communication are unified by the aspect that the respective signal is chemical in nature at all stages, and is produced intracellularly and directly prior to release into the extracellular space.[81]
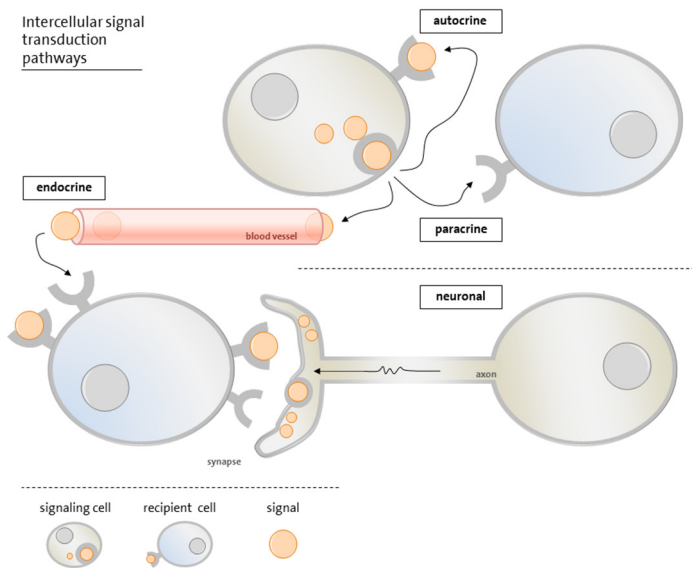


**Figure 12**: Schematic illustration of intercellular cell-communication pathways found in higher-developed organisms like mammals. Paracrine signaling affects cells in the close proximity of the signaling cell. In autocrine signaling, the signaling cell or cells of the same type are addressed. Endocrine signaling in contrast is effective over long distances. Special in this context is the neuronal signal transduction which relies on entirely different mechanisms, proceeds in a targeted manner and is generally faster than the before mentioned processes. Adapted from [80,81].

*Neuronal signal transduction* in contrast is characterized by the transformation of an intra-cellular electric signal into an extracellular chemical signal (Fig. 12). This is implemented by

the release of neurotransmitters from storages, and their successive diffusion from the neuronal membrane to the target cell receptors. This process is reversible and localized within the synaptic cleft that is formed between the synapse of a neuron and a subordinated cell. Hence, spatial and temporal restriction as well as precise targeting constitute further aspects that differentiate neuronal signal transduction form the mechanisms described before.[80]

Lastly, the contact-dependent signal transduction via *gap junctions* constitutes a fourth variant of cell-communication for neighboring cells. The process allows both a direct chemical communication through the transmission of secondary messengers and a direct electric communication between cells. Also, an exchange of small molecules proceeds via gap junctions which are formed out of the transmembrane protein connexin.[80,81]

THE RECEIVER

Cell-cell communication and signaling processes using chemical signals always imply the recognition of these by a certain receptor. In all cases, the receptor is a protein and often the proteins are glycosylated. A majority of the receptor proteins is localized at the cell membrane with the recognition site facing the extracellular space since a range of exocrine signaling molecules cannot enter cells passively. Once a signaling molecule coordinates to its receptor and forms a ligand-receptor complex, an activation of a signaling cascade is promoted. Following this signaling cascade, the received signal is implemented by the cell and respective actions and reactions are initiated.

*Nuclear receptors* constitute an exception from this general procedure. They are located in the cytoplasm since the respective substrates, commonly hormones, are able to traverse across the cell membrane (Fig. 13). The active, ligand-bound form binds to the promotor region of a target gene, influences thereby the transcription, and thus acts as a transcription factor.[81,89]
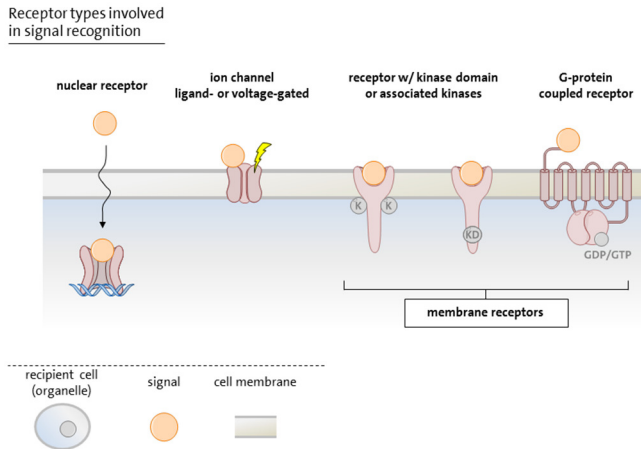
Receptor types involved
in signal recognition

**Figure 13:** Schematic overview of the receptor-types in cell-communication processes. Adapted from [81].

*Ion channels* constitute a fundamental part of signaling processes in basically all cells (Fig. 13). The proteins are localized in the cell membrane, but are found also on intracellular organelles where they participate in intracellular signaling. This concludes to the ability to be gated by extracellular ligands like neurotransmitters, as well as intracellular ligands like purinergic second messengers or $Ca^{2+}$. Ion channels are separated into two classes based on their mode of excitation: *voltage-gated* and *ligand-gated*. (Fig. 13) In neurons, for example, voltage-gated ion channels are responsible for the mediation of action potentials to trigger the release of neurotransmitters via exocytosis. These neurotransmitters constitute first messenger-substrates and successively activate the respective ligand-gated ion channels by binding to an extracellular recognition site. Upon this, channels open, and cations or anions are conducted at high rates of approximately $10^7$ ions per second.[90]

Ligand-gated ion channels commonly are composed of a homo- or hetero-oligomeric association of subunits that surround a central ion pore. Examples for first messenger activated ligand-gated ion channels are the Cys-loop receptor superfamily, the glutamate receptor family and the P2X receptor family.[89–91]

The former receptor families are gated by the 'classic' neurotransmitters acetylcholine (Ach), γ-aminobutyric acid (GABA), serotonin (5-HT), glycine (G) and glutamate (E).

In contrast, the P2X receptor family takes part in purinergic signaling, a form of extra- and intracellular signaling mediated by purine nucleotides. P2X channels are activated by adenosine triphosphate (ATP) which is not only the universal intracellular energy currency, but also an important signaling molecule and neurotransmitter.[86,89,90]

Ionotropic P2X receptors mainly gate $Na^+$, $K^+$ and $Ca^{2+}$. They are expressed on e.g. nerve terminals, glia cells, muscle cells (heart, skeletal muscle and smooth muscle tissue) and cells of the immune system like leukocytes. With respect to this variety, it stringently is observed that P2X signaling correlates with different physiologic and pathologic processes.[84] Controlled co-release of ATP with glutamate for example was found to contribute to long-term potentiation (LTP) of CA1 neurons, a process associated with learning and memory, since according P2X signaling served as a low-frequency filter that prevented weak stimuli from interfering with LTP.[90,92] Under pathologic conditions, e.g. in inflammatory or apoptotic cells, a connexin- or pannexin-mediated release of intracellular ATP constitutes a danger- and 'find-me'-signal. It promotes pro-inflammatory processes and recruits cells of the immune system for clearance of the respective cell. This corresponds to the exemplary observation that ATP-based activation of $P2X_7$ receptors is specifically involved in apoptosis via formation of large conductance pores and induction of pro-inflammatory cytokine release like interleukin 1β (IL-1β).[85,86,93] Studies with P2 receptor-knockout mice assisted the hypothesis that under physiologic conditions ATP induced P2X signaling is reduced to subtype-specific signaling. The respective mice were typically viable but developed unexpected phenotypes indicating uncompensated functional roles of certain P2XRs. Under pathologic conditions however, mutations in the P2X receptor have been linked to e.g. elevated susceptibility to tuberculosis and chronic lymphocytic leukemia, which underlined the implication in important regulatory mechanisms in inflammation and disease.[85,86,90]

Another class of ligand-gated ion channel related to immunologic regulation in physiologic and pathologic condition is the transient receptor protein (TRP) cation channel. This protein superfamily consists of six subtypes in mammals which in general are characterized by a tetrameric composition of six putative transmembrane domains that form non-selective, $Ca^{2+}$ permeable cation channels.[89] The activation of TRP channels proceeds, in contrast to

the transmitter-dependent P2X receptor, downstream of other receptors and is linked for many members of the protein family to a depletion of intracellular $Ca^{2+}$ storages. This indicates that TRP channels commonly are activated through intracellular signals, so called second messengers.[89,94,95]

A member of the subfamily TRPM, the TRPM2 channel, recently gained attention in the context of immune modulation. TRPM2 is regulated, similar to the P2X receptor family, by distinctive purine nucleotides, namely adenosine diphosphoribose (ADPR) and 2'-deoxy-adenosine diphosphoribose (dADPR, Fig. 14). In contrast to the ATP/P2X system, these two nucleotides constitute intracellular signals/second messengers that are formed upon activation of certain hydrolases from distinctive precursors. Besides this, the channel is modulated by intracellular $Ca^{2+}$, temperature and pH.[89,90,94,95]

TRPM2 was found to be expressed exclusively in certain areas of the brain as well as on cells of the immune system, with highest expression levels on differentiating effector T ($T_{eff}$) cells, dendritic and phagocytic cells. In these cell types, signaling through free cytosolic $Ca^{2+}$ intervenes in processes ranging from cell activation, proliferation and differentiation to the release of pro-inflammatory cytokines and apoptosis.[95] The ability of TRPM2 to gate $Ca^{2+}$ influx and efflux in combination with the condensed expression on immune cells substantiates the hypothesis that the ion channel is an essential component in protective and pathological inflammation. On this basis, studies with TRPM2-knock out models (dendritic cells, mice) were performed and acute as well as chronic inflammation conditions were induced. The respective results pointed to an implication of the receptor in chronic inflammation in particular.[94,95]

Two examples for intracellular ionotropic channels of interest in the context of $Ca^{2+}$-related immune regulation are ryanodine receptors (RYR) and two-pore channels (TPC) (Fig. 14). Both receptor families are involved in the release of $Ca^{2+}$ from intracellular storages into the cytoplasm and thus located on distinctive $Ca^{2+}$ storing organelles: the endoplasmic reticulum (ER) and acidic organelles like endosomes or lysosomes (Fig. 14). Activation of RYR and TPC is the result of a second messenger-based forwarding of a preceding signal and associated with early stages of $Ca^{2+}$ signaling. As mentioned in the section above, intracellular $Ca^{2+}$ constitutes a fundamental signal in the activation of immune cells of the adaptive immune system, and related ion channels are thus of particular interest for a better

understanding of immunologic processes. For both receptor types, studies on the respective activation mechanisms indicate again the involvement of a purine nucleotide, the second messenger nicotinic acid adenine dinucleotide phosphate (NAADP).[89,96,97]

Many aspects of the biochemical pathways on which NAADP is generated and the regulatory processes in which it is subsequently involved remain elusive. However, there is substantial evidence that links the $Ca^{2+}$ mobilizing properties of NAADP to the activation of, for example, T cells in inflammation.[98–105]

A further remarkably diverse and large class of membrane receptors is the *G protein coupled receptor* (GPCR) family (Fig. 13). Analysis of the human genome sequence predicted approximately 800 different genes to encode for GPCRs. The common motif they share is composed of a seven α-helical transmembrane region while high heterogeneity is found in the extracellular N-terminals. Here, a variety of functional domains is incorporated which corresponds to the multitude of signals GPCRs respond to, ranging from hormones over cytokines, neurotransmitters and odorants to ions and even photons (Fig. 13).[89,106] Signal transduction is performed by the associated heterotrimeric G-protein. In the inactive GDP bound state, the subunits Gα and Gβγ form a trimer. Coordination of a ligand to the receptor domain of GPCRs induces an allosteric activation of the inactive trimer which is promoted by the dissociation of GDP and association of GTP at the nucleotide binding site. Consequently, Gα undergoes a change in conformation that triggers the successive dissociation of Gα and Gβγ. Both subunits were shown to act regulatory on downstream effector proteins with prominent examples being adenylyl cyclases (Fig. 14), phospholipase C and voltage-dependent $Ca^{2+}$ channels.[106,107]

The GPCR types P2Y and P1, which are activated by ATP (as well as ADP, UTP & UDP) and adenosine (A), respectively, complement the group of membrane receptors involved in purinergic signaling (Fig. 14). P2Y receptors, similarly to the ATP-dependent ion channel receptor P2X, are related to pro-inflammatory processes whereas the A-activated P1 receptor family is linked to anti-inflammatory actions. These apparently opposing effects constitute a tool to fine-tune immune response in inflammation and are balanced by ecto-enzymes of the *cluster of differentiation* family (CD), namely CD39 and CD73 (Fig. 14).

The accentuated role of P2Y receptors in inflammation was underlined by studies on knock out mice carrying deletions for individual P2YRs. These mice showed only slightly altered phenotypes and were generally viable when left unchallenged.[85,108]

In inflammation however, balanced P2Y and P1 signaling constitutes a central aspect of neutrophil chemotaxis. Neutrophils, as part of the innate immune system and first responders to acute inflammation, are activated through specific *N*-formylated oligopeptides released under pathologic conditions by bacteria or damaged cells. Successively, they migrate to the site of inflammation within minutes. The movement is based on chemotaxis which itself is regulated through autocrine purinergic signaling systems. Upon activation, neutrophils rapidly release ATP through pannexin 1 hemichannels which in turn activates $P2Y_2$ receptors on the neutrophil-surface. The P2Y activation amplifies the pathogenic signal and creates a chemotactic gradient field which the granulocyte senses. Consequently, the cell polarizes and translocates components of the purinergic signaling system to the leading edge of the cell, where additional ATP is released. Translocated CD39 receptors degrade ATP to adenosine which promotes an autocrine activation of the P1-type receptor A3. The feedback signal additionally drives the movement of the neutrophil towards the source of the chemotactic field and accordingly source of inflammation.[84,85]

The main downstream events that P1 and P2Y signaling regulate are associated with $Ca^{2+}$ signaling processes in general. However, the various receptor-subtypes of each family couple with different G proteins. Receptors of the same superfamily thus can exert contrary effects on subsequent second messenger (im-)mobilization, and consequently $Ca^{2+}$ homeostasis.
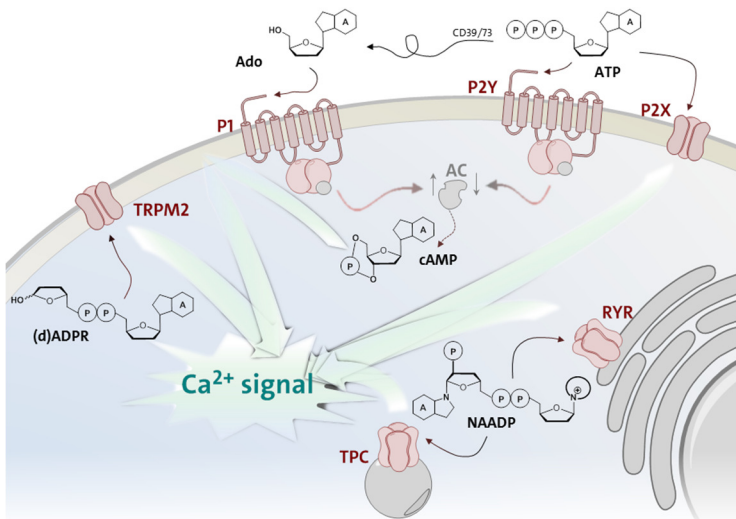
**Figure 14:** Summarized depiction of the ways in which adenine nucleosides and nucleotides are involved in the mediation of inter- and intracellular signals as primary and secondary messengers, respectively. The direct or indirect impact on $Ca^{2+}$ signaling processes constitutes a mutual as well as central aspect in this context.

The P1 receptors A2A and A2B, for example, mediate production of 3',5'-cyclic adenosine monophosphate (cAMP) by activation of adenylyl cyclases (AC), whereas A1 and A3 inhibit cAMP generation (Fig. 14). In P2Y signaling, (down-)regulation of cAMP is often accompanied by the activation of phospholipase Cβ which promotes the formation of another $Ca^{2+}$ mobilizing second messenger, inositol triphosphate ($IP_3$).

Summarizing all these examples, receptors that are modulated by adenine nucleotides like ATP, ADPR or NAADP are particularly and in high complexity involved in processes related to inflammation and regulation of the immune system. The different adenine nucleotides show a joint engagement in the modulation of intracellular $Ca^{2+}$ concentrations.

Intracellular $Ca^{2+}$ constitutes, together with phosphate ($PO_4^{2-}$), the central signal cells evolved to assimilate external stimuli. This consequently implies a substantial involvement of the ion in aspects as diverse as cell motility, gene transcription or exocytosis, examples of processes which are relevant e.g. in immune cell activation.[88,98] However, the underlying molecular mechanisms of these are largely unclear to date as a range of extra challenges

has to be solved to effectively look into cells. This accounts in particular for the precise role of those adenine nucleotides that act as second messengers in the mobilization of $Ca^{2+}$.

ADENINE NUCLEOTIDE SECOND MESSENGERS ASSOCIATED WITH $Ca^{2+}$ SIGNALING

The ubiquitous second messenger *cAMP* plays an important role in many biological processes, in addition to its implication in $Ca^{2+}$ mobilization. The cyclic mononucleotide is generated from ATP through GPCR-based activation of AC. Signaling by cAMP proceeds via two general pathways which rely either on direct binding and thus regulation of distinctive cyclic nucleotide-gated (CNG) ion channels, or on the activation of protein kinase A (PKA) to further forward the signal.[109–111] Activated PKA promotes the phosphorylation of a variety of enzymes, which can be subsumed as regulators of metabolic processes, muscle contraction and gene transcription.[111] In contrast, signaling through CNG channels allows a faster processing and implementation of increased cAMP levels. The ion channels are generally non-selective for cations. However, the entry of $Na^+$ depolarizes the membrane which promotes the combined influx of $Ca^{2+}$. Additionally, voltage-gated $Ca^{2+}$ channels open in response to membrane depolarization and thus enhance the $Ca^{2+}$ signal further.[109,110]

The inflow of cations is terminated finally by opening of $K^+$ channels which restore polarization of the cell membrane. Signals of cAMP are ceased through its degradation to AMP by phosphodiesterase.[109,110]

The role of cAMP signaling in the context of inflammation and regulation of immune response constitutes a research field of rising interest, based on the ubiquitous involvement in cellular processes. It was for example found that regulatory T cells ($T_{reg}$) exert their suppressive effect on effector T cells ($T_{eff}$) through increasing concentrations of cAMP. The rise of cAMP levels in $T_{eff}$ could either be induced via a paracrine mechanism, or by a direct transfer of cAMP via gap junctions between $T_{reg}$ and $T_{eff}$. [112,113] However, the transfer of cAMP between a pair of T cells could not be visualized directly yet, and also the underlying mechanisms allowing $T_{reg}$ cells to produce such significantly higher cAMP levels than $T_{eff}$ cells are not elucidated to date.

A loss of the immune suppressive mechanism would contribute to the generation of autoimmune reactions. Understanding the role of cAMP in T cell regulation and identifying the

associated molecular pathways thus could enable the identification of novel targets in the treatment of autoimmune disease.

The dinucleotide second messenger *ADPR* exhibits, in contrast to cAMP, a rather narrow field of target proteins with TRPM2 being the only clearly allocated one to date.[94,114] The TRPM2 channel was found to be one of a few cases of ion channels that are fused with an enzymatic domain. The domain belongs to the Nudix family of pyrophosphatases and displays an ADPR-hydrolase activity. Thus, the Nudix-motif is presumed to be the ADPR binding site that, upon direct interaction with ADPR, activates TRPM2 and gates $Ca^{2+}$ influx until hydrolysis of the substrate.[115]

Biosynthesis of ADPR uses nicotinamide adenine dinucleotide (NAD) as substrate and was found to proceed via two different pathways. One of these uses extracellular NAD, which analogously to extracellular ATP constitutes a 'danger-signal' of cells. The extracellular NAD is degraded by the plasma membrane-bound ectoenzyme CD38, and ADPR (as well as small amounts of cyclic ADPR (1 – 3%)) results. Successively, ADPR can be hydrolyzed further to AMP and, lastly, A by the enzymes CD203 and CD73.[116,117]
This pathway excludes an ADPR-based activation of e.g. TRPM2 channels at first sight, since the membrane-impermeable second messenger is formed extracellularly while the Nudix-binding site is located intracellularly.
However, studies showed that CD38 regulated $Ca^{2+}$ signaling in various cell types, and that its metabolites ADPR and cADPR modulated ion channels associated with $Ca^{2+}$ signaling. For example, the chemotaxis of neutrophils and dendritic cells (mouse and human) was found to critically rely on the presence of CD38 as well as ADPR and cADPR. In this context, the formation of ADPR on the CD38-pathway upon chemokine-/-attractant stimulation was probed and confirmed. Further, the $Ca^{2+}$ signals measured in response were related to an ADPR-gated channel, likely being the TRPM2 channel.[118]

These findings illustrate the controversy stated above well, and in order to address it, several hypotheses raised which for example theorize an intracellular transfer of ADPR via nucleotide transporters.[119] Another supposition considers the presence of CD38 partially in a special conformation (type III) where the catalytically active N-terminus is located inside the cell.[97]

However, the processes in-between formation of ADPR by CD38 and gating of TRPM2 are not elucidated yet and constitute a matter of ongoing debate.[115]

The second pathway on which ADPR can be generated involves activation of the nuclear enzymes poly(ADPR)polymerase (PARP) and poly(ADPR)glycohydrolase (PARG). They are activated by sensing single-/double stranded DNA breaks through e.g. oxidative stress. PARP responds with the synthesis of polyADPR on further enzymes involved in DNA repair as an activating signal. Additionally, transcription processes driven by nuclear factor κB are initiated. Once DNA repair is completed, polyADPR is hydrolyzed to free ADPR by PARG. In the case of extensive DNA damage however, PARP gets over activated so that the associated NAD turnover can lead to a depletion of storages and successively lower ATP levels to such a degree that cell death or lysis are initiated.[115,120–122] Cell studies, which demonstrated that TRPM2 channels were activated under oxidative stress and linked to PARP/PARG mobilization, underlined the contribution of this pathway to ADPR-mediated TRPM2-based $Ca^{2+}$ signaling.[115,120–122] However, the precise role of TRPM2 in pathophysiological processes associated with oxidative stress remains unclear.

More broadly, the two independent ways for the generation of ADPR illustrate the complexity of intracellular signaling, and the difficulty of clearly allocating triggers and targets of biologic mechanisms. The recent discovery of a new player in TRPM2 activation, 2'-deoxy-ADPR, adds to this. Respective studies revealed a significantly higher affinity of dADPR to TRPM2 than displayed by ADPR. These findings led to the hypothesis that dADPR might be involved in physiological processes like chemotaxis whereas ADPR-signaling was related to pathologic reactions on e.g. oxidative stress.[123] Hence, the dependencies and intersections between the several derivatives of ADPR constitute a further aspect of ongoing research. To this, chemical probes that enable cell assays with reduced complexity could contribute, and a better understanding of (d/c)ADPR-associated biological processes and implications on cell regulation could be gained. Such probes would include membrane-permeable derivatives of (d/c)ADPR to avoid e.g. patch-clamp stimulation as a source of possible biological side reactions and thus false positive results.

The adenine dinucleotide *NAADP* complements the main group of nucleotidic $Ca^{2+}$ mobilizing-second messengers identified to date. From first hints on its existence to the

confirmation of its chemical structure and involvement in $Ca^{2+}$ signaling, it took eight years.[105,124] Today, more than 20 years after resolution of structure and implication in $Ca^{2+}$ metabolism, many aspects of the biologic mechanisms environing NAADP still remain elusive and matters of discussion.[97]

Regarding the formation of NAADP, nicotin*amide* adenine dinucleotide phosphate (NADP) has long been investigated as the biologic precursor. This assumption was substantiated by the discovery of the 'base-exchange' reaction mediated by CD38.[125] However, the reaction conditions, acidic pH and high concentrations of nicotinic acid as a co-substrate, are unlikely to be found in the cytosol of living cells. Furthermore, knockout of the gene encoding for CD38 did not affect intracellular NAADP levels in some tissues and cell types.[97]

Alternatively proposed reactions for the formation of NAADP include amide-to-acid conversion of NADP, phosphorylation of NAAD through NAD kinases, or reduction of NAADPH to NAADP.[126–128] However, enzymes displaying corresponding activities have not been clearly allocated yet, and initial studies on e.g. NADPH oxidase are ongoing.[97] Candidates for target channels of NAADP are similarly manifold as hypotheses for pathways of its generation, and proof for one or the other is pending. The target search initially focused on the ER and in particular RYRs type 1 and 2, since this organelle constitutes the common address for intracellular $Ca^{2+}$ release and mobilization. However, the probability of RYR2 in open state, reconstituted from heart cells into lipid planar bilayers, was increased only above 1 μM concentrations of added NAADP. This would by far exceed the determined values of endogenous NAADP concentrations for a range of cell types.[97,129,130] For RYR1 in contrast, indication is mounting that the channel could be a target of NAADP. Stimulation of native RYR1 from skeletal muscle integrated into lipid planar bilayers showed an increase in open probability at NAADP concentrations in between 20 – 100 nm. This range would coincide with endogenous concentrations of NAADP found in various cell types.[97,130] Further evidence pointing to RYR1 was gained by experiments where NAADP-derived $Ca^{2+}$ signals were deactivated by the addition of the RYR blockers ryanodine and ruthenium red (assays used nuclei from pancreatic acinar cells & human T-lymphoma cells). In a Jurkat T cell system lacking RYR1, $Ca^{2+}$ signals were found to be largely diminished, further substantiating the implication of RYR1 in NAADP signaling.[97,99,130]

In 2002, CHURCHILL and colleagues published results that relocated the search for NAADP target channels as they showed that NAADP mobilized $Ca^{2+}$ from a store other than the ER. Their studies on sea urchin eggs (homogenate) revealed the reserve granule, a lysosome-analogue organelle, to be an acidic $Ca^{2+}$ store activated by NAADP exclusively. [102] Successive investigations on the identification of the associated $Ca^{2+}$ releasing channel took until 2009, when three publications concordantly stated that TPCs release $Ca^{2+}$ from acidic organelles in dependency on NAADP.[131–133] The authors showed that TPCs responded to NAADP signals at NAADP concentrations in the physiologic (nanomolar) range and were inhibited at micromolar NAADP concentrations.[133] Further, overexpression of TPCs potentiated $Ca^{2+}$ signals mediated by NAADP, and, on the contrary, TPC gene knockout resulted in the abrogation of NAADP signals as well as associated $Ca^{2+}$ dependent processes.[131,132] Conversely, continued research in this field featured cases in which no regulatory effects of NAADP on TPCs were observed, adding thus further controversy and complexity to the matter.[96]

Approaches to unify these controversial results for target channels of NAADP include hypotheses of an NAADP-binding protein being involved in the activation of RYRs, and with regard to TPCs, a potential action of NAADP not as full- but co-regulator of the channel.[96,97] The former theory was raised already in 2003, and substantiated by photoaffinity labelling experiments conducted by WALSETH & LIN-MOSHIER *et al.* pointing to small (ca. 22 kDa) cytosolic proteins as binding protein candidates. Their precise identity however is still a subject of ongoing investigation.[97,134]

It is generally accepted that NAADP mediates initial release of $Ca^{2+}$ which then amplifies to global $Ca^{2+}$ events. Accordingly, in T-lymphocytes a rapid formation of NAADP was confirmed, which reached peak-concentrations within a few seconds after stimulation.[99,130] However, the spatiotemporal response to NAADP stimulation differs in between cell types, and the underlying mechanisms including initial organelles and potential co-messengers, are not clarified yet.[130] In T cells, interaction of the T cell receptor/CD3 complex with an antigen presented by the MHC complex induced formation of NAADP and triggered the generation of $Ca^{2+}$ microdomains. The process was shown to be dependent on the presence of RYR1. Additionally, an implication of extracellular $Ca^{2+}$ was observed in this very early stage of $Ca^{2+}$ signaling.[97–99] Thus, it could be concluded that NAADP is involved essentially in the initiation of $Ca^{2+}$ signaling events, which successively are amplified through further second messengers like cADPR and $IP_3$.

In distinctive infection models (e.g. experimental autoimmune encephalomyelitis (EAE), a model for multiple sclerosis (*MS*)), this initial interaction mechanism was found to be crucially involved in the regulation of motility and re-activation of autoaggressive $T_{eff}$ cells. In EAE like *MS*, presentation of myelin-antigens by macrophages drives T cells to invade central nervous system (CNS) tissues. Here, local encounters with the specific antigen re-activates the $T_{eff}$ cells, which consequently promote a release of pro-inflammatory signals, subsequently the recruiting of further immune cells and finally the onset of disease.[97,135,136] Interestingly, the course of EAE was shown to be significantly alleviated when a NAADP inhibitor was added to the treatment. This approach in combination with further techniques like live two photon imaging strengthened the findings and substantiated the hypothesis of NAADP's essential involvement in early $Ca^{2+}$ signals and T cell activation.[135]

Taken together the particular pathologic implications with the persisting controversy on the biologic mechanisms environing NAADP, the need for further investigation and novel tools in support of this becomes obvious. However, the setup of cell-based studies mostly involves mechanic strain for the application of second messengers in general, and is restricted to single-cell techniques.[99] The assays further are especially sensitive and prone to false-positives. The transient character of the NAADP signals further compliments to eventual complications. Concluding, already slight damages to the cell membrane can provoke an unintended influx of $Ca^{2+}$ and hence formation of NAADP, which consequently interferes with or impedes the envisaged experiment.

With all the described, yet not clarified aspects of intracellular signaling in general, and the particular complications associated with studies on these in mind, the steady demand for novel tools enabling improved assay setups appears natural. One highly desirable innovation in this general context are membrane permeable, bio-reversibly modified chemical derivatives of the so sophisticated to study second messengers.

BIO-REVERSIBLY MASKED PRO-ADENINE NUCLEOTIDE SECOND MESSENGERS

As mentioned previously in Part I (see chapter 4), the neutralization of negative charges constitutes an option to overcome membrane permeability issues, and can be implemented by conversion of the respective acid into its corresponding ester
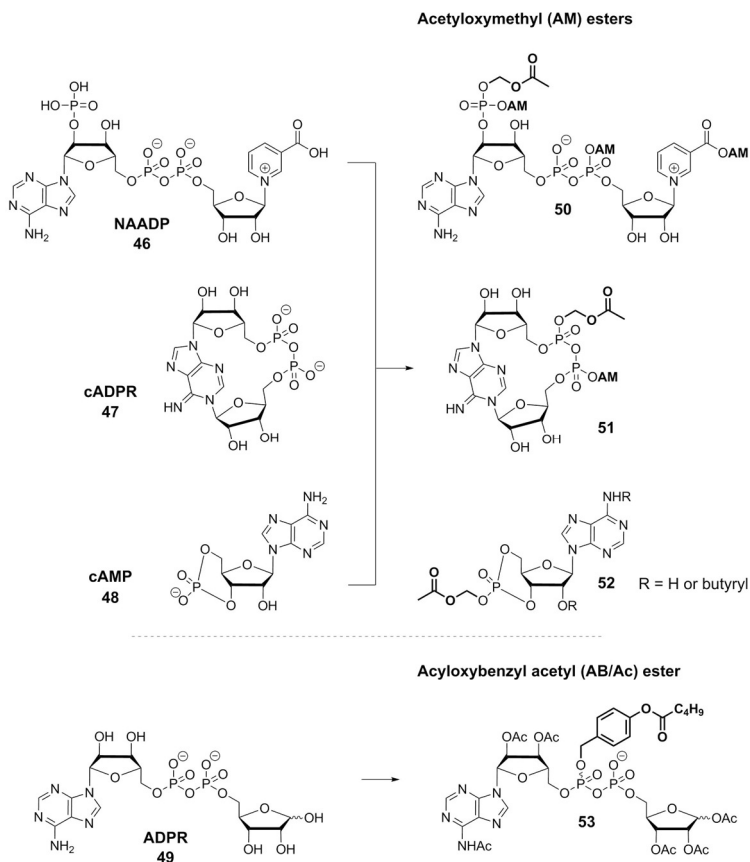
**Scheme 16:** Overview of the membrane-permeable derivatives of NAADP, cADPR (proposed structures), cAMP and ADPR that are found in the literature. In case of NAADP, cADPR and cAMP, membrane-permeable acyloxymethyl esters have been reported whereas the 4-acyloxybenzyl/acetyl (AB/Ac) pro-ADPR constitutes the first bio-reversible derivative synthesized from ADPR.[142–147]

This modification is reversible by means of chemical or enzymatic hydrolysis of the ester moiety, and thus, under the conditions of most biological assays, the free acid is released again.

Such approaches are well-known and established for nucleotides, in particular nucleoside (analogue) monophosphates. A main field of application constitutes the prodrug-design and -synthesis of nucleoside analogues that display pharmacologic activity but suffer from

poor pharmacokinetics and metabolization. Accordingly, a variety of monophosphate pro-drug approaches has been developed to date, and some of these prodrugs, like *sofosbuvir* or *adefovir dipivoxil*, even reached the market and are applied in therapy.[137–139]

However, bio-reversibly masked derivatives of polyphosphorylated nucleosides are rarely described despite their promising use as e.g. chemical probes. Regarding the second messengers NAADP, cADPR and cAMP, reports on membrane-permeant derivatives are limited to acetyloxymethyl (AM) and benzyl esters (only of cAMP & cGMP[140,141]) (Scheme 16). In this context, HUGHES and colleagues reported the synthesis and biologic evaluation of a dibutyryl cAMP-AM ester (Scheme 16).[142] The synthesis started from $N^6$, $O^{2'}$-dibu-tyryl cAMP, which was converted with AM bromide (AMBr) under DIEA-basic conditions in acetonitrile over 4 days at room temperature, and yielded the pro-nucleotide in 59% (two fractions from column chromatography, first contained 38% pure product, second 21% of the product (determined by NMR) plus salt impurities).[142] In successive whole-cell incuba-tion studies, they successfully observed activation of PKA, but only 15 min after the addi-tion of di(Bu)cAMP-AM (10 µM) to the cell medium.[142]

In further studies of SCHULTZ *et al.*, cAMP-AM was synthesized via a transient protection of the 2'-OH function of cAMP with the trimethylsily (TMS) group, which was followed by es-terification of the phosphate under the before described conditions.[145] The protected nu-cleotide was studied similarly to di(Bu)cAMP-AM with regard to its potential of PKA activa-tion. Despite an activating effect the researchers found that cAMP-AM was less potent than di(Bu)cAMP-AM and metabolized so rapidly that it rather mimicked transient cAMP sig-nals.[145] These findings were underpinned by BARTSCH *et al.* who performed extensive HPLC studies on membrane permeability, intracellular accumulation and biotransformation of cAMP derivatives and selected AM esters thereof.[148] The authors could confirm a beneficial effect of phosphate-masking on membrane permeation, and showed that the enzymatic hydrolysis of di(Bu)cAMP-AM proceeded mainly via the mono-$N^6$-butyrylated intermedi-ate.[148]

Concluding these studies, room for optimization of the activation profile for bio-reversibly masked cAMP exists. A respective approach should include a variation of the phosphate masking unit in a way that the chemical stability is improved (over cAMP AM) while

activation of the masked nucleotide proceeds rapidly still. Further, the mask should provide higher lipophilicity to make the 2'-OH protecting group redundant, and thus reduce the amount of enzymatic reactions needed. Modification at $N^6$ however should be retained to eventually benefit from a two-stage hydrolysis mechanism which offers the possibility of $N$-derivatized cAMP intermediate accumulation.

For NAADP and cADPR, reports on photo-caged derivatives preceded those on membrane-permeant derivatives by more than a decade. LEE and co-workers published respective articles on synthesis and use of caged NAADP and cADRR in 1995 and 1997 already.[149,150] The caging approach enabled a controlled release of NAADP and cADPR by means of UV-light excitation at 350 nm. However, photolysis efficiencies for uncaging were calculated to only 1% which consequently demanded the application of high concentrations of the caged nucleotides in cell studies. The syntheses of the caged agents, however, went along with only modest yields. Apart from this and with regard to the assay setup, both caged agents were unable to traverse across the cell membrane passively so that effortful single-cell microinjection was still required.[149,150]

CHURCHILL and colleagues picked up on the approach of SCHULTZ *et al.* and envisioned the synthesis of cell-permeant AM esters of both NAADP and cADPR. Respective publications followed in 2008 (NAADP-AM) and 2012 (cADPR-AM, Scheme 16).[144,147] The presented synthetic procedures were adapted largely from HUGHES and SCHULTZ. In both cases, DIEA was used as base, acetonitrile as solvent and AMBr as reagent. The nucleotides were pretreated with DIEA in acetonitrile for 15 min to 2 h, until AMBr was added (one to two portions, in approx. fivefold excess). The reactions were stirred at rt for 24 – 48 h, and then concentrated to dryness. Reactions were followed by TLC and anion exchange HPLC (Fig. 15).
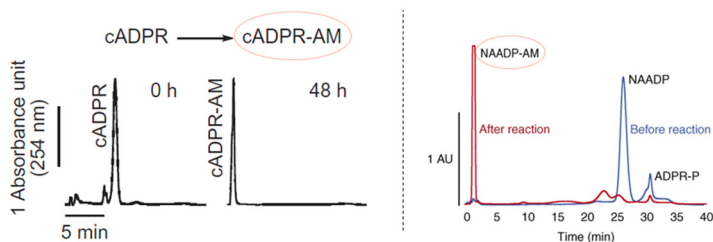
**Figure 15:** By CHURCHILL and colleagues presented HPLC traces of the reaction of cADPR to cADPR-AM (left) and NAADP to NAADP-AM (right) taken from in their respective publications. HPLC runs were performed using strong anion exchange resin (AGMP1) packed into 3 x 150 mm borosilicate glass columns, and a concave upwards trifluoroacetic acid (TFA) gradient over 40 min. UV-detection of compounds was done at 254 nm.[144,147]

According to the authors, the newly formed peak during the reaction, which showed no retention on the column, "suggests that most of the negative charges of NAADP have been removed by esterification" (Fig. 15, right, compare blue and red traces).[147] The obtained product was further analyzed by NMR spectroscopy, but the proton spectrum presented by PARKESH *et al.* featured a multitude of signals which are difficult to correlate with the proposed molecular structure of NAADP-AM. In contrast, the section shown from the $^{31}$P-NMR spectrum contained diffuse signals only hardly above the background noise. Correlation spectra were not recorded, and mass spectrometric analysis stated to be impeded due to "the labile nature of this compound" since "excessive breakdown of the compound occurred during this process".[147] In contrast, for cADPR-AM it was described with regard to the peak showing no retention on the column (Fig. 15, left) that "mass spectroscopy was consistent with cADPR with multiple AM groups" since "mass spectroscopy revealed a family of peaks separated by 73 atomic mass units indicating multiple species with varying numbers of AM groups".[144] However, "due to the low yields and instability of cADPR esters (…) we were unable to obtain enough material for NMR for absolute structural assignment".[144]

Apparently, the esterification reactions afforded more than one (by-)product under the described conditions, leaving e.g. the interpretation of the presented HPLC traces (Fig. 15), open to discussion. Thus, a successful synthesis of both NAADP-AM and cADPR-AM in general appears rather arguable which is complemented by further inconsistencies observed for bioassays using the respective AM ester-labeled samples.[151]

Despite these discouraging reports, the interest in membrane permeable derivatives of adenine-nucleotide second messengers persists as they offer such great advantages for the setup of whole-cell studies on respective signaling processes. However, synthetic approaches towards bio-reversible phosphate esters that start from the intact dinucleotide showed several weak spots, ranging from inefficient synthesis protocols to the accuracy of analytics. Regarding the conceptual basis, a straight forward approach further limits the possibility to control site and degree of esterification as e.g. the discrimination between phosphate groups is not guaranteed. A twofold esterification at the pyrophosphate backbone of e.g. NAADP would considerably destabilize the anhydride bond, thus promoting its breakage. Hence, an approach enabling the directed modification of definite functional groups would be ideal. Lastly, the masking group strategy itself could be revisited bearing in mind that AM esters of cAMP were hydrolyzed particularly fast and lacked stability.[142,144,145,148]

THE ACYLOXYBENZYL MOIETY AS AN ESTABLISHED MASKING UNIT IN PRODRUG APPROACHES

Originally developed for the delivery of amines as carbamate prodrugs, FREEMAN and co-workers were the first to transfer the use of 4-acyloxybenzyl (AB) esters as bio-reversible protecting groups on phosphonates and phosphates with pharmaceutical relevance.[152–154] The adaption was prompted by the observation that di(acyloxymethyl)esters of phosphates were hydrolyzed particularly slow in the second stage of enzymatic hydrolyses. FREEMAN assumed the respective phosphate monoesters to be poorer substrates for esterases due to the negative charge adjacent to the cleavage site. Consequently, it was reasoned that a distance-adding linker like the benzyl moiety could be advantageous and would facilitate in particular the second enzymatic activation.[152,153]

This hypothesis was confirmed successfully in HPLC studies for both compound classes, mono/di(AB)phosphonate esters and mono/di(AB)phosphate ester of the nucleoside analogue azidothymidine (AZT). Porcine liver carboxylesterase (PLE) was used as a model enzyme for the hydrolysis studies. [152,155] Hence, the integration of AB moieties into prodrug approaches tailored for mononucleotides appeared indeed advantageous.

Adding to this, the bio-reversible AB-protecting group system was the first and so far only one to be transferred effectively on prodrug approaches for nucleoside diphosphates (DiP-Pro-concept) and triphosphates (TriPPPro-concept).[156–161] Further, it was expanded on compound classes like sugar nucleotides (Scheme 16).[143]
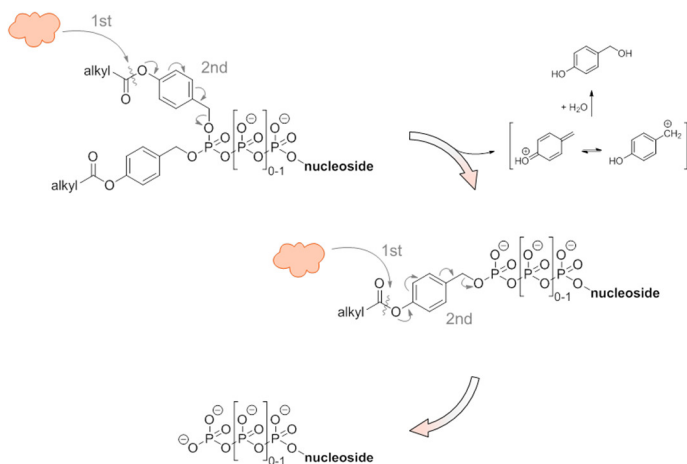


**Figure 16:** Mechanism of the enzymatic activation of AB-phosphate ester prodrugs. Two subsequent enzymatic cleavages of the phenolic acyl ester initiate the elimination of the oxybenzyl linker which finally releases the free nucleotide, and the byproducts 4-hydroxybenzyl alcohol as well as the corresponding acid of the acyl ester.

The broad synthetic applicability of the AB-masking group is complimented by meeting the essential features of a prodrug concept: high chemical stability, efficient enzymatic activation and sufficient lipophilicity to pass cell membranes. Moreover, the two-part composition of the AB-masks allows variation of e.g. lipophilicity or enzymatic activatability which adds further versatility to the concept.[156–161]

The enzymatic release mechanism of AB ester prodrugs was shown to rely on an initial cleavage of the phenolic acyl ester by ubiquitous esterases. The former acceptor substituent is thus turned into a donor substituent which induces a spontaneous decomposition of the oxybenzyl linker according to a 1,6-elimination. Successively, the mono(AB)ester and, lastly, 4-hydroxybenzyl alcohol are released (Fig. 16). This process takes place a second time to finally release the free nucleotide.[152]

The chemically driven cleavage of AB-units was shown to proceed significantly slower. Further studies on the hydrolysis behavior revealed a correlation between the rate of prodrug activation and the length of the acyl ester chain. While the AB-cleavage rate decreased with increasing chain length, this was at the cost of stability of the pyrophosphate bond.[159] Here, several further developments of the DiPPro- and TriPPPro-concepts enabled the tuning of hydrolysis properties so that activation, lipophilicity and stability were balanced to an optimum.[161,162] The successful entry of diphosphate and triphosphate prodrugs into cells was confirmed with the aid of fluorescent nucleoside analogue prodrugs.[163,164]

All these aspects encouraged the transfer of this approach on further nucleotide classes. A first example in this context was presented by PAHNKE *et al.* with the synthesis and evaluation of an AB/Ac ADPR derivative (Scheme 16).[143] The compound, in contrast to the earlier mentioned AM esters of cAMP, NAADP and cADRP, was built up in a convergent synthesis approach that generated the pyrophosphate linkage in the last steps. The route used selectively acetylated adenosine (2',3'-*O*Ac), a 4-pentanoyloxybenzyl (PB) bis(*N*,*N*-di*iso*propyl-amino)phosphorous diamidite and per-acetylated ribose-5-phosphate as key building blocks which were assembled stepwise to the final product. By this, the PB moiety was selectively introduced at a distinct site of the molecule.

Hydrolysis studies of the PB/Ac ADPR derivative with PLE confirmed a rapid removal of the PB group. Enzymatic cleavage of the acetyl groups, in contrast, was surprisingly slow since even after three days of incubation only small amounts of released ADPR were detected (HPLC/MS). Complete turnover of the pro-nucleotide took ca. seven days, but anyhow, quantities of free ADPR were low due to a range of persisting intermediates.[143] Nevertheless, the AB/Ac ADPR derivative constitutes a valuable first indication of the applicability of AB-groups in approaches aiming at effective bio-reversibly masked derivatives of sugar nucleotides and purine nucleotide second messengers.

Consequently, an expansion of the AB-pro-nucleotide approach on the second messenger NAADP appears promising, as does also the development of AB-masked derivatives of cNMPs, to ultimately allow studies on e.g. calcium signaling in bulk settings on a variety of cells and without the need of microinjection. A further development of the described PB/Ac-ADPR derivative would potentially enable studies regarding the signaling and

function of TRPM2 channels and their role in cells. These studies are imperative to advance our understanding of intracellular signaling pathways and their implication in cell communication and regulation, and ultimately, pathological conditions.

## 7.  Aim of the Work

The adenine nucleotide (AN) 2nd messenger cAMP, ADPR and NAADP are crucial parts of $Ca^{2+}$ signaling processes. However, many aspects of their precise involvement in the complex cellular signaling system as well as the physiologic and pathologic implications of their contribution to $Ca^{2+}$ mobilization are not understood yet.

Cell-based studies on 2nd messengers are generally difficult to perform as application of the highly polar compounds is carried out via effortful, single-cell preparative methods like electroporation, microinjection or patch clamp. These methods require highly trained staff, careful preparation and significant amounts of time in advance of each experiment while at the same time the invasive application raises the potential for interfering artefacts or false-positives.

The development of efficient membrane-permeant, bio-reversibly protected derivatives of cAMP, ADPR and NAADP constitutes an approach to overcome the limitations of current setups. Further, an expansion of cell assays to medium- or high-throughput formats becomes possible and cell-based settings generally simplified.

An established bio-reversible protecting group, particularly for phosphates, is the acyloxybenzyl (AB) moiety (Fig. 17). It was used successfully in prodrug approaches for mono-, di- and triphosphates of nucleoside analogues with antiviral activity.[152,153,156,157,160] The respective prodrugs were shown to efficiently diffuse across cell membranes and release the corresponding nucleotide intracellularly upon enzymatic activation.[157] Hence, integration of the AB-concept into approaches towards membrane-permeant AN 2nd messenger derivatives was envisaged (Fig. 17).

This thesis aimed at developing synthetic access towards AB-masked derivatives of cNMPs, ADPR and NAADP. Introduction of the AB-mask in a (site-) specific way and thus total synthesis approaches were preferably considered.
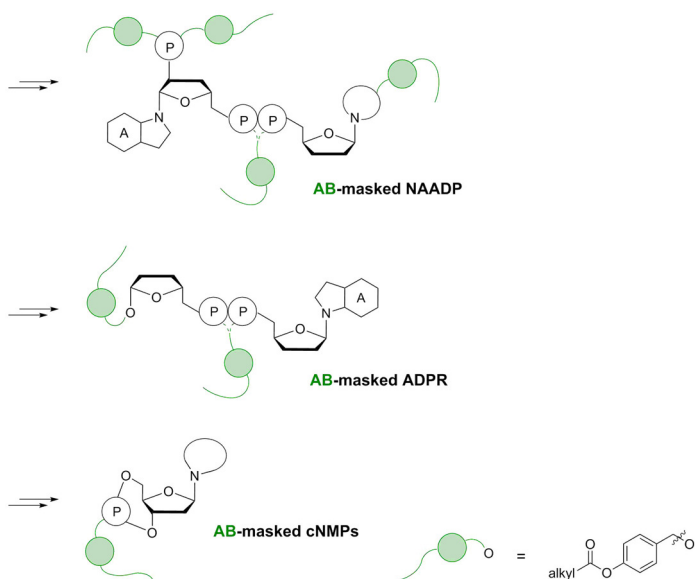
**Figure 17:** Overview of anticipated membrane-permeant, bio-reversibly protected AN 2$^{nd}$ messenger derivatives including the envisaged positions for AB-masking.

Based on the complexity of the dinucleotides in molecular structure, convergent synthesis routes with a final coupling step were designed. In this context, protecting group strategies allowing for directed modifications at the specified sites needed to be set up (Fig. 17). Here, the chemical lability of the AB-mask towards nucleophiles was to regard just as the distinctive sensitivities of phosphoranhydride bonds and glycosidic bonds.

The obtained membrane-permeant, bio-reversibly masked AN 2$^{nd}$ messenger derivatives further were to evaluate with regard to their chemical stability, enzymatic activation and performance as efficient AN 2$^{nd}$ messenger releasers in cell-based settings. In this context, particular focus laid on the potentials of the masked AN derivatives to induce Ca$^{2+}$ signals.

This work was carried out in cooperation with the groups of A. GUSE, V. NIKOLAEV, and C. GEE (University Medical Center Hamburg-Eppendorf (UKE)) in the framework of the READ ME project.

# 8. Results and Discussion

A first synthesis of membrane-permeant AN 2nd messenger derivatives was pursued by re-tracing the approaches of PARKESH and ROSEN *et al.* towards AM-protected NAADP and cADPR derivatives. [144,147] The according synthetic protocol was reproduced for NAADP and its outcome evaluated with respect to feasibility and efficiency of the straight-forward ap-proach bearing in mind the drawbacks mentioned before (see chapter 6).

## 8.1. Approaches towards masked NAADP-derivatives starting from NAADP

### 8.1.1. Studies on the synthesis of NAADP-AM

According to PARKESH *et al.*, NAADP (as its sodium salt) was evaporated several times with di*iso*propylethylamine (DIPEA) or triethylamine (TEA) prior to reaction. The residue (which the authors described as the respective NAADP alkylammonium salt) was dissolved in ace-tonitrile and mixed with another 5 equivalents base. After stirring at rt for 15 min, 5 equiv-alents acetyloxymethyl bromide (AMBr) were added and reacted with NAADP at rt for 24 h. TLC and HPLC monitoring of the reaction indicated conversion of the starting material, so that the reaction was terminated by filtration and evaporation of the filtrate. This afforded a yellow solid. The solid was washed with ether to remove unreacted AMBr, and used with-out further purification in cell-based assays. Analysis of the crude product included ^{1}H- and ^{31}P-NMR spectroscopy only (see previous chapter).[147]

Attempts to reproduce the procedure were accompanied by various complications and, overall, did not lead to the desired product (Scheme 17).

The solubility of the NAADP sodium salt was poor in acetonitrile and DMF. Dissolution of NAADP in DMSO was generally possible but only at high dilution. Further, upon dissolution the mixture of NAADP and DMSO underwent a change of color from colorless to yellow which might indicate a potential reactivity of compound and solvent.

The ion exchange method described by PARKESH *et al.* further was insufficient, and the res-idues obtained upon evaporation did not show any improved solubility in e.g. acetonitrile or DMF. In this context, a successful ion exchange from sodium to the respective alkyl

ammonium counter ion appears generally dubious since protons for the formation of alkyl ammonium ions were missing and neither could a volatile sodium species have formed under the applied conditions. Hence, successively performed reactions were characterized by insufficient dissolution and thus no conversion.

Enhanced solubility of NAADP was achieved by ion exchange chromatography on a DOWEX stationary phase loaded with triethylammonium or tetra-*n*-butylammonium. The NAADP TEAH$^+$ salt was obtained by freeze-drying and was soluble in acetonitrile and DMF, so that DMSO was excluded as a solvent in successive attempts to synthesize NAADP-AM.

The reagents, 3.3 equivalents AMBr and nitrogen base (TEA or DIEA), were added to the NAADP solution. Potassium carbonate was studied as an alternative base since it displays a salt character and higher nucleophilicity in relation to the sterically hindered tertiary amines, and thus potentially advances conversion. All reactions were carried out at rt and the reactions were followed by HPLC (Scheme 17).

Reactions were terminated via removal of all volatile components, and crude mixtures successively purified on an automated RP purification system (6 g $C_{18}$-RP silica gel, acetonitrile gradient in water, 0 – 100%, 20 min at 6 ml/min). Reaction products were analyzed by NMR spectroscopy and MALDI mass spectrometry.

An efficient formation of NAADP-AM was not observed under any of the applied conditions. At best, traces of one- or twofold AM-modified NAADP-species were found in MALDI mass spectra. This, however, could not be linked to a specific reaction procedure and thus constituted rather single than reproducible events. More frequently observed (via HPLC-reaction monitoring) was a decomposition of NAADP, likely through loss of nicotinic acid or cleavage of the pyrophosphate backbone. Respective fragments were assigned in MALDI mass spectra. However, additional decomposition during work up, purification, sample preparation or ionization could not be excluded. Regardless, the described observations were more pronounced under potassium carbonate-basic conditions in DMF (Scheme 17).
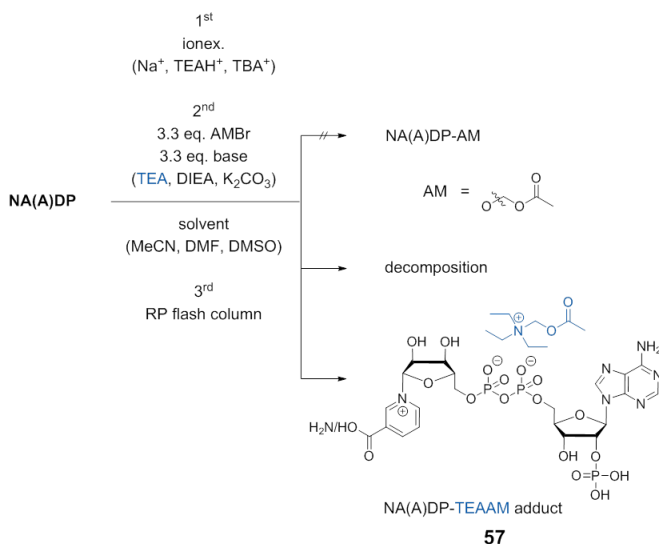
**Scheme 17:** Overview of reaction conditions investigated for a straight forward synthesis of NA(A)DP-AM. In parts, NADP, which is almost identical to NAADP with exception of the nicotinic amide versus acid function, was used as a model compound to evaluate reaction conditions prior to application on NAADP.

Esterification reactions carried out in the presence of TEA (and DIEA) led to less decomposition. However, an efficient formation of NAADP-AM did not take place either. Instead, a Menshutkin-type side reaction between nitrogen base and AMBr proceeded and led to the formation of acetyloxymethyl(triethyl)ammonium. Anyhow, NAADP and the quaternary ammonium salt formed surprisingly stable adducts which, at first sight and with mass spectrometry analysis, could lead to the guess that NAADP-AM with TEAH⁺ as a counter ion was successfully formed, just as PARKESH *et al.* reported it. A thorough analysis of 2D-correlation NMR spectra however clarified that the reaction led to a NAADP TEAAM⁺ adduct (**57**) instead of actual NAADP-AM (Scheme 17, Fig. 18).

The result illustrates the low reactivity of the functional groups of intact NAADP under the applied conditions as almost no modification of these proceeded. In summary, esterification conditions based on a reaction between alkyl halide and acid under basic conditions, were not successful for NA(A)DP.

**Figure 18:** $^1$H-, $^{31}$P- & HMBC-NMR spectra (D$_2$O, 600 MHz, 243 MHz & 151 MHz, 25 °C, shifts δ in [ppm]) of NAADP TEAAM$^+$ adduct **57**. The formation of **57** was repeatedly observed for esterification attempts conducted under TEA or DIEA basic conditions. Proton and phosphorous signals correspond to an intact NAADP molecule. Signals at lower field (highlighted in blue) corresponded to AM- and TEA-moieties. An intense correlation between protons and carbons of these moieties was found in the HMBC spectrum.

As an alternative, AM-esterification was attempted via 1.) ion exchange from NAADP Na$^+$ to NAADP Ag$^+$ and 2.) reacting the silver(I) salt with AMBr in DMF. AgBr precipitated from the solution as anticipated. However, the desired product was not obtained and mainly starting material resulted from RP column chromatography instead.

Consequently, this linear approach aiming at directly modifying NAADP with AM-groups proved impractical due to the low reactivity of the functional groups of the dinucleotide with the reagent AMBr under the studied esterification conditions which, however, had proven highly successful with various other substrates (s. chapter 3, end). Still, the attempts to directly synthesize NAADP-AM allowed retracing the observations re-ported by PARKESH *et al.* The AM(alkyl)ammonium salt generated from nitrogen base and AMBr, and the successively formed NAADP AM(alkyl)ammonium salt were mistakenly in-terpreted as NAADP-AM. Correlation spectra however clearly showed strong couplings

between protons and carbons of AM- and TEA-moieties whereas no correlation between NA(A)DP and AM-groups was visible (Fig. 18).

Samples of the obtained NAADP TEAAM[+] salt **57** were analyzed with regard to a $Ca^{2+}$ mobilizing effect on cells (Jurkat T cells, cardiomyocytes from mice) in incubation assays performed in cooperation with the group of A. GUSE. Surprisingly, $Ca^{2+}$ signals were observed in some cases leading to the hypothesis that the lipophilic NAADP salt was able to enter cells somehow. Similar to observations made for samples of "NAADP-AM" provided by PARKESH and collegues, GUSE *et al.*'s results of the incubation experiments with the NAADP TEAAM[+] salt were inconsistent and poorly reproducible. These findings substantiated doubts regarding the actual synthesis of NAADP-AM as reported, and contributed further to the hypothesis that instead a Menshutkin-type side reaction and successively the formation of NAADP AM(alkyl)ammonium salt were observed.

In summary, the esterification of the dinucleotides NADP and NAADP starting from the intact natural compound using an alkyl halide and base failed under various conditions due to either decomposition or ineffective conversion. Accordingly, this approach was not pursued further.

### 8.1.2. Studies on the reaction between NADP and diazo-mask derivatives

Another approach towards modified nucleotides that starts from the natural compounds makes use of diazo-derivatives of the respective masking unit. This was successfully applied in the synthesis of photo-caged ATP and ADPR.[165,166] The photo groups were purchased as hydrazones and converted to the reactive diazo compounds via treatment with $MnO_2$ in DMF. After stirring at rt, the reaction mixtures were filtered and the filtrate added to the respective nucleotide. In some cases, this process was repeated up to four times, despite the use of excess diazo compound (min. 12.5 equivalents per portion). Reaction products were purified by semipreparative HPLC.[165,166] Evaluation of the photo-caged compounds via NMR spectroscopy and mass spectrometry led to the identification of mono- and multi-caged compounds which indicated a lack of chemo-selectivity or regio-control. More importantly in the context of this thesis, the results, however, showed a sufficient reactivity of the reagent with the nucleotides.

Consequently, the approach was transferred first on NADP as a model compound for NAADP. The required diazo-mask derivative was synthesized starting from 4-(hydroxyme-thyl)-phenyl octanoate **58** which was oxidized to its corresponding aldehyde **58a** first, and subsequently converted to hydrazine **59**.[167] Oxidation to diazo-compound **60** was per-formed *in situ* with excess $MnO_2$, which was then removed by filtration over Celite®.[165,166] Following described protocols,[165,166] the filtrate containing the reactive compound was added to a solution of NADP in water. The reaction mixture was stirred at rt for 24 h and the course of the reaction monitored via HPLC. Successively, the solvent was removed to terminate the reaction and the crude mixture purified via automated RP chromatography.

The desired product, however, was not isolated.
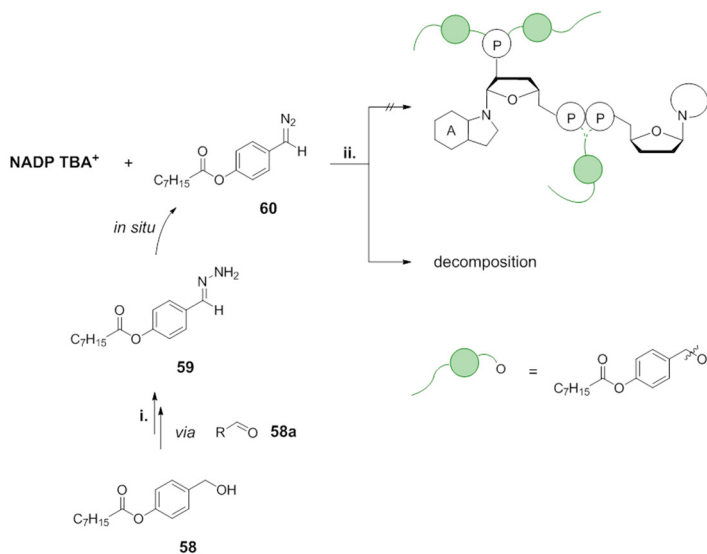


**Scheme 18:** Synthesis of (4-(phenyloctanoyl)-benzylidene) hydrazine starting from the corresponding alcohol, and its ap-plication in the modification of NADP (used as TBA$^+$ salt): **i.** $1^{st}$: 1.1 eq. Dess-Martin periodinane, dichloromethane, 0 °C to rt, 2 h, 88%, $2^{nd}$: 1.2 eq. hydrazine monohydrate (80%), MeOH, rt, 60 min, **59**: 74%, **ii.** 7- 15 eq. **59**, 46 – 150 eq. MnO$_2$, (46 eq. KH$_2$PO$_4$), DMF, rt, 1 h for oxidation, filtration over Celite®, then addition to NADP TBA$^+$ in H$_2$O, rt, 24 h, decompo-sition.

Instead fractions containing the nucleobases adenine and nicotinic amide only were obtained indicating a decomposition of the dinucleotide.

Residual $MnO_2$ seemingly remained in the filtrate added to the NADP solution despite its thorough removal and repeated filtration over Celite®. Like other twofold positive cations, $Mn^{2+}$ can be chelated by the N- and O-atoms of nucleobases. Such coordination might exert strain on the NADP molecule on the one hand, and on the other hand the Lewis acidity of $Mn^{2+}$ potentially promoted the cleavage of the nucleobases.

In summary, the approach to use *in situ* generated diazo masks for the modification of NADP with octanoyloxybenzyl (OB) groups was not practicable. Instead of product formation major breakdown of the dinucleotide was observed, presumably resulting from coordination of residual $MnO_2$ from the first reaction mixture between the nucleobases and successive cleavage of these due to the Lewis acidity of $Mn^{2+}$. Consequently, the conditions were not transferred on NAADP further.

Overall, the attempts for direct masking of the dinucleotides did not yield any of the desired products. Analysis of reaction- and decomposition products pointed out the infeasibility of the available direct approaches when applied to NAADP or NADP. In addition to the observed reaction outcomes, a lack of regio-control or chemo-selectivity constituted drawbacks (in the case of successful reaction) resulting in randomly and/or excessively masked derivatives (see NPE-ADPR).[165]

The development of a synthesis route in which the dinucleotide is modified in a directed fashion while being built up stepwise and convergent clearly constituted a great advantage against this backdrop.

### 8.1.3.    Development of a total synthesis route towards membrane-permeant, bio-reversibly protected derivatives of NAADP

The targeted structure of a membrane-permeant, bio-reversibly masked NAADP derivative was envisaged to carry AB-moieties at the 2'-phosphate and the carboxylic acid function (Fig. 19). A retrosynthetic analysis was chosen to design respective synthesis routes. Here, aspects to particularly consider next to the structural complexity of NAADP were the various labilities that NAADP as well as AB-masks exhibit.

AB-masked NAADP

**Figure 19:** Envisaged structure of the bio-reversibly protected NAADP-AB derivative with chemically labile sites indicated by grey flashes.

The general sensitivity of purine nucleosides and nucleotides towards (strong) acids, especially in aqueous solutions, needed to be regarded to begin with. Similarly, the phosphorous anhydride bond is prone to hydrolysis under acidic conditions. The masking AB moieties in contrast are instable under basic and nucleophilic conditions as attacks on the partially positively charged benzylic carbon and the ester bond would cause a cleavage of the groups (Fig. 16.). Hydrogenolytic and Lewis acidic conditions were further to avoid based on expected labilities of the AB ester as well as the nicotinic acid (NA) nucleobase. Lastly, the exceptional instability of the glycosidic bond between ribose and NA, in particular under basic conditions, needed to be considered.

The nitrogen atom of the pyridine-derived nucleobase is positively charged, and thus highly sensitive towards attack of even mild bases or nucleophiles. Aqueous acidic conditions on the other hand promote hydrolysis of the glycosidic bond.

In summary, the listed limitations exclude a range of reaction conditions depending on the stage of synthesis and nucleoside/-tide dealt with. Thus, the development of a suitable convergent route, in particular regarding the combination of PGs and coupling reagents, constituted a sophisticated and iteratively continued process.

#### 8.1.3.1. Retrosynthetic analysis of synthesis pathways to NAADP-AB derivatives

The complexity of NAADP's different functionalities and thus reactivities together with the envisaged masking in selected positions gave priority to a convergent approach. Hence, the first disconnection was set "in the middle" of NAADP - the pyrophosphate backbone - giving two nucleotide building blocks to be coupled preferably late in the synthesis sequence (Scheme 19).

Coupling of the NA nucleotide building block and adenine nucleotide (AN) building block was set late (last or penultimate) in the synthesis sequence to allow maximum flexibility in the modification of each building block before. Further, this strategy would allow a straight-forward transfer to analogues containing further modifications or simply different nucleotides. In this context, also the definition of an 'attacking' nucleophilic and 'attacked' electrophilic phosphorous species was required (Scheme 19).
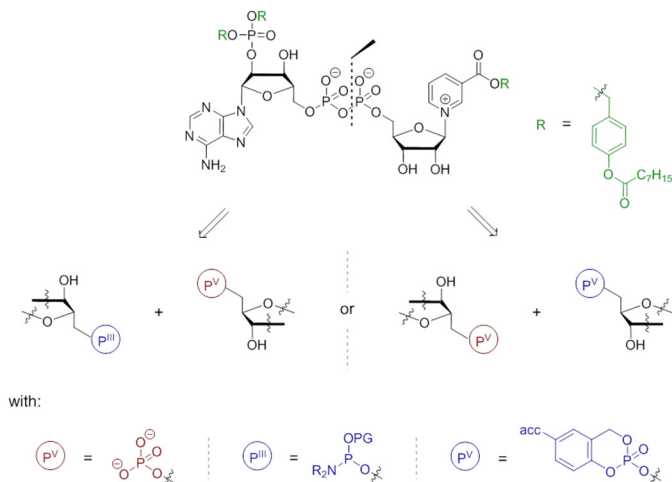


**Scheme 19:** First step of the retrosynthetic disconnection of an NAADP-AB derivative. Potential coupling methods derived were conversion of a nucleoside monophosphate with a P$^{III}$-building block (phosphoramidite) or an activated P$^{V}$-*cyclo*Sal-nucleotide.

Phosphates generally display nucleophilic properties and are therefore fit to react with an electrophile. Regarding phosphorous centers, such electrophiles constitute for instance $P^{III}$-compounds like phosphoramidites. These, however, afford an additional oxidation step subsequent to coupling to generate the corresponding phosphate. Activated $P^V$-compounds like *cyclo*Sal-phosphate triesters circumvent this and constitute thus a valuable alternative to $P^{III}$-chemistry in phosphate-phosphate coupling reactions (Scheme 19).[168,169]

For the design of routes towards the nucleotide monophosphate (NMP) building blocks of adenosine (A) and the nicotinic acid nucleoside (NAN), respectively, the order and fashion, in which the 5'-phosphorylations were performed, constituted a central aspect (Scheme 20).

Regarding the A-part, introduction of the 5'-phosphate was set last and importantly after the introduction of the 2'-bis-(OB)-phosphate (Scheme 20). Both modifications should make use of phosphoramidite chemistry as this generally goes along with high coupling rates and relatively mild reagents and conditions. A directed introduction of the phosphate moieties should be facilitated by selective protection of the respective hydroxy functions.

The NA mononucleotide (NAMN) derivative should be obtained from first 5'-phosphorylation of a selectively protected ribose building block using a phosphoramidite reagent, and second glycosylation (Scheme 20). This unusual reaction order acknowledged the concept of a late NA introduction, and thus allowed flexibility in the setup of the 5'-phosphorylation and access to the synthesis of potential analogues. Further, it accounts for the redox reactivity of NA nucleosides/-tides and its potential interference with phosphorylation methods that make use of $P^{III}$-reagents.

This approach, 1.) phosphorylation & 2.) glycosylation, required consequently a PG strategy suitable for the selective release and phosphorylation of the 5'-OH function as well as the subsequent glycosylation (Scheme 20). The strategy leading to the NAMN-building block thus strongly differed from the methodology envisaged for the synthesis of the A-building block.
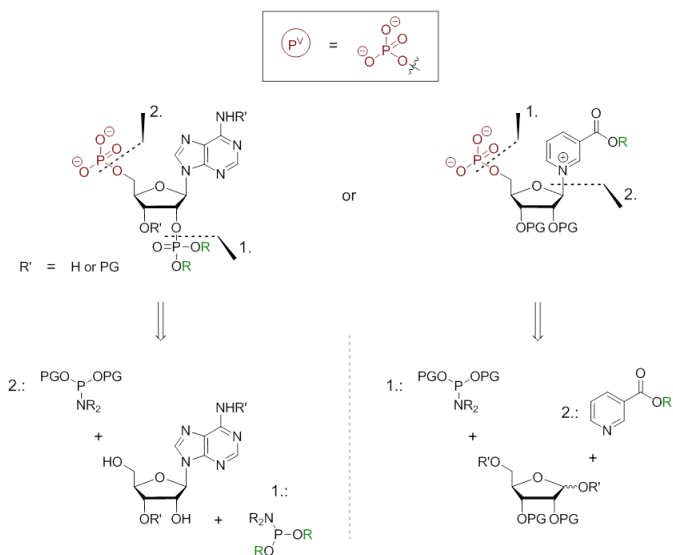
**Scheme 20:** Second step of the disconnection approach for the synthesis of nucleotide monophosphate building blocks of A and NAN. A central aspect of this stage was the order in which 5'-phosphorylation and remaining modifications would be performed.

The synthesis of an activated P$^{III}$-building block was only considered for the adenosine part as NAN was regarded unfit for phosphoramidite chemistry (mentioned above, Scheme 21).

Introduction of the P$^{III}$-moiety to the A-building block was set last, and modification of the 2'-position arranged ahead. Again, phosphoramidite chemistry should be applied. Concluded, the potential synthesis routes towards an A-5'-phosphate or -5'-phosphoramidite combined the advantage to diverge only at the very last reaction step. However, the oxidation after coupling was regarded as critical step for this P$^{III}$-based approach due to the mentioned adverse redox behavior of NA. Hence, a further approach avoiding an oxidation step was explored.

*Cyclo*Sal-nucleotides constitute electrophilic P$^V$-building blocks that exhibit high reactivity and thus would allow an oxidation-free coupling to an NAADP-AB derivative.
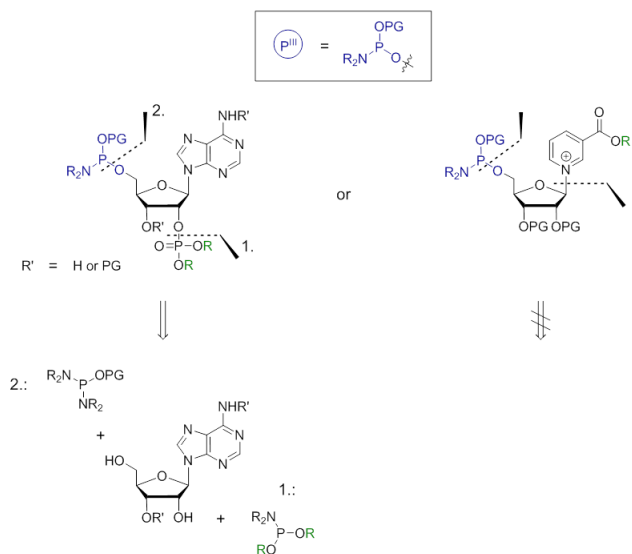
**Scheme 21:** Retrosynthetic considerations for the synthesis of a P$^{III}$-coupling partner.

A retrosynthetic analysis of potential synthesis routes was performed from both perspectives with the A- or the NAN-part being the electrophilic reaction partner (Scheme 22). In both cases, introduction of the *cyclo*Sal-moiety was set last in acknowledgment of this group's inherent high reactivity. Consequently, 2'-phosphorylation and glycosylation, respectively, were placed ahead which again required the setup of an appropriate PG strategy (Scheme 22).

Summarizing the considerations for the A-building block, the retrosynthetic analysis yielded a 2'-bis-(OB)-phosphorylated AN as central component of all routes. The building block would successively be subjected to different 5'-modifications (Scheme 23). Access to a 2'-bis-(OB)-phosphorylated AN was planned by selective 2'-phosphorylation, which would be enabled from selective 3',5'-OH protection. Here, bifunctional silyl ethers like the di-*tert*-butylsilyl- or tetra*iso*propyldisiloxanediyl-group constitute established options (Scheme 23).
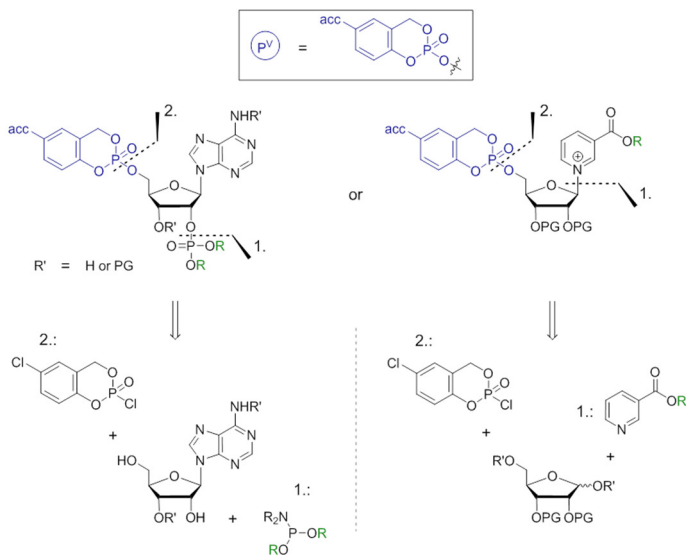
**Scheme 22:** Retrosynthetic analysis of the synthesis of *cyclo*Sal-nucleotides of the adenosine and NAN part as activated P$^V$-coupling partner.

In contrast to the A-building block synthesis, generation of a NAMN derivative or a NA-*cyclo*Sal-nucleotide appeared to require two entirely different synthesis routes including different PG strategies (Scheme 24).

For the NAMN derivative, access to the building block was expected from glycosylation of an acetylated ribose-5-bis(9-fluorenylmethyl)-phosphate using *Vorbrüggen*-conditions. The ribose-5-phosphate in turn should be obtained from phosphoramidite-based 5-modification of the appropriately acetylated ribose (Scheme 24).

Following this route, the late introduction of the labile nucleobase would constitute an advantage. However, the ultimate cleavage of the various PGs could potentially turn out critical.

**Scheme 23:** Retrosynthesis from the coupling building block to the starting material adenosine includes the 5'-modification as the last step, preceded by deprotection, 2'-phosphorylation, and selective protection of 3'-OH and 5'-OH function. Preparation of the bis-(OB)-phosphoramidite requires synthesis of the dichloro phosphoramidite and OB alcohol.

The route towards a NA-*cyclo*Sal-nucleotide afforded a different approach: 5'-phosphorylation was set last here based on the inherent lability of the *cyclo*Sal-moiety, particularly towards nucleophilic attack (Scheme 24). Accordingly, the selective deprotection of the 5'-position and glycosylation would precede. This required adaptation of the PG strategy, where silyl ethers were identified as suitable.

The realization of the different synthesis strategies is described in the following chapters.

**Scheme 24:** Retrosynthetic pathways for the synthesis of a NA-*cyclo*Sal-nucleotide and NAMN derivative.

### 8.1.3.2. Synthesis of the AB-masked adenosine building blocks

ESTABLISHMENT OF A PROTECTING GROUP STRATEGY AND 2'-PHOSPHORYLATION

The selective, simultaneous protection of 3'-OH and 5'-OH function was accessible using the *Markiewicz* reagent as well as di-*tert*-butylsilyl bis(trifluoromethanesulfonate). Starting from adenosine, the respective silyl-protected products **62** and **63** were obtained in good yields of 71% and 80%.
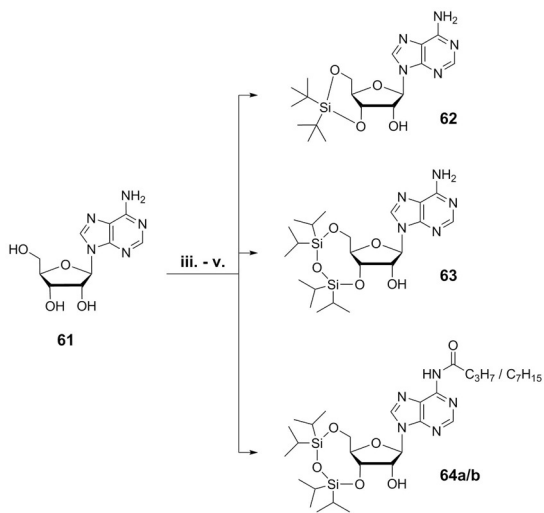
**Scheme 25:** Synthesis of the 3,5-protected adenosine building blocks: **iii.** 1.1 eq. ($t$Bu)$_2$Si(OTf)$_2$, DMF, rt, 20 h, **62**: 71%. **iv.** 1.1 eq. *Markiewicz* reagent (TIPDSCl$_2$), pyridine, -30 °C to rt, 20 h, **63**: 80%. **v.** 1$^{st}$: 1.1 eq. TIPDSCl$_2$, pyridine, -30 °C to rt, 20 h, 2$^{nd}$: 1.1 eq. TMSCl, 1.1 eq. acyl chloride, pyridine/THF 1:1, rt, 30min and 6 h, 3$^{rd}$: 4 eq. 1 – 1.2 M HCl, THF, rt, 30 – 60 min, **64a**: 56%, **64b**: 56%.

In addition to these two compounds, two mono-*N*-acylated, 3',5'- protected adenosine derivatives, **64a** (with R = C$_7$H$_{15}$) and **64b** (with R = C$_3$H$_7$), were synthesized.

The *N*-selective acylation was facilitated by transient 2'-OH-silylation using trimethylsilyl chloride (TMSCl). Removal of the TMS-group was promoted by diluted HCl. Prior attempts of restoring the hydroxy function under basic conditions or addition of methanol were not successful and revealed the silyl ether to be unexpectedly stable. Under acidic conditions however, cleavage of the silyl group proceeded efficiently within short time (30 min), but also a cleavage of the nucleobase was observed. Hence, the reaction was monitored by TLC closely and terminated once nucleobase cleavage set in notably (formation of a further new TLC spot).

Following this protocol, the *N*-butyryl derivative **64b** and *N*-octanoyl derivative **64a** were obtained in yields of 56% each.

The next step constituted the 2'-phosphorylation which was carried out using phosphoramidite (PA) chemistry.

The symmetrically OB-masked PA **68** was synthesized following established standard conditions.[158,159,162] Synthesis of the required alcohol **58** started from 4-hydroxy benzyl alcohol **65** and acid chloride **66** and gave the desired product in a competitive yield of 62% following the established standard conditions.[157–159]
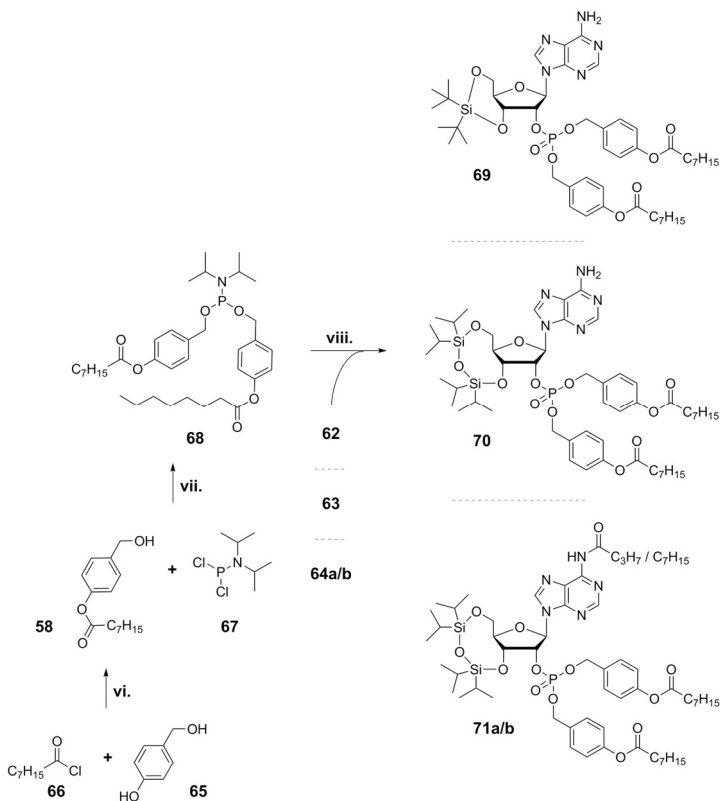


**Scheme 26:** Synthesis of the symmetrically masked OB$_2$PA: **vi.** 0.9 eq. octanoyl chloride, 1 eq. 4-hydroxy benzyl alcohol, 1 eq. TEA, THF, rt, 3 h, **58**: 62%. **vii.** 2.1 eq. **58**, 2.3 eq. TEA, THF, rt, 20 h, **68**: 63%. Synthesis of 2'-phosphorylated adenosine derivatives: 1 – 1.3 eq. OB$_2$PA **68**, 1.3 – 2 eq. DCI (0.25 M in MeCN), 1.3 – 1.5 eq. *t*BuOOH (5.5 M in *n*-decane), rt, 60 min and 30 min, **69**: 43%, **70**: 60%, **71a**: 92%, **71b**: 78%.

Successively, 2.1 equivalents of alcohol **58** were reacted with dichloro PA **67**, and the desired OB$_2$PA **68** was isolated in a yield of 63% which is comparable to those reported.[157–159]

Coupling of PA **68** and the 3',5'-protected adenosine building blocks **62** – **64b** was mediated by 4,5-dicyanoimidazole (DCI) as activator. Oxidation of the intermediate phosphites to the adenosine-2'-phosphates **69** – **71b** was achieved by *tert*butyl hydroperoxide (*t*BuOOH). [157–159]

The comparably low yield of maximum 43% obtained for **69** pointed towards steric hindrance at the 2'-position that impeded an efficient coupling of PA and nucleoside. Increasing equivalents of PA **68** or DCI did not improve the generally low conversion which further substantiated the steric-hindrance hypothesis.

In contrast, the TIPDS-protected building block **63** showed higher conversion for the coupling reaction and gave 2'-phosphate **70** in 60% yield.
Reactions of *N*-acylated adenosine derivatives **64a** and **64b** with PA **68** showed best conversions and gave phosphorylation products **71a** and **71b** in 92% and 78% yield, respectively. From these results, it was deduced that the reaction between PA and purine nucleoside additionally benefitted from protection of the NH$_2$-function.

Losses in yields, particularly for **71b**, resulted from the demanding purification by automated NP flash column chromatography. Partial co-elution of the desired product and residual phosphoramidate complicated the process, and occurred regardless of solvent composition or gradient setup. Thus, a complete separation of phosphoramidate and nucleotide was not achieved and respective mixed fractions were discarded.

In conclusion, the combination of TIPDS group for 3',5'-OH protection and acylation of the 6-amino function gave fast access to an adenosine derivative that, successively, was efficiently phosphorylated in the 2'-position in yields of up to 92%. For this purpose, phosphoramidite chemistry proved very convenient.

Subsequently, removal of the TIPDS group was investigated and turned out to constitute a first crucial step of the route towards the adenosine coupling component.
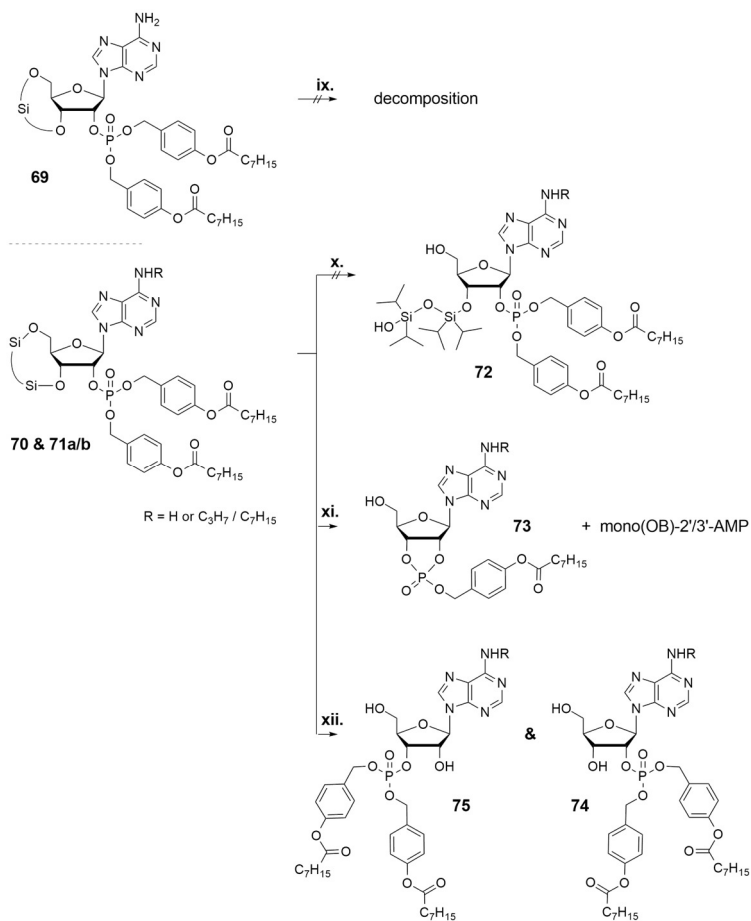
**Scheme 27:** Desilylation of **69**: **ix.** 3 eq. HF-pyridine (70:30 wt%), pyridine/dichloromethane 1:3, 0 °C to rt, decomposition. Removal of TIPDS group: **x.** TFA/H$_2$O/THF 1:1:4, 0 °C, 2 h, quenched w/ 1 pt. NaHCO$_3$ (sat. aq. sol), reverse-reaction, and inseparable mixtures of starting material and product. **xi.** 2 eq. TBAF, (4.1 eq. AcOH), THF, 0 °C to rt, 15 min to 2 h, cyclisation and OB-mask cleavage. **xii.** 12 eq. TEA · 3 HF (37 wt% in TEA), MeCN, rt, 3 h to 5 h, **74** & **75**: up to 84%.

Desilylation of the di-*tert*-butyl silyl protected derivative **69** with hydrogen fluoride pyridine (70:30 wt%) lead largely to a decomposition of the starting material, and fractions obtained from RP flash chromatography contained only traces of phosphorylated species, as concluded from NMR analysis (Scheme 27, upper part). As a consequence, di-*tert*-butyl

silyl protected building blocks were abandoned taking this result together with the difficult 2'-phosphorylation.

Selective opening of the TIPDS PG at the 5'-position giving compound **72** was investigated following a protocol reported by ZHU *et al.*[170] which used trifluoroacetic acid in water/tetrahydrofuran 1:1:4. Conversion to the desired product proceeded smoothly as indicated by TLC monitoring of the reaction course. However, while isolation and purification of the crude product, the reverse reaction to the respective starting material (**70** – **71a/b**) set in and **72** was obtained in unsatisfying yields or mixtures of product and starting material. Reasons for this could not be clearly identified. The reaction was followed by neutralization with sat. NaHCO₃ sol., extraction with dichloromethane and a further washing step with brine, before layers were separated and the organic layer was dried, concentrated and purified by NP flash column chromatography, as described in the literature.[170] Still, any of these conditions apparently promoted the nucleophilic attack of either of the formed hydroxy functions leading thus to substantial re-formation of the starting material (Scheme 27).

Adding to this outcome, further attempts to phosphorylate the 5'-position of **72** using e.g. phosphoramidite chemistry were not successful due to low conversions. Steric hindrance induced by the spacious silyl-group at the 3'-position was assumed to impede an efficient reaction at the 5'-position. Accordingly, the approach was not pursued further.

The full desilylation at 3'- and 5'-position was envisaged consequently (Scheme 27, middle part). For this purpose, a variety of reaction conditions was studied, including different fluoride sources and Lewis acids.

Treatment of silyl-protected derivatives **70** & **71a/b** with tetra-*n*-butylammonium fluoride led largely to the formation of OB-2',3'-cyclic AMP derivative **73**. Further loss of the OB-mask was observed, as well as the loss of an OB mask in combination with migration of the phosphate group from 2'- to 3'-position giving the isomers **74a** and **75a** (Scheme 27 & 28).
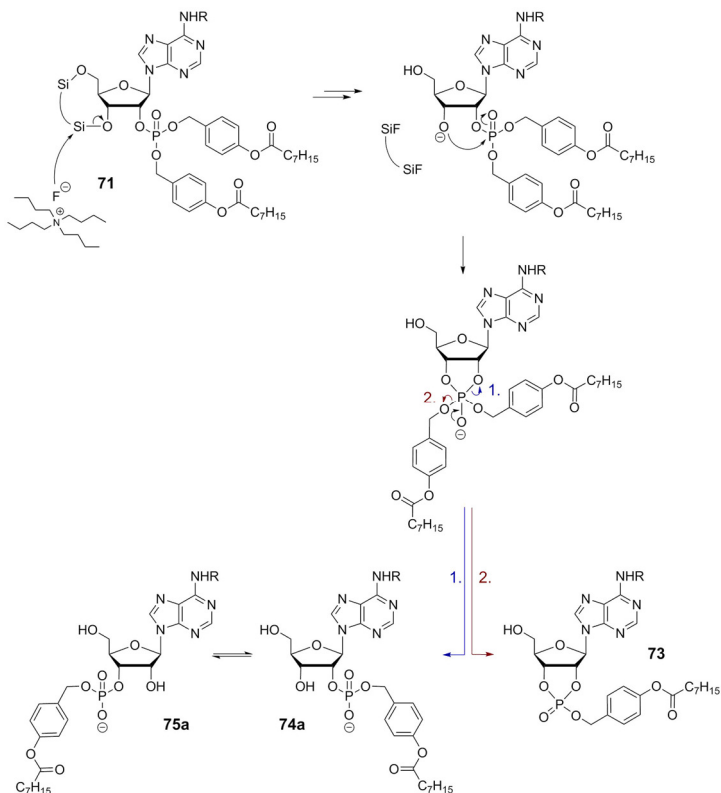
**Scheme 28**: Formation of OB-2′,3′-cyclic AMP derivative **73** and mono-OB-masked 2′/3′ AMP derivatives **74a** and **75a**. Upon nucleophilic opening of the silyl ring at the 3′-position, the 3′-oxygen attacks the adjacent phosphate group. This process is followed by either a ring-opening reaction resulting in migration of the phosphate or cleavage of one of the OB masks. Further loss of OB groups is promoted by nucleophilic attack on the respective labile positions through nucleophiles like OH (which results from residual water usually contained in TBAF solutions).

Buffering of the basic TBAF solution (1 M in THF) with AcOH, as described by Higashibayashi *et al.*, was no improvement and product fractions from RP flash column chromatography continued to consist of **74a** & **75a** and **73** and its de-masked derivative, respectively.[171]

Lewis acids like BF₃ · Et₂O, TMSI or TMSOTf were reported to mediate efficient cleavage of silyl ethers as well, and were thus included in test approaches. [172–175] However, these procedures generally promoted a complete cleavage of masks and/or decomposition of the

starting materials. Hence, further in-depth studies were ruled out. Another procedure involving *N*-iodosuccinimide (NIS) as desilylation agent was not efficient as well.[174]

Finally, the milder fluoride-source triethylamine trihydrofluoride (TEA · 3 HF)[176] enabled a complete removal of the TIPDS-group without cleavage of one of the OB-masks.

Migration of the phosphate however could not be suppressed and was likely induced by the generally acidic pH of the reagent. Accordingly, mixtures of bis-(OB)-masked 2'- and 3'-AMPs **74** and **75** with varying compositions were obtained in yields of up to 84% (Scheme 27). Losses in yield were caused by cyclisation as by-product **73** was isolated by RP purification as well. This by-product formation progressed with increasing time. As a consequence, the reaction protocol was set up as follows: upon addition of TEA · 3 HF at 0 °C, the mixture was allowed to warm to rt and the reaction course monitored by TLC. After 3 h to 5 h, the cyclisation reaction was observed to significantly gain while conversion of the starting material **71b** was incomplete still. Nevertheless, and to avoid substantial losses in yield, the reaction was terminated at this point and the crude product purified by automated RP flash chromatography. From the purification, products **74** and **75** were obtained in one single fraction. Further, the unconsumed starting material was recovered, and successively reacted with TEA · 3 HF again for maximum 5 h. Analogously, products and unconverted starting material were isolated, and the described reaction-cycle was repeated until <10% starting material were re-covered.

Following this approach, a cleavage of the TIPDS-group while maintaining all OB-masks was feasible and side reactions were reduced to a low level (down to 16%). Hence, migration of the phosphate and consequently isolation of OB-masked 2'/3'-AMP **74** and **75** as a single fraction were tolerated in turn. Moreover, separation of the regio-isomers was anticipated to be possible in the next reaction step, where the introduction of the 5'-P$^{III}$/P$^V$-group was expected to significantly influence the polarity of the isomers and as a consequence their elution behavior while chromatography.

Implementation of the 5'-phosphorylation was studied following three general and well-established concepts: the *cyclo*Sal-approach, the monophosphorylation-approach with POCl$_3$ developed by SOWA and OUCHI, and a phosphoramidite-based monophosphorylation-approach.[161,177–179]

EVALUATION OF 5′-PHOSPHORYLATION OPTIONS
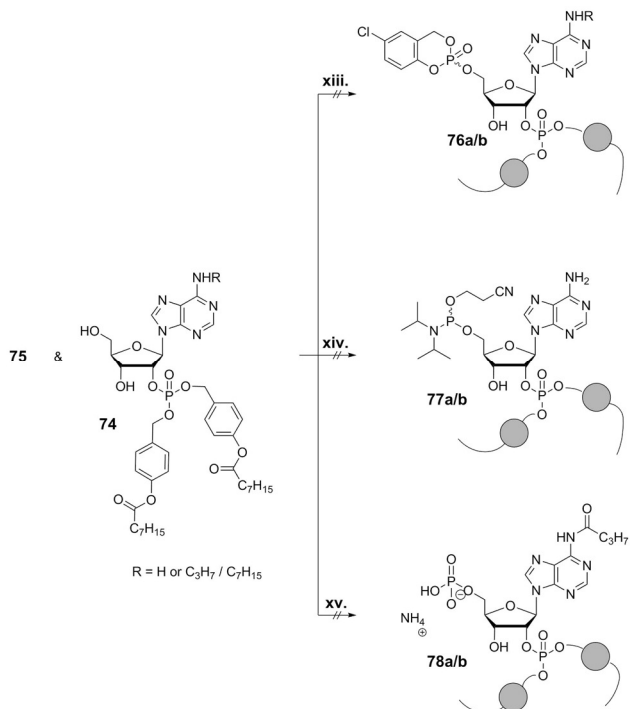


**Scheme 29:** Approaches towards 5′-P^III- or P^V-functionalized adenosine derivatives **76a/b** to **78a/b**. **xii.** 1.3 eq. 5-chloro-*cyclo*Saligenyl chlorophosphate, pyridine/THF, -40 °C to rt, 18 h, no conversion. **xiv.** 1.5 eq. 2-cyanoethoxy bis(*N,N*-di*iso*-propylamino)phosphoramidite, 2 eq. DCI (0.25 M in MeCN), DMF, rt, 25 h, no conversion; or 1 eq. 2-cyanoethoxy-(*N,N*-di*iso*propyl)chlorophosphine, 1.2 eq. TEA, THF, rt, 18 h, no conversion. **xv.** 4.4 eq. POCl₃, 4.4 eq. pyridine, 2.2 eq. water, MeCN, 0 °C, 30 min, **78a/b**: (4%).

Synthesis of *cyclo*Sal-compound **76a/b** was studied as a route towards an activated cou-pling component for conversion with a NAMN derivative (Scheme 29). The phosphorylation was carried out under mild conditions with 5-chloro-*cyclo*Saligenyl-chlorophosphate in pyridine/tetrahydrofuran. Control over the regioselectivity of the reaction should be achieved from addition of the reagent at low temperatures (-40 °C). However, no conver-sion was detected, and thus the temperature was allowed to stepwise warm up to rt.

Still no conversion of the starting material was observed from TLC monitoring and accordingly, from the crude mixture obtained from evaporation no product was isolated.

Synthesis of phosphoramidites **77a/b** was studied on two ways, making use first of cyanoethoxy bis(*N*,*N*-di*iso*propylamino)phosphoramidite and second of 2-cyanoethoxy-(*N*,*N*-di*iso*propyl)chlorophosphine (Scheme 29).

The phosphordiamidite-based approach proved insufficient as no conversion of the starting materials was seen by TLC monitoring. Accordingly, the more reactive chlorophosphine was studied in a next reaction. Again, conversion was low and formation of the desired product proceeded poorly as concluded from crude $^1$H- and $^{31}$P-NMR spectra. Instead, $^{31}$P-NMR signals in the range of phosphites and activated phosphoramidites constituted the main components of the crude reaction mixture. These signals could indicate a self-induced phosphoramidite coupling-like side-reaction resulting in cyclisation reactions involving the 5'- and 3'-positions.

Taking these attempts towards activated P$^{III}$- or P$^v$-adenosine coupling components in total, an efficient synthesis of any of these was not achieved. Consequently, the focus was set on the synthesis of a 5'-monophosphate which would instead constitute the nucleophilic building block in coupling reactions with a respective electrophilic NAMN derivative.

The monophosphorylation according to SOWA and OUCHI was carried out precisely as described by the authors for natural ribonucleosides (Scheme 29).[178] However, the respective products **78a/b** were obtained only in unsatisfying 4% yield and as an inseparable mixture of regioisomers after purification of the crude product by automated RP flash chromatography. Consequently, this approach was not pursued further since the obtained yield was unsatisfying and a separation of 2',5'- and 3',5'-adenosine-bis(OB)-bis phosphates was not feasible.

The consecutive approach included phosphoramidite chemistry making use of a bis(9*H*-fluoren-9-ylmethyl)-protected phosphoramidite (Fm$_2$PA). With this, a stepwise synthesis of the desired product **79** was anticipated as 1.) synthesis and purification of the protected bis(Fm)-5'-monophosphate should be performed and 2.) removal of the Fm-PGs under

anhydrous mild basic conditions (Scheme 30). This concept was presented for the synthesis of di- and triphosphates by CREMOSNIK *et al.* and refined further by HUCHTING et al.[179,180]

Conversion of the protected 5'-monophosphate **79a** was performed under standard conditions with DCI as activator and *t*BuOOH as oxidizer.[157–159,180] The obtained crude product was re-solved in dichloromethane and washed with aq. NH$_4$OAc (1 M) and water to remove DCI-salts and, by this, simplify the successive purification via automated NP flash chromatography (MeOH gradient in dichloromethane, 0% to 10%). As anticipated and indicated from TLC monitoring while reaction, the elution behavior of the Fm-protected 2',5'- and 3',5'-bisphosphates differed so that a sufficient separation of the regioisomers was possible at this stage. It also became apparent, that 3'-bis-(OB)-phosphate **75b** was converted to a lower extend than **74b**, presumably due to steric interference between the adjacent spacious OB- and Fm-groups.

The almost regioisomerically pure, protected bisphosphate **79a** was successively treated with TEA in acetonitrile (10 vol%) under anhydrous conditions to remove the Fm-groups without affecting the OB-esters at the 2'-phosphate.
Upon completion of this reaction, the crude product was purified by automated RP flash column chromatography which afforded pure product **79** in a yield of 16% over two steps (Scheme 30, Fig. 20).

The seemingly low yield was based first of all on the starting material being a 1:1 mixture of 2'- and 3'-phosphate on average. In addition, coupling between nucleotide and Fm$_2$PA did not go to completion for both regioisomers which caused further decreases in yield. These were complemented lastly by two successive and each demanding purification processes.
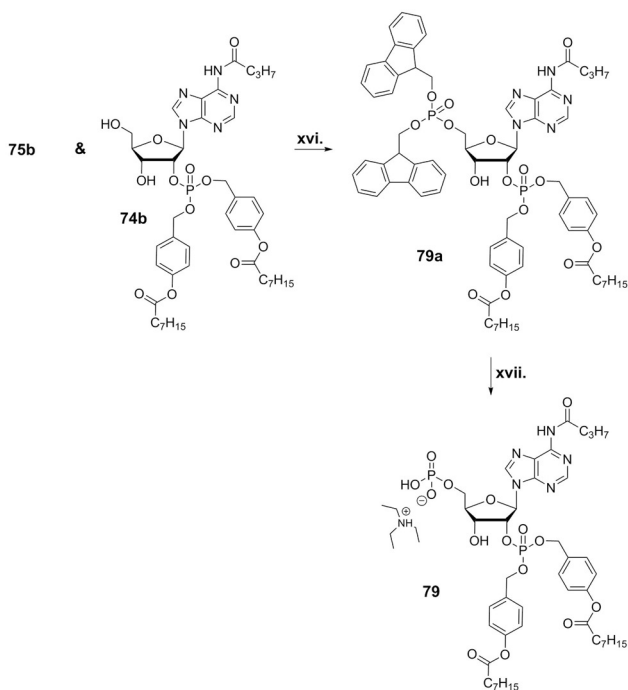
**Scheme 30:** Stepwise synthesis of $N^6$-butylamino adenosine bis-(2'-bis-(OB))-5'-phosphate **79**: **xvi.** 1.2 eq. Fm$_2$PA, 1.5 eq. DCI (0.25 M in MeCN), 1.5 eq. $t$BuOOH (5.5 M in $n$-decane), MeCN, rt, 60 min. **xvii.** 10 vol% TEA in MeCN, rt, 20 h, **79**: 16 % over two stages.

Importantly, following the described approach, the preparation and isolation of the first coupling component for synthesis of an OB-masked NAADP derivative was accomplished and pure adenosine-2'-bis-(OB)-5'-bisphosphate **79** obtained.

In summary, the adenosine building block **79** was synthesized successfully over four steps starting from adenosine, which was first protected selectively in the 3'- and 5'-position as well as the 6-amino function. Successively, the 2'-phosphorylation was conducted using phosphoramidite chemistry and was followed by 3',5'-desilylation. Lastly, the 5'-mono-phosphorylation was successful using phosphoramidite chemistry again.
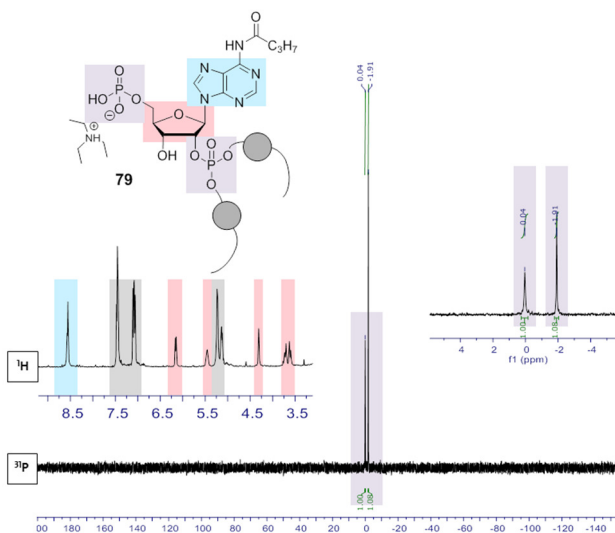
**Figure 20:** $^1$H- and $^{31}$P-NMR spectra (MeCN-d$_3$, 400 MHz & 162 MHz, 25 °C, shifts δ in [ppm]) of $N^6$-butanoyl adenosine-bis-(2'-bis-(OB))-5'-phosphate **79**. Signals of phosphates are highlighted in violet; proton signals of the ribose core are highlighted in red, proton signals of the nucleobase framed in blue and proton signals of the OB-mask in grey.

The complementing NAMN building blocks were studied in parallel and synthesis strategies towards NAN monophosphate as well as activated NAMN derivative were investigated accordingly.

### 8.1.3.3. Approaches towards masked NAMN derivatives

The first route towards the labile nucleotide (s. section 8.1.3.) envisaged the synthesis of a NAMN derivative following an approach where the 5'-phosphorylation preceded the glycosylation reaction (Scheme 31). The rather unusual reaction order was chosen since by this, the above discussed redox-reactivity and acid-sensitivity of the NA nucleobase was acknowledged. Simultaneously, it was profited from the generally higher reactivity of P$^{III}$-reagents as opposed to P$^V$-reagents. In addition, introduction of the nucleobase at a later stage of the synthesis sequence allowed a broader scope of synthesis conditions during earlier steps (compare w/ section 8.1.3.1.).

The synthesis of OAc- and Fm-protected ribose monophosphate **84** proceeded smoothly over three steps starting from D-ribose (Scheme 31). Conveniently, the separation of anomers was not necessary during any of these stages as the C1 configuration was irrelevant for the successive step, the glycosylation with NA benzyl ester (NA-OBn) **83**. The preparation of protected ribose phosphate **84** was therefore attractive even in bigger scales (2 – 30 mmol) since purifications were convenient to perform (one NP column chromatography sufficed) and each respective starting material easy to access.

*Vorbrüggen*-type reaction conditions facilitated the successive introduction of the NA nucleobase as anticipated by the choice of PGs.

Hence, NA-OBn **83** and ribose monophosphate **84** were reacted in the presence of TMSOTf as Lewis acid to yield the desired protected NAMN **85** as pure β-anomer and in good yields of up to 76%.
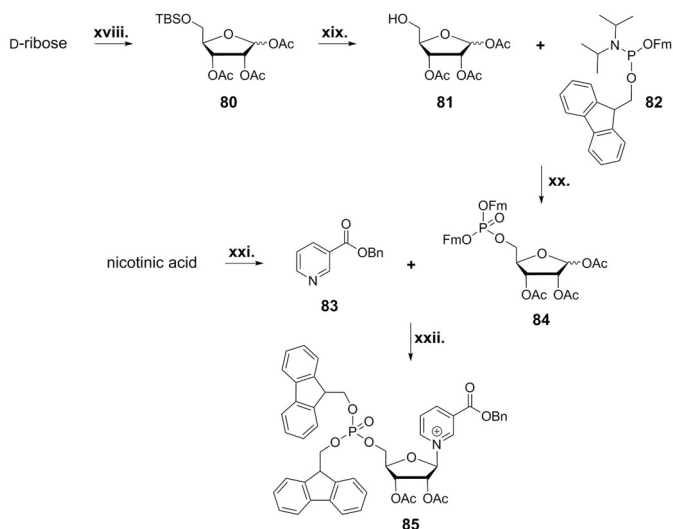


**Scheme 31:** Synthesis route towards the protected NAMN derivative **85**: **xvii.** 1.3 eq. TBSCl, 9 eq. acetic anhydride, pyridine, rt, 20 h, **80**: 63%. **xix.** 3 eq. TEA · 3 HF, dichloromethane, rt, 5 h, **81**: 87%. **xx.** 1.3 eq. Fm₂PA, 1.3 eq. DCI (0.25 M in MeCN), 1.3 eq. *t*BuOOH (5.5 M in *n*-decane), dichloromethane, 60 min, rt, **84**: 97%. **xxi.** 1 eq. benzyl bromide, 1.1 eq. TEA, THF, rt, 18 h, **83**: 33%. **xxii.** 1.4 eq. **83**, 1 eq. **84**, 1.2 eq. TMSOTf, MeCN, rt, 3 h, **85**: 76%.

Summarizing these four steps, the inverted standard procedure (first phosphorylation, second glycosylation) allowed efficient synthesis of the protected NAMN derivative **85**. Considering also the convenient preparation of the ribose monophosphate, an application of the re-ordered procedure on further nucleotides could be attractive since phosphorylation often constitutes a limiting step within the synthesis sequence towards a respective NMP.

A second glycosylation protocol using 1,1,1,3,3,3-hexamethyldisilazan (HMDS) as silylating agent and tin(IV)chloride as Lewis acid was applied and allowed the use of unprotected NA. The desired product **86** was obtained in a lower yield of 27% compared to 76% for **85** due to poorer conversion. In addition, the anomeric ratio of α/β 1:9 was not as satisfying as for the reaction mediated by TMSOTf (only β-NAMN isolated).
Nonetheless, this glycosylation procedure was as well applied successfully on the phosphorylated riboside **84** and thus underlined the versatility the building block offers for further conversion to NMPs.
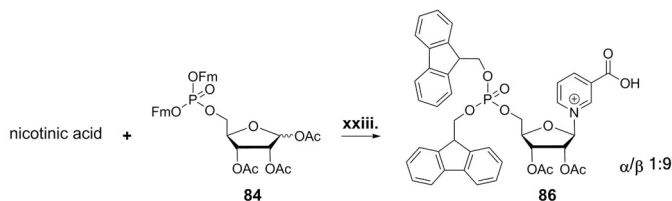


**Scheme 32:** Alternative synthesis of a NAMN with the unprotected NA: **xxiii.** 1 eq. **85**, 1.4 eq. NA, 2.5 mL/mmol (NA) HMDS, 1.4 eq. SnCl$_4$, MeCN, first reflux, then rt, 4 h, **86**: 27%.

The successive deprotection of ester-protected nucleotides is in general performed using e.g. triethylamine in acetonitrile or methanol and water, or ammonia in methanol. These conditions are well tolerated by most nucleobases and nucleotides.
In the case of NAMN, aqueous basic conditions were to avoid based on the lability of the glycosidic bond (compare 8.1.3.1.). Accordingly, milder deprotection protocols were studied for **85**.
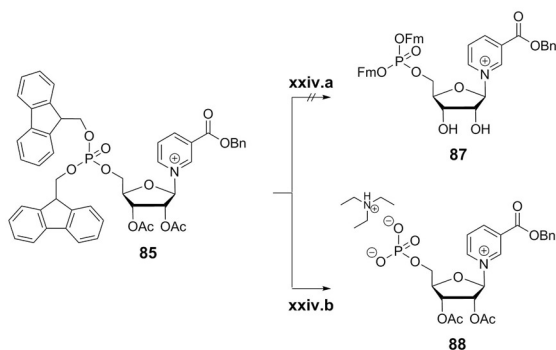
**Scheme 33:** Deprotection approaches towards partially unprotected NAMN **86** and **87**: **xxiv.a** 0.5 eq. Bu$_2$SnO, MeOH, rt to reflux, 30 min, **87**: decomposition. **xxiv.b** TEA in MeCN (4 - 25 vol%), rt, 5 h, **86**: (41%).

Removal of OAc-groups was attempted following a method reported by L$_{IU}$ *et al.* who used dibutlytin oxide (Bu$_2$SnO) in methanol for a mild and neutral transesterification applicable also on nucleophile-sensitive, multifunctional starting materials, e.g. the ribonucleoside of favipiravir.[181,182]

However, in the case of NAMN **85**, the reaction conditions promoted decomposition of the nucleotide as indicated by NMR-analysis of the fractions obtained from automated NP flash chromatography.

Removal of Fm-groups from the phosphate of **85** was performed similarly as for adenosine-2'-bis-(OB)-5'-bis(OFm)-bisphosphate **79a** in acetonitrile with triethylamine (4 – 25 vol%) under anhydrous conditions. The desired product was formed and isolated in a yield of 41%, but a complete purification of monophosphate **88** was not achieved since significant traces of cleaved nucleobase co-eluted during RP chromatography. Varying the amount of triethylamine did not improve the reaction course and cleavage of NA continued to occur. Also, no optimization of the purification was achieved by variation of the gradient or solvent composition while automated RP flash column chromatography.

In summary, an efficient deprotection protocol for all PGs of NAMN **85** could not be developed since the tested conditions promoted decomposition of the nucleotide which took place preferably by cleavage of the glycosidic bond.

Thus, access to NAN monophosphate **88** was gained, but a complete purification of the compound was not possible, likely due to salt-formation between phosphate and cleaved nucleobase.

In complementation, the synthesis of a potential coupling partner, namely the *cyclo*Sal-phosphate **76a/b**, was neither successful.

The further focus was consequently set on the synthesis of an electrophilic $P^V$-NAMN-derivate. Also, the PG strategy was redesigned since the former concept was not compatible with the inherent limitations given by NAN. Nonetheless, any potential PG strategy was required to be compatible with glycosylation reactions as well as partial or full removal of PGs under mild conditions.

An approach including per-TBS protected ribose as a starting point was considered based on the following observations: from studies on bis-(OB)-masked 2'- and 3'-AMPs **74** and **75** (s. section 8.1.3.2.) it was known that OB groups, which were envisaged to mask the carboxylic acid of NA, tolerated desilylation with TEA · 3 HF. These slightly acidic conditions were hypothesized to also be applicable on NAN as the positive charge at the nucleobase was reasoned to have a delaying effect on glycosidic bond hydrolysis here. Lastly, Baldoni and Marino reported an efficient glycosylation method that used per-TBS protected sugars as starting material and TMSI as promoting reagent.[183]

Accordingly, fully protected ribose **89** was synthesized (Scheme 34). Conducting the reaction with TBSCl and imidazole in DMF at rt, as described in the literatur,[184] led to the formation of a mixture of pyranose and furanose-form. This mixture was demanding to purify and thus, significant loss in yield was caused. This outcome was improved when the addition of the reagents was carried out slowly and at 0 °C. By this, pure β-ribofuranoside **89** was obtained in 67% yield from one single NP column chromatography. The improved selectivity was likely based on a preferred formation of the kinetic furano-product at the low temperatures. The predominant formation of the β-anomer was deduced to also rely on kinetic preference resulting from a higher nucleophilicity of the β-furano oxide compared to the α-oxide. Similar effects were observed for e.g. pyranosyl-trichloroacetimidate-formations under mild basic conditions.[185]

NA ester **90** was prepared from NA chloride and alcohol **58** under similar conditions as applied for synthesis of **58** itself and obtained in a yield of 46%. Successively, NA-OB ester **90** was converted with riboside **89** (Scheme 34). The glycosylation was performed in a *one pot* reaction and initiated by generation of the corresponding ribofuranosyl-iodide using TMSI at low temperatures (-30 to -50 °C). After 10 to 30 min, NA-OB ester **90** and triethyl-amine were added to the intermediate ribosyl iodide.
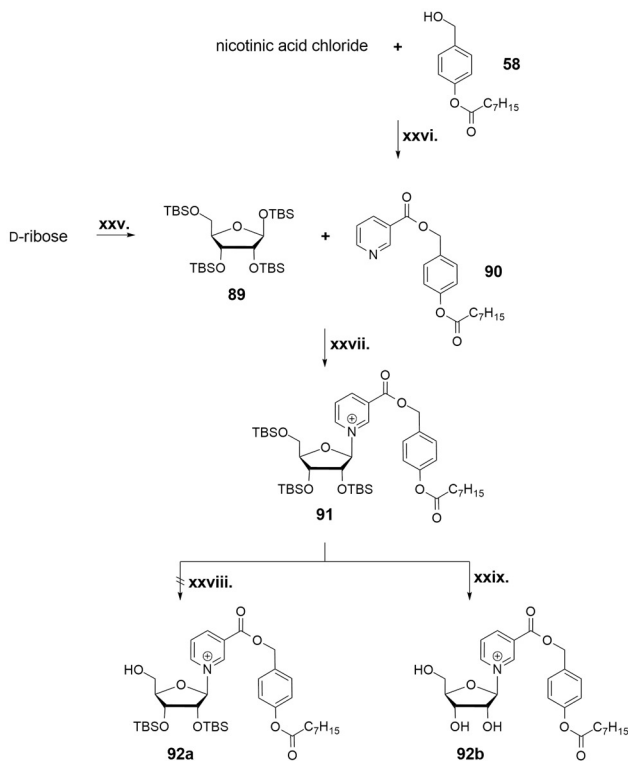


**Scheme 34**: Synthesis route towards NAN-OBs **92** and **93**: **xxv.** 5 eq. imidazole, 5.6 eq. TBSCl, DMF, 0 °C to rt, 48 h, **89**: 67%. **xxvi.** 2 eq. TEA, 0.9 eq. **58**, cat. DMAP, THF, rt, 4 h, **90**: 42%. **xxvii.** 1 eq. **89**, 1.2 eq. **90**, 1.1 eq. TMSI, 2.4 eq. TEA, -50 °C to rt, 3 h, **91**: quantitative. **xxviii.** 4 eq. TEA · 3 HF, MeCN, rt, 5 h to 18 h, decomposition. **xxix.** TEA · 3 HF/MeCN 10 vol%, rt, 85 h, **92b**: 60%.
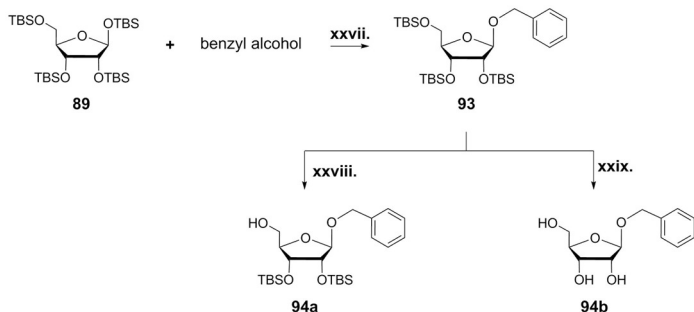
**Scheme 35:** Synthesis of fully, partially and unprotected 1-*O*-benzylated ribosides **93**, **94a** and **94b**: **xxvii.** 1 eq. **89**, 1.2 eq. benzyl alcohol, 1.1 eq. TMSI, 2.4 eq. TEA, -50 °C to rt, 3 h, **93**: quantitative. **xxviii.** 4 eq. TEA · 3 HF, MeCN, rt, 5 h to 18 h, **94a**: 46%. **xxix.** TEA · 3 HF/MeCN 10 vol%, rt, 85 h, **94b**: quantitative.

Upon consumption of the starting materials (monitored by TLC), the reaction was terminated by addition of aq. NH$_4$OAc (1 M). After an aqueous work up and NP flash column chromatography, the fully protected NAN-OB **91** was obtained in up to quantitative yield and as single anomer.

The observed anomeric selectivity of the reaction was confirmed by synthesis of two further ribosides carrying an OB-group (s. section 8.2.2.1) and benzyl alcohol as aglycone (Scheme 35). During the respective reactions, only one new compound was formed out of the intermediate ribofuranosyl-iodide and the respective aglycone (TLC control). Furthermore, only one isomer was contained in the product fractions obtained from NP column chromatography. The isolated ribosides were identified as the β-anomers, lastly from NOESY-NMR analysis.

The full or partial removal of TBS groups was investigated subsequently using TEA · 3 HF as desilylating agent. For 1-*O*-benzylated riboside **93**, the 5-OH as well as complete desilylation proceeded smoothly, and the respective products **94a** and **94b** were isolated in decent to excellent yields of 46% and 100%, respectively (Scheme 35). The comparably low yield for **94a** resulted from incomplete conversion of the starting material which, however, was recovered while NP flash column chromatography so that a further desilylation cycle could be pursued and yields increased.

In summary, synthesis of a 5-O-unprotected as well as fully unprotected riboside was feasible so that the PG strategy met the sought requirements. Accordingly, the reaction conditions were transferred on NAN **91**.

Treatment of NAN **91** with TEA · 3 HF lead to a large extent to the formation of one new compound (TLC control). However, the newly formed compound assumed to be **92a** could not be isolated since it decomposed while evaporation of volatile parts from the reaction mixture and/or successive NP column chromatography. Consequently, product fractions contained a mix of components.

NMR-analysis of these fractions indicated an extensive cleavage of the glycosidic bond which could result from either too acidic pH or an intramolecular attack of the free 5'-OH group at the anomeric carbon atom leading to the 1,5-anhydro derivative (Scheme 36). Similar side-reactions were reported by BALDONI and MARINO for their glycosides as well.[183]

The fully unprotected NAN-OB **92b** was successfully obtained from treatment of precursor **91** with 10 vol% TEA · 3 HF in acetonitrile at rt over 85 h. The crude reaction product was purified by automated RP flash column chromatography and yielded the desired nucleoside **92b** in up to 60% yield (Scheme 34, Fig. 21).

Partial but minor decomposition of the nucleobase caused losses in yield. However, the successful isolation and purification of NAN-OB **92b** proved lastly the applicability of the PG concept on the sensitive nucleoside. The glycosylation went along with excellent conversion leading to quantitative yields for this step, the desilylation conditions were feasible and the purification by RP column chromatography was efficient with one column sufficing. This gave the masked nucleoside overall in high purity and satisfying amounts (Fig. 21).
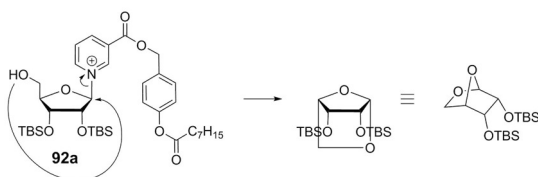


**Scheme 36:** Mechanism of the potential side reaction leading to an 1,5-anhydro-riboside derived from **92**.
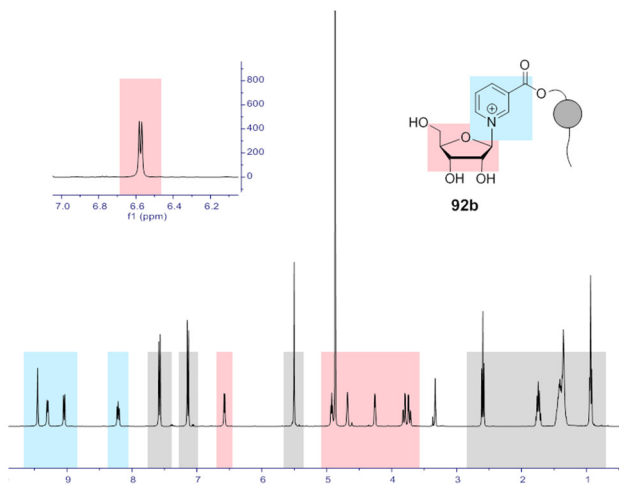
**Figure 21:** $^1$H-NMR spectrum (MeOD, 400 MHz, 25 °C, shifts δ in [ppm]) of NAN-OB **93**. Proton signals of the ribose core are highlighted in red, proton signals of the nucleobase framed in blue and signals of the OB-mask in grey.

The synthesis of an activated $P^V$-coupling partner for adenosine-2'-bis-(OB)-5'-bisphosphate **79** was studied successively.

The *cyclo*Sal approach was chosen as it enables the oxidation-free preparation of electrophilic $P^V$-building blocks under relatively mild conditions. Furthermore, the regio-selectivity of the reaction can be controlled and guided towards the 5'-OH group of unprotected nucleosides at low temperatures ($\sim$ -30 °C).[186,187]

Hence, NAN-OB **92b** was converted with 5-chloro-*cyclo*Saligenylchlorophoshpate.
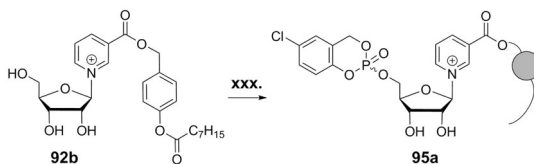


**Scheme 37:** Synthesis conditions for the preparation of *cyclo*Sal-phosphortriester **95a**: **xxx.** 1 – 1.3 eq. 1-methyl imidazole, 1.2 – 1.3 eq. 5-chloro-*cyclo*Saligenyl chlorophosphate, (1.2 eq. TEA), DMF or acetonitrile plus 5% pyridine, -30 °C – rt, 5 – 7 h, n.d., **95a** was used crude in the subsequent reaction.

In a first attempt, the reaction was carried out in DMF and the addition of 5-chloro-*cy-cloSaligenyl* chlorophosphate was performed at -30 °C. To accelerate conversion, 1-methyl imidazole and triethylamine were added. The reaction was allowed to slowly reach rt, and was terminated after 5 h by removal of all volatile components.

The second reaction protocol used acetonitrile plus 5% pyridine as solvents and waived triethylamine. Addition of the *cycloSal-*reagent was done again at -30 °C, and the reaction was successively stirred 7 h while slowly warming up 0 °C. Removal of all volatile components terminated the reaction.

In both cases, $^{31}$P-NMRs of the obtained crude residues were recorded (Fig. 22).
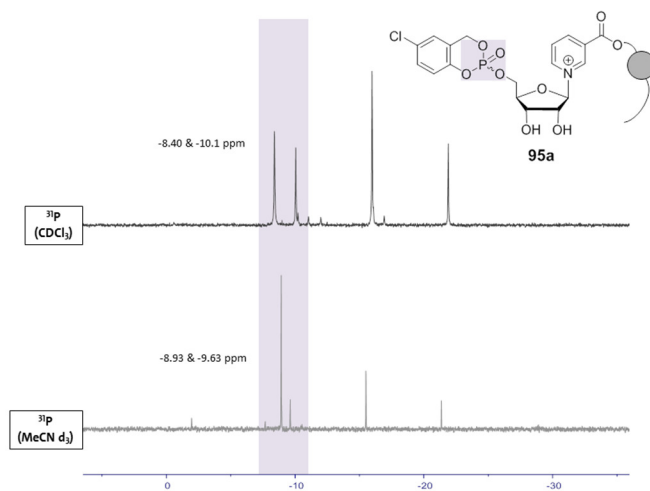


**Figure 22:** $^{31}$P-NMR spectrum (CDCl$_3$ and MeCN d$_3$, 400 MHz, 25 °C, shifts δ in [ppm]) of crude reaction mixtures of **95a**. Despite different solvents, a similar signal pattern was observed for phosphorous signals. Typically, phosphorous signals of *cyclo*Sal-nucleotides give chemical shifts in the respective $^{31}$P-NMR spectra between -8.0 to -11 ppm.[186,187]

Despite the use of different solvents (due to solubility issues), similar signal patterns were found in the $^{31}$P-NMR spectra and two signals featuring shifts in the range reported for *cyclo*Sal-nucleotides were prominent (Fig. 22).[186,187]

Encouraged by this finding, purification of the crude product was attempted by NP column chromatography with a methanol gradient in dichloromethane containing 1% acetic acid to stabilize the *cyclo*Sal-triester. However, no product was isolated and instead compound-containing fractions comprised cleaved mask only. It was assumed that

decomposition due to too acidic pH or adsorption to the stationary phase due to too high polarity impeded the purification of the crude product **95a**.

Consequently, the crude reaction mixture of **95a** was applied together with monophosphate **79** in a coupling attempt. Both reagents were thoroughly dried under high vacuum prior to reaction and stored over molecular sieves for 2 h additionally. Then, the in DMF solved reaction partners were mixed and reacted with another at rt for 48 h. Successively, all volatile components were removed under high vacuum, and the crude residue obtained was analyzed $^{31}$P-NMR spectroscopically.
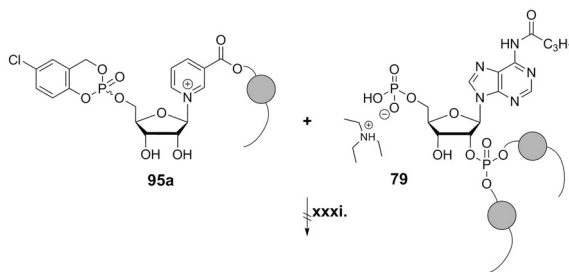


**Scheme 38:** Attempted coupling reaction towards OB-masked NAADP: **xxxi.** DMF, rt, 48 h, no conversion.

The desired product, however, was not formed and no signals indicating the formation of a diphosphate were found. Unsatisfyingly, hints towards impeding factors or side-reactions could neither be drawn clearly from the $^{31}$P-NMR spectrum. Mass spectrometric analysis hinted towards cleavage of the nucleobase. Further, peaks for unreacted monophosphate **79** could be assigned.

Subsumed, synthesis attempts towards *cyclo*Sal-NAMN-OB **95a** went along with the drawbacks that purification of the crude reaction mixture and accordingly definite identification of **95a** were not possible, and that a direct conversion of the crude product with monophosphate **79** failed.

The PG-free approach towards the *cyclo*Sal-nucleotide was consequently rated inefficient, and an alternative protocol including PGs was studied. Further, the order of

phosphorylation and glycosylation was intended to be inverted again to acknowledge the ever-present lability of NA as nucleobase.

For this purpose, the selectively desilylated riboside **94a** was first converted into the *cyclo*Sal-(ribose-5)-phosphate **94c** following standard conditions (Scheme 39).[186,187] The *cyclo*Sal-compound was obtained as a mixture of diastereomers in 39% yield after purification by column chromatography.

The successive step was designed to include a *one pot* debenzylation followed by glycosylation with NA-OB **90** (Scheme 39). Both steps should be promoted by TMSI which proved to mediate glycosylation and cleavage of benzyl groups efficiently in previous own studies (s. chapter 5.3.3.1. & 8.1.3.3, synthesis of **93**).

Accordingly, *cyclo*Sal-(ribose-5)-phosphate **94c** was treated with a first portion (1.1 equivalents) of TMSI at -50 °C to rt over 4 h for debenzylation. NA-OB **90**, triethylamine and further 1.1 equivalents TMSI were added successively at low temperatures for glycosylation of the expected intermediate 1-*O*-TMS-ribose-5-phosphate. $^{31}$P-NMR spectroscopic analysis of the crude reaction mixture prompted the further purification of the crude mixture.
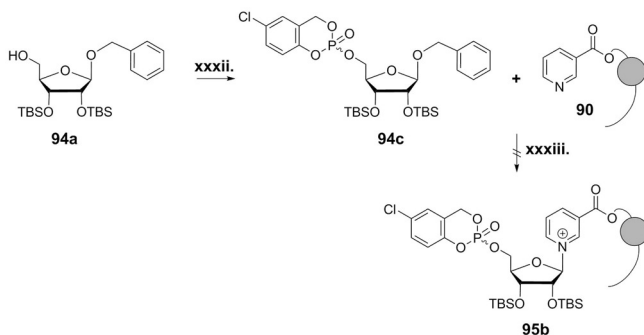


**Scheme 39:** Alternative approach towards a *cyclo*Sal-NAMN: **xxxii.** 1.2 eq. 5-chloro-*cyclo*Saligenyl chlorophosphate, pyridine, -30 °C to rt, 4 h, **94c**: 39%. **xxxiii.** 2.2 eq. TMSI, 2.4 eq. TEA, 1.2 eq. **90**, dichloromethane, -50 °C to rt, **95b**: -.

However, after a quick aqueous work up and automated NP column chromatography, the desired product was not isolated. Fragments of NA and silylated ribose were obtained instead but no phosphor-containing species were found.

The approach did not facilitate the synthesis of *cyclo*Sal- NAMN-OB **95b** and, thus, the synthesis of a coupling partner for monophosphate **79** was not completed.

Nevertheless, several conclusions and indications for optimization of approaches towards nucleophilic and/or electrophilic phosphorous NAN-building blocks were drawn from the different syntheses routes investigated.

The first approach towards fully protected NAMN **85** showed that glycosylation reactions in the presence of a protected phosphate group are feasible, and nucleotide **85** was isolated in yields up to 76% with excellent β-selectivity.

The choice of PGs, however, needed adaption, and TBS-ethers in combination with a TMSI-driven glycosylation were found to enable the efficient synthesis of silyl-protected NAN-OB **91** in quantitative amounts. The removal of silyl ethers using TEA · 3 HF was feasible and NAN-OB **92b** repeatedly synthesized successfully in yields up to 60%.

The preparation of a *cyclo*Sal-NAMN was not achieved satisfyingly.

In summary, the syntheses of a carboxyl-modified NA nucleoside and protected NA nucleotide were achieved. Pursuing these approaches further, very mild deprotection or phosphorylation protocols likely facilitate access to NAMN-building blocks suitable for coupling reactions. The coupling of two phosphates is for example successfully used in the approach towards Tri*PPP*ro-compounds where an activated masked pyrophosphate reagent is converted with a NMP.[164] In analogy to this procedure, first adenosine-2'-bis-(OB),5'-bisphosphate **79** could be activated with trifluoroacetic anhydride and 1-methyl imidazole, and second a NAMN would be added.

Subsumed, the synthesis of modified NA nucleotides and, overall, modified NAADP derivatives apparently requires elevated considerateness and unconventional approaches in the design and setup of synthesis routes. Against this backdrop, the developed protocols constitute a valuable basis for the further development of the total synthesis approaches towards NAADP-ABs.

## 8.2. Total synthesis approach towards AB-masked (d)ADPR derivatives

The total synthesis of (d)ADPR-AB derivatives was explored as such compounds would constitute interesting biologically inactive precursors of the important yet little studied second messengers dADPR and ADPR for non-invasive cell studies.

Again, key aspects of the conceptualization were the defined positioning of AB-masking groups within a convergent synthesis strategy to allow for a flexible alignment of moieties. Accordingly, the development approach chosen for (d)ADPR-AB synthesis started with a retrosynthetic analysis of the anticipated target structures.

### 8.2.1. Retrosynthetic analysis of routes towards (d)ADPR-AB

The AB-derivatives of ADPR and dADPR were envisaged to carry one AB-unit at one of the phosphates of the pyrophosphate backbone to neutralize and mask the negative charges. A further AB-group was planned to occupy the anomeric hydroxy group of the ribose in order to block the reactive position during synthesis and to convey additional lipophilicity (Scheme 40).

Similar as for NAADP-AB, a convergent approach was chosen to increase the flexibility of the synthesis route and to broaden the possible scope of reaction conditions for the various envisaged modifications.

Consequently, the first disconnection set at the pyrophosphate moiety led to two building blocks that would be coupled to yield the respective (d)ADPR-OB derivative at a late stage of the synthesis sequence. Hence, an electrophilic and a nucleophilic phosphorous species were required as coupling components. For the latter, the synthesis of a respective phosphate was envisaged. The former was planned to compose a $P^{III}$-building block since these usually show higher reactivity and therefore better coupling rates. Further, oxidation was not regarded detrimental for the targeted molecules (Scheme 40). Another advantage in this context was the possibility to alternate the order of nucleophilic and electrophilic coupling component.

Thus, the synthesis of the respective building blocks was drafted in two versions (Scheme 40).
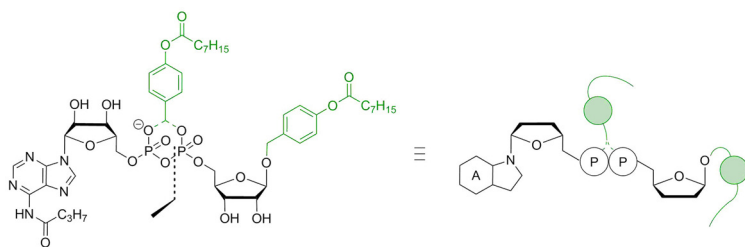
**AB-masked ADPR**
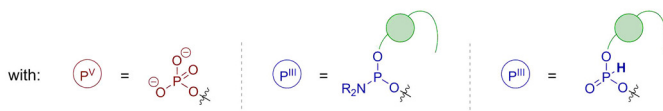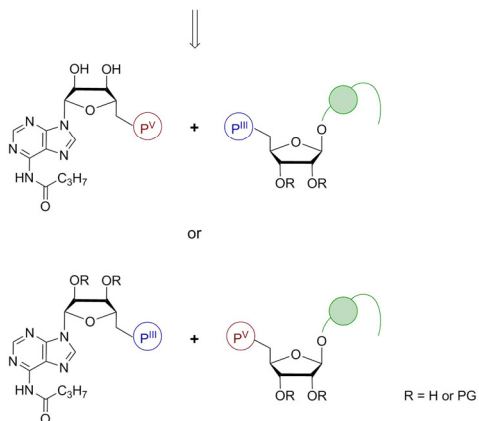
**Scheme 40:** Retrosynthetic analysis of approaches towards (d)ADPR-AB derivatives. The disconnection for a convergent approach was set within the pyrophosphate bridge to give two phosphorous-containing building blocks derived from adenosine and ribose, respectively. Efficient coupling was expected from a combination of nucleophilic $P^V$- and electrophilic $P^{III}$-species. Hence, a phosphate group was identified as a suitable nucleophile whereas a non-symmetric phosphoramidite or H-phosphonate constituted the $P^{III}$-moiety. Both building blocks displayed no lability towards oxidation so that the functionalization to the $P^{III}/P^V$-compound was invertible.

### 8.2.2. Routes towards AB-riboside and adenosine coupling partners

The synthesis routes towards the respective $P^{III}$- and $P^V$-coupling pairs were explored in parallel. Prior to this, a suitable protection group strategy allowing for site-specific modification and deprotection of the ribose-moiety was elaborated.

### 8.2.2.1. Synthesis of 1-*O*-AB-masked ribosides as precursors for $P^{III/V}$-modification

The protecting group strategy developed for NAN-OB **91** was used since similar criteria as for the synthesis of **91** applied for the ribose building block (Scheme 41).

Accordingly, per-TBS protected ribose **89** was reacted with TMSI first and second with alcohol **58** in the presence of TEA to give the riboside **96** in up to quantitative yield. Treatment of **96** with different amounts of TEA · 3 HF yielded the 5-OH free as well as fully desilylated ribosides **97** and **98** in 80% and 69% yield, respectively. It was found here, that an intermediate purification of **96** by NP flash column chromatography was necessary to obtain **97** and **98** in high purity since unreacted alcohol **58** was demanding to remove from the respective reaction mixtures by chromatographic procedures.

As observed before, the glycosylation reaction went along with high β-selectivity as concluded from ¹H-NMR spectra of crude product which confirmed the formation of only one anomer. It was identified as the β-riboside form evaluation of the purified ribosides **97** and **98** by NOESY-NMR spectroscopy.

The desilylation reactions, partial of the 5-OH group as well as complete, proceeded smoothly and without the formation of glycoside cleavage- or other by-products (Scheme 41). Losses in yield ($\sim$ 20%) resulted from incomplete conversion since, in particular, the secondary 2'- and 3'-silyl ethers proved remarkably stable.

The obtained ribosides **97** and **98** as well as the nucleosides A and dA were successively studied in terms of conversion into the respective phosphates or $P^{III}$ building blocks envisaged for the couplings to (d)ADPR-AB derivatives.
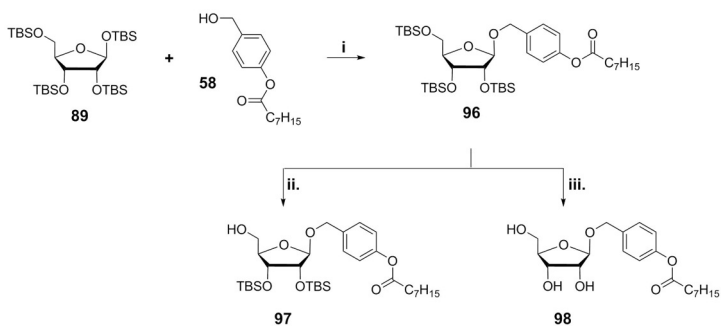
**Scheme 41:** Synthesis of the fully as well as partially and unprotected 1-*O*-OB ribosides **96**, **97** and **98**: **i.** 1 eq. **89**, 1.2 eq. **58**, 1.1 eq. TMSI, 2.4 eq. TEA, -50 °C to rt, 3 h, **96**: quantitative. **ii.** 4 eq. TEA · 3 HF, MeCN, rt, 5 h to 18 h, **97**: 80%. **iii.** TEA · 3 HF/MeCN 10 vol%, rt, 85 h, **98**: 69%.

### 8.2.2.2.  Strategies towards riboside and nucleoside P$^V$- and P$^{III}$-building blocks

A first approach towards an ADPR-AB derivative was pursued in orientation on that re-ported by PAHNKE *et al.*, where a per-acetylated ribose monophosphate was coupled with a non-symmetric phosphoramidite bearing an AB-mask and an acetyl-protected adenosine moiety to form the respective ADPR derivative (s. end of chapter 6).[143]

1-*O*-OB ribose **98** was converted analogously to the corresponding 5'-monophosphate **99** by treatment with Fm$_2$PA under the PA-chemistry standard conditions described above (s. section 8.1.3.2.). The Fm-protected intermediate **99a** was deprotected under dry basic con-ditions to yield 33% of the desired monophosphate **99** after automated RP flash column chromatographic purification (Scheme 42).
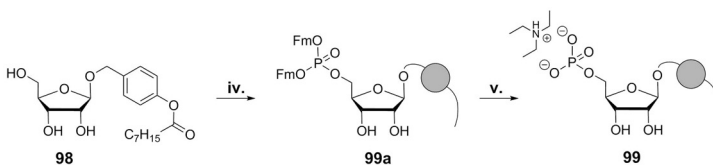


**Scheme 42:** Synthesis of 1-*O*-OB ribose-5-phosphate: **iv.** 1.3 eq. Fm$_2$PA, 1.3 eq. DCI (0.25 M in MeCN), 1.5 eq. *t*BuOOH (5.5 M in *n*-decane), dichloromethane/MeCN, rt, 60 min, **v.** 10 eq. TEA, MeCN, rt, 24 h, **99**: 33% over two steps.

The relatively low yield for **99** likely resulted from the multiple free hydroxy groups present during PA-coupling which inherited a substantial potential for side reactions. Removal of Fm-groups, however, proceeded quantitatively as seen from TLC-monitoring of the reaction, and the final automated RP flash column chromatography yielded the desired monophosphate **99** in high purity.

In complementation to the monophosphate building block, the synthesis of an non-symmetrically substituted PA carrying an OB-mask and an A-moiety was studied (Scheme 43). The phosphordiamidite (PA₂) approach towards non-symmetrical PAs described by WEINSCHENK *et al.* was chosen for this purpose. Accordingly, the synthesis of OBPA₂ was performed as described in the literature starting from chlorophosphine **100**, and OBPA₂ **101** was obtained in a competitive yield of 71% (Scheme 43).[162]
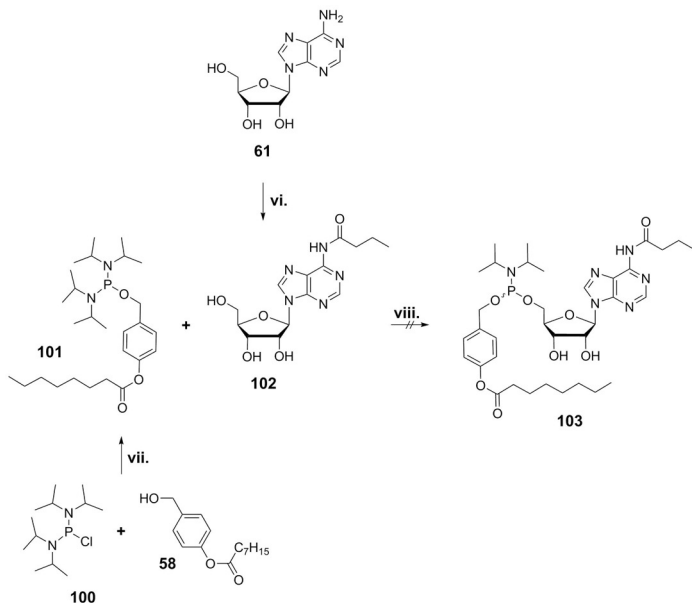


**Scheme 43:** Synthesis approach towards the non-symmetrical PA **103**: **vi.** 3.2 eq. TMSCl, 1.1 eq. butyryl chloride, pyridine/THF 1:1, rt 20 h, **102** 61%. **vii.** 1 eq. **58**, 1.3 eq. TEA, THF, rt, 18 h, **101**: 71%. **viii.** 1 eq. **102**, 1.1 eq. **101**, 1 eq. DCI (0.25 M in MeCN), **103**: not formed.

$N^6$-Butanoyl-adenosine **102** was synthesized starting from adenosine **61** via transient si-lylation of all hydroxy groups to selectively introduce the butyryl moiety at the $N^6$-position.[188] The desired precursor **102** was obtained in 61% yield after automated RP flash column chromatography (Scheme 43). The yield was lowered by the formation of $N,N$-diacylated adenosine as well as partial cleavage of the glycosidic bond while concentration of the crude reaction mixture.

For the preparation of PA **103**, nucleoside **102** and the activator DCI were first mixed and then slowly treated with a solution of PA₂ **101** in acetonitrile at 0 °C to rt (Scheme 43). After 60 min, all volatile reaction components were removed and the crude residue purified by automated NP flash column chromatography using a methanol gradient in dichloro-methane (0% to 10%) with additional 5% TEA to stabilize the PA on the silica phase. How-ever, isolated fractions included mainly impurities from unreacted PA₂ **101** and $N$(Bu)-A **102** as concluded from $^1$H- and $^{31}$P-NMR analysis. Additionally, $^{31}$P NMR-signals in the range of phosphites were found which pointed towards a twofold substitution of the amidite groups, either inter- or intramolecularly. Consequently, PA **103** was not formed as desired, and thus, the approach was changed by inverting the roles of ribose- and adenosine-build-ing blocks.

Accordingly, $N$(Bu)-A **102** was converted into the corresponding NMP **104** using again the Fm₂PA approach (Scheme 44). The procedure described for the synthesis of ribose phos-phate **99** was pursued similarly for nucleoside **102**, and the desired NMP **104** obtained in a comparable yield of 26% (Scheme 44). This outcome underlined to the assumption that multiple free hydroxy groups likely interfere with an efficient 5'-phosphitylation (compare with section 8.1.3.2 and synthesis of **99**).
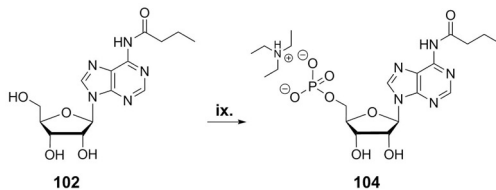


**Scheme 44:** Synthesis of $N^6$-butanoyl AMP **104**: 1$^{st}$: 1.1 eq. Fm₂PA, 1.3 eq. DCI, 1.3 eq. $t$BuOOH, MeCN/DMF, rt, 2 h, 2$^{nd}$: 10 vol% TEA in aq. MeCN, rt, 22 h, **104**: 26%.

Still, this PG-free procedure was preferred to a PG-involving alternative, since like this no additional and time- or resource-consuming protection/deprotection steps prolonged the synthesis route. Further, the convenient reaction setup and efficient purification constituted another advantage of the approach.

The synthesis of non-symmetric PA **105**, the coupling partner for $N$(Bu)-AMP **104**, was studied in parallel. Therefore, PA$_2$ **101** was reacted with 1-$O$-OB ribose **97** in the presence of DCI (Scheme 45).
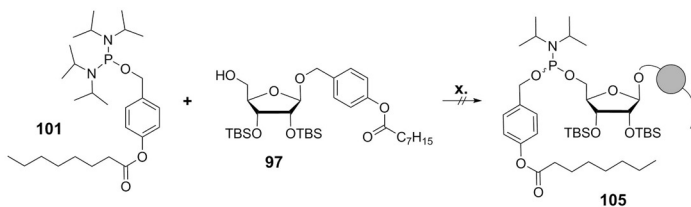


**Scheme 45:** Attempt of the synthesis of non-symmetric PA **105**: 1 eq. **97**, 1.1 eq. **101**, 1 eq. DCI (0.25 M in MeCN), **105**: insufficient formation.

The conversion to the desired non-symmetric PA **105** proceeded only insufficiently despite full activation of the PA$_2$ (Fig. 22). $^{31}$P-NMR spectra of the reaction between riboside **97** and PA$_2$ **101** were recorded at reaction points where no DCI (top), 0.5 equivalents DCI (middle) and 1 equivalent DCI (bottom) were added (Fig. 22).

Apparently, no reaction took place between the compounds without the activator. The addition of 0.5 equivalents DCI however sufficed to fully activate PA$_2$ **101** as indicated by the absence of the PA$_2$-typical signal at 123.0 ppm (Fig. 22, top). Instead, a prominent signal at 13.2 ppm was formed as well as two singlets at 148.0 ppm and 148.3 ppm. Comparison with literature-data indicated that the former signal likely corresponded to the activated amidite.[189] The latter lied within the area expected for the desired PA **105**, which was seemingly formed as a 1:1 mixture of two diastereomers. However, the proportion of formed product was low, and decreased even further when 1 eq. of DCI was added. This was potentially based on the successive formation of the corresponding phosphite substituted with two ribose moieties (Fig. 22, middle, signal at 140.2 ppm). Over time, only this signal at 140.2 ppm increased while the signals at around 148 ppm decreased and the signal at 13.2 ppm appeared to be constant (Fig. 22, bottom).
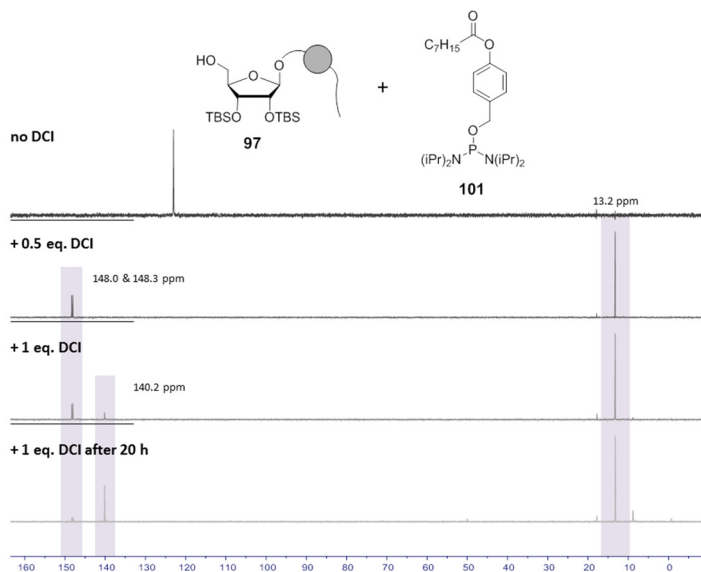
**Figure 22:** $^{31}$P-NMR spectra (MeCNd$_3$, 162 MHz, 25 °C, shifts δ in [ppm]) of the reaction between riboside **97** and PA$_2$ **101** upon subsequent addition of DCI (0.25 M in MeCN).

The results of this NMR-study explained the low isolated amounts of product **105**. Lastly, steric interference between the spacious TBS- and *i*Pr-groups was assumed to hamper the efficient formation of PA **105**. The approach aiming at non-symmetric PAs as coupling part-ners for the respective monophosphates was consequently discontinued since both varia-tions towards PAs **103** and **105** did not lead to the anticipated coupling components.

An alternative approach in orientation on the synthesis pathways established for Tri*PPP*ro-compounds was explored successively: the synthesis of a non-symmetric H-phos-phonate carrying a ribose- and an OB-moiety (Scheme 46). The synthesis protocol was adapted from REIMER with minor changes and started with the conversion of alcohol **58** with diphenyl phosphine (DPP) at low temperatures (-30 °C) in pyridine.[163] The reaction was allowed to warm to rt within 30 to 60 min, and was then cooled down to -30 °C again to add riboside **97** which was left to react with intermediate **106a** for 20 h (Scheme 46).

135
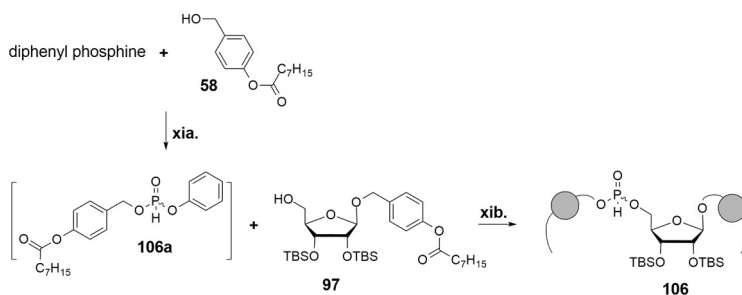
**Scheme 46:** Synthesis of non-symmetric H-phosphonate **106**: **xia.** 1.2 eq. DPP, 1 eq. **58**, pyridine, -30 °C to rt, 30 – 60 min. **xib.** 1 eq. **97**, pyridine, -30 °C to rt, 20 h, **106**. 48%.

Purification of the crude reaction mixture was performed via automated NP flash column chromatography with an ethyl acetate gradient in petroleum ether (0% to 100%) with additional 2% acetic acid to stabilize the H-phosphonate on the silica phase.
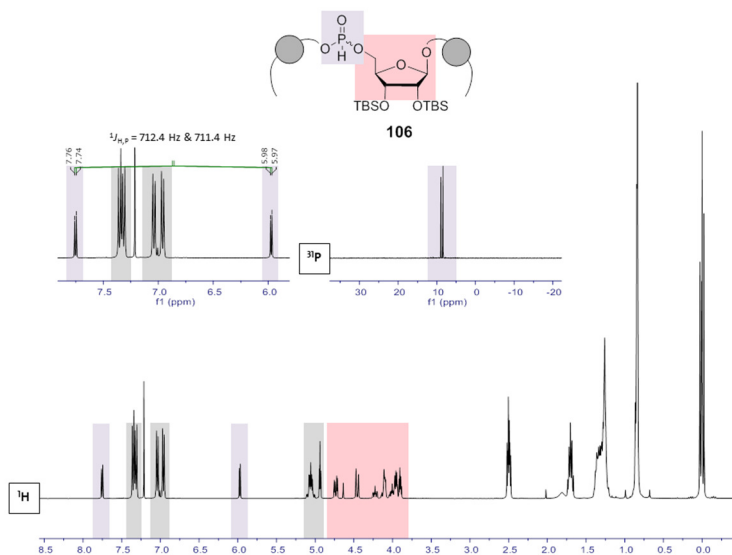


**Figure 23:** $^1$H-and $^{31}$P-NMR spectrum (CDCl$_3$, 400 MHz & 162 MHz, 25 °C, shifts δ in [ppm]) of non-symmetric H-phosphonate **106**. Protons of the ribose core are highlighted in red and protons of the OB-mask in grey. Signals belonging to the H-phosphonate are framed in violet.

136

The desired product was obtained in a good yield of 48% and, furthermore, its purification was successful after only one chromatographic separation. From the course of the purification it was concluded further that particularly the second step of the reaction did not go to completion.

H-phosphonate **106** was obtained as the expected mixture of diastereomers and in high purity (>98%, determined by NMR) (Fig. 23). Successively, the coupling reaction between H-phosphonate **106** and NMP **101** was investigated.

### 8.2.2.3. Coupling of building blocks to the protected (d)ADPR-AB precursors

The coupling conditions for NMP **101** and H-phosphonate **106** were adapted again from procedures previously established for the synthesis of Tri*PPP*ro-compounds.[157,163,164] In these cases, *N*-chlorosuccinimide (NCS) was applied for the oxidative activation of the respective H-phosphonate to its corresponding chlorophosphate which subsequently was reacted with tetra-*n*-butylammonium phosphate to the corresponding masked pyrophosphate.

Analogously, H-phosphonate **106** was treated with 2 equivalents NCS at rt to 50 °C. The oxidative activation to chlorophosphate **106b** was followed by NMR-spectroscopy and found to be completed within 20 h (Scheme 47, Fig. 24).
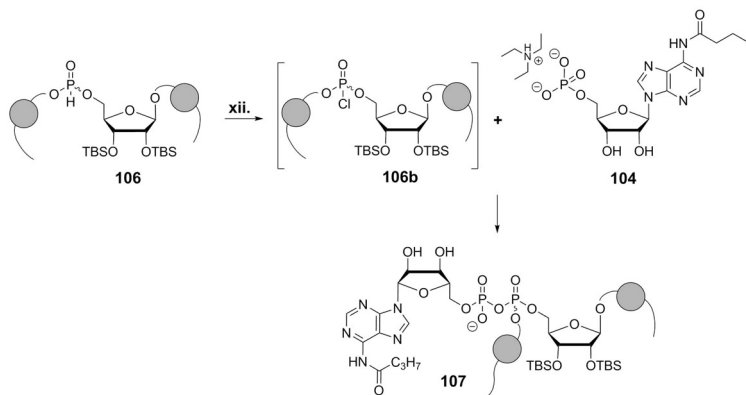


**Scheme 47:** Synthesis of TBS-protected ADPR-OB **107**: **xii.** 1$^{st}$: 2 eq. NCS, MeCN, rt to 50 °C, 20 h, 2$^{nd}$: 1.2 eq. **101**, MeCN/DMF, rt, 2 h **107**: (18%)
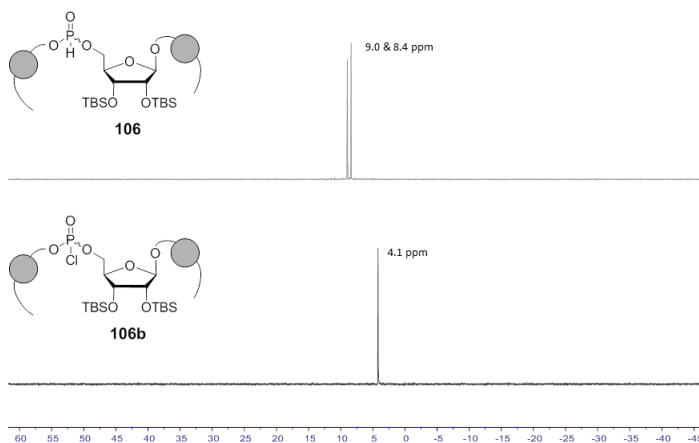
**Figure 24:** $^{31}$P-NMR (CDCl$_3$, 162 MHz, 25 °C, shifts δ in [ppm]) monitoring of the oxidative activation of H-phosphonate **106** to chlorophosphate **106b** with NCS over 20 h between 50 °C to rt.

NMP **101** was added as a solution in MeCN/DMF upon completed activation. The reaction mixture was stirred at rt for two hours and successively concentrated to dryness.

The obtained crude residue was subjected to automated RP flash column chromato-graphy but fractions containing product **107** could not be separated entirely from impurities by monophosphate **101**. Still, $^{31}$P-NMR-spectroscopic analysis of the obtained product con-firmed the formation of **107** showing distinct diphosphate signals. The H-phosphonate route thus proved to be generally applicable as a coupling method in this context but required further adaption.

The scope of the investigation was broadened on 2'-deoxyadenosine encouraged by these results (Scheme 48).

The respective NMP **110** was synthesized analogously to N(Bu) AMP **101**. Accordingly, nu-cleoside **108** was selectively N-butyrylated via transient TMS-protection, and successively 5'-phosphorylated via the Fm$_2$PA-approach (Scheme 48).[179,188] The formation and isolation of **109** was reduced through elevated nucleobase cleavage under the acidic reaction con-ditions and two-fold reaction of the $N^6$-amino group with butyryl chloride, so that N(Bu)-dA **109** was isolated in a yield of 32%. The successive phosphorylation gave the desired monophosphate **110** in 31% yield.
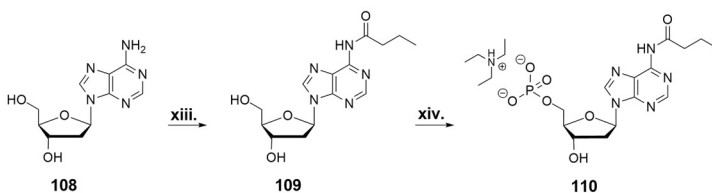
**Scheme 48:** Synthesis of $N^6$-butanoyl-2'-deoxyAMP **110**: **xiii.** 2.1 eq. TMSCl, 1.1 eq. butyryl chloride, pyridine/dichloromethane 1:2, 0 °C to rt, 22 h, **109**: 32%. **xiv.** 1st: 1.2 eq. Fm$_2$PA, 1.1 eq. DCI (0.25 M in MeCN), 2.2 eq. $t$BuOOH (5.5 M in $n$-decane), MeCN/DMF, rt, 60min, 2nd: 10 vol% TEA in aq. MeCN, rt, 18 h, **110**: 31%.

Coupling between NMP **110** and H-phosphonate **106** was repeated as described for NMP **104** with minor changes (Scheme 49). The oxidative activation with NCS proceeded again smoothly and was completed within 18 h as monitored by $^{31}$P-NMR spectroscopy (analog to Fig. 24). Then, NMP **110** was pretreated with tetra-$n$-butylammonium hydroxide in aqueous acetonitrile to increase solubility and nucleophilicity of the monophosphate. Once all monophosphate was soluble in acetonitrile, it was thoroughly concentrated to dryness one more time. NMP **110** was successively dissolved in acetonitrile at high concentration and then added to the activated chlorophosphate in one portion. The coupling reaction was carried out at rt to 50 °C in order to increase conversion. Also, the reaction time was prolonged to 18 h for the same reason.
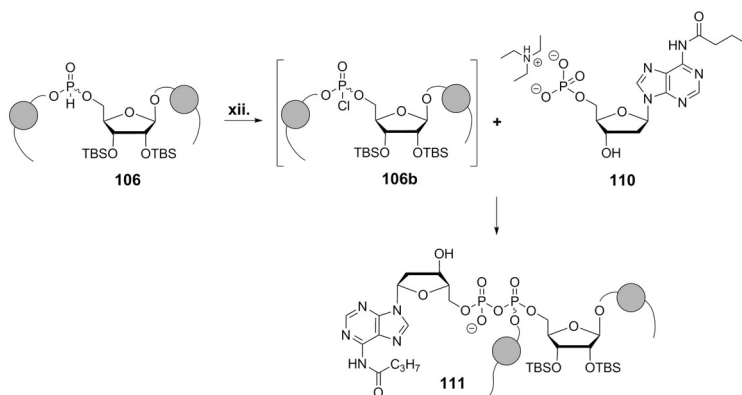


**Scheme 49:** Synthesis of TBS-protected dADPR-OB **107**: **xxi.** 1st: 2 eq. NCS, MeCN, rt to 50 °C, 20 h, 2nd: 2 eq. **110**, MeCN, rt to 50 °C, 18 h, **111:** 26%.

139
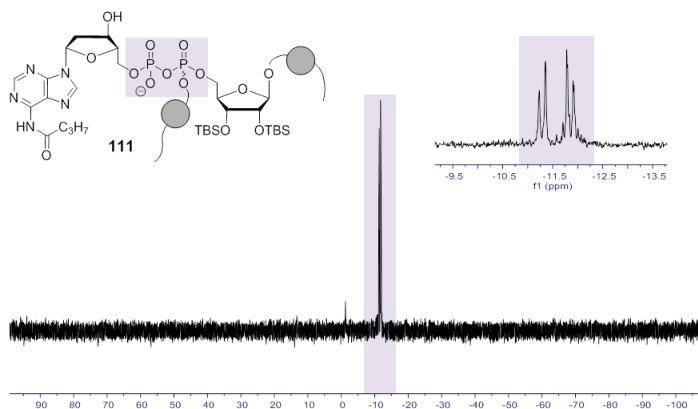
**Figure 25:** ^{31}P-NMR (MeCN d$_3$, 162 MHz, 25 °C, shifts δ in [ppm]) of TBS-protected dADPR-OB **111** after a single automated RP flash column chromatographic purification (MeCN gradient in water, 0% to 100%). Phosphorous signals of TBS-protected OB dADPR **111** are framed in violet.

Finally, all volatile components were removed under vacuum, and the obtained crude product subjected to automated RP flash column chromatography. This time, the TBS-protected dADPR-OB **111** was obtained in good purity (>92%, determined by NMR) from one single column chromatographic purification in a yield of 26% (Fig. 25).

This optimized reaction outcome and protocol underlined the feasibility of the coupling reaction. In contribution, the preparation of the required building blocks was on the one hand convenient to perform and allowed on the other hand for a flexible arrangement of components with regard to AB mask, nucleotide and riboside.

After the successful coupling to the (d)ADPR derivatives **107** and **111**, the last step towards the targeted (d)ADPR-OB was the development of a desilylation protocol.

### 8.2.2.4.     Desilylation to AB-masked (d)ADPR derivatives

From previous experiments on the desilylation of ribosides **91** & **96** and nucleotides **71a** & **71b**, it was known that OB esters, phosphates or labile nucleobases tolerated conditions using TEA · 3 HF to remove TBS ethers.
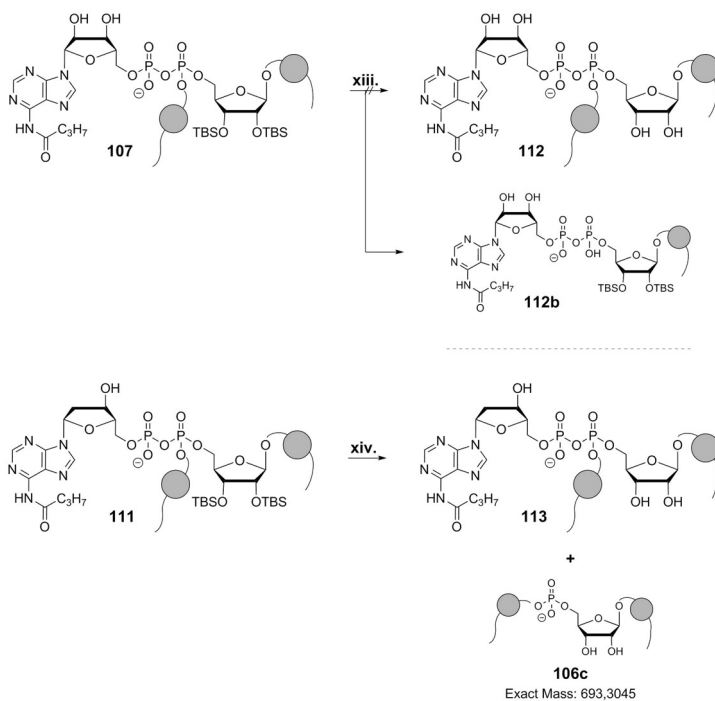
**Scheme 50:** Approaches to desilylate the TBS-protected (d)ADPR-OB derivatives **107** and **111**. **xiii.** 10 eq. TEA · 3 HF, 12.5 eq. TEA, MeCN/H₂O 19:1, rt, 30 h, **112**: -. **xiv.** 8 eq. TEA · 3 HF, MeCN, rt, 20 h, **113**: (25%).

Thus, TEA · 3 HF constituted the reagent of choice to attempt the desilylation of protected (d)ADPR derivatives **107** and **111** (Scheme 50).

Two protocols were studied; the first protocol using TEA · 3 HF in acetonitrile was adapted from the desilylation procedures for ribosides **91** and **96** whereas the second one made use of TEA · 3 HF buffered with triethylamine in acetonitrile (+ 5% water) in acknowledgment of the lability of pyrophosphate moieties under acidic conditions.

Following the second protocol, the pyrophosphate backbone stayed largely intact as anticipated. However, the applied conditions promoted a dissociation of the phosphate-OB mask rather than a cleavage of the 2',3'-silyl ethers (Scheme 50). These conclusions were drawn from respective ³¹P-NMR- and ESI-mass spectra and **112b** was identified as mayor reaction product after RP purification of the crude reaction mixture accordingly (Scheme 50, Fig. 26).

141

The former conditions (TEA · 3 HF, acetonitrile) mediated the formation of the desired dADPR-OB derivative **113** successfully (Scheme 50). Unfortunately, the reaction went also along with significant cleavage of the pyrophosphate backbone. This was deduced from NMR and MS analysis of the fractions obtained from purification of the crude reaction mixture by automated RP column chromatography (Scheme 50, Fig. 27). It was further found that the monophosphate fragment **106c** co-eluted with dADPR-OB **113**, so that a complete purification of the desired product was not achieved (Fig. 27).

The applied protocol, however, was feasible and the synthesis of OB-masked dADPR **113** achieved successfully so that a valuable basis for further optimization was established.
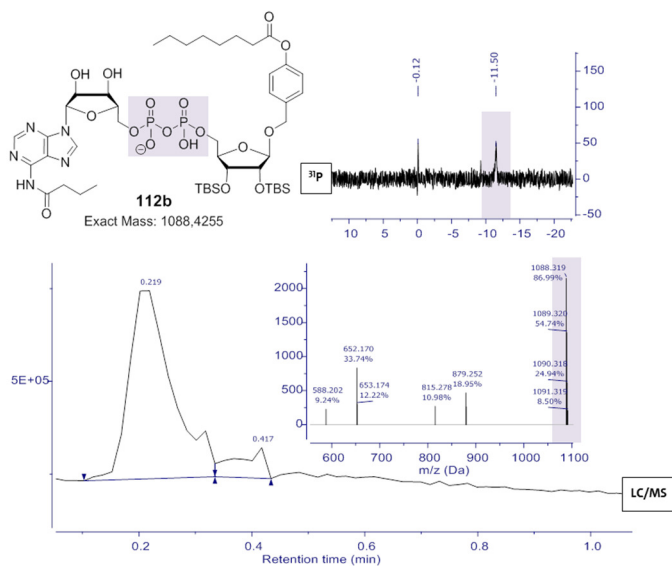


**Figure 26:** $^{31}$P-NMR (MeCN d$_3$, 162 MHz, 25 °C, shifts δ in [ppm]) and HPLC/ESI-MS spectra of the main reaction product **112b** from desilylation of **107** with TEA-buffered TEA · 3 HF in acetonitrile (+ 5% water).
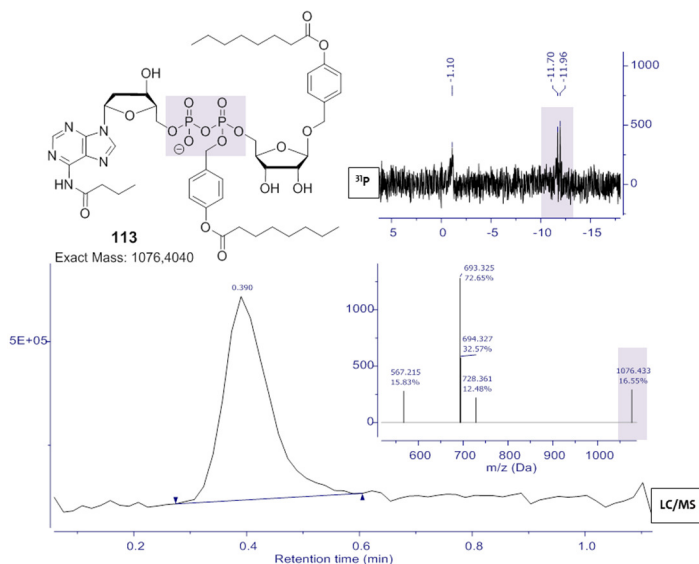
**Figure 27:** $^{31}$P-NMR (MeCN d$_3$, 162 MHz, 25 °C, shifts δ in [ppm]) and HPLC/ESI-MS spectra of the product fraction obtained from desilylation of **111** with TEA · 3 HF in acetonitrile.

These optimizations should aim at reducing the dissociation rates of the pyrophosphate backbone and phosphate-OB-mask which could be achieved by adjusting the amounts and ratio of TEA · 3 HF and triethylamine used for desilylation.

Further, a preparation of unprotected H-phosphonate **106b** would be an interesting modification of the synthesis route. In this case, the desired dinucleotide would be obtained directly from coupling of H-phosphonate **106** and a respective NMP, and no PGs would be needed to be cleaved afterwards (Scheme 51). A test reaction towards **106b** was performed and seemed feasible as indicated by TLC monitoring.

The activation of the H-phosphonate, however, could turn out sophisticated since the unprotected 2′,3′-hydroxy functions display potential for side reactions from nucleophilic attack on the intermediate chlorophosphate. Here, transient TMS-protection prior to H-phosphonate activation would constitute a solution to temporarily block the reactive positions.
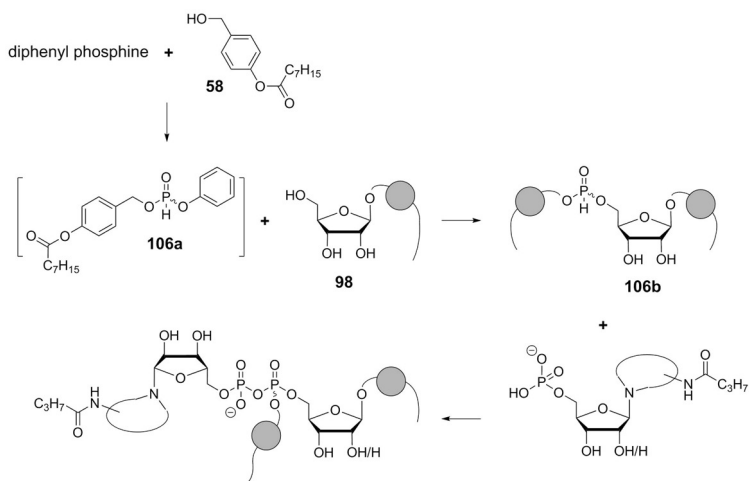
**Scheme 51:** Suggestion of a further development of the synthesis route towards OB-masked (d)ADPR derivatives via the unprotected H-phosphonate **106b**.

In summary and against this backdrop, the route developed for the synthesis of (d)ADPR-OB derivatives to this stage resembles a very promising basis for further development. The assembly of mask is adaptable based on the mode of composition of the non-symmetric H-phosphonate as well as the riboside. In both cases, the respective mask is introduced via its corresponding alcohol. The coupling step between the P$^{III}$-building block and an NMP of choice holds further versatility so that a synthesis of e.g. nucleoside-analogues of (d)ADPR-AB would be possible on this route as well. In prospect, these aspects make the developed approach a valuable and promising foundation for the convenient synthesis of further membrane-permeant (d)ADPR derivatives.

### 8.3. Synthesis and evaluation of AB-masked cNMPs

Cyclic mononucleotides like the two prominent examples cAMP and cGMP complement the group of nucleosidic second messengers with a demand for further investigation. Membrane permeable, bio-reversibly protected derivatives of cNMPs constitute valuable compounds for the investigation of intracellular signaling pathways in non-invasive setups, and consequently, the synthesis of AB-masked cNMPs was studied. The focus of the synthesis approach laid on the development of a flexible route allowing for variation of AB-mask and nucleoside.

#### 8.3.1. Elaboration and evaluation of a synthesis approach towards AB-cNMPs

Inspiration for a potential synthetic access to AB-masked cNMPs was drawn from own studies on the synthesis of non-symmetric phosphoramidites (PAs) that included an unprotected nucleoside moiety (see sections 8.1.3.2 & 8.2.2.2). In these cases, the isolation of the desired PAs was usually impeded due to significant proportions of side reactions amongst which the formation of phosphites was repeatedly observed. These phosphites were concluded to result either from an intermolecular or an intramolecular substitution of the remaining *N*-di*iso*propyl-group by a second nucleosidic hydroxy group. In the latter case, a cyclic nucleoside phosphite would constitute the reaction product, and further oxidation would result in a cyclic NMP derivative.

Bearing these observations and hypothesis in mind, a synthesis approach involving the respective nucleoside and an AB-masked phosphordiamidite (ABPA$_2$) was set up and investigated in more detail, starting with the reaction towards an AB-cUMP derivative.

#### 8.3.1.1. Formation of AB-cUMP as model system

The starting conditions for the synthesis of OB-cUMP **115** were adapted from the approaches towards the non-symmetric PAs **77**, **103** and **105** using the respective PA$_2$ **101**. DCI (0.25 M in acetonitrile) was used as activator for the reaction, and *t*BuOOH (5.5 M in n-decane) was applied as oxidizing agent. The reaction was carried out in a mixture of acetonitrile and DMF due to the limited solubility of uridine in acetonitrile (Scheme 52).
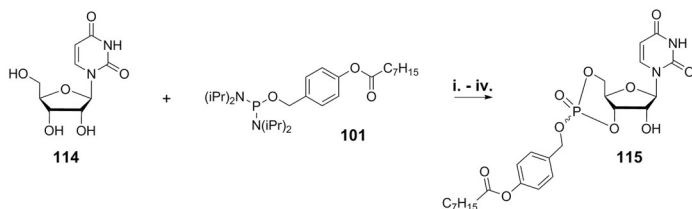
**Scheme 52: i.** 1.1 eq. **101**, 2.2 eq. DCI (0.25 M in MeCN), 1.5 eq. *t*BuOOH (5.5 M in *n*-decane), MeCN/DMF 5:4, 0 °C to rt, 60 min, **115**: 13%. **ii.** 1.1 eq. **101**, 1st 1.3 eq. DCI (0.25 M in MeCN), 2nd 1.3 eq. DCI (0.25 M in MeCN), 1.5 eq. *t*BuOOH (5.5 M in *n*-decane), MeCN/DMF 5:1, rt, 60 min, **115**: 15%. **iii.** 1.1 eq. **101**, 1st 1.3 eq. DCI (0.25 M in MeCN), 2nd 1.3 eq. BTT (0.3 M in MeCN), 1.5 eq. *t*BuOOH (5.5 M in *n*-decane), MeCN/DMF 5:1, rt, 60 min, **115**: 13 – 19%. **iv.** 1 – 1.2 eq. **101**, 1st 1 – 1.2 eq. saccharin & 1 – 1.2 eq. 1-methylimidazole, 2nd 1 – 1.2 eq. saccharin & 1 – 1.2 eq. 1-methylimidazole, 1.5 eq. *t*BuOOH (5.5 M in *n*-decane), MeCN/DMF 5:1, rt, 60 min to 72 h, **115**: 16 – 19%.

In a first attempt, a solution of nucleoside **114** and OBPA₂ **101** was treated with 2.2 equivalents DCI that were added dropwise at 0 °C. The reaction mixture was allowed to warm to rt and stirred 30 min more before *t*BuOOH was added for oxidation (Scheme 52). Lastly, the crude reaction mixture was purified by automated RP flash column chromatography, and the cyclic nucleotide **115** was obtained as a mixture of two diastereomers in a yield of 13%.

Prompted by the surprisingly low yield, the reaction course was studied $^{31}$P-NMR spectroscopically (Fig. 28). Interestingly, upon just mixing uridine **114** and OBPA₂ **101**, the activation of the diamidite proceeded almost quantitatively which was indicated by the formation of the earlier observed signal at 13.2 ppm (compare section 8.2.2.2., Fig. 28). As well, signals in the range of PAs and phosphites were formed already (Fig. 28 top).
The addition of DCI apparently promoted the formation of the intermediate PA **115a**, but formation of the anticipated cyclic phosphite **115b** seemed to occur only at low proportion (Fig. 28 bottom, Scheme 53). Steric obstruction of the attack of the 3'-hydroxy group on the phosphorous atom or an insufficient nucleophilicity was lastly estimated to interfere with the efficient formation of phosphite **115b** (Scheme 53).

The synthesis of OB-cUMP **115** consequently was repeated with several changes to the protocol in order to evaluate the influence of the reaction conditions and in particular the impact of the activator.
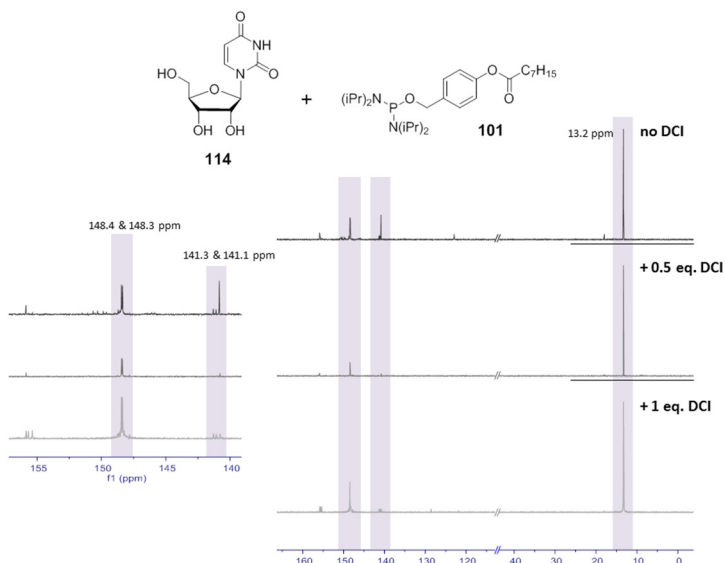
**Figure 28:** ^{31}P-NMR spectra (MeCN d$_3$, 162 MHz, 25 °C, shifts δ in [ppm]) of the reaction monitoring between uridine **114** and OBPA$_2$ **101**.

In a second approach, the ratio between acetonitrile and DMF was altered to 5:1 and the mode of addition of reagents was changed (Scheme 52). This time, the nucleoside was placed in the reaction flask and dissolved in acetonitrile/DMF 5:1. A separate solution of OBPA$_2$ **101** in acetonitrile and one equivalent of DCI were added slowly and dropwise to the nucleoside at rt. Once the addition was completed, a second equivalent of DCI was added, and the reaction mixture stirred at rt for 60 min. After the successive oxidation, the concentrated crude product was purified by automated RP flash column chromatography and OB-cUMP **115** obtained in 15% yield.

Consequently, the outcome of the reaction was almost identical to that of the attempt before.

The activator was changed to 5-(benzylthio)-1H-tetrazole (BTT) next. BTT displays a higher acidity and lower nucleophilicity than DCI. These properties were anticipated to be beneficial in particular for the second reaction step, the formation of phosphite **115b** (Scheme 53 lower part).

147
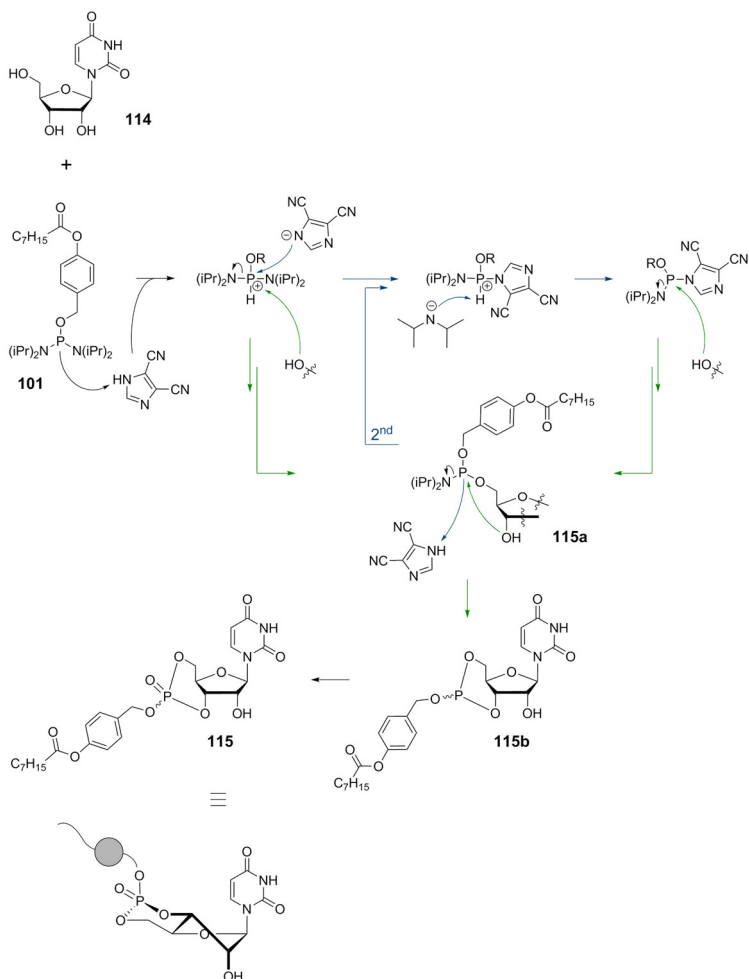
**Scheme 53:** Mechanism of the reaction between uridine **114** and OBPA₂ **101** to OB-cUMP **115** via the intermediate species **115a** and **115b**. DCI was used as activator. Bottom: theoretically preferred conformation of OB-cUMP **115** (*northern*/C3' endo-C2' exo).

It was assumed, that the better acid BTT facilitated the protonation of PA **115a** while competing less with the 3'-hydroxy group for substitution of the *N*-di*iso*propyl-group. These effects should advance the phosphite formation.

The reaction protocol was varied as follows: uridine **114** was again dissolved in acetonitrile/DMF 5:1 and successively treated with a solution of OBPA$_2$ **101** in acetonitrile and one equivalent DCI (Scheme 52). Both reagents were added dropwise in small portions over a period of 30 min. Upon completed addition, the reaction mixture was stirred another 30 – 120 min at rt. Then, one equivalent BTT was added slowly and dropwise over 10 min, and the reaction kept stirring for further 15 – 60 min. After the subsequent oxidation with *t*BuOOH, all volatile components were removed and the crude reaction mixture purified by automated RP column chromatography. The isolated yields of OB-cUMP **115** varied between 13 – 19% which again constituted no significant improvement of the reaction outcome.

Lastly, an alternative activator-system composed of saccharine and 1-methylimidazole was tested as it was reported to efficiently mediate also reactions between PAs and poorly nucleophilic alcohols like tertiary alcohols.[190]

Saccharine and 1-methylimidazole were dissolved in a 1:1 ratio in acetonitrile prior to reaction to generate the activating salt. Simultaneously with OBPA$_2$ **101**, one equivalent of the activator salt was added dropwise to a solution of uridine **114** in MeCN/DMF 5:1 (scheme 52). Upon completion of the first addition, the reaction mixture was stirred for 30 min, then treated with a second equivalent of the activator solution and successively stirred for another 60 min to 72 h. After addition of *t*BuOOH, all volatile components were removed and the crude residue was again subjected to automated RP column chromatography. The desired product **115** was obtained in yields between 16 – 19%.

Monitoring of the reaction course via $^{31}$P-NMR spectroscopy indicated an incomplete activation of OBPA$_2$ **101** even after 72 h. Further, the activated intermediates were again not converted efficiently to the desired phosphite as concluded from the persistence of the respectively attributed phosphorous signals.[190]

Subsumed, this alternative approach constituted no improvement in comparison to the previous protocols.

In summary, the isolation of OB-masked cUMP succeeded repeatedly despite poor yields (13 – 19%), and thus prompted the expansion of the synthesis approach on further nucleosides like adenosine or guanosine.

### 8.3.1.2. Expansion of the reaction scope on further nucleosides

Adenosine and the *N*-butyrylated derivatives of A, dA and G were employed as starting materials for the further syntheses of OB-cNMPs.

The synthesis of $N^2$-butanoyl guanosine **117** was performed similarly the procedure applied for the preparation of 2'-deoxy-$N^6$-butanoyl A **109**.[188] After automated RP column chromatographic purification of the respective crude reaction mixture, nucleoside **117** was isolated in a yield of 48% (Scheme 54).
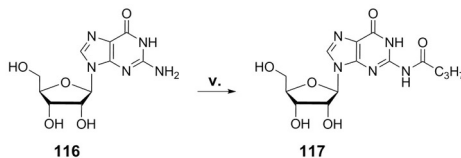


**Scheme 54:** Synthesis of $N^2$-butanoyl guanosine **117**: **v.** 9 eq. TMSCl, 1.1 eq. butyryl chloride, pyridine/dichloromethane 1:2, 0 °C to rt, 22 h, **117**: 48%

OB-cAMP **118** was synthesized analogously to OB-cUMP **115** starting from nucleoside **61** and following synthesis variant **ii.** which made use of a stepwise addition of the in total applied 2.4 equivalents DCI (Scheme 55).
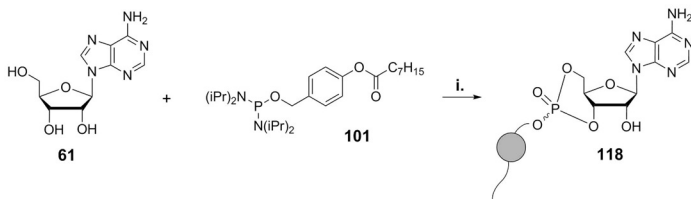


**Scheme 55:** Preparation of OB-cAMP **118** following the 2nd synthesis variant: **ii.** 1.1 eq. **101**, 2.4 eq. DCI (0.25 M in MeCN), 1.5 eq. *t*BuOOH (5.5 M in *n*-decane), MeCN/DMF 1:1, rt, 60 min, **118**: 12%.

The desired OB-cAMP **118** was isolated in a yield of 12% after final purification by automated RP flash column chromatography.

The *N*-butyrylated OB-cNMPs **119** to **121** were obtained analogously following the synthesis protocols **ii.** and **iii.** described above. The yields generated for OB-*N*(Bu)-cAMP **119** and OB-*N*(Bu)-cdAMP **120** were in a similar range as found for OB-cNMPs **115** and **118** with 14% and 13%, respectively (Scheme 56). The reaction towards OB-*N*(Bu)-cGMP **121** proceeded to a lower extent and the desired OB-cNMP **121** was isolated in a comparably low yield of 4% (Scheme 56). Interestingly, in the case of **121** the formation of only one of the two possible diastereomers seemed favored as crude $^{31}$P-NMR spectra indicated. Here, only one of the possible two phosphate signals was prominent, and consequently, **121** was isolated as a single diastereomer.

The masked cNMPs **118** to **121** in contrast were obtained as mixtures of the two possible diastereomers with diastereomeric ratios of approximately 1:1.
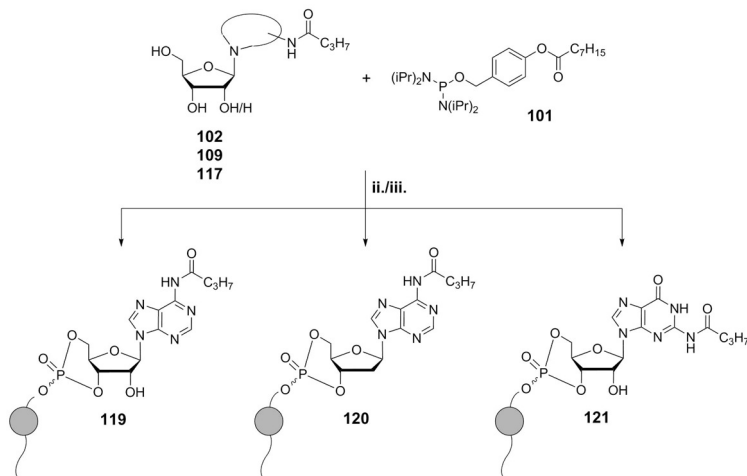


**Scheme 56:** Syntheses of the *N*-butyrylated OB-cNMPs **119** to **121**: to **119**: **iii.** 1.1 eq. **101**, 1st 1.3 eq. DCI (0.25 M in MeCN), 2nd 1.3 eq. BTT (0.3 M in MeCN), 1.5 eq. *t*BuOOH (5.5 M in *n*-decane), MeCN/DMF 3:1, rt, 60 min, **119**: 14%. to **120**: via **ii.** 1.1 eq. **101**, 1st 1.3 eq. DCI (0.25 M in MeCN), 2nd 1.3 eq. DCI (0.25 M in MeCN), 1.5 eq. *t*BuOOH (5.5 M in *n*-decane), MeCN/DMF 1:1, rt, 60 min, **120**: 13%. to **121**: via **ii.** 1.1 eq. **101**, 1st 1.5 eq. DCI (0.25 M in MeCN), 2nd 1.5 eq. DCI (0.25 M in MeCN), 1.5 eq. *t*BuOOH (5.5 M in *n*-decane), MeCN/DMF 1:1, rt, 60 min, **121**: 4%.

Concluding the successful syntheses of five different OB-cNMPs, their functional evaluation proceeded next. A first focus was set on determination of the chemical stability versus the enzymatic activation of masked cNMPs by esterases. Further, the compounds were studied with regard to their performance in cell-based settings and the effects they provoke in living cells. These investigations were performed in close collaboration with A. GUSE, V. NIKO-LAEV and C. GEE and their co-workers at the University Medical Center Hamburg Eppendorf.

### 8.3.2.    Functional evaluation of AB-cNMPs

Ideally, masked precursors of bio-active compounds are biologically inactive and display a stability in physiologic media that on the one hand exceeds their specific activation significantly, and on the other hand guarantees sufficient time for their approximation to their respective target structure. Once activated, the previously inactive compound re-gains its biologic activity and, accordingly, should display respective effects from interaction with its target. These demands applied for the prepared OB cNMPs equally as e.g. for prodrugs like *cyclo*Sal-, Di*PP*ro- or Tri*PPP*ro-compounds.

Consequently, the chemical stability of the OB-cNMPs under physiological conditions as well as the efficiency of the enzymatic activation of the OB-mask by an exemplary esterase was evaluated. In complementation, the masked nucleotides were applied in various cell assays to analyze their biologic effects e.g. in the context of $Ca^{2+}$ mobilization and cell activation.

### 8.3.2.1.      Investigation of chemical stability and enzymatic activation by PLE

Stability determinations for OB-cNMPs **115**, **119** and **120** (as 5 mM stock sol. in DMSO) were performed in PBS (50 mM, pH 7.3) as physiological pH mimic. The compounds (2 mM, final conc. in PBS/DMSO) were incubated over 120 – 200 h at 37 °C. Hydrolysis samples were taken at distinctive times and analyzed via HPLC/MS (Fig. 29).

The recorded HPLC chromatograms and ESI mass spectra showed that the OB-cNMPs released only their respective parent cNMP from cleavage of the OB-mask without the formation of further cleavage byproducts (Fig. 29).

It was found that after 8 h circa 50% of the OB-cNMPs were hydrolyzed (**115**: $t_{1/2}$ = 8.6 h, **119**: $t_{1/2}$ = 7.4 h, **120**: $t_{1/2}$ = 7.5 h) (Fig. 30).

This half-life implied a stability of the OB-cNMPs that should facilitate convenient setups of cell-based assays and allow for satisfactory time to run e.g. even (pre-) incubation experiments with the masked nucleotides.
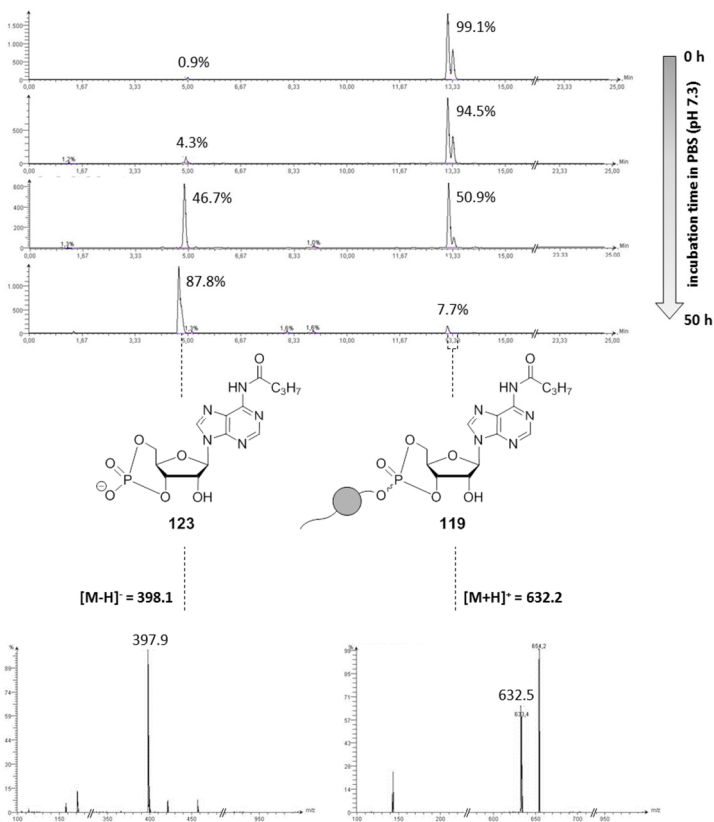


**Figure 29:** HPLC chromatograms and ESI mass spectra of the chemical hydrolysis of OB-*N*(Bu)-cAMP **119** in PBS (50 mM, pH 7.3) at 0 h, 1 h, 8 h & 50 h. The two signals of the diastereomers vanished over time while the signal for *N*(Bu)-cAMP **123** increased. The compounds were assigned from the mass spectra recorded at the retention times coinciding with the signals found in the HPLC chromatograms.

153

The hydrolysis behavior of **115**, **119** and **120** was assessed further, and the relative areas of signals for OB-cNMP and cNMP were determined (in percent). These values were normalized and then averaged for all three hydrolyses under determination of the corresponding standard deviation. Following this procedure, the individual hydrolysis courses were numerically compared with another.

The progress of hydrolyses was expected to be largely similar since the dissociation of the OB-mask constituted the determinant process in theory.

The average deviation of the hydrolysis progress for OB-cNMPs **115**, **119** and **120** at the time points measured was 5% with a single value maximum of 12%. From these calculations, it was deduced that the hydrolysis course was indeed analog for all OB-cNMPs tested and subject to the pace of the cleavage of the masking group and was almost independent of the nucleotide employed.

Accordingly, the stability (and lipophilicity) of AB-cNMPs should be adjustable by the choice of masking unit (see chapter 6, last part).[160,164] The relatively easy synthetic realization of such a venture underlines the adaptability of the chosen approach (synthesis of a respective PA$_2$ and coupling to the nucleoside of choice).
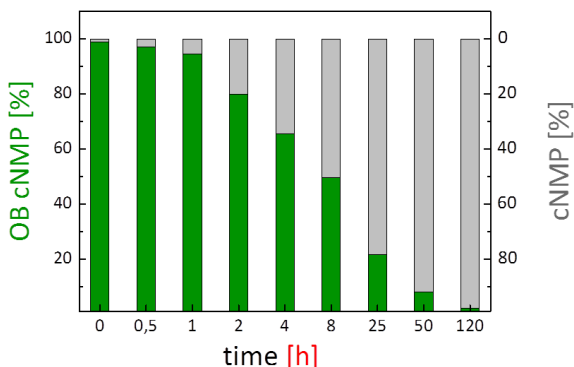


**Figure 30:** Course of the chemical hydrolysis of OB-*N*(Bu)-cAMP **118** to *N*(Bu)-cAMP **123** given as normalized values for each time point analyzed. Similar hydrolysis courses were measured for OB-cNMPs **115** and **120**.

Successively to successfully probing the chemical stability of the OB-cNMPs satisfying, their enzymatic activation by pig liver esterase (PLE) as an exemplary esterase was evaluated.

The conditions described by GOLLNEST *et al*. were used as a starting point for the respective incubation experiments and OB-cUMP **115** taken as model compound again.[156]
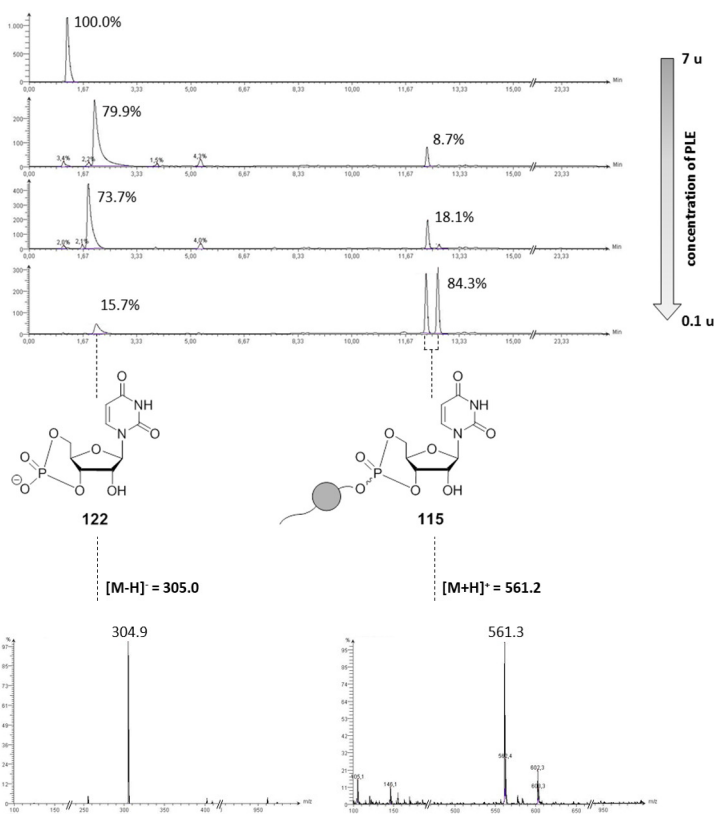


**Figure 31:** HPLC chromatograms and ESI mass spectra of the enzymatic hydrolysis OB-cUMP **115** in PBS (50 mM, pH 7.3) at 1 min with decreasing contents of PLE (7, 0.75, 0.25 & 0.1 u). With progressively lower PLE concentrations, the enzymatic reaction became more and more traceable. The compounds **115** and **122** were assigned from the mass spectra recorded at the retention times coinciding with the signals found in the HPLC chromatograms.

Accordingly, **115** (2 mM final conc. in PBS/DMSO) was incubated with PLE in PBS (50 mM) at 37 °C, and the enzymatic reaction terminated after distinctive points of time via the addition of methanol and deep-freezing in liquid nitrogen. The outcome of the hydrolysis was evaluated again by HPLC/MS analysis.

The applied amount of PLE following the described procedure, however, was far too high and the masked nucleotide entirely consumed just upon addition of the enzyme solution.

Thus, incubation experiments with varying contents of PLE were performed in the following to identify a concentration range where the enzymatic reaction could be observed in more detail (Fig. 31). The accordingly prepared PLE hydrolysis samples of OB-cUMP **115** contained 7 to 0.05 units PLE (per hydrolysis sample), and incubations were terminated after 0, 1, 2 and 5 min (Fig. 31).
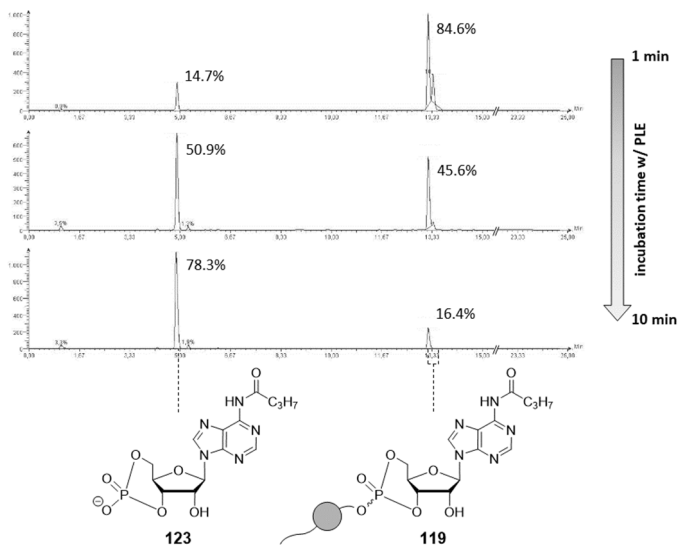


**Figure 32:** HPLC chromatograms and ESI mass spectra of the enzymatic hydrolysis of OB-*N*(Bu)-cAMP **119** in with PLE (0.05 u/hydrol. sol.) in PBS (50 mM, pH 7.3) at 1, 5 & 10 min. The two signals of the diastereomers vanished over time while the signal for *N*(Bu)-cAMP **123** increased. The compounds were assigned from mass spectra recorded at the retention times coinciding with the signals found in the HPLC chromatograms.
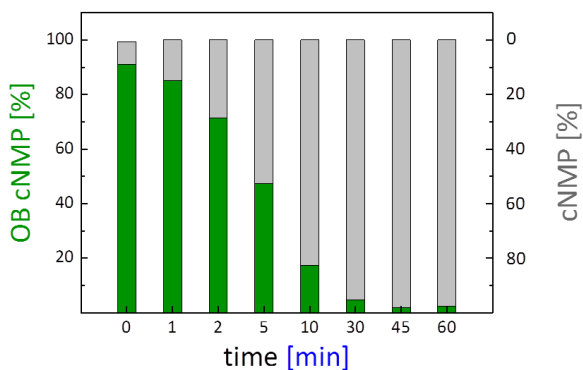
**Figure 33:** Course of the enzymatic hydrolyses of of OB-*N*(Bu)-cAMP **119** to *N*(Bu)-cAMP **123** given as normalized values for each time point analyzed. Similar hydrolysis courses were measured for OB-cNMPs **115** and **120**.

OB-cUMP **115** was detected just in traces when PLE amounts were around 1 u. The PLE concentration was thus lowered further by factor ten which finally slowed down the enzymatic reaction enough to observe the masked nucleotide well at 1 min (Fig. 31).

The final incubations of OB-cNMPs **115**, **119** and **120** with PLE were carried out with 0.05 u PLE per hydrolysis sample (V = 20 μL) which enabled good traceability of the enzymatic conversion (Fig. 32). Again, no further cleavage products apart from the respective cNMPs **122**, **123** and *N*(Bu)-cdAMP were determined. The *N*-butyryl group was not cleaved by PLE, even at longer incubation times (up to 60 min), as expected.

The acquired chromatograms were processed as described for the chemical hydrolysis to compare the progresses of the individual incubations with PLE (Fig. 33).

The half-lives of the studied OB-cNMPs were around 5 min under the applied conditions, which, however and as shown before, depended significantly on the amount present of esterase. More importantly in this context, the enzymatic activation of OB-cNMPs proceeded even at low PLE concentrations significantly faster than their decomposition in PBS by a factor of approximately 100.

In addition, the enzymatic hydrolyses showed analog progression as indicated by a mean deviation of normalized signal areas for OB-cNMPs and cNMPs of 4% with a maximum deviation of 9% for single time point values.

This permitted again the conclusion that the enzymatic reaction was almost independent of the type of nucleotide and relied on the OB-mask applied.

In summary, the results of both hydrolysis studies, chemical and enzymatic, went well along with the initial criteria as they showed that the stability of the prepared OB-cNMPs was significantly higher than the rate of enzymatic activation. Further, the masked nucleotides proved to be satisfactory stable for application in cell-based assays as they allow for incubations even over several hours ($t_{1/2} \approx 8$ h). This would enable setups where direct effects could be measured as well as experiments that envisage e.g. a pre-incubation with the OB-cNMPs to load the respective nucleotides into cells prior to a successive stimulation of the cell.

The similar hydrolysis behavior of OB-cNMPs **115**, **119** and **120** underlined the adaptability of the masking approach since the nucleotide structure had apparently very little influence on the course of hydrolysis, and thus could be exchanged readily. In addition, the properties of masked cyclic nucleotides could be tuned by the choice of mask[162,164], and this could be conveniently realized synthetically by the developed flexible synthesis approach.

Encouraged by the promising hydrolysis properties, the ability of the OB-cNMPs to cross cellular membranes as well as their potential to induce cellular processes was studied successively. The respective experiments were carried out in cooperation with the groups of A. GUSE, V. NIKOLAEV and C. GEE.

### 8.3.2.2. Performance of selected AB cNMPs in cell-based settings

Primary mouse cardiomyocytes carrying a FRET-sensor with a cAMP binding site were used in live cell imaging experiments to examine the membrane-permeability of OB-*N*(Bu)-cAMP **119** in particular. The binding of intracellular cAMP to the FRET sensor is indicated by a decreasing FRET-signal and an increasing fluorescence ratio between cyan-fluorescent protein (CFP) and yellow-fluorescent protein (YFP). The effect is monitored microscopically, and the acquired images are processed post-experiment for determination of FRET ratios and accordingly intracellular levels of cAMP (Fig. 34).[191]

In a second setup, Jurkat T cells were loaded with the $Ca^{2+}$-sensitive fluorescent dye Fura-2. Upon intracellular elevation of $Ca^{2+}$, Fura-2 coordinates the cation. Consequently, the absorption ratio between its two excitation wavelengths at 340 nm and 380 nm increases. This effect correlates directly with the amount of free cytosolic $Ca^{2+}$ (Fig. 34).
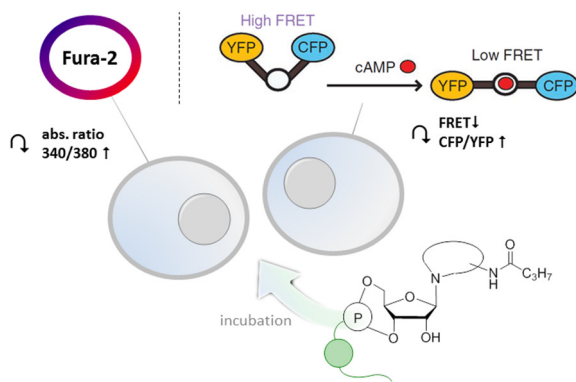


**Figure 34:** Schematic illustration of the experimental live cell imaging-setups applied to investigate the membrane permeability and biologic activity of selected OB-cNMPs. Left: OB-cNMPs **115**, **119** and **120** were incubated with cells loaded with the $Ca^{2+}$-sensitive fluorescent dye Fura-2. Upon increase of $Ca^{2+}$ levels, the absorption ratio between 340 nm and 380 nm increases in these cells. Right: OB-*N*(Bu)-cAMP **119** was incubated with cells that carry a FRET-sensor containing a cAMP binding site. Upon cAMP binding, the FRET signal decreases and the absorption ratio between CFP and YFP increases.

FRET-sensor carrying mouse cardiomyocytes were incubated with OB-*N*(Bu)-cAMP **119** (20 mM stock sol. in DMSO, diluted 1:1000 with FRET buffer) at approximately 60 s after data acquisition was started (Fig. 35). Immediately after addition of **119** to the extracellular medium, the ratio between CFP and YFP started to increase and reached a steady maximum state at circa 110 s (Fig. 35).

These results imply clearly that OB-*N*(Bu)-cAMP **119** instantaneously crossed the cell membrane and was also rapidly activated by intracellular esterases. Further, the product of this process was successfully recognized by the cAMP binding site of the FRET sensor. For the studied substrate, OB-*N*(Bu)-cAMP **119**, this implied that the $N^6$-butyryl group was either removed by enzymatic hydrolysis, or that its presence had no detrimental effect on receptor interaction.

The masked nucleotide successfully entered the cardiomyocytes within seconds, was metabolized within seconds and furthermore displayed effects similar to those of intracellularly generated cAMP. All these aspects were substantially required to make up a suitable membrane-permeable, bio-reversibly masked second messenger derivative for application in cellular assays.

The findings from this incubation study were complimented by the results from the in parallel performed live cell imaging experiments on Jurkat T-cells. Accordingly, Jurkat T-cells loaded with Fura-2 were stimulated with OB-cNMPs **115**, **119** and **120** (20 µM in DMSO, at t ≈ 120 s)) which were added to the extracellular medium (Fig. 36).

The absorption ratio of Fura-2 rose rapidly almost immediately after addition of the masked nucleotide **119**, and reached its maximum after approximately 200 s. Then, the $Ca^{2+}$ signal slowly decreased as indicated by the degression of the signal. A similar trend was observed for OB-cUMP **115** but the induced $Ca^{2+}$ signal was significantly reduced compared to compound **119** (Fig. 36).
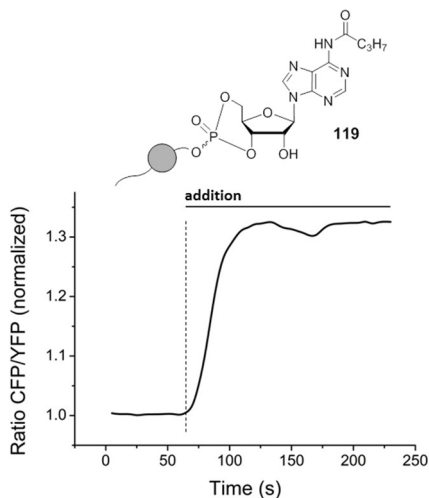


**Figure 35:** Normalized FRET ratio (between CFP and YFP) over the course of OB-N(Bu)-cAMP **119** addition to mouse cardiomyocytes Epac1-camps biosensor for intracellular cAMP. An instantaneous increase of FRET ratio after addition of **119** to the extracellular medium indicated intracellular release of cAMP and its binding to the FRET biosensor. Representative experiments (n=5).
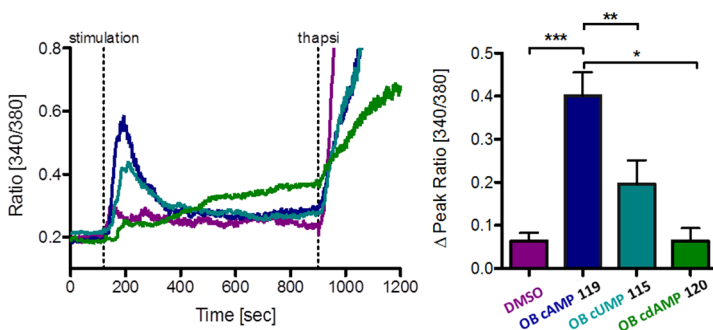
**Figure 36:** Stimulation of the of Jurkat T cells with OB-cNMPs **115, 119** and **120**. Left: Jurkat T cells were stimulated after 120 s with the respective OB-cNMPs (20 μM) or DMSO (as negative control). Furthermore, as positive control Thapsigargarin (1.67 μM) was added after 900 s. Mean signal ratio between 340 nm and 380 nm from single cells are shown (DMSO n=26; OB cAMP n=77; OB cUMP n=37; OB cdAMP n=14). The addition of **119** and **115** resulted in a transient increase of the $Ca^{2+}$ concentration, while no transient increase is visible for **120** or DMSO. Right: Statistical analysis of the mean delta peak for the OB-cNMPs and DMSO (data represent mean ± SEM). The most pronounced effect is measured for **119** and statistically significant differences between are marked by asterisks (* $p < 0.05$, ** $p<0.01$, *** $p<0.001$, Kruskal-Wallis Test).

In the case of OB-*N*(Bu)-cdAMP **120**, no initial increase of the intracellular Calcium concentration was measured. The absorption ratio, however, seemed to increase slightly over time and, overall, showed a subtly different course compared to OB-cNMPs **115** and **119** or the negative control DMSO (Fig. 36).

The results confirmed again that the OB-masked cNMPs were able to traverse across cell membranes and, importantly, triggered cellular responses immediately. In this context, it was concluded that de-masked cNMPs promoted the observed effects based on the results described just before.

In addition, $Ca^{2+}$ signaling events are substrate specific since they are mediated by receptor-interactions (s. chapter 6, "the receiver"), and cUMP **122**, the hydrolysis product of **115**, was just recently identified to be a 2nd messenger associated with $Ca^{2+}$ signaling. However, the compound is only little studied yet.[192]

The hydrolysis product of **119** behaved as it would be expected for cAMP supporting the assumption that the $N^6$-butyryl group was either removed enzymatically, too, or that its presence did not impede receptor activation.

Comparison of the measured effects with those evoked by an $NH_2$-unmodified OB-cAMP and e.g. further nucleobase derivatives of adenosine or uridine in combination with incubation studies in cell homogenate could help to finalize the analysis and clarify whether the $N^6$-butyryl group is cleaved or the interacting receptors and binding sites lack selectivity in the corresponding region.

In summary, the performed cell assays confirmed excellent membrane-permeability of the OB-cNMPs synthesized. Further, the cellular effects observed allow the conclusion that the bio-reversible protection at the phosphate was removed rapidly and efficiently. A fast enzymatic activation of the prepared OB-cNMPs was shown analogously in hydrolysis studies using pig liver esterase. The esterase cleaved the OB-mask even at low concentration within very short time, so that similar effects can be expected to proceed in cells.

Finally, the observed FRET-sensor binding site interaction and induced $Ca^{2+}$ mobilization proved that biologically active compounds were released from the masked cNMPs. Moreover, the compounds triggered processes like they are attributed to their parent cNMPs (if existent in nature/identified yet).

The chosen synthesis approach bears the potential for flexible interchange of building blocks meaning that different nucleosides can be combined with different masked $PA_2$s. An improvement of yields, however, would be desirable despite the fact that starting materials can be pursued or prepared conveniently.

An interesting approach could be the use of H-phosphonate chemistry (Scheme 57). First, a cyclic nucleoside H-phosphonate would be synthesized using diphenyl phosphine as reagent. At the same time, this step presumably constitutes the bottleneck of the synthesis sequence. Successive oxidative chlorination to the corresponding $P^V$-chlorophosphate and direct conversion with the mask of choice as its corresponding alcohol would give the AB-masked cNMP in only two steps. Hence, this route would be as short and adaptable as the $PA_2$ approach developed and thus constitutes an auspicious option to explore.
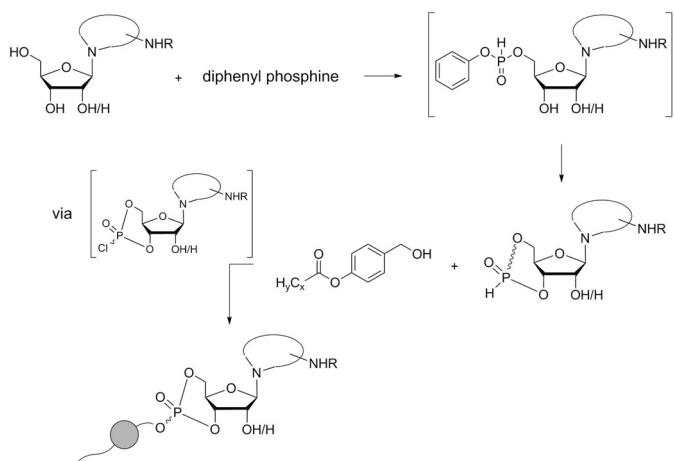
**Scheme 57:** Synthesis sequence for an alternative route towards AB-masked cNMPs using H-phosphonate chemistry.

In summary, the prepared OB-cNMPs fulfilled all requirements in terms of synthetic configurability, which is inherent in the chosen approach, satisfying chemical stability and rapid enzymatic activation to be valuable new tools for the use in and the setup of novel cellular assays.

## 9.   Experimental Part

### 9.1.    General

All reactions involving water-sensitive reagents were conducted under anhydrous condi-tions and a dry atmosphere of nitrogen.

Reagents were used as purchased from commercial suppliers.

The reagents bis(9*H*-fluoren-9-ylmethyl)-di*iso*propylamino phosphoramidite and 5-chloro-*cyclo*Saligenylchlorophosphate were gratefully obtained from S. WEISING.

Triethylamine (TEA) was dried by heating under reflux over calcium hydride for several days followed by distillation. Anhydrous *N,N*-dimethylformamide (DMF) was purchased as such and stored over 4 Å molecular sieves.

All *other anhydrous solvents* were purified and dried using a solvent purification system (MB SPS-800 from Braun), and were stored over appropriate molecular sieves.

Solvents for *normal phase* (NP) chromatography were distilled prior to use. Acetonitrile and tetrahydrofuran were purchased in HPLC grade for *reverse phase* (RP) chromatography and HPL chromatography .

Evaporation of solvents was performed under reduced pressure on a rotary evaporator or using a high-vacuum pump.

Reactions were monitored via *thin layer chromatography* (TLC) carried out on pre-coated Macherey-Nagel TLC plates Alugram® Xtra SIL G/UV$_{254}$, and compounds stained with Van-illin (Vanillin (5 g), 1000 mL MeOH/AcOH 9:1, 35 mL H$_2$SO$_4$) under heating. Manual NP column chromatographic purification was performed with Macherey-Nagel sil-ica gel 60 M (0.04 mm-0.063 mm). For automated NP or RP chromatography, two flash systems (Interchim Puriflash 430 or Sepacore® Flash System, combined with Chromabond® Flash RS 80 SiOH (NP) or RS40 C$_{18}$ ec (RP) columns) were used. For purifications of phos-phor(di)amidites, a chromatotron (Harrison Research 7924T) with glass plates coated with 2 mm or 4 mm layers of VWR60 PF$_{254}$ silica gel containing a fluorescent indicator (VWR no. 7749) was used.

Analytical RP-*High Performance Liquid Chromatography* (RP-HPLC) was carried out on a VWR-Hitachi LaChromElite HPLC system (L-2130, L-2200, L-2455) using EzChromElite soft-ware and a Nucleodur 100-5 C$_{18}$ec column (Macherey-Nagel).

Analytical RP-*High Performance Liquid Chromatography-Mass Spectrometry* (RP-HPLC/MS) was performed with an Agilent 1260 Infinity instrument (pump G1311B, autosampler G1329B, column compartment G1316A, diode array detector G4221B, column Agilent Poroshell 120 EC-C18, 2.7 mm, 4.6x50 mm) coupled with a single-quad MS (Advion expression$^L$ CMS)

*Ultrapure water* was generated by a Sartorius Aurium® pro unit (Sartopore 0.2 µm, UV). As elution buffer for RP-HPLC served tetra-*n*-butylammonium acetate (10 mM, pH 7.2). HPLC runs were performed according to the following method: 0 – 20 min: tetra-*n*-butylammonium acetate (TBAA) buffer/acetonitrile gradient (5% – 80% B) with a flow of 1 mL/min and UV detection at 310 nm. HPLC/MS runs were performed according to the following method: 0 – 15 min: water/acetonitrile gradient (2% – 98% B) with a flow of 0.5 mL/min, 20 °C column temperature and UV detection at 259 nm and 270 nm, MS scans from 150 to 1100 m/z.

*Nuclear magnetic resonance* (NMR) spectra were recorded at room temperature on Bruker Fourier 300 (300 MHz for $^1$H acquisitions), Bruker AMX 400 (400 MHz for $^1$H 101 MHz for $^{13}$C and 152 MHz for $^{31}$P acquisitions) or Bruker AVIII 600 (600 MHz for $^1$H and 151 MHz for $^{13}$C acquisitions) spectrometers in automation mode. All chemical shifts (δ) are given in parts per million (ppm) with the solvent resonance as internal standard. Coupling constants *J* are given in Hertz (Hz). Two-dimensional NMR experiments (HSQC, HMBC) were used for the assignment of quaternary carbons.

For *mass spectrometric* (MS) analytics, spectra were acquired on an Agilent 6224 ESI-TOF spectrometer in positive and negative mode as required.

*Infrared spectroscopy* (IR) was carried out with a Bruker Alpha P FT-IR in attenuated total reflection (ATR) mode at room temperature ranging from 400 cm$^{-1}$ to 4000 cm$^{-1}$. *Ultraviolet visible spectrophotometry (UV-Vis)* was performed using a peqlab NanoDrop 2000c Spectrophotometer in cuvette measurement mode.

*Optical rotations* were measured with a P8000 polarimeter (A. Krüss Optonic GmbH) at the temperatures and concentrations indicated.

## 9.2.    Syntheses

### 9.2.1.    Part I - Functionalized Prodrugs of a Bacterial RNAP-Inhibitor

GENERAL PROCEDURE (GP) I: PREPARATION OF ALKANOYL METHANESULFONATES:

Under anhydrous conditions, the alcohol (1 eq.) was dissolved in dichloromethane and the solution cooled to 0 °C. Methanesulfonyl chloride (1.3 eq.) and triethylamine (1.3 eq.) were added simultaneously and dropwise to the solution. The reaction mixture was stirred at 0 °C for 10 min and then allowed to warm to rt. Upon complete consumption of the starting material, the mixture was poured into a cool, diluted NaHCO₃ solution. The layers were separated and the aqueous phase extracted with dichloromethane. The organic layers were combined, washed once with brine, dried over Na₂SO₄, filtered and the solvent was removed under reduced pressure.

GP II: PREPARATION OF CHLOROMETHYL(ALKYL)CARBONATE MASK REAGENTS:

Under anhydrous conditions, a solution of chloromethyl chloroformate (0.17 – 1.1 eq.) in dichloromethane was cooled to 0 °C and pyridine added dropwise (2 – 2.5 eq., calculated on chloromethyl chloroformate). The resulting suspension was stirred 15 min at 0 °C, followed by addition of the in dichloromethane dissolved alcohol (1 eq.). The reaction mixture was kept further 30 min at 0 °C and then allowed to warm up to rt. After stirring for 18 h, the mixture was diluted with dichloromethane and washed once with each, sat. NaHCO₃ (aq. sol.) and sat. NaCl (aq. sol.). The organic layer was separated, dried over Na₂SO₄, filtered, and the filtrate was evaporated under reduced pressure.

GP III: BASIC ESTERIFICATION OF CARBOXYLIC ACIDS WITH OMS-MASK REAGENTS:

Under anhydrous conditions, the carboxylic acid (1 eq.) was suspended in DMF and mixed with TEA (1.75 eq. – 3 eq.) and the mask reagent-halide/-mesylate (1.85 eq. – 3 eq.). The reaction mixture was stirred at rt for 18 h and terminated by removal of all volatile components under reduced pressure. The crude residue was purified by flash column chromatography on silica gel with an ethyl acetate gradient in petroleum ether.

GP IV: TBAI-AIDED BASIC ESTERIFICATION OF CARBOXYLIC ACIDS WITH HALIDE-MASK REAGENTS:

The carboxylic acid (1 eq.) was suspended in DMF under anhydrous conditions and mixed with TEA (1.75 eq.), the mask reagent-halide (1.85 eq.) and tetra-*n*-butylammonium iodide (TBAI, 0.5 eq.). The reaction was stirred at rt for 18 h and terminated by removal of all volatile components under reduced pressure. The crude residue was purified by flash column chromatography on silica gel with an ethyl acetate gradient in petroleum ether.

GP V: DE-*O*-BENZYLATION VIA TRANSIENT TMS-PROTECTION:

Under anhydrous conditions and an atmosphere of nitrogen, the benzylated diphenol (1 eq.) was dissolved in dichloromethane, the solution cooled to -30 °C and trimethylsilyl iodide (5 eq., 1 M in dichloromethane) added slowly and dropwise. The resulting mixture was allowed to slowly warm up to 0 °C or rt. Upon consumption of the starting material, the mixture was hydrolyzed with cooled phosphate buffer (pH 7) and all volatile components were removed subsequently under high vacuum. The crude product was purified by automated RP$_{18}$ chromatography with an acetonitrile gradient in water (5% – 100%).

Experimental Part

SYNTHESIS OF 3-(3,4-DIBENZYLOXYPHENYL)PROPANOIC ACID BENZYL ESTER **18**:

4.10 g (22.5 mmol) 3-(3,4-dihydroxyphenyl)propionic acid were dissolved in 81 mL acetonitrile plus 4% demin. water (3 mL/mmol), mixed with 14.0 g (101 mmol, 4.5 eq.) potassium carbonate and cooled to 0 °C. Then, 16.1 mL (135 mmol, 6 eq.) benzyl bromide were added slowly. The reaction mixture was heated to 95 °C and stirred for 18 h. To terminate the reaction, the mixture was cooled to rt and then poured into ice water/NaHCO$_3$ sol. 1:1. After extraction with dichloromethane, the combined organic layers were washed with water, dried over Na$_2$SO$_4$, filtered and concentrated in vacuum. Purification was performed via flash column chromatography on silica gel with a petroleum ether/ethyl acetate gradient (5:1 → 3:1) to yield the product as pale yellowish wax.

*Yield*: 8.92 g (19.7 mmol, 88%).
*Formula*: C$_{30}$H$_{28}$O$_4$.
*Molecular weight*: 452.550.
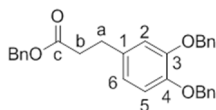


*$^1$H-NMR (400 MHz, chloroform-d)*: δ [ppm] = 7.50 – 7.26 (m, 15 H, C*H*(aromatic)), 6.84 (d, $^3J_{H,H}$ = 8.1 Hz, 1 H, H5), 6.80 (d, $^4J_{H,H}$ = 2.1 Hz, 1 H, H2), 6.69 (dd, $^3J_{H,H}$ = 8.1 Hz, $^4J_{H,H}$ = 2.1 Hz, 1 H, H6), 5.12 (s, 2 H, C*H$_2$*(benzylic)), 5.10 (s, 2 H, C*H$_2$*(benzylic)), 5.09 (s, 2 H, C*H$_2$*(benzylic)), 2.87 (t, $^{2,3}J_{H,H}$ = 7.7 Hz, 2 H, C*H$_2$*(a)), 2.62 (t, $^{2,3}J_{H,H}$ = 7.7 Hz, 2 H, C*H$_2$*(b)).
*$^{13}$C-NMR (101 MHz, chloroform-d)*: δ [ppm] = 172.9 (C$_q$(c)), 149.2 (C4), 147.7 (C3), 137.6 (C$_q$(aromatic)), 137.5 (C$_q$(aromatic)), 136.1 (C$_q$(aromatic)), 134.1 (C1), 128.7 (*C*H(aromatic)), 128.6 (*C*H(aromatic)), 128.4 (*C*H(aromatic)), 128.3 (*C*H(aromatic)), 127.9 (*C*H(aromatic)), 127.5 (*C*H(aromatic)), 127.4 (*C*H(aromatic)), 121.3 (C6), 115.7 (C2), 115.6 (C5), 71.6 (*C*H$_2$(benzylic)), 71.5 (*C*H$_2$(benzylic)), 66.4 (*C*H$_2$(benzylic)), 36.2 (*C*H$_2$(b)), 30.6 (*C*H$_2$(a)).

*IR (ATR)*: ṽ in [cm$^{-1}$] = 3063.3, 3032.1, 2903.9, 2147.2, 1732.9, 1605.4, 1588.1, 1510.8, 1454.1, 1425.7, 1380.4, 1259.4, 1221.2, 1151.1, 1136.1, 1079.9, 1023.3, 907.5, 850.4, 806.9, 735.2, 696.1, 603.9, 463.7.

*MS (ESI-HR)*: m/z [M+NH$_4$]$^+$ calc. for C$_{30}$H$_{29}$NO$_4^+$: 470.2320, found: 470.2323.

SYNTHESIS OF CHLOROMETHYL-(3-(3,4-DIBENZYLOXYPHENYL)PROPANOATE **21**:

*a) Deprotection of 3-(3,4-dibenzyloxyphenyl)propanoic acid benzyl ester*:

To debenzylate the carboxylic acid, 500 mg (1.11 mmol) 3-(3,4-dibenzyloxyphe-nyl)propa-noic acid benzyl ester **18** were dissolved in THF/demin. water 1:1 (5 mL/mmol) and treated with 124 mg (2.21 mmol, 2 eq.) potassium carbonate. The reaction mixture was stirred 5 h at 50 °C. After cooling to rt, the solution was diluted with dichloromethane and the organic layer separated. The aqueous phase was adjusted to pH 3 and extracted two further times with dichloromethane. The combined organic layers were washed with demin. water, dried over $Na_2SO_4$, filtered and the solvent evaporated under reduced pressure. The crude product was purified via NP column chromatography on silica gel with a petroleum ether/ethyl acetate gradient (3:1 → EE) yielding the free carboxylic acid as colorless solid.

*Yield*: 330 mg (0.910 mmol, 82%).

*Formula*: $C_{23}H_{22}O_4$.

*Molecular weight*: 362.425.
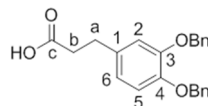


*$^1$H-NMR (400 MHz, chloroform-d)*: δ [ppm] = 7.51 – 7.26 (m, 10 H, C*H*(aromatic)), 6.86 (d, $^3J_{H,H}$ = 8.2 Hz, 1 H, H5), 6.81 (d, $^4J_{H,H}$ = 2.1 Hz, 1 H, H2), 6.72 (dd, $^3J_{H,H}$ = 8.1 Hz, $^4J_{H,H}$ = 2.1 Hz, 1 H, H6), 5.14 (s, 2 H, C*H$_2$*(benzylic)), 5.13 (s, 2 H, C*H$_2$*(benzylic)), 2.85 (t, $^{2,3}J_{H,H}$ = 7.7 Hz, 2 H, C*H$_2$*(a)), 2.61 (t, $^{2,3}J_{H,H}$ = 7.7 Hz, 2 H, C*H$_2$*(b)).

*$^{13}$C-NMR (101 MHz, chloroform-d)*: δ [ppm] = 177.2 ($C_q$(c)), 149.1 (C4), 147.8 (C3), 137.6 ($C_q$(aromatic)), 137.5 ($C_q$(aromatic)), 133.8 (C1), 128.6 (*C*H(aromatic)), 128.0 (*C*H(aromatic)), 127.9 (*C*H(aromatic)), 127.6 (*C*H(aromatic)), 127.5 (*C*H(aromatic)), 121.3 (C6), 115.8 (C2), 115.6 (C5), 71.7 (*C*H$_2$(benzylic)), 71.6 (*C*H$_2$(benzylic)), 35.6 (*C*H$_2$(b)), 30.3 (*C*H$_2$(a)).

*IR (ATR)*: ṽ in [cm$^{-1}$] = 3032.8, 2930.7, 2865.4, 2088.7, 1960.7, 1701.5, 1590.0, 1517.0, 1453.7, 14329.0, 1382.7, 1302.0, 1262.7, 1213.9, 1163.3, 1138.1, 912.2, 849.3, 799.0, 736.7, 695.7, 575.4.

*MS (ESI-HR)*: m/z [M+H]$^+$ calc. for $C_{23}H_{23}O_4{}^+$: 363.1590, found: 363.1537.

*b) Chloromethylation of carboxylic acid **19***:

In 5 mL demin. water/dichloromethane (1:1), 190 mg (0.524 mmol) 3-(3,4-dibenzyloxy-phenyl)propanoic acid **19** were dissolved and mixed with 176 mg (2.10 mmol, 4 eq.) so-dium bicarbonate and 17.8 mg (52.4 µmol, 0.1 eq.) tetra-*n*-butylammonium hydrogensul-fate. Last, 59.4 µL (0.576 mmol, 1.1 eq.) chloromethyl chlorosulfate were added to the sus-pension under vigorous stirring. After 60 min, the reaction mixture cleared up which indi-cated largely complete conversion of the starting material. The layers were subsequently separated, and the organic layer was washed with a diluted NaHCO₃ solution. After drying over Na₂SO₄ and filtration, dichloromethane was removed under reduced pressure. The product was obtained as clear, pale yellowish syrup.

*Yield*: 182 mg (0.443 mmol, 85%).

*Formula*: $C_{24}H_{23}ClO_4$.

*Molecular weight*: 410.894.
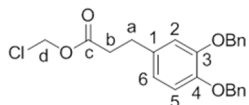


*¹H-NMR (400 MHz, chloroform-d)*: δ [ppm] = 7.51 – 7.27 (m, 10 H, C*H*(aromatic)), 6.86 (d, ³$J_{H,H}$ = 8.1 Hz, 1 H, H5), 6.80 (d, ⁴$J_{H,H}$ = 2.1 Hz, 1 H, H2), 6.71 (dd, ³$J_{H,H}$ = 8.1 Hz, ⁴$J_{H,H}$ = 2.1 Hz, 1 H, H6), 5.66 (s, 2 H, C*H₂*(d)), 5.14 (s, 2 H, C*H₂*(benzylic)), 5.13 (s, 2 H, C*H₂*(benzylic)), 2.88 (t, ²,³$J_{H,H}$ = 7.6 Hz, 2 H, (C*H₂*(a)), 2.64 (t, ²,³$J_{H,H}$ = 7.7 Hz, 2 H, (C*H₂*(b)).

*¹³C-NMR (101 MHz, chloroform-d)*: δ [ppm] = 171.0 (C_q(c)), 149.2 (C4), 147.8 (C3), 137.6 (C_q(aromatic)), 137.4 (C_q(aromatic)), 133.4 (C1), 128.6 (C*H*(aromatic)), 128.0 (*C*H(aro-matic)), 127.9 (C*H*(aromatic)), 127.6 (*C*H(aromatic)), 127.5 (*C*H(aromatic)), 121.3 (C6), 115.7 (C2), 115.6 (C5), 71.6 (C*H₂*(benzylic)), 71.5 (C*H₂*(benzylic)), 68.8 (C*H₂*(d)) 35.9 (C*H₂*(b)), 30.1 (*C*H₂*(a)).

*IR (ATR)*: ṽ in [cm⁻¹] = 3062.9, 3031.9, 2930.0, 2870.1, 2044.6, 1759.5, 1605.1, 1588.8, 1509.9, 1453.5, 1439.5, 1426.0, 1377.8, 1334.7, 1258.3, 1215.4, 1158.2, 1119.1, 1014.1, 907.0, 848.8, 806.5, 731.7, 694.4, 621.8, 605.1, 461.3, 400.8.

*MS (ESI-HR)*: m/z [M+H]⁺ calc. for $C_{24}H_{24}ClO_4^+$: 411.1357, found: 411.1355.

SYNTHESIS OF 3-(3,4-DIBENZYLOXYPHENYL)PROPANOL **20**:

In a Schlenk flask, 1.45 g (3.20 mmol) 3-(3,4-dibenzyloxyphenyl)propanoic acid benzyl ester **18** were dissolved in THF (5 mL/mmol) and the solution was cooled to 0 °C. Under vigorous stirring, 9.61 mL (9.61 mmol, 3 eq.) borane-THF complex (1 M in THF) was added slowly. The reaction mixture was allowed to warm to rt and stirred for further 18 h. To terminate the reaction, 1 M hydrochloric acid was added and the solution diluted with dichloromethane. The aqueous phase was separated, extracted once with dichloromethane, and the combined organic layers were washed with brine and demin. water. After drying over $Na_2SO_4$ and filtration, the crude product was concentrated in vacuum. Purification on NP silica gel with a petroleum ether/ethyl acetate gradient (5:1 → 1:1) yielded the product as colorless wax.

*Yield*: 1.01 g (2.91 mmol, 91%).

*Formula*: $C_{23}H_{24}O_3$.

*Molecular weight*: 348.442.
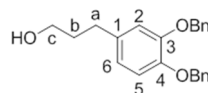
*$^1$H-NMR (400 MHz, chloroform-d)*: δ [ppm] = 7.58 – 7.26 (m, 10 H, C*H*(aromatic)), 6.87 (d, $^3J_{H,H}$ = 8.1 Hz, 1 H, H5), 6.79 (d, $^4J_{H,H}$ = 2.0 Hz, 1 H, H2), 6.71 (dd, $^3J_{H,H}$ = 8.1 Hz, $^4J_{H,H}$ = 2.0 Hz, 1 H, H6), 5.15 (s, 2 H, C*H$_2$*(benzylic)), 5.13 (s, 2 H, C*H$_2$*(benzylic)), 3.72 – 3.50 (m, 2 H, C*H$_2$*(c)), 2.61 (t, $^{2,3}J_{H,H}$ = 7.6 Hz, 2 H, C*H$_2$*(a)), 1.88 – 1.76 (m, 2 H, C*H$_2$*(b)).

*$^{13}$C-NMR (101 MHz, chloroform-d)*: δ [ppm] = 149.0 (C4), 147.4 (C3), 137.7 ($C_q$(aromatic)), 137.6 ($C_q$(aromatic)), 135.5 (C1), 128.6 (*C*H(aromatic)), 127.8 (*C*H(aromatic)), 127.5 (*C*H(aromatic)), 127.4 (*C*H(aromatic)), 121.4 (C6), 116.0 (C2), 115.6 (C5), 71.8 (*C*H$_2$(benzylic)), 71.5 (*C*H$_2$(benzylic)), 62.3 (*C*H$_2$(c)), 34.3 (*C*H$_2$(b)), 31.7 (*C*H$_2$(a)).

*IR (ATR)*: ṽ in [cm$^{-1}$] = 3356.1, 3031.4, 2932.4, 2863.5, 1605.5, 1587.7, 1509.2, 1453.6, 1423.7, 1379.4, 1259.0, 1217.5, 1156.2, 1134.4, 1014.1, 909.1, 848.2, 807.0, 733.2, 695.1, 624.1, 464.5.

*MS (ESI-HR)*: m/z [M+H]$^+$ calc. for $C_{23}H_{25}O_3^+$: 349.1797, found: 349.1758.

SYNTHESIS OF 3-(3,4-DIBENZYLOXYPHENYL)PROPANOYL MESYLATE **34**:

According to GP I, 1.0 g (2.8 mmol) 3-(3,4-dibenzyloxyphenyl)propanol **20** was converted with 0.28 mL (3.6 mmol, 1.3 eq.) methanesulfonyl chloride and 0.51 mL (3.6 mmol, 1.3 eq.) triethylamine. After the aqueous work up, the solvent was removed to yield the product as clear colorless syrup.

*Yield*: 0.93 g (2.2 mmol, 76%).

*Formula*: $C_{24}H_{26}O_5S$.

*Molecular weight*: 426.527.
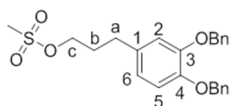


*$^1$H-NMR (400 MHz, chloroform-d)*: δ [ppm] = 7.51 – 7.28 (m, 10 H, C$H$(aromatic)), 6.87 (d, $^3J_{H,H}$ = 8.1 Hz, 1 H, H5), 6.78 (d, $^4J_{H,H}$ = 2.2 Hz, 1 H, H2), 6.73 – 6.66 (m, 1 H, H6), 5.16 (s, 2 H, C$H_2$(benzylic)), 5.14 (s, 2 H, C$H_2$(benzylic)), 4.17 (t, $^{2,3}J_{H,H}$ = 6.3 Hz, 2 H, C$H_2$(c)), 2.96 (s, 3 H, C$H_3$(OMs)), 2.65 (t, $^{2,3}J_{H,H}$ = 7.3 Hz, 2 H, C$H_2$(a)), 2.04 – 1.95 (m, 2 H, C$H_2$(b)).

*$^{13}$C-NMR (101 MHz, chloroform-d)*: δ [ppm] = 149.1 (C4), 147.7 (C3), 137.7 (C$_q$(aromatic)), 137.4 (C$_q$(aromatic)), 133.8 (C1), 128.6 (C$H$(aromatic)), 127.9 (C$H$(aromatic)), 127.5 (C$H$(aromatic)), 127.4 (C$H$(aromatic)), 121.4 (C6), 115.8 (C2), 115.6 (C5), 71.6 (C$H_2$(benzylic)), 71.5 (C$H_2$(benzylic)), 69.2 (C$H_2$(c)), 37.4 (C$H_3$(OMs)), 31.1 (C$H_2$(b)), 30.8 (C$H_2$(a)).

*IR (ATR)*: ṽ in [cm$^{-1}$] = 3031.1, 2937.0, 2035.0, 1588.4, 1511.8, 1454.4, 1425.5, 1352.0, 1262.0, 1224.3, 1172.5, 1136.7, 1079.9, 1010.0, 971.9, 925.1, 835.9, 811.7, 737.6, 697.2, 620.7, 528.3, 468.4.

*MS (ESI-HR)*: m/z [M+Na]$^+$ calc. for $C_{24}H_{26}O_5SNa^+$: 449.1399, found: 449.1494.

SYNTHESIS OF CHLOROMETHYL(3-(3,4-DIBENZYLOXYPHENYL) PROPYL)CARBONATE **22**:

According to GP II, 56 µL (0.63 mmol, 1.1 eq.) chloromethyl chloroformate were reacted with 200 mg (0.574 mmol) 3-(3,4-dibenzyloxyphenyl) propanol **20** in the presence of 117 µL (1.44 mmol, 2.5 eq.) pyridine. After washing, dichloromethane was removed under high vacuum and the product obtained as clear yellowish liquid.

*Yield*: 239 mg (0.543 mmol, 95%).

*Formula*: $C_{25}H_{25}ClO_5$.

*Molecular weight*: 440.920.
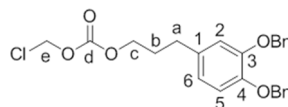


*$^1$H-NMR (400 MHz, chloroform-d)*: δ [ppm] = 7.56 – 7.27 (m, 10 H, C*H*(aromatic)), 6.87 (d, $^3J_{H,H}$ = 8.1 Hz, 1 H, H5), 6.78 (d, $^4J_{H,H}$ = 2.0 Hz, 1 H, H2), 6.69 (dd, $^3J_{H,H}$ = 8.1 Hz, $^4J_{H,H}$ = 2.0 Hz, 1 H, H6), 5.73 (s, 2 H, C*H$_2$*(e)), 5.14 (s, 2 H, C*H$_2$*(benzylic)), 5.13 (s, 2 H, C*H$_2$*(benzylic)), 4.19 (t, $^{2,3}J_{H,H}$ = 6.4 Hz, 2 H, C*H$_2$*(c)), 2.61 (t, $^{2,3}J_{H,H}$ = 7.6 Hz, 2 H, C*H$_2$*(a)), 1.96 (dt, $^{2,3}J_{H,H}$ = 6.4 Hz, $^{2,3}J_{H,H}$ = 8.4 Hz, 2 H, C*H$_2$*(b)).

*$^{13}$C-NMR (101 MHz, chloroform-d)*: δ [ppm] = 153.5 (C$_q$(d)), 149.1 (C4), 147.7 (C3), 137.6 (C$_q$(aromatic)), 137.5 (C$_q$(aromatic)), 134.2 (C1), 128.6 (C*H*(aromatic)), 127.9 (C*H*(aromatic)), 127.8 (C*H*(aromatic)), 127.6 (C*H*(aromatic)), 127.5 (C*H*(aromatic)), 121.4 (C6), 115.9 (C2), 115.6 (C5), 72.3 (C*H$_2$*(e)), 71.7 (C*H$_2$*(benzylic)), 71.6 (C*H$_2$*(benzylic)), 68.5 (C*H$_2$*(c)), 31.4 (C*H$_2$*(a)), 30.2 (C*H$_2$*(b)).

*IR (ATR)*: ṽ in [cm$^{-1}$] = 3661.3, 3064.2, 3031.5, 2938.8, 2206.5, 2087.5, 1961.0, 1765.0, 1605.4, 1588.4, 1512.1, 1454.1, 1425.5, 1384.2, 1343.1, 1251.4, 1158.4, 1136.9, 1116.5, 1080.2, 1017.7, 970.7, 900.4, 851.7, 787.9, 735.7, 696.7, 621.3.

*MS (ESI-HR)*: m/z [M+NH$_4$]$^+$ calc. for $C_{25}H_{29}ClNO_5^+$: 458.1657, found: 458.1721.

S<small>YNTHESIS OF</small> 5-B<small>ENZYLOXY</small>-2-(<small>HYDROXYMETHYL</small>)-4-<small>PYRONE</small> **23**:

Following the procedure described by B<small>ROWN</small> *et al.*, 500 mg (3.52 mmol) Kojic acid were suspended in methanol and mixed with 5.28 mL (5.28 mmol, 1.5 eq.) sodium hydroxide (1 M aq. sol.) and 1.25 mL (10.6 mmol, 3 eq.) benzyl bromide under cooling. The reaction mixture was heated to 100 °C for 18 h. Upon completion, the mixture was allowed to cool to rt and 30 mL hydrochloric acid (1 M aq. sol.) were added. The precipitation of the prod-uct was completed by stirring at 0 °C for 60 min. The obtained solids were filtered of and washed with water and petroleum ether/ethyl acetate 3:2. The filtrate was resolved in methanol and the solution concentrated to dryness in high vacuum. The product was af-forded as beige to colorless solid.

*Yield*: 680 mg (2.92 mmol, 83%).

*Formula*: $C_{13}H_{12}O_4$.

*Molecular weight*: 232.235.
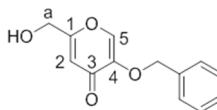
*$^1$H-NMR (400 MHz, methanol-d$_4$)*: δ [ppm] = 8.04 (s, 1 H, H5), 7.56 – 7.31 (m, 5 H, C*H*(aro-matic)), 6.55 (d, $^4J_{H,H}$ = 1.0 Hz, 1 H, H2), 5.07 (s, 2H, C*H$_2$*(benzylic)), 4.44 (d, $^4J_{H,H}$ = 0.9 Hz, 2 H, C*H$_2$*(a)).

*$^{13}$C-NMR (101 MHz, methanol-d$_4$)*: δ [ppm] = 177.0 (C3), 170.6 (C1), 148.3 (C4), 143.2 (C5), 137.3 (C$_q$(aromatic)), 129.6, 129.4, 129.1 (*C*H(aromatic)), 112.1 (C2), 72.6 (*C*H$_2$(benzylic)), 61.0 (*C*H$_2$(a)).

*IR (ATR)*: ṽ in [cm$^{-1}$] = 3316.2, 3094.7, 2920.3, 2851.7, 2228.1, 2150.0, 2105.7, 2021.6, 1978.3, 1961.8, 1646.3, 1611.7, 1261.3, 1203.7, 1081.2, 985.6, 946.2, 863.6, 826.5, 779.0, 748.5, 736.6, 697.8, 653.8, 627.3, 612.2, 586.5, 552.4, 538.9, 515.0.

*MS (ESI-HR)*: m/z [M+Na]$^+$ calc. for $C_{13}H_{12}O_4Na^+$: 255.0634, found: 255.0635.
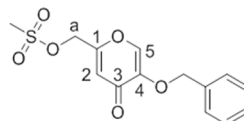
SYNTHESIS OF 5-BENZYLOXY-4-PYRONE-2-METHYLMESYLATE **32**:

According to GP I, 150 mg (0.646 mmol) 5-benzyloxy-2-(hydroxymethyl)-4-pyrone **23** were treated with 62.5 µL (0.807 mmol, 1.3 eq) methanesulfonyl chloride and 113 µL (0.807 mmol, 1.3 eq.) triethylamine. The product was obtained as pale beige solid.

*Yield*: 171 mg (0.552 mmol, 85%).

*Formula*: $C_{14}H_{14}O_6S$.

*Molecular weight*: 310.320.



*$^1$H-NMR (400 MHz, chloroform-d)*: δ [ppm] = 7.45 (s, 1 H, H5), 7.35 – 7.06 (m, 5 H, C*H*(aromatic)), 6.39 (s, 1 H, H2), 4.59 (s, 2H, C*H$_2$*(benzylic)), 4.82 (s, 2 H, C*H$_2$*(a)), 2.96 (s, 3 H, C*H$_3$*(mesyl)).

*$^{13}$C-NMR (101 MHz, chloroform-d)*: δ [ppm] = 174.1 (C3), 158.9 (C1), 147.6 (C4), 141.7 (C5), 135.5 (C$_q$(aromatic)), 128.9, 128.7, 127.9 (*C*H(aromatic)), 115.8 (C2), 72.1 (*C*H$_2$(benzylic)), 65.2 (*C*H$_2$(a)), 38.4 (*C*H$_3$(mesyl)).

*IR (ATR)*: ṽ in [cm$^{-1}$] = 3064.9, 3031.8, 2955.2, 2920.1, 2850.9, 2181.7, 2165.2, 2024.0, 1984.9, 1952.5, 1734.7, 1652.7, 1625.2, 1595.6, 1497.7, 1455.4, 1434.1, 1358.5, 1265.9, 1208.9, 1175.1, 1081.5, 1029.9, 958.1, 919.7, 867.4, 811.1, 735.5, 699.0, 647.6, 583.4, 527.0, 509.7.

*MS (ESI-HR)*: m/z [M+Na]$^+$ calc. for $C_{14}H_{14}O_6SNa^+$: 333.0403, found: 333.0407.

SYNTHESIS OF 5-BENZYLOXY-2-HYDROXYMETHYL-*N*-BENZYLOXY PYRIDINE-4-ON **25**:

608 mg (2.62 mmol) 5-benzyloxy-2-(hydroxymethyl)-4-pyrone **23** were dissolved in 6 mL *N*-methyl-2-pyrrolidone, mixed with 910 mg (13.1 mmol, 5 eq.) hydroxylamine hydrochloride and 1.81 g (13.1 mmol, 5 eq.) potassium carbonate and heated to 75 °C for 24 h. At room temperature, 0.46 mL (3.93 mmol, 1.5 eq.) benzyl bromide and 633 mg (4.58, 1.8 eq.) potassium carbonate were added. The reaction mixture was heated to 75 °C for further 24 h. Successively, the reaction mixture was poured into ice water and the product extracted with ethyl acetate. The organic layer was washed with water, dried over $Na_2SO_4$, filtered and concentrated. A final column chromatographic purification on silica gel with dichloromethane/methanol 9:1 as eluent afforded the product as colorless solid.

*Yield*: 501 mg (1.48 mmol, 56%).

*Formula*: $C_{20}H_{19}NO_4$.

*Molecular weight*: 337.375.
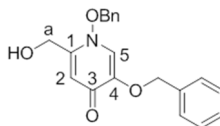


*$^1$H-NMR (400 MHz, methanol-$d_4$)*: δ [ppm] = 7.77 (s, 1 H, H5), 7.50 – 7.29 (m, 10 H, C*H*(aromatic)), 6.50 (s, 1 H, H2), 5.23 (s, 2H, C*H$_2$*(benzylic), 5.04 (s, 2H, C*H$_2$*(benzylic), 4.40 (s, 2 H, C*H$_2$*(a)).

*$^{13}$C-NMR (101 MHz, methanol-$d_4$)*: δ [ppm] = 173.5 (C3), 149.8 (C1), 148.3 (C4), 137.4, 134.2 ($C_q$(aromatic)), 131.5, 131.0, 130.0, 129.6, 129.4, 129.1 (*C*H(aromatic)), 124.5 (C5),112.4 (C2), 82.6, 72.4 (*C*H$_2$(benzylic)), 58.6 (*C*H$_2$(a)).

*IR (ATR)*: ṽ in [cm$^{-1}$] = 3330.9, 3254.0, 3210.5, 3066.4, 3035.2, 2923.9, 2850.5, 2154.4, 2045.7, 2032.6, 1992.1, 1956.4, 1613.2, 1562.5, 1527.2, 1498.7, 1454.5, 1388.6, 1279.5, 1218.9, 1107.3, 1078.8, 984.8, 911.2, 861.0, 749.7, 697.4, 642.1.

*MS (ESI-HR)*: m/z [M+H]$^+$ calc. for $C_{20}H_{20}NO_4^+$: 338.1386, found: 338.1404

SYNTHESIS OF CHLOROMETHYL(5-BENZYLOXY-*N*-BENZYLOXY PYRIDINE-4-ON-2-METHYL)CARBONATE **28**:

Following GP II, 25 µL (0.29 mmol, 1.1 eq.) chloromethyl chloroformate were reacted with 88 mg (0.26 mmol) 5-benzyloxy-2-hydroxymethyl-*N*-benzyloxy pyridine-4-on **25** in the presence of 53 µL (0.65 mmol, 2.5 eq.) pyridine to afford the product as clear syrup.

*Yield*: 39 mg (0.09 mmol, 35%).

*Formula*: $C_{22}H_{20}ClNO_6$.

*Molecular weight*: 429.850.
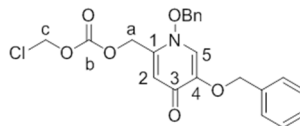


*$^1$H-NMR (400 MHz, methanol-$d_4$)*: δ [ppm] = 7.91 (s, 1 H, H5), 7.51 – 7.30 (m, 10 H, C*H*(aromatic)), 6.44 (s, 1 H, H2), 5.83 (s, 2 H, C*H$_2$*(c)), 5.27 (s, 2 H, C*H$_2$*(benzylic)), 5.12 (s, 2 H, C*H$_2$*(a)), 5.07 (s, 2 H, C*H$_2$*(benzylic)).

*$^{13}$C-NMR (101 MHz, methanol-$d_4$)*: δ [ppm] = 173.0 (C3), 154.2 ($C_q$(c)), 149.1 (C1), 142.8(C4), 137.4, 134.2 ($C_q$(aromatic)), 131.5, 131.0, 130.0, 129.6, 129.4, 129.1 (*C*H(aromatic)), 129.1 (C5), 114.3(C2), 83.0(*C*H$_2$(benzylic)), 74.0 (*C*H$_2$(c)), 72.5 (*C*H$_2$(benzylic)), 64.1 (*C*H$_2$(a)).

*IR (ATR)*: ṽ in [cm$^{-1}$] = 3032.9, 2955.8, 2924.2, 2870.9, 2154.8, 2100.5, 2040.9, 2028.9, 1990.9, 1932.2, 1887.1, 1770.0, 1612.8, 1578.7, 1498.0, 1378.3, 1229.8, 1104.0, 1081.4, 962.7, 909.2, 852.3, 785.0, 752.4, 698.0, 605.5, 584.2.

*MS (ESI-HR)*: m/z [M+H]$^+$ calc. for $C_{22}H_{21}ClNO_6^+$: 430.1051, found 430.1068.

SYNTHESIS OF 5-(3',4'-DICHLOROPHENYL)-3-[(*N*-ETHYL BENZYL AMINO)CARBONYL AMINO]-THIOPHENE-2-CARBOXYLIC ACID-(3-(3,4-DIBENZYLOXYPHENYL) PROPIONYLOXYMETHYL ESTER **38**:

In accordance with GP IV, 15 mg (33 µmol) 5-(3',4'-dichlorophenyl)-3-[(*N*-ethyl benzyl amino)-carbonyl amino]-thiophen-2-carboxylic acid were reacted with 25 mg (62 µmol) chloromethyl-(3-(3,4-dibenzyloxy-phenyl)propanoate **21** in the presence of 8 µL (58 µmol) triethylamine and 11 mg (31 µmol) tetra-*n*-butyl-ammonium iodide in a total volume of 2.5 mL of DMF. After 18 h at 40 °C, all volatile components were removed and the crude residue was purified to afford the product as yellowish resin.

*Yield*: 23 mg (28 µmol, 84%).

*Formula*: $C_{45}H_{40}Cl_2N_2O_7S$.

*Molecular weight*: 823.782.
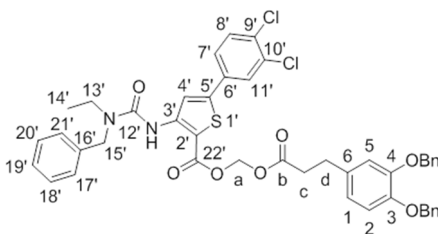


$^1$*H-NMR (400 MHz, chloroform-d)*: δ [ppm] = 9.83 (bs, 1 H, N*H*),8.39 (s, 1 H, H4'), 7.76 (d, $^4J_{H,H}$ = 2.1 Hz, 1 H, H11'), 7.47 (dd, $^3J_{H,H}$ = 8.4 Hz, $^4J_{H,H}$ = 2.1 Hz, 1 H, H7'), 7.44 – 7.37 (m, 5 H, H8', C*H*(aromatic)), 7.36 – 7.27 (m, 11 H, C*H*(aromatic)), 6.82 – 6.78 (m, 2 H, H2, H5), 6.68 (dd, $^3J_{H,H}$ = 8.2 Hz, $^4J_{H,H}$ = 2.1 Hz, 1 H, H6), 5.89 (s, 2 H, C*H$_2$*(a)), 5.11 (s, 2 H, C*H$_2$*(benzylic)), 5.06 (s, 2 H, C*H$_2$*(benzylic)), 4.63 (s, 2 H, H15'), 3.44 (q, $^{2,3}J_{H,H}$ = 7.2 Hz, 2 H, H13'), 2.87 (t, $^{2,3}J_{H,H}$ = 7.6 Hz, 2 H, C*H$_2$*(d)), 2.65 (t, $^{2,3}J_{H,H}$ = 7.7 Hz, 2 H, C*H$_2$*(c)), 1.28 – 1.23 (m, 3 H, H14').

$^{13}$*C-NMR (126 MHz, chloroform-d)*: δ [ppm] = 171.7 (C$_q$(b)), 163.3 (C22'), 153.8 (C12'), 149.1 (C4), 148.2 (C5'), 147.8 (C3), 137.6 (C16') 137.5 (C$_q$(aromatic) *O*Bn), 137.4 (C$_q$(aromatic) *O*Bn), 133.6 (C6'), 133.4 (C1), 130.9 (C8'), 128.8 (C*H*(aromatic)), 128.6 (C*H*(aromatic)), 128.5 (C*H*(aromatic)), 128.0 (C*H*(aromatic)), 127.8 (C11'), 127.5 (C*H*(aromatic)), 127.4 (C*H*(aromatic)), 125.2 (C7'), 121.1 (C6), 118.6 (C4') 115.7 (C2), 115.6 (C5), 105.9 (C3'), 78.1 (C*H$_2$*(a)), 71.6 (C*H$_2$*(benzylic)), 71.5 (C*H$_2$*(benzylic)), 50.2 (C15'), 42.2 (C13'), 35.8 (C*H$_2$*(c)), 30.3 (C*H$_2$*(d)), 13.3 (C14').

*IR (ATR)*: ṽ in [cm$^{-1}$] = 3346.8, 2959.7, 2919.4, 2848.5, 2356.0, 2343.7, 2197.3, 2035.4, 1989.4, 1952.3, 1820.8, 1757.7, 1671.5, 1574.3, 1453.0 1434.9, 1379.0, 1258.9, 1138.2, 1079.1, 1025.7, 850.1, 757.7, 731.5, 649.8, 640.2.

*MS (ESI-HR)*: m/z [M+H]$^+$ calc. for C$_{45}$H$_{41}$Cl$_2$N$_2$O$_7$S$^+$: 823.2005, found: 823.1999.

SYNTHESIS OF 5-(3′,4′-DICHLOROPHENYL)-2-[(N-ETHYL BENZYL AMINO)CARBONYL AMINO]-THIOPHENE-3-CARBOXYLIC ACID-[OXYMETHYL(3-(3,4-DIBENZYLOXYPHENYL)-PROPYL)-CARBONATE] ESTER **39**:

The synthesis was performed according to GP IV and 15 mg (33 µmol) 5-(3′,4′-dichlorophenyl)-2-[(N-ethyl benzyl amino)-carbonyl amino]-thiophen-3-carboxylic acid treated with 27 mg (62 µmol) chloromethyl(3-(3,4-dibenzyloxy-phenyl)-propyl)-carbonate **22** in the presence of 8 µL (58 µmol) triethylamine and 11 mg (31 µmol) tetra-*n*-butyl-ammonium iodide in a total volume of 2.5 mL of DMF. The reaction mixture was stirred 18 h at 40 °C. After all volatile components were removed in high vacuum; the obtained residue was purified and gave the product as yellowish resin.

*Yield*: 19 mg (22 µmol, 65%).
*Formula*: C$_{46}$H$_{42}$Cl$_2$N$_2$O$_8$S.
*Molecular weight*: 853.808.
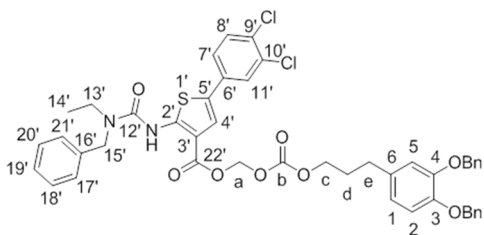


$^1$*H-NMR (400 MHz, chloroform-d)*: δ [ppm] = 10.62 (bs, 1 H, N*H*), 7.79 (d, $^4J_{H,H}$ = 2.1 Hz, 1 H, H11′), 7.45 – 7.38 (m, 6 H, H4′, H7′, H8′, C*H*(aromatic)), 7.39 – 7.27 (m, 11 H, C*H*(aromatic)), 6.84 (d, $^3J_{H,H}$ = 8.2 Hz, 1 H, H5), 6.76 (d, $^4J_{H,H}$ = 2.0 Hz, 1 H, H2), 6.67 (dd, $^3J_{H,H}$ = 8.2 Hz, $^4J_{H,H}$ = 2.1 Hz, 1 H, H6), 5.95 (s, 2 H, C*H$_2$*(a)), 5.12 (s, 2 H, C*H$_2$*(benzylic)), 5.11 (s, 2 H, C*H$_2$*(benzylic)), 4.64 (s, 2 H, H15′), 4.17 (t, $^{2,3}J_{H,H}$ = 6.5 Hz, 2 H, C*H$_2$*(c)) 3.44 (q, $^{2,3}J_{H,H}$ = 7.5 Hz, 2 H, H13′), 2.60 (t, $^{2,3}J_{H,H}$ = 7.6 Hz, 2 H, C*H$_2$*(e)), 1.99 – 1.89 (m, 2 H, C*H$_2$*(d)), 1.29 – 1.23 (m, 3 H, H14′).

*¹³C-NMR (126 MHz, chloroform-d)*: δ [ppm] = 164.2 (C22'), 154.2 (C$_q$(b)), 153.4 (C12'), 149.2 (C4), 147.7 (C3), 137.6 (C$_q$(aromatic) *O*Bn), 137.5 (C16'), 137.4 (C$_q$(aromatic) *O*Bn), 134.3 (C1), 133.3 (C6'), 130.4 (C8'), 128.9 (CH(aromatic)), 128.6 (CH(aromatic)), 128.0 (CH(aromatic)), 127.5 (CH(aromatic)), 127.4 (CH(aromatic)), 127.0 (C11'), 124.4 (C7'), 121.4 (C6), 120.1 (C4') 115.9 (C2), 115.6 (C5), 110.3 (C3'), 81.6 (*C*H$_2$(a)), 71.7 (*C*H$_2$(benzylic)), 71.6 (*C*H$_2$(benzylic)), 68.2 (*C*H$_2$(c)), 50.3 (C15'), 42.2 (C13'), 31.5 (*C*H$_2$(e)), 30.3 (*C*H$_2$(d)), 13.2 (C14').

*IR (ATR)*: ṽ in [cm$^{-1}$] = 2954.8, 2920.1, 2851.2, 1759.6, 1666.0, 1554.0, 1522.9, 1455.3, 1424.7, 1377.9, 1259.6, 1202.0, 1160.7, 113.2, 1080.2, 1025.3, 999.6, 963.0, 907.1, 847.5, 814.6, 789.7, 776.3, 733.0, 696.3, 674.1, 647.7.

*MS (ESI-HR)*: m/z [M+H]$^+$ calc. for C$_{46}$H$_{43}$Cl$_2$N$_2$O$_8$S$^+$: 853.2112, found: 853.2326.

SYNTHESIS OF 5-(3',4'-DICHLOROPHENYL)-3-[(*N*-ETHYL BENZYL AMINO)CARBONYL AMINO]-THIOPHENE-2-CARBOXYLIC ACID-(3-(3,4-DIHYDROXYPHENYL) PROPIONYLOXYMETHYL ESTER **43**:

In accordance with GP V, 19 mg (23 µmol) 5-(3',4'-dichlorophenyl)-3-[(*N*-ethyl benzyl amino)carbonyl amino]-thiophene-2-carboxylic acid-(3-(3,4-dibenzyl-oxyphenyl)-propionyloxymethyl ester **38** were treated with 115 µL (115 µmol) TMSI (1 M in dichloro-methane) in 2.5 mL dichloromethane. The product was obtained as colorless wax after purification.

*Yield*: 12 mg (18 µmol, 77%).
*Formula*: C$_{31}$H$_{28}$Cl$_2$N$_2$O$_7$S.
*Molecular weight*: 643.532.
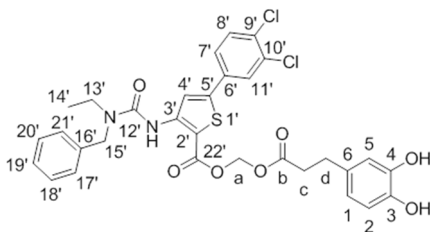
*$^1$H-NMR (400 MHz, acetonitrile-d$_3$)*: δ [ppm] = 9.67 (bs, 1 H, N*H*), 8.34 (s, 1 H, H4'), 7.84 (d, $^4J_{H,H}$ = 2.1 Hz, 1 H, H11'), 7.61 (dd, $^3J_{H,H}$ = 8.4 Hz, $^4J_{H,H}$ = 2.1 Hz, 1 H, H7'), 7.55 (d, $^3J_{H,H}$ = 8.4 Hz, 1 H, H8'), 7.40 – 7.25 (m, 5 H, H17' – H21'), 6.66 (d, $^4J_{H,H}$ = 2.1 Hz, 1 H, H2), 6.61 (d, $^3J_{H,H}$ = 8.4 Hz, 1 H, H5), 6.57 – 6.47 (m, 3 H, H6, 2x O*H*), 5.83 (s, 2 H, C*H$_2$*(a)), 4.62 (s, 2 H, H15'), 3.43 (q, $^{2,3}J_{H,H}$ = 7.2 Hz, 2 H, H13'), 2.77 (t, $^{2,3}J_{H,H}$ = 7.3 Hz, 2 H, C*H$_2$*(d)), 2.63 (t, $^{2,3}J_{H,H}$ = 7.3 Hz, 2 H, C*H$_2$*(c)), 1.23 (t, $^{2,3}J_{H,H}$ = 7.2 Hz, 3 H, H14').

*$^{13}$C-NMR (126 MHz, acetonitrile-d$_3$)*: δ [ppm] = 172.2 (C$_q$(b)), 163.8 (C22'), 154.4 (C12'), 148.2 (C5'), 145.4 (C4), 143.7 (C3), 139.2 (C16'), 134.3, (C10'), 133.7 (C6'), 133.6 (C9'), 133.3 (C1), 132.8 (C8'), 129.5, 128.3, 128.2 (C17' – C21'), 128.8 (C11'), 126.9 (C7'), 120.8 (C6), 119.8 (C4') 116.2 (C2), 116.0 (C5), 80.0 (*C*H$_2$(a)), 50.6 (C15'), 43.1 (C13'), 36.2 (*C*H$_2$(c)), 30.5 (*C*H$_2$(d)), 13.5 (C14').

*IR (ATR)*: ṽ in [cm$^{-1}$] = 3324.6, 2977.3, 2928.9, 1757.6, 1651.2, 1574.3, 1513.9, 1495.5, 1436.9, 1385.6, 1363.7, 1259.0, 1199.0, 1140.2, 1112.2, 1079.6, 1044.7, 1027.9, 978.6, 866.2, 815.6, 776.3, 760.9, 726.7, 699.7, 674.4, 605.8, 448.3, 432.8, 400.4.

*MS (ESI-HR)*: m/z [M+H]$^+$ calc. for C$_{31}$H$_{29}$Cl$_2$N$_2$O$_7$S$^+$: 643.1067, found: 643.1110.

S$_{\text{YNTHESIS OF}}$ 5-(3',4'-$_{\text{DICHLOROPHENYL}}$)-2-[(*N*-$_{\text{ETHYL BENZYL AMINO}}$)$_{\text{CARBONYL AMINO}}$]-$_{\text{THIOPHENE-3-}}$ $_{\text{CARBOXYLIC ACID}}$-[$_{\text{OXYMETHYL}}$(3-(3,4-$_{\text{DIHYDROXYPHENYL}}$)-$_{\text{PROPYL}}$)-$_{\text{CARBONATE}}$] $_{\text{ESTER}}$ **44**:

According to GP V, 19 mg (22 µmol) 5-(3',4'-dichlorophenyl)-2-[(*N*-ethyl benzyl amino)car-bonyl amino]-thiophene-3-carboxylic acid-[oxymethyl(3-(3,4-dibenzyloxy-phenyl)-propyl)-carbonate] ester **39** were treated with 108 µL (108 µmol) TMSI (1 M in dichloromethane). After RP purification, the product was obtained as colorless wax.

*Yield*: 10 mg (14 µmol, 66%).

*Formula*: $C_{46}H_{42}Cl_2N_2O_8S$.

*Molecular weight*: 673.558.
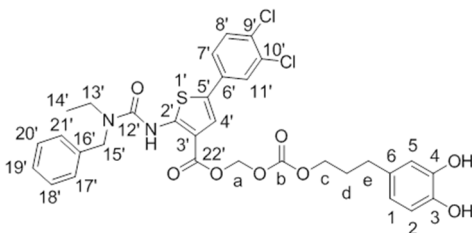


*1H-NMR (400 MHz, acetonitrile-d₃)*: δ [ppm] = 10.49 (bs, 1 H, N*H*), 7.74 (t, $^{4,5}J_{H,H}$ = 1.3 Hz, 1 H, H11'), 7.49 – 7.48 (m, 2H, H7', H8'), 7.46 (s, 1 H, H4'), 7.40 – 7.26 (m, 5 H, H17' – H21'), 6.68 (d, $^{3}J_{H,H}$ = 8.0 Hz, 1 H, H5), 6.65 (d, $^{4}J_{H,H}$ = 2.1 Hz, 1 H, H2), 6.53 (dd, $^{3}J_{H,H}$ = 8.0 Hz, $^{4}J_{H,H}$ = 2.1 Hz, 1 H, H6), 6.50 (bs, 1 H, O*H*), 6.46 (bs, 1 H, O*H*), 5.88 (s, 2 H, C*H₂*(a)), 4.62 (s, 2 H, H15'), 4.15 (t, $^{2,3}J_{H,H}$ = 6.5 Hz, 2 H, C*H₂*(c)), 3.44 (q, $^{2,3}J_{H,H}$ = 7.2 Hz, 2 H, H13'), 2.57 – 2.47 (m, 2 H, C*H₂*(e)), 1.92 – 1.85 (m, 2 H, C*H₂*(d)), 1.21 (t, $^{2,3}J_{H,H}$ = 7.2 Hz, 3 H, H14').

*13C-NMR (126 MHz, acetonitrile-d₃)*: δ [ppm] = 164.9 (C22'), 155.3 (C5'), 154.8 (C$_q$(b)), 154.0 (C12'), 145.4 (C4), 143.6 (C3), 135.2 (C16'), 134.4 (C1), 133.5 (C6'), 131.8 (C8'), 131.2 (C10'), 130.2 (C9'), 129.6, 128.4, 128.3 (C17' – C21'), 127.6 (C11'), 125.8 (C7'), 121.6 (C4'), 120.9 (C6), 116.3 (C2), 116.1 (C5), 110.9 (C3'), 83.2 (*C*H₂(a)), 69.0 (*C*H₂(c)), 50.8 (C15'), 42.3 (C13'), 31.7 (*C*H₂(e)), 31.1 (*C*H₂(d)), 13.5 (C14').

*IR (ATR)*: ṽ in [cm⁻¹] = 3294.3, 3066.8, 2926.9, 2132.6, 2105.9, 1761.0, 1667.5, 1650.2, 1603.5, 1556.1, 1524.2, 1488.2, 1453.6, 1426.7, 1384.1, 1363.8, 1264.0, 1112.7, 1079.8, 1026.9, 1001.0, 960.0, 900.5, 847.9, 816.7, 776.9, 746.3, 700.0, 631.9, 595.3, 537.5, 513.9, 481.2, 469.9, 457.7, 423.6.

*MS (ESI-HR)*: m/z [M+H]⁺ calc. for $C_{32}H_{31}Cl_2N_2O_8S^+$: 673.1173, found: 673.1164.

Synthesis of 5-(3′,4′-dichlorophenyl)-2-[(*N*-ethyl benzyl amino)carbonyl amino]-thiophene-3-carboxylic acid (3-(3,4-dihydroxyphenyl)-propyl) ester **42**:

Under anhydrous conditions, 15 mg (33 μmol) 5-(3′,4′-dichlorophenyl)-2-[(*N*-ethyl benzyl amino)-carbonyl amino]-thiophen-3-carboxylic acid were reacted with 26 mg (62 μmol, 1.9 eq.) 3-(3,4-dibenzyloxyphenyl)-propanoyl mesylate **34** in the presence of 8 μL (58 μmol, 1.8 eq.) triethylamine in a total volume of 2.5 mL of DMF. After 18 h at 40 °C, the reaction was terminated. Upon purification of the crude residue via flash column chromatography on silica gel with a petroleum ether/ethyl acetate gradient (5:1 → 1:1) the obtained product (18 mg, 22 μmol) was converted according to GP V. Treatment with 112 μL (112 μmol, 5 eq.) TMSI (1 M in dichloromethane) in 2.5 mL dichloromethane afforded the product as colorless solid after purification.

*Yield*: 10 mg (16 μmol, 48%, two stages).

*Formula*: $C_{30}H_{28}Cl_2N_2O_5S$.

*Molecular weight*: 599.523.
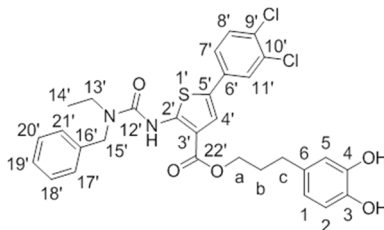


$^1$*H-NMR (600 MHz, acetonitrile-d₃)*: δ [ppm] = 10.73 (bs, 1 H, N*H*), 7.74 (m, 1 H, H11′), 7.47 (m, 2 H, H7′, H8′), 7.42 (s, 1 H, H4′), 7.37 – 7.26 (m, 5 H, H17′ – H21′), 6.73 – 6.68 (m, 2 H, H2, H5), 6.59 (dd, $^3J_{H,H}$ = 8.0 Hz, $^4J_{H,H}$ = 2.1 Hz, 1 H, H6), 6.55 (bs, 1 H, O*H*), 6.48 (bs, 1 H, O*H*), 4.61 (s, 2 H, H15′), 4.20 (t, $^{2,3}J_{H,H}$ = 6.4 Hz, 2 H, C*H₂*(a)), 3.42 (q, $^{2,3}J_{H,H}$ = 7.2 Hz, 2 H, H13′), 2.63 (t, $^{2,3}J_{H,H}$ = 7.5 Hz, 2 H, C*H₂*(c)), 1.98 (q, $^{2,3}J_{H,H}$ = 7.0 Hz, 2 H, C*H₂*(b)), 1.20 (t, $^{2,3}J_{H,H}$ = 7.2 Hz, 3 H, H14′).

$^{13}$*C-NMR (151 MHz, acetonitrile-d₃)*: δ [ppm] = 166.6 (C22′) , 154.2 (C12′), 153.5 (C5′), 145.4 (C4), 143.5 (C3), 137.8 (C16′), 135.5 (C6′), 134.7 (C1), 133.4 (C10′), 131.8(C8′), 130.9 (C9′), 129.7, 129.6, 128.4, 128.3 (C17′ – C21′), 127.5 (C11′), 125.7 (C7′), 122.0 (C4′), 121.0 (C6), 116.4 (C2), 116.1 (C5), 112.4 (C3′), 65.1 (*C*H₂(a)), 50.8 (C15′), 43.1 (C13′), 32.1 (*C*H₂(c)), 31.1 (*C*H₂(b)), 13.5 (C14′).

*IR (ATR)*: ṽ in [cm⁻¹] = 3272.9, 3032.8, 2929.7, 1635.6, 1590.0, 1557.5, 1521.9, 1490.8, 1453.4, 1414.1, 1381.6, 1362.8, 1241.5, 1135.0, 1114.2, 1079.6, 1026.8, 980.7, 952.6, 868.8, 814.8, 778.7, 745.1, 699.41, 635.4, 594.9, 512.5.

*MS (ESI-HR)*: m/z [M+H]⁺ calc. for $C_{30}H_{29}Cl_2N_2O_5S^+$: 599.1169, found: 599.1135.

Synthesis of 5-(3′,4′-dichlorophenyl)-2-[(*N*-ethyl benzyl amino)carbonyl amino]-thiophene-3-carboxylic acid (5-hydrox-4-pyrone-2-methyl) ester **42**:

Under a dry atmosphere of nitrogen, 15 mg (33 µmol) 5-(3′,4′-dichlorophenyl)-2-[(*N*-ethyl benzyl amino)-carbonyl amino]-thiophen-3-carboxylic acid were mixed with 26 mg (83 µmol, 2.5 eq.) 5-benzyloxy-4-pyrone-2-methylmesylate **32** in the presence of 8 µL (58 µmol, 1.8 eq.) triethylamine in a total volume of 2.5 mL of DMF. The reaction mixture was stirred 18 h at 40 °C. Upon completion, all volatile components were removed in high vacuum and the crude residue purified via flash column chromatography on silica gel with a dichloromethane/methanol gradient (34:1 → 14:1). The obtained product (21 mg, 31 µmol) was subsequently converted according to GP V and treated with 155 µL (155 µmol, 5 eq.) TMSI (1 M in dichloromethane) in 2.5 mL dichloromethane. After purification, the product was obtained as colorless solid.

*Yield*: 4 mg (7.0 µmol, 20%, two stages).

*Formula*: $C_{27}H_{22}Cl_2N_2O_6S$.

*Molecular weight*: 573.441.
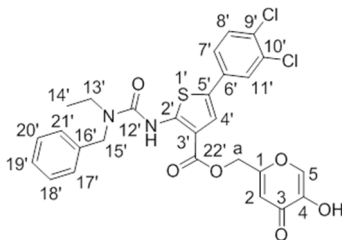


*¹H-NMR (600 MHz, acetonitrile-d₃)*: δ [ppm] = 10.53 (bs, 1 H, N*H*), 7.92 ( s, 1 H, H5), 7.79 (d, $^3J_{H,H}$ = 1.8 Hz, 1 H, H11′), 7.57 – 7.46 (m, 2 H, H7′, H8′), 7.42 – 7.24 (m, 6 H, H4′, H17′ – H21′), 6.66 (bs, 1 H, O*H*), 6.53 (s, 1 H, H2), 5.09 (s, 2 H, C*H₂*(a)) 4.61 (s, 2 H, H15′),

3.43 (q, $^{2,3}J_{H,H}$ = 7.0 Hz, 2 H, H13'), 1.20 (t, $^{2,3}J_{H,H}$ = 7.2 Hz, 3 H, H14').

*$^{13}$C-NMR (151 MHz, acetonitrile-d$_3$)*: δ [ppm] = 174.5 (C3), 165.6 (C1), 164.0 (C22'), 154.0 (C12'), 146.8 (C4), 138.8 (C16'), 135.5 (C6'), 133.5 (C10'), 131.5(C8'), 130.7 (C9'), 129.1, 128.1, 128.0 (C17' – C21'), 127.3 (C11'), 125.5 (C7'), 121.3 (C4'), 112.1 (C2), 111.1 (C3') 62.2 (*C*H$_2$(a)), 50.5 (C15'), 42.9 (C13'), 13.2 (C14').

*IR (ATR)*: ṽ in [cm$^{-1}$] = 3293.2, 3092.3, 2925.2, 2850.5, 1652.9, 1589.1, 1554.6, 1520.7, 1485.8, 1434.5, 1382.6, 1207.8, 1136.0, 1080.4, 1027.7, 981.6, 920.4, 865.8, 814.2, 774.5, 743.3, 698.5, 672.9, 634.0, 595.2, 574.2.

*MS (ESI-HR)*: m/z [M+H]$^+$ calc. for C$_{27}$H$_{23}$Cl$_2$N$_2$O$_6$S$^+$: 573.0648, found: 573.0641.

#### 9.2.2.    Part II - Bio-reversibly masked purinergic 2nd Messenger derivatives

GENERAL PROCEDURE (GP) VI: GLYCOSYLATION OF PER-*O*-TBS PROTECTED D-RIBOSE:

Under anhydrous conditions, 1,2,3,5-tetra-*O-tert*butyldimethylsilyl-β-D-ribose was dissolved in dichloromethane (15 mL/mmol) and the mixture cooled to -50 °C. Trimethylsilyl iodide (TMSI, 1.1 eq., 1 M in dichloromethane) was added to the solution and the reaction mixture allowed to warm to rt. Formation of the iodo-ribose was followed by TLC (dichloromethane/methanol 24:1) and upon completion, the reaction mixture was cooled down to -30 °C again. In a separate flask, triethylamine (2.4 eq.) and the respective aglycone (1.2 eq.) were dissolved in dichloromethane (12.5 mL/mmol) and added dropwise to the cooled reaction mixture which successively was allowed to warm to rt and stirred for further 2 – 18 h. The glycosylation was terminated by dilution with dichloromethane and the addition of aq. $NH_4OAc$ sol. (1 M). After extraction and washing with demin. water, the organic layer was dried over $Na_2SO_4$, filtered, concentrated to dryness and the obtained residue purified by automated NP flash chromatography using an ethyl acetate gradient in petroleum ether (0% to 100 %) or methanol gradient in dichloromethane (0% to 10%).

GP VIIa: 5'-DESILYLATION TO 1-*O*-GLYCOSYLATED-2,3-DI-*O*-TBS-β-D-RIBOSIDES:

The 1-*O*-glycoslyated-2,3,5-tri-*O-tert*butyldimethylsilyl-β-D-riboside was treated with triethylamine trihydrofluoride (37 wt.% HF in TEA, 4 eq.) in acetonitrile at rt over 18 h. The reaction was terminated by removing all volatile components from the reaction mixture. Final purification of the obtained residue was performed using an automated NP flash chromatography system and an ethyl acetate gradient in petroleum ether (0% to 100%) or methanol gradient in dichloromethane (0% to 10%).

GP VIIb: COMPLETE DESILYLATION TO 1-*O*-GLYCOSYLATED-β-D-RIBOSIDES:

The 1-*O*-glycoslyated 2,3,5-tri-*O-tert*butyldimethylsilyl-β-D-riboside was treated with triethylamine trihydrofluoride (37 wt.% HF in TEA, 27 eq.) in acetonitrile at rt over 18 h. The reaction was terminated by removal of all volatile components from the reaction mixture.

Final purification of the obtained residue was performed using an automated RP flash chromatography system and an acetonitrile gradient in water (0% to 100%).

GP VIIIa: 3',5'-*O*-TIPDSILYLATION OF ADENOSINE:

Under an atmosphere of nitrogen, adenosine was suspended in pyridine (10 eq.) and cooled to -30 °C. To the cooled solution, 1,3-dichloro-1,1,3,3-tetra*iso*propyldisiloxane (TIPDSCl$_2$, 1.1 eq.) was added and the reaction mixture allowed to warm to rt while stirring. After 18 h, the reaction was terminated via removal of all volatile reaction components. The crude residue was co-evaporated several times with toluene and dichloromethane, finally taken up in little dichloromethane and purified by NP column chromatography on silica gel with dichloromethane/methanol 14:1 as eluents.

GP VIIIb: 3',5'-*O*-TIPDSILYLATION AND *N*$^6$-ACYLATION OF ADENOSINE VIA TRANSIENT 2'-*O*-TMS PROTECTION:

Under an atmosphere of nitrogen, adenosine was suspended in pyridine (10 or 15 eq.) and cooled to -30 °C. To the cooled solution, 1,3-dichloro-1,1,3,3-tetra*iso*propyldisiloxane (TIPDSCl$_2$, 1.1 eq.) was added and the reaction mixture allowed to warm up to rt while stirring. After 18 h, the reaction mixture was diluted with tetrahydrofuran (same volume as pyridine) and trimethylsily chloride (TMSCl, 1.1 or 1.3 eq.) was added. After 15 – 30 min further stirring, acid chloride (1.1 or 1.3 eq.) was mixed to the reaction and another 5 – 18 h of stirring succeeded. The reaction was terminated by removal of all volatile components under high vacuum. The obtained residue was co-evaporated several times with toluene and dichloromethane, then taken up in dichloromethane and washed with sat. NaHCO$_3$ (aq.) and brine, was then dried over Na$_2$SO$_4$, filtered and the filtrate concentrated to dryness. The crude product was taken up in tetrahydrofuran again and treated with hydrochloric acid (1 M aq. sol., 4 eq.) for 30 – 60 min between 0 °C to rt. The solution was neutralized, extracted again with dichloromethane, dried over Na$_2$SO$_4$ and concentrated to dryness. Final purification of the crude product was performed by means of automated NP flash column chromatography using a methanol gradient in dichloromethane (0 to 10%).

GP IX: 2'-PHOSPHORYLATION OF PROTECTED ADENOSINE DERIVATIVES:

Under anhydrous conditions, 3',5'-$O$-silylated ($N^6$-acylated) adenosine was dissolved in DMF, acetonitrile or dichloromethane and reacted stepwise in five portions with bis(4-octanoyloxybenzyl)-$N$,$N$-di*iso*propylamino phosphoramidite ((OB)$_2$PA, 1 to 1.3 eq., dissolved in the same solvent) and 4,5-dicyanoimidazole (DCI, 0.25 M in acetonitrile, 1.3 to 2 eq.). After addition, the reaction mixture was stirred further 60 min at rt, and then *tert*bu-tyl hydroperoxide (*t*BuOOH, 5.5 M in *n*-decane, 1.3 to 1.5 eq.) was added for oxidation. After further 30 min, all volatile components were removed from the reaction mixture, and the crude residue was taken up in dichloromethane, washed with sat. NaHCO$_3$ (aq.) or NH$_4$OAc (1 M aq. sol.), brine and demin. water, then dried over Na$_2$SO$_4$, filtered and the filtrate concentrated in vacuum. The crude product was purified finally by means of an automated NP flash chromatography system with a methanol gradient in dichloromethane (0% to 10%).

GP X: $N$-BUTANOYLATION OF NUCLEOSIDES VIA TRANSIENT TMS-PROTECTION:

The respective nucleoside (adenosine, guanosine or 2'-deoxyadenosine) was co-evapo-rated three times with and then dissolved in anhydrous pyridine (2 – 5 mL/mmol), and fur-ther diluted with either the same volume of tetrahydrofuran or double the volume of di-chloromethane. At 0 °C, TMSCl (1.1 – 1.8 eq.) was added. The reaction mixture was succes-sively allowed to warm to rt and stirred for 18 h. Next, butyryl chloride (1.1 eq.) was added under cooling and the reaction mixture was stirred for another 6 h at rt. Cleavage of TMS ethers was promoted by the addition of either hydrochloric acid (1 M aq. sol., 0.5 mL/mmol) under vigorous stirring for 5 min, or methanol (2 - 5 mL/mmol) under stir-ring for further 12 h.

The reaction was terminated by removal of all volatile components under high vacuum. The crude residue was co-evaporated with toluene and dichloromethane several times, was then taken up in acetonitrile/demin. water and purified by means of automated RP flash column chromatography on C$_{18}$ modified silica gel with an acetonitrile gradient in wa-ter (0% to 100%).

GP XI: 3',5'-Phosphorylation of nucleosides to their AB-masked cyclic Nucleotide Monophosphate analogues:

Under an atmosphere of nitrogen, the respective nucleoside was dissolved in DMF/acetonitrile (25 mL/mmol). In a separate flask, bis(*N,N*-di*iso*propylamino)-4-octanoyloxybenzyl phosphoramidite (1 eq.) was dissolved in acetonitrile (25 mL/mmol total volume). The phosphordiamidite solution and DCI (0.25 M in acetonitrile, 1.3 – 1.5 eq.) were added slowly and dropwise in five to ten portions to the nucleoside solution. The addition of more DCI (0.25 M in acetonitrile, 1.2 – 1.5 eq.) or 5-(benzylthio)-1*H*-tetrazole (BTT, 0.3 M in acetonitrile, 1.3 eq.) followed, and the reaction mixture was stirred 1 h further. Then, *t*BuOOH (5.5 M in *n*-decane, 1.5 eq.) was added and the solution stirred for 10 min more. Successively, all volatile components were removed in vacuum, and the obtained residue was taken up in acetonitrile/demin. water for purification by means of automated RP flash column chromatography on $C_{18}$ modified silica gel with an acetonitrile gradient in water (0% to 100%).

GP XII: 5- & 5'-Monophosphorylation of ribosides and nucleosides via the (OFm)₂PA route:

The respective nucleoside was dissolved in anhydrous DMF or acetonitrile (10 mL/mmol or 20 mL/mmol) and slowly and dropwise mixed with DCI (0.25 M in acetonitrile, 1.1 - 1.2 eq.) and a solution of bis(9*H*-fluoren-9-ylmethyl)-di*iso*propylamino phosphoramidite ((OFm)₂PA, 1.2 – 2.2 eq) in acetonitrile (5 mL/mmol). After addition, the reaction mixture was stirred 30 min at rt and then treated with *t*BuOOH (5.5 M in *n*-decane, 1.3 - 2.2 eq.). After further 15 min at rt, all volatile components were removed, and the crude residue was resolved in anhydrous acetonitrile. Successively, triethylamine (10 vol.%) was added, and after 2 h of stirring at rt, demin. water (same volume as acetonitrile) was mixed to the solution. After 18 h at rt, the reaction was terminated by concentrating the mixture to a volume of approximately 1 mL. The solution was directly purified via automated RP flash column chromatography on $C_{18}$ modified silica gel with an acetonitrile gradient in water (0% to 100%).

GP XIII: Coupling of asymmetric H-Phosphonate and Monophosphate to ADPR derivatives:

Under anhydrous conditions, the asymmetric H-phosphonate was dissolved in acetonitrile and reacted with *N*-chlorosuccinimide (2 eq., NCS) between rt and 50 °C. Upon completed activation to the corresponding chlorophosphate, the respective monophosphate (1.2 – 2 eq.) was added dissolved in acetonitrile. The reaction mixture was warmed twice with a warm water bath and successively stirred at rt for 5 h – 18 h. Then, all volatile components were removed and the crude product purified by automated RP flash column chromatography on $C_{18}$ modified silica gel with an acetonitrile gradient in water (0% to 100%).

Experimental Part

SYNTHESIS OF 4-(HYDROXYMETHYL) PHENYL OCTANOATE **58**:

In 180 mL dichloromethane, 8.63 g(69.6 mmol) 4-hydroxybenzylic alcohol **65** were dissolved and cooled to 0 °C. The addition of 9.78 mL (69.6 mmol, 1 eq.) triethylamine and 10.7 mL (62.6 mmol, 0.9 eq) octanoic acid chloride **66** succeeded slowly and dropwise. Upon completed addition, the reaction was allowed to warm to rt and stirred for further 2 h before quenching with water. The organic layer of the biphasic mixture was separated and washed with sat. NaHCO₃ (aq.), 1 M HCl (aq.) and demin. water, dried over Na₂SO₄, and filtered. The residue obtained from removal of the solvent under reduced pressure was finally purified via NP column chromatography on silica gel with petroleum ether/ethyl acetate 5:1 to 2:1 as eluents to afford the product as a colorless wax.

*Yield*: 9.74 g (38.9 mmol, 62%,).

*Formula*: $C_{15}H_{22}O_3$.

*Molecular weight*: 250.338.
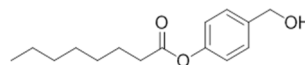


The analytical data obtained were consistent with those reported in the literature.[158]

SYNTHESIS OF 4-OCTANOYLOXYBENZALDEHYDE **58a**:

Under anhydrous conditions, 0.81 g (3.26 mmol) 4-(hydroxymethyl)-phenyloctanoate **58** were dissolved in 30 mL dichloromethane, cooled to 0 °C and mixed with 1.45 g (3.42 mmol, 1.1 eq.) Dess-Martin periodinane. After warming to rt and further stirring over 60 min, the reaction was terminated via the addition of a 1:1:1 solution of sat. NaHCO₃, brine and 10% NaS₂O₃. The extracted organic layer was washed with brine and demin. water, the solvent evaporated under reduced pressure and the obtained residue purified by NP column chromatography on silica gel with a petroleum ether/ethyl acetate gradient (10:1 → 5:1) as eluents. The product was obtained as colorless syrup.

*Yield*: 0.72 g (2.88 mmol, 88%).

*Formula*: $C_{15}H_{20}O_3$

*Molecular weight*: 248.322.
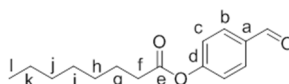


*¹H-NMR (600 MHz, chloroform-d)*: δ [ppm] = 9.98 (s, 1 H, C*H*O), 7.98 – 7.85 (m, 2 H, Hb), 7.35 – 7.20 (m, 2 H, Hc), 2.58 (t, $^{2,3}J_{H,H}$ = 7.5 Hz, 2 H, Hf), 1.76 (p, $^{2,3}J_{H,H}$ = 7.5 Hz, 2 H, Hg), 1.52 – 1.23 (m, 8 H, Hh – k), 0.89 (t, $^{2,3}J_{H,H}$ = 6.9 Hz, 3 H, Hl).

*¹³C-NMR (151 MHz, chloroform-d)*: δ [ppm] = 191.0 (CHO), 171.7 ($C_q$e), 155.6 ($C_q$d), 134.0 ($C_q$a), 131.3 (Cb), 122.5 (Cc), 34.5 (Cf), 31.7, 29.1, 29.0, 24.9, 22.7 (Cg – k), 14.2 (Cl).

*IR (ATR)*: ṽ in [cm⁻¹] = 2926.7, 2855.5, 2735.3, 2066.2, 1760.5, 1698.0, 1598.3, 1455.4, 1364.9, 1262.5, 1237.8, 1205.8, 1154.9, 1129.9, 1098.8, 1012.3, 917.8, 857.9, 782.9, 745.4, 693.4, 675.4, 621.7, 508.6, 470.1.

*MS (ESI-HR)*: m/z [M+H]⁺ calc. for $C_{15}H_{21}O_3^+$: 249.1491, found: 249.1959.

SYNTHESIS OF (4-OCTANOYLOXYBENZYLIDENE) HYDRAZINE **59**:

250 mg (1.01 mmol) 4-octanoyloxybenzaldehyde **58a** were dissolved in 5 mL chloro-form/ethanol 1:3 and treated with 0.08 mL (1.31 mmol, 1.3 eq.) hydrazine monohydrate (80%). After stirring the reaction mixture at rt for 12 h, the solvent was evaporated, and the remaining residue taken up in a little amount of ethanol. The solid parts were filtered of and dried in high vacuum giving the desired product as a yellowish solid.

*Yield*: 158 mg (0.60 mmol, 60%).

*Formula*: $C_{15}H_{22}N_2O_2$

*Molecular weight*: 262.353.
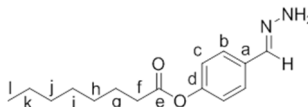
*$^1$H-NMR (500 MHz, methanol-$d_4$)*: δ [ppm] = 8.54 (s, 1 H, C*H*(N)NH$_2$), 7.76 – 7.66 (m, 2 H, H2), 6.98 – 6.85 (m, 2 H, H3), 2.22 – 2.09 (m, 2 H, C*H$_2$*C(O)OR), 1.61 (p, $^{2,3}J_{H,H}$ = 7.3 Hz, 2 H, C*H$_2$*CH$_2$C(O)OR), 1.50 – 1.20 (m, 8 H, C*H$_2$*), 1.00 – 0.83 (m, 3 H, C*H$_3$*).

*$^{13}$C-NMR (151 MHz, methanol-$d_4$)*: δ [ppm] = 174.0 (*C*(O)OR), 161.1 (*C*H(N)NH$_2$), 130.0 (C2), 125.3 (C1), 115.4 (C3), 33.6, 31.5, 28.8, 28.6, 25.5, 22.3 (*C*H$_2$), 13.0 (*C*H$_3$).

*IR (ATR)*: ṽ in [cm$^{-1}$] = 3213.4, 2954.4, 2924.2, 2855.1, 2091.2, 1995.6, 1914.7, 1758.2, 1659.8, 1603.9, 1506.4, 1464.6, 1415.4, 1377.1, 1273.2, 1233.0, 1197.4, 1161.2, 1137.7, 1100.0, 1015.7, 0918.2, 836.7, 776.9, 745.3, 723.6, 698.3, 568.1, 527.7.

*MS (ESI-HR)*: m/z [M+H]$^+$ calc. for C$_{15}$H$_{23}$N$_2$O$_2$$^+$: 263.1754, found: 263.1967 .
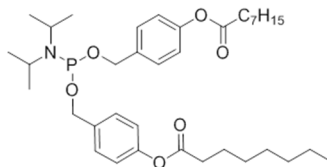

SYNTHESIS OF BIS(4-OCTANOYLOXYBENZYL)-*N,N*-DI*ISO*PROPYLAMINO PHOSPHORAMIDITE **68**:

Under an atmosphere of nitrogen, 1.20 mL (10.6 mmol) dichloro-*N,N*-di*iso*propylamino phosphoramidite were dissolved in 30 mL tetrahydrofuran and cooled to 0 °C. In a separate flask, 3.44 mL (24.5 mmol, 2.3 eq.) triethylamine and 5.46 g (21.8 mmol, 2.1 eq.) 4-(hy-droxymethyl)-phenyloctanoate **58** were dissolved in 15 mL tetrahydrofuran as well, and added dropwise to the cooled phosphoramidite solution. The reaction mixture was allowed to warm up to rt, stirred for further 20 h and was then quenched by filtration and concentration to dryness. The obtained residue was purified via NP chromatography on silica gel with petroleum ether/ethyl acetate 10:1 + 5% triethylamine as eluents. The product was isolated as colorless syrup.


*Yield*: 3.10 g (5.05 mmol, 63%).

*Formula*: C$_{36}$H$_{56}$NO$_6$P.

*Molecular weight*: 629.818.



The analytical data obtained were consistent with those reported in the literature.[158]

SYNTHESIS OF BIS(*N*,*N*-DI*ISO*PROPYLAMINO)-4-OCTANOYLOXYBENZYL PHOSPHORDIAMIDITE **101**:

1.00 g (3.75 mmol) bis(*N*,*N*-di*iso*propylamino)-chlorophosphine were dissolved in 15 mL anhydrous tetrahydrofuran. In a separate flask, 0.68 mL (4.87 mmol, 1.3 eq.) triethylamine and 0.94 g (3.75 mmol, 1 eq.) 4-(hydroxymethyl)-phenyloctanoate **58** were mixed with 7 mL anhydrous tetrahydrofuran, and the mixture was added dropwise to the chlorophosphine. The reaction mixture was stirred at rt for 20 h, then filtered and the filtrate concentrated to dryness in vacuum. The remaining residue was purified by NP chromatography on silica gel with petroleum ether/triethylamine 98:2 as eluents, and the desired product obtained as colorless syrup.

*Yield*: 1.28 g (2.67 mmol, 71%).

*Formula*: $C_{27}H_{49}N_2O_3P$.

*Molecular weight*: 480.637.
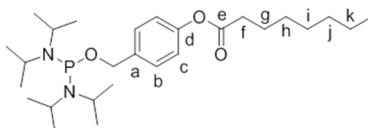


*$^1$H-NMR (600 MHz, chloroform-d)*: δ [ppm] = 7.36 (d, $^2J_{H,H}$ = 8.2 Hz, 2 H, Hb), 7.14 – 6.95 (m, 2 H, Hc), 4.63 (d, $^2J_{H,H}$ = 7.2 Hz, 2 H, C*H*$_2$(benzylic)), 3.66 – 3.51 (m, 4 H, NC*H*), 2.54 (t, $^{2,3}J_{H,H}$ = 7.5 Hz, 2 H, Hf), 1.75 (p, $^{2,3}J_{H,H}$ = 7.4 Hz, 2 H, Hg), 1.51 – 1.23 (m, 8 H, Hh – k), 1.21 (d, $^2J_{H,H}$ = 2.7 Hz, 12 H, C*H*$_3$(*i*Pr)), 1.20 (d, $^2J_{H,H}$ = 2.8 Hz, 12 H, C*H*$_3$(*i*Pr)), 0.88 (t, $^{2,3}J_{H,H}$ = 7.3 Hz, 3 H, Hl).

*$^{13}$C-NMR (151 MHz, chloroform-d)*: δ [ppm] = 172.6 (C$_q$e), 149.7 (C$_q$d), 138.2 (C$_q$a), 127.9 (Cb), 121.5 (Cc), 65.8 (C*H*$_2$(benzylic)), 44.69, 44.56 (NC*H*), 34.6 (Cf), 31.8, 29.2, 29.1, 25.1 (Cg – j), 24.8, 24.7, 24.1, 24.0 (C*H*$_3$(*i*Pr)), 22.75 (Ck), 14.22 (Cl).

*$^{31}$P-NMR (162 MHz, chloroform-d)*: δ [ppm] = 123.5.

*IR (ATR)*: ṽ in [cm$^{-1}$] = 2963.3, 2927.8, 2861.4, 2079.0, 2025.5, 1761.3, 1607.8, 1507.4, 1457.5, 1416.5, 1390.1, 1361.6, 1300.3, 1194.2, 1184.8, 1162.9, 1140.3, 1116.2, 1045.2, 1016.9, 952.7, 916.5, 866.3, 779.6, 748.7, 706.7, 642.7, 566.1, 527.6.

*MS (MALDI)*: m/z [M-H] calc. for $C_{27}H_{48}N_2O_3P^-$: 479.340, found: 479.245.

SYNTHESIS OF NICOTINIC ACID BENZYL ESTER **83**:

In 90 mL tetrahydrofuran, 4.50 g (36.6 mmol) nicotinic acid were suspended and successively mixed with 5.65 mL (40.2 mmol, 1.1 eq.) triethylamine and 4.34 mL (36.6 mmol, 1 eq.) benzyl bromide. The reaction mixture was stirred at rt for 18 h, and the reaction then quenched via filtration and concentration of the filtrate to dryness. The obtained residue was taken up in petroleum ether/ethyl acetate/dichloromethane 3:2:0.5 and purified via NP column chromatography on silica gel with petroleum ether/ethyl acetate 3:2 as eluents. The desired product was obtained as orange syrup.

*Yield*: 2.57 g (12.1 mmol, 33%).

*Formula*: $C_{13}H_{11}NO_2$.

*Molecular weight*: 213.236.
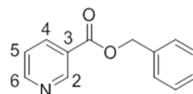


*$^1$H-NMR (400 MHz, chloroform-d)*: δ [ppm] = 9.26 (dd, $^4J_{H,H}$ = 2.2 Hz, $^4J_{H,H}$ = 0.9 Hz, 1 H, H2), 8.77 (dd, $^3J_{H,H}$ = 4.9 Hz, $^3J_{H,H}$ = 1.7 Hz, 1 H, H6), 8.32 (dt, $^{3,4}J_{H,H}$ = 8.0 Hz, $^4J_{H,H}$ = 2.0 Hz, 1 H, H4), 7.51 – 7.35 (m, 6 H, H5 & C*H*(aromatic)), 5.40 (s, 2 H, C*H$_2$*(benzylic)).

*$^{13}$C-NMR (151 MHz, chloroform-d)*: δ [ppm] = 165.1 (C(O)OR), 153.5 (C6), 151.0 (C2), 137.3 (C4), 135.6 (C$_q$(aromatic)), 128.8, 128.6, 128.4 (C*H*(aromatic)), 126.2 (C3), 123.4 (C5), 67.2 (C*H$_2$*(benzylic)).

*IR (ATR)*: ṽ in [cm$^{-1}$] = 3293.2, 3034.9, 2956.9, 2034.1, 1957.5, 1722.8, 1590.6, 1498.0, 1476.1, 1455.6, 1420.1, 1377.4, 1327.3, 1278.9, 1237.3, 1214.1, 1194.2, 1110.9, 1024.1, 959.9, 913.3, 828.8, 740.3, 699.2, 620.9, 600.3, 586.9, 521.7, 414.5.

*MS (EI)*: m/z [M]$^+$ calc. for $C_{13}H_{11}NO_2^+$: 213.08, found: 213.15.

SYNTHESIS OF NICOTINIC ACID-(4-OCTANOYLOXYBENZYL) ESTER **90**:

500 mg (2.81 mmol) nicotinic acid chloride were dissolved in 10 mL tetrahydrofuran and successively mixed with a solution of 0.79 mL (5.62, 2 eq.) triethylamine and 633 mg (2.53, 0.9 eq.) 4-(hydroxymethyl)-phenyloctanoate **58** in 10 mL tetrahydrofuran. To this, a small amount of DMAP was added to accelerate the reaction. After stirring 18 h at rt, the reaction mixture was filtered, the filtrate concentrated to dryness, and the obtained residue purified by NP column chromatography on silica gel with dichloromethane/methanol 24:1 as eluents. The product was obtained as pale yellowish wax.

*Yield*: 373 mg (1.05 mmol, 42%).

*Formula*: $C_{21}H_{25}NO_4$.

*Molecular weight*: 355.434.
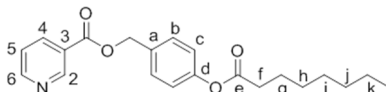


*$^{1}$H-NMR (400 MHz, chloroform-d)*: δ [ppm] = 9.27 (dd, $^{4}J_{H,H}$ = 2.1 Hz, $^{4}J_{H,H}$ = 0.9 Hz, 1 H, H2), 8.80 (dd, $^{3}J_{H,H}$ = 5.0 Hz, $^{3}J_{H,H}$ = 1.7 Hz, 1 H, H6), 8.40 (dt, $^{3,4}J_{H,H}$ = 8.0 Hz, $^{4}J_{H,H}$ = 2.0 Hz, 1 H, H4), 7.58 – 7.42 (m, 3 H, H5 & Hb), 7.19 – 7.08 (m, 2 H, Hc), 5.39 (s, 2 H, $CH_2$(benzylic)), 2.56 (t, $^{2,3}J_{H,H}$ = 7.5 Hz, 2 H, Hf), 1.75 (p, $^{2,3}J_{H,H}$ = 7.5 Hz, 2 H, Hg), 1.50 - 1.19 (m, 8 H, Hh – k), 1.02 – 0.74 (m, 3 H, Hl).

*$^{13}$C-NMR (101 MHz, chloroform-d)*: δ [ppm] = 172.3 ($C_q$e), 164.9 (C(O)OR$_{OB\ ester}$), 152.2 (C6), 151.1 ($C_q$d), 150.0 (C2), 138.4 (C4), 132.6 ($C_q$a), 129.9 (Cb), 126.7 (C3), 123.9 (C5), 122.1 (Cc), 66.9 ($CH_2$(benzylic)), 34.5 (Cf), 31.8, 29.2, 29.1, 25.1, 22.7 (Cg – k), 14.2 (Cl).

*IR (ATR)*: ṽ in [cm$^{-1}$] = 3056.8, 2955.6, 2927.8, 2857.0, 2514.4, 2361.3, 2168.5, 2045.3, 1999.0, 1989.7, 1978.5, 1958.4, 1921.8, 1890.2, 1759.1, 1726.8, 1652.9, 1610.1, 1591.6, 1558.3, 1540.5, 1508.9, 1452.7, 1419.6, 1376.1, 1329.6, 1278.9, 1200.0, 1167.0, 1132.0, 1107.8, 1023.8, 917.3, 381.9, 765.6, 741.5, 702.5, 667.6, 620.5, 592.8, 563.2, 520.9, 506.9, 495.4.

*MS (ESI-HR)*: m/z [M+H]$^{+}$ calc. for $C_{27}H_{22}Cl_2N_2O_6S$: 356.1851, found: 356.1882.
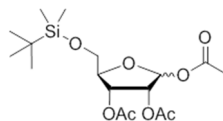
SYNTHESIS OF 1,2,3-TRI-*O*-ACETYL-5-*O*-*TERT*BUTYLDIMETHYLSILY-D-RIBOSE **80**:

Under anhydrous conditions, 5.05 g (33.6 mmol) D-ribose were dissolved in 84 mL pyridine and mixed with 6.59 g (43.7 mmol, 1.3 eq.) *tert*butyldimethylsilyl chloride in small portions. The mixture was stirred at rt for 20 h, and successively 28.6 mL (302 mmol, 9 eq.) acetic anhydride were added. After another 5 h reaction time at rt, the solvent was removed in vacuum and the remaining residue co-evaporated with toluene and dichloromethane until the absence of pyridine. The residue was taken up in ethyl acetate and washed with sat. NaHCO$_3$ (aq.), 1 M HCl (aq.) and demin. water, was then dried over Na$_2$SO$_4$, filtered and the filtrate concentrated in vacuum. The obtained crude residue was purified via NP column chromatography on silica gel with petroleum ether/ethyl acetate 3:1 as eluents. The desired product was obtained colorless resin.

*Yield*: 8.22 g (21.0 mmol, 63%).
*Formula*: C$_{17}$H$_{30}$O$_8$Si.
*Molecular weight*: 390.504.



The analytical data obtained were consistent with those reported in the literature.[143]
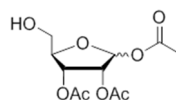
SYNTHESIS OF 1,2,3-TRI-*O*-ACETYL-D-RIBOSE **81**:

In 20 mL dichloromethane, 3.30 g (8.46 mmol) 1,2,3-*O*-acetyl-5-*O*-*tert*butyldimethylsily-D-ribose **80** were dissolved and treated with 4.13 mL (25.4 mmol, 3 eq.) triethylamine trihydrofluoride (37 wt.% HF in TEA) at rt for 5 h. The reaction was quenched by addition of silica gel. The solvent was successively removed under reduced pressure and the obtained residue purified via NP column chromatography on silica gel with ethyl acetate as eluent. The desired product was obtained as colorless resin.

*Yield*: 2.04 g (7.37 mmol, 87%).

*Formula*: $C_{11}H_{16}O_8$.

*Molecular weight*: 276.241.

The analytical data obtained were consistent with those reported in the literature.[143]

<small>SYNTHESIS OF 1,2,3-TRI-*O*-ACETYL-D-RIBOSE-5-BIS(9*H*-FLUOREN-9-YLMETHYL)-PHOSPHATE **84**:</small>

Under an atmosphere of nitrogen, 0.43 g (1.57 mmol) 1,2,3-tri-*O*-acetyl-D-ribose **81** were dissolved in 11 mL dichloromethane and mixed with a solution of 1.10 g (2.10 mmol, 1.3 eq.) bis(9*H*-fluoren-9-ylmethyl)-di*iso*propylamino phosphoramidite **82** in 7 mL dichloro-methane. To this, 7.80 mL (1.96 mmol, 1.25 eq.) DCI (0.25 M in acetonitrile) were added in five portions over a period of 30 min. Upon completed addition, the reaction was stirred another 30 min at rt. For oxidation, 0.36 mL (1.96 mmol, 1.25 eq.) *t*BuOOH (5.5 M in *n*-decane) were added to the reaction mixture. After further 30 min at rt, the reaction was terminated and all volatile components evaporated. The residue was taken up in dichloro-methane, washed with aq. $NH_4OAc$ (1 M) and demin. water, dried over $Na_2SO_4$, filtered and concentrated to dryness again. Lastly, the crude product was purified by NP column chro-matography using an automated flash-chromatography system and a methanol gradient in dichloromethane (0% to 10%). The desired product was obtained as a colorless resin and 1:1 mixture of anomers.

*Yield*: 1.09 g (1.52 mmol, 97%).

*Formula*: $C_{39}H_{37}O_{11}P$.

*Molecular weight*: 712.687.
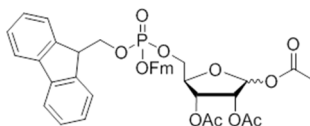
*1H-NMR (600 MHz, chloroform-d)*: δ [ppm] = 7.83 – 7.64 (m, 8 H, C*H*(aromatic)), 7.60 – 7.46 (m, 8 H, C*H*(aromatic)), 7.43 – 7.21 (m, 16 H, C*H*(aromatic)), 6.36 (d, $^3J_{H,H}$ = 4.5 Hz, 1 H, H1α), 6.13 (s, 1 H, H1β), 5.35 (dd, $^3J_{H,H}$ = 7.1 Hz, $^3J_{H,H}$ = 4.9 Hz, 1 H, H3β), 5.31 (dd, $^3J_{H,H}$ = 4.9 Hz, 1.0 Hz, 1 H, H2β), 5.23 (dd, $^3J_{H,H}$ = 6.8 Hz, $^3J_{H,H}$ = 3.0 Hz, 1 H, H3α), 5.09 (dd, $^3J_{H,H}$ = 6.8 Hz, $^3J_{H,H}$ = 4.5 Hz, 1 H, H2α), 4.34 – 4.00 (m, 14 H, H4α/β, H5$_{a,b}$α/β, C*H*$_2$(benzylic) & C*H*CH$_2$(OFm)), 4.18 – 3.97 (m, 9H), 2.12 (s, 3 H, C*H*$_3$(OAc)), 2.10 (2 x s, 6 H, C*H*$_3$(OAc)), 2.07 (s, 3 H, C*H*$_3$(OAc)), 2.01 (s, 3 H, C*H*$_3$(OAc)), 1.92 (s, 3 H, C*H*$_3$(OAc)).

*13C-NMR (151 MHz, chloroform-d)*: δ [ppm] = 170.1, , 169.7, 169.6, 169.5, 169.3, 169.2 (*C*$_q$(OAc)), 143.2, 143.1, 143.0, 141.5, 141.4 (*C*$_q$(aromatic)), 128.0, 127.9, 127.3, 127.2, 125.3, 125.2, 120.1, 120.0 (*C*H(aromatic)), 98.1 (C1β), 94.2 (C1α), 82.5 (C4α), 79.9 (C4β), 74.2 (C2), 70.2 (C3β), 69.6 (C3α) 69.5, 69.4 (*C*H$_2$(benzylic)), 66.6, 66.4 (C5), 48.0, 47.9 (*C*HCH$_2$(OFm)), 21.1, 21.0, 20.7, 20.6, 20.5, 20.4 (*C*H$_3$(OAc)).

*MS (ESI-HR)*: m/z [M+H]$^+$ calc. for C$_{39}$H$_{38}$O$_{11}$P$^+$: 713.2146, found: 713.2150.

<small>SYNTHESIS OF 1,2,3,5-TETRA-*O-TERT*BUTYLDIMETHYLSILYL-β-D-RIBOSE **89**:</small>

In 22 mL anhydrous DMF, 1.60 g (10.7 mmol) D-ribose and 3.63 g (53.4 mmol, 5 eq.) imidazole were dissolved and cooled to 0 °C. Separately, 9.01 g (59.8 mmol, 5.6 eq.) *tert*butyldimethylsilyl chloride were dissolved in 43 mL DMF. The reagent solution was added dropwise over the course of 2 h to the cooled solution of sugar and base. Upon completed addition, the cooling bath was removed, and the reaction mixture stirred at rt for further 48 h. The reaction was terminated by first removing a part of the DMF under high vacuum, and then pouring the remaining solution into ice water. Extraction with dichloromethane was followed by washing with sat. NaHCO₃ (aq.), 1 M HCl (aq.) and demin. water, drying over Na₂SO₄ and concentration of the filtrate to dryness. The residue was purified by column chromatography on silica gel with petroleum ether/dichloromethane 4:1 as eluents, and afforded the desired product as colorless syrup and single anomer.

*Yield*: 4.35 g (7.17 mmol, 67%).

*Formula*: $C_{29}H_{66}O_5Si_4$.

*Molecular weight*: 607.182.
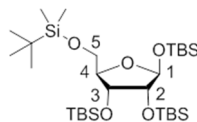


$[\alpha]_{589\,nm}^{23}$ = -5.0 (c = 0.04, MeOH)

*$^1$H-NMR (400 MHz, chloroform-d)*: δ [ppm] = 5.10 (d, $^3J_{H,H}$ = 1.9 Hz, 1 H, H1), 4.05 (dd, $^3J_{H,H}$ = 6.1 Hz, $^3J_{H,H}$ = 4.1 Hz, 1 H, H4), 3.93 (td, $^3J_{H,H}$ = 5.9, $^{3,4}J_{H,H}$ = 3.5 Hz, 1 H, H3), 3.82 – 3.71 (m, 2 H, H2 & H5$_a$), 3.60 (dd, $^2J_{H,H}$ = 10.9, $^3J_{H,H}$ = 5.7 Hz, 1 H, H5$_b$), 1.03 – 0.79 (m, 36 H, $CH_3$(*t*Bu)), 0.15 - 0.01 (m, 24 H, $CH_3$Si).

*$^{13}$C-NMR (151 MHz, acetonitrile-d$_3$)*: δ [ppm] = 102.1 (C1), 83.2 (C3), 78.5 (C2), 72.5 (C4), 65.0 (C5), 26.2, 26.1, 26.0, 25.9 ($CH_3$(*t*Bu)), 18.7, 18.3, 18.2, 18.1 ($C_q$(*t*Bu)), -4.0, -4.1, -4.2, -4.4, -4.7, -4.9, -5.1, -5.2 ($CH_3$Si).

*IR (ATR)*: ṽ in [cm$^{-1}$] = 2953.8, 2929.5, 288.3, 2857.8, 1472.4, 1463.2, 1389.2, 1361.6, 1252.5, 1222.5, 1158.7, 1130.2, 1111.1, 1058.7, 1029.9, 1003.9, 970.9, 939.5, 877.1, 834.6, 775.6, 669.1.

*MS (ESI-HR)*: m/z [M+H]$^+$ calc. for $C_{29}H_{66}O_5Si_4$: 629.3880, found: 629.3881.

SYNTHESIS OF 1-*O*-BENZYL-2,3-DI-*O*-*TERT*BUTYLDIMETHYLSILYL-β-D-RIBOSE **94a**:

According to GP VI, 524 mg (0.86 mmol) 1,2,3,5-tetra-*O*-*tert*butyldimethylsilyl-β-D-ribose **89** were dissolved in 13 mL dichloromethane and converted with 0.95 mL (0.95 mmol, 1.1 eq.) TMSI (1 M in dichloromethane), 0.29 mL (2.07 mmol, 2.4 eq.) triethylamine and 0.10 mL (1.01 mmol, 1.2 eq.) benzyl alcohol. The reaction was terminated after 2 h, and the desired product obtained as yellowish syrup in quantitative yield (427 mg, 0.86 mmol) after purification by means of automated NP flash column chromatography with an ethyl acetate gradient in petroleum ether.

Successively, the fully protected riboside was desilylated partially in accordance with GP

VIIa. Therefore, 427 mg (0.86 mmol) of the riboside were treated with 0.56 mL (3.45 mmol, 4 eq.) TEA x 3 HF (37 wt.%). After 18 h at rt, the reaction was terminated by concentration to dryness, and the crude product was purified by automated NP flash chromatography with an ethyl acetate gradient in petroleum ether (0% to 100%). The desired product was obtained as a single anomer and colorless syrup.

*Yield*: 186 mg (0.40 mmol, 46%).

*Formula*: $C_{24}H_{44}O_5Si_2$.

*Molecular weight*: 468.781.
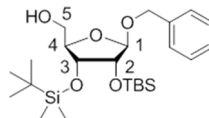


$[\alpha]_{589\,nm}^{21}$ = +65,7 (c = 0.07, CHCl$_3$)

*$^1$H-NMR (600 MHz, chloroform-d)*: δ [ppm] = 7.44 – 7.35 (m, 3 H, C*H*(aromatic)), 7.34 - 7.29 (m, 2 H, C*H*(aromatic)), 5.02 (d, $^3J_{H,H}$ = 3.8 Hz, 1 H, H1), 4.84 (d, $^2J_{H,H}$ = 12.2 Hz, 1 H, C*H*$_2$(benzylic)), 4.55 (d, $^2J_{H,H}$ = 12.2 Hz, 1 H, C*H*$_2$(benzylic)), 4.10 (dt, $^3J_{H,H}$ = 4.6 Hz, $^3J_{H,H}$ = 3.4 Hz, 1 H, H4), 4.04 (dd, $^3J_{H,H}$ = 5.5 Hz, $^3J_{H,H}$ = 4.7 Hz, 1 H, H3), 3.96 (dd, $^3J_{H,H}$ = 5.5 Hz, $^3J_{H,H}$ = 3.8 Hz, 1 H, H2), 3.81 (dd, $^2J_{H,H}$ = 12.0 Hz, $^3J_{H,H}$ = 2.9 Hz, 1 H, H5$_a$), 3.60 (d, $^2J_{H,H}$ = 12.0 Hz, 1 H, H5$_b$), 0.90 (s, 9 H, C*H*$_3$(*t*Bu)), 0.89 (s, 9 H, C*H*$_3$(*t*Bu)), 0.09 (s, 3 H, C*H*$_3$Si), 0.07 (s, 3 H, C*H*$_3$Si), 0.06 (s, 3 H, C*H*$_3$Si), 0.03 (s, 3 H, C*H*$_3$Si).

*$^{13}$C-NMR (151 MHz, acetonitrile-d$_3$)*: δ [ppm] = 138.5 (C$_q$(aromatic)), 128.7, 128.2, 127.7, 127.4, 127.1 (C*H*(aromatic)), 101.9 (C1), 84.4 (C4), 74.3 (C2), 71.4 (C3), 69.3 (C*H*$_2$(benzylic)), 62.4 (C5), 26.1, 26.0 (C*H*$_3$(*t*Bu)), 18.6, 18.3 (C$_q$(*t*Bu)), -4.1, -4.2, -4.4, -4.8 (C*H*$_3$Si).

*IR (ATR)*: ṽ in [cm$^{-1}$] = 3390.2, 2953.9, 2924.6, 2853.5, 2328.7, 2199.0, 2180.8, 2166.1, 2155.7, 2092.2, 2051.2, 1987.0, 1737.9, 1495.8, 1462.8, 1377.6, 1361.7, 1252.1, 1180.2, 1121.8, 1022.5, 922.2, 836.6, 776.7, 733.5, 696.7.

*MS (ESI-HR)*: m/z [M+Na]$^+$ calc. for $C_{24}H_{44}NaO_5Si_2^+$: 491.2619, found: 491.2621.

SYNTHESIS OF 1-*O*-BENZYL-β-D-RIBOSE **94b**:

Following GP VI for the glycosylation and GP VIIb for the desilylation, 524 mg (0.86 mmol) 1,2,3,5-tetra-*O-tert*butyldimethylsilyl-β-D-ribose were dissolved in 13 mL dichloromethane, cooled to -50 °C and converted with 0.95 mL (0.95 mmol, 1.1 eq.) TMSI (1 M in dichloromethane). After 30 min, 0.29 mL (2.07 mmol, 2.4 eq.) triethylamine and 0.11 mL (1.02 mmol, 1.2 eq.) benzyl alcohol were added to the cooled solution. The reaction was allowed to warm up slowly and was terminated after further 2 h. The fully protected riboside was obtained as yellowish syrup in quantitative yield (427 mg, 0.86 mmol) after purification by means of automated NP flash column chromatography. Successively, 28 mg (0.06 mmol) of fully protected riboside were desilylated completely by treatment with 0.10 mL (0.59 mmol, 10 eq.) TEA x 3 HF (37 wt.%) in 1.2 mL acetonitrile. After 4 d at rt, the reaction was terminated and the crude product purified via automated RP flash chromatography with an acetonitrile gradient in water (0% to 100%). The desired product was obtained as colorless resin and a single anomer.

*Yield*: 14 mg (0.06 mmol, quantitative).

*Formula*: $C_{12}H_{16}O_5$.

*Molecular weight*: 240.255.
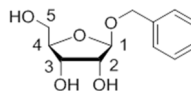
$[\alpha]_{589\,nm}^{23}$ = +92.7 (c = 0.11, $H_2O$)

*$^1$H-NMR (400 MHz, DMSO-$d_6$)*: δ [ppm] = 7.44 – 7.22 (m, 5 H, C*H*(aromatic)), 4.94 (d, $^3J_{H,H}$ = 4.3 Hz, 1 H, H1), 4.76 – 4.66 (m, 2 H, O*H*(H5) & C*H$_2$*(benzylic)), 4.61 (d, $^3J_{H,H}$ = 5.8 Hz, 1 H, O*H*(H3)), 4.51 (d, $^2J_{H,H}$ = 12.4 Hz, 1 H, C*H$_2$*(benzylic)), 4.27 (d, $^3J_{H,H}$ = 9.0 Hz, 1 H, O*H*(H2)), 3.92 – 3.85 (m, 2 H, H2 & H4), 3.81 (td, $^3J_{H,H}$ = 6.2 Hz, $^3J_{H,H}$ = 3.3 Hz, 1 H, H3), 3.45 (ddd, $^2J_{H,H}$ = 6.1 Hz, $^3J_{H,H}$ = 4.3 Hz, $^3J_{H,H}$ = 1.8 Hz, 2 H, H5$_a$ & H5$_b$).

*$^{13}$C-NMR (101 MHz, DMSO-$d_6$)*: δ [ppm] = 138.4 (C$_q$(aromatic)), 128.1, 127.4, 127.2 (*C*H(aromatic)), 101.1 (C1), 85.2 (C4), 71.4 (C2), 69.3 (C3), 68.4 (*C*H$_2$(benzylic)), 61.7 (C5).

*IR (ATR)*: ν̃ in [cm⁻¹] = 3422.6, 3063.4, 3030.8, 2932.1, 2360.0, 2224.7, 2214.7, 2118.9, 2095.8, 1496.9, 1454.5, 144.4, 1353.0, 1211.5, 1123.4, 1087.5, 1021.6, 903.4, 855.7, 739.7, 698.8, 612.3, 556.8, 470.9.

*MS (ESI-HR)*: m/z [M+Na]⁺ calc. for $C_{12}H_{16}NaO_5^+$: 263.0890, found: 263.0885.

S<small>YNTHESIS OF</small> 5-C<small>HLORO-</small>*<small>CYCLO</small>S<small>AL-</small>(1-*O*-<small>BENZYL-</small>2,3-<small>DI-</small>*O*-<small>TERT</small>BUTYLDIMETHYLSILYL-β-<small>D-RIBOSE-</small>5)-<small>PHOSPHATE</small> **95c**:

In 7.2 mL anhydrous pyridine, 68 mg (0.14 mmol) 1-*O*-benzyl-2,3-di-*O*-*tert*butyldimethylsi-lyl-β-D-ribose were dissolved, cooled to -30 °C and mixed with 41 mg (0.17 mmol, 1.2 eq.) 5-chloro-*cyclo*Saligenylchlorophoshpate. The reaction mixture was allowed to warm to rt and stirred for 4 h. Then, all volatile components were removed under vacuum, and the crude residue was taken up in dichloromethane, washed with demin. water (three times), dried over Na₂SO₄, filtered and concentrated again. Purification of the crude product was performed by automated NP flash column chromatography with an ethyl acetate gradient in petroleum ether (+ 1% AcOH) as eluents. The product was obtained as colorless syrup and mixture of two diastereomers.

*Yield*: 38 g (0.05 mmol, 39%).
*Formula*: $C_{31}H_{48}ClO_8PSi_2$
*Molecular weight*: 671.311.
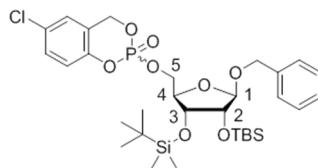


*¹H-NMR (500 MHz, acetonitrile-d₃)*: δ [ppm] = 7.46 – 7.27 (m, 12 H, C*H*(aromatic)), 7.05 ( 2 x d, $^4J_{H,H}$ = 10.1 Hz, 2 H, C*H*(aromatic)), 6.99 (d, $^3J_{H,H}$ = 8.8 Hz, 1 H, C*H*(aromatic)), 6.93 (d, $^3J_{H,H}$ = 8.8 Hz, 1 H, C*H*(aromatic)), 5.32 – 5.27 (m, 4 H, 2 x C*H₂*(benzylic)), 4.92 (d, $^3J_{H,H}$ = 3.8 Hz, 1 H, H1), 4.88 (d, $^3J_{H,H}$ = 3.8 Hz, 1 H, H1), 4.77 (dd, $^2J_{H,H}$ = 12.2 Hz, $^3J_{H,H}$ = 8.6 Hz, 2 H, 2 x C*H₂*(benzylic)), 4.53 (2 x d, $^2J_{H,H}$ = 11.7 Hz, 2 H, 2 x C*H₂*(benzylic)), 4.44 – 4.27 (m, 2 H, 2 x H5ₐ), 4.26 – 4.18 (m, 2 H, 2 x H5ᵦ), 4.19 – 4.14 (m, 2 H, H2 & H4), 4.10 (dt,

$^3J_{H,H}$ = 4.7 Hz, $^3J_{H,H}$ = 3.2 Hz, 1 H, H2), 4.04 (t, $^3J_{H,H}$ = 5.1 Hz, 1 H, H3), 4.02 – 3.95 (m, 1 H, H3), 3.96 (td, *J* = 4.3, 2.2 Hz, 2H), 0.90 (2 x s, 18 H, C*H*$_3$(*t*Bu)), 0.14 – 0.04 (m, 12 H, C*H*$_3$Si).

*$^{13}$C-NMR (126 MHz, chloroform-d)*: δ [ppm] = 148.8, 148.7 (C$_q$(aromatic)), 138.5 (C$_q$(aromatic)), 129.7, 129.6, 128.7, 128.2, 127.6, 127.3, 127.1, 125.3, 125.2, 120.4, 120.3 (*C*H(aromatic)), 101.7, 101.6 (C1), 82.3, 82.2 (C4), 73.9, 73.8 (C2), 71.4, 71.33 (C3), 69.3, , 68.3, 68.1 (*C*H$_2$(benzylic)), 68.0, 67.9 (C5), 26.1, 25.9 (*C*H$_3$(*t*Bu)), 18.6, 18.5, 18.2 (*C*$_q$(*t*Bu)), -4.0, -4.1, -4.2, -4.3, -4.4, -4.5, -4.6, -4.8 (*C*H$_3$Si).

*$^{31}$P-NMR (162 MHz, chloroform-d)*: δ [ppm] = -10.0, -10.1.

*MS (ESI-HR)*: m/z [M+Na]$^+$ calc. for C$_{31}$H$_{48}$ClNaO$_8$PSi$_2{}^+$: 693.2206, found: 693.2208.

SYNTHESES OF ADENOSINE BUILDING BLOCKS FOR NAADP AB DERIVATIVES

SYNTHESIS OF 3',5'-O-DI-*TERT*-BUTYLSILYL ADENOSINE **62**:

In 6 mL DMF, 0.75 g (2.81 mmol) adenosine were reacted with 0.98 mL (3.03 mmol, 1.1 eq.) di-*tert*butylsilyl bis(trifluoromethanesulfonate) at rt for 18 h. The reaction was terminated by addition of diluted $NaHCO_3$ (aq.) After extraction with dichloromethane, the organic layer was washed with brine, dried over $Na_2SO_4$, filtered and concentrated to dryness. The crude product was purified by NP column chromatography on silica gel with dichloromethane/methanol 14:1 as eluents, and the desired product was obtained as colorless amorphous solid.

*Yield*: 0.81 g (1.99 mmol, 71%).

*Formula*: $C_{18}H_{29}N_5O_4Si$.

*Molecular weight*: 407.539.
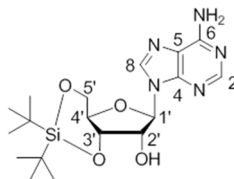


$^1$*H-NMR (400 MHz, methanol-d₄)*: δ [ppm] = 8.23 (s, 1 H, H2), 8.21 (s, 1 H, H8), 6.02 (s, 1 H, H1'), 4.80 (dd, $^3J_{H,H}$ = 8.8 Hz, $^3J_{H,H}$ = 4.8 Hz, 1 H, H3'), 4.65 (d, $^3J_{H,H}$ = 4.9 Hz, 1 H, H2'), 4.47 (dd, $^3J_{H,H}$ = 8.8 Hz, $^3J_{H,H}$ = 4.8 Hz, 1 H, H4'), 4.22 (td, $^2J_{H,H}$ = 9.9 Hz, $^3J_{H,H}$ = 4.8 Hz, 1 H, H5$_a$'), 4.12 (dd, $^2J_{H,H}$ = 10.5 Hz, $^3J_{H,H}$ = 8.9 Hz, 1 H, H5$_b$'), 1.16 (s, 9 H, C$H_3$(*t*Bu)), 1.11 (s, 9 H, C$H_3$(*t*Bu)).

$^{13}$*C-NMR (101 MHz, methanol-d₄)*: δ [ppm] = 155.8 (C6), 153.5 (C2), 148.8 (C4), 141.1 (C8), 119.3 (C5), 92.4 (C1'), 77.4 (C3'), 75.7 (C4'), 74.8 (C2'), 68.5 (C5'), 27.9, 27.6 (C$H_3$(*t*Bu)), 23.5, 21.2 (C$H$(*t*Bu)).

IR (ATR): ṽ [cm$^{-1}$] = 3668.2, 3334.2, 3217.1, 2176.7, 2066.4, 20333.7, 2000.7, 1645.6, 1600.6, 1538.6, 1474.0, 1296.5, 1253.3, 1209.5, 1129.6, 1065.8, 1057.0, 1013.1, 853.9, 828.9, 798.4, 740.6, 724.2, 705.9, 652.6, 595.4, 565.9, 495.3, 460.6.

MS (ESI-HR): m/z = [M+H]$^+$ calc. for $C_{18}H_{30}N_5O_4Si^+$: 408.2068, found: 408.3141.

Sʏɴᴛʜᴇsɪs ᴏꜰ 3',5'-*O*-(1,1,3,3-Tᴇᴛʀᴀ*ɪsᴏ*ᴘʀᴏᴘʏʟᴅɪsɪʟᴏxᴀɴᴇ-1,3-ᴅɪʏʟ) ᴀᴅᴇɴᴏsɪɴᴇ **63**:

According to GP VIIIa, 2.00 g (7.48 mmol) adenosine were dissolved in 34 mL pyridine and treated with 2.60 mL (8.08 mmol, 1.1 eq.) TIPDSCl$_2$ between -30 °C to rt over 18 h. After work up and purification, the desired product was obtained as colorless amorphous solid.

*Yield*: 3.04 g (5.96 mmol, 80%).

*Formula*: C$_{22}$H$_{39}$N$_5$O$_5$Si$_2$.

*Molecular weight*: 509.754.
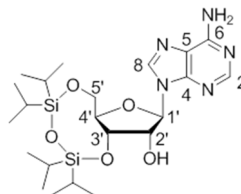


*$^1$H-NMR (400 MHz, chloroform-d)*: δ [ppm] = 8.29 (s, 1 H, H2), 7.96 (s, 1 H, H8), 5.97 (d, $^3J_{H,H}$ = 1.1 Hz, 1 H, H1'), 5.70 (s, 2 H, N*H$_2$*), 5.10 (dd, $^3J_{H,H}$ = 7.8 Hz, $^3J_{H,H}$ = 5.4 Hz, 1 H, H3'), 4.59 (d, $^3J_{H,H}$ = 5.4 Hz, 1 H, H2'), 4.21 – 3.96 (m, 3 H, H4', H5'a, H5'b), 3.39 (s, 1 H, -O*H*), 1.15 – 1.20 (m, 4 H. C*H*(*i*Pr)), 1.20 – 0.88 (m, 21 H, C*H$_3$*(*i*Pr)).

$^{13}$C-NMR (101 MHz, Chloroform-d): δ [ppm] = 155.6 (C6), 153.2 (C2), 149.4 (C4), 139.7 (C8), 120.6 (C5), 89.8 (C1'), 82.3 (C4'), 75.3 (C2'), 71.0 (C3'), 62.0 (C5'), 17.6, 17.5, 17.5, 17.4, 17.3, 17.2, 17.1, 17.1 (C*H$_3$*(*i*Pr)), 13.8, 13.2, 12.9, 12.8 (C*H*(*i*Pr))

IR (ATR): ṽ [cm$^{-1}$] = 3327.2, 2165.3, 2944.7, 2894.6, 2867.6, 2730.0, 2540.6, 1644.2, 1598.9, 1576.9, 1502.2, 1465.9, 1418.6, 1386.2, 1367.6, 13330.8, 1295.2, 1247.6, 1208.5, 1158.0, 1121.3, 1060.3, 1037.1, 1011.8, 991.5, 906.2, 884.3, 859.2, 822.1, 797.3, 773.8, 729.0, 699.1, 647.8, 611.5, 596.5, 562.0, 546.8.

MS (ESI-HR): m/z = [M+H]$^+$ calc. for C$_{22}$H$_{39}$N$_5$O$_5$Si$_2$: 510.2560, found: 510.2580.

SYNTHESIS OF 3',5'-*O*-(1,1,3,3-TETRA*ISO*PROPYLDISILOXANE-1,3-DIYL)-6-*N*-BUTANOYL-ADENOSINE **64b**:

In accordance with GP VIIIb, 2.60 g (9.74 mmol) adenosine were dissolved in 25 mL (10 eq.) pyridine and converted with 3.38 mL (10.5 mmol, 1.1 eq.) TIPDSCl$_2$ between -30 °C to rt over 18 h. Then, the reaction mixture was diluted further with 25 mL tetrahydrofuran and 1.36 mL (10.7 mmol, 1.1 eq.) TMSCl as well as 1.11 mL (10.7 mmol, 1.1 eq.) butyryl chloride were added. After an intermediate work up, cleavage of the TMS ether was carried out in 25 mL tetrahydrofuran mixed with 33 mL (4 eq.) HCl (1.2 M, aq.). After work up and column chromatographic purification, the desired product was obtained as colorless resin.

*Yield*: 3.61 g (5.44 mmol, 56%).

*Formula*: C$_{26}$H$_{45}$N$_5$O$_6$Si$_2$.

*Molecular weight*: 426.527.
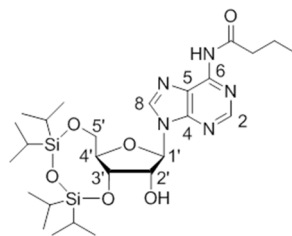


$^1$*H-NMR (400 MHz, chloroform-d)*: δ [ppm] = 8.81 (s, 1 H, N*H*R), 8.64 (s, 1 H, H2), 8.14 (s, 1 H, H8), 6.02 (d, $^3J_{H,H}$ = 1.2 Hz, 1 H, H1'), 5.18 – 5.00 (m, 1 H, H3'), 4.60 (d, $^3J_{H,H}$ = 5.4 Hz, 1 H, H2'), 4.24 – 4.08 (m, 2 H, H4' & H5$_a$'), 4.08 – 3.96 (m, 1 H, H5$_b$'), 3.32 (bs, 1 H, O*H*), 2.85 (t, $^3J_{H,H}$ = 7.4 Hz, 2 H, C*H*$_2$C(O)NR), 1.80 (h, $^3J_{H,H}$ = 7.4 Hz, 2 H, C*H*$_2$CH$_2$C(O)NR), 1.22 – 0.87 (m, 31 H, C*H*$_3$(*i*Pr), C*H*(*i*Pr), C*H*$_3$(alkyl)).

$^{13}$*C-NMR (101 MHz, chloroform-d)*: δ [ppm] = 172.9 (*C*(O)NR), 152.6 (C2), 150.6 (C6), 149.5 (C4), 141.9 (C8), 122.6 (C5), 89.9 (C1'), 82.4 (C4'), 75.2 (C2'), 70.8 (C3'), 61.7 (C5'), 39.9 (*C*H$_2$C(O)NR), 18.5, 17.7, 17.6, 17.5, 17.4, 17.3, 17.2, 17.1, 17.0 (*C*H$_3$(*i*Pr) & *C*H$_2$(alkyl)), 13.91 (*C*H$_3$(alkyl)), 13.4, 13.2, 12.9, 12.7 (*C*H(*i*Pr)).

*IR (ATR)*: ṽ in [cm$^{-1}$] = 3272.9, 2944.2, 2894.6, 2867.3, 1687.9, 1606.9, 1584.0, 1520.2, 1462.5, 1382.5, 1366.6, 1352.5, 1327.0, 1291.2, 1220.9, 1121.6, 1087.5, 1035.4, 992.1, 904.7, 883.9, 859.6, 825.4, 776.8, 736.3, 693.7, 644.9, 609.8, 552.8, 454.3.

*MS (ESI-HR)*: m/z [M+H]$^+$ calc. for C$_{26}$H$_{46}$N$_5$O$_6$Si$_2$$^+$: 580.2981, found: 580.2983.
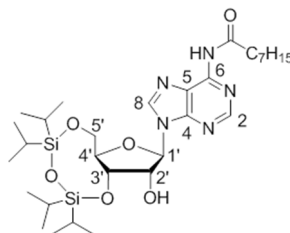
SYNTHESIS OF 3',5'-*O*-(1,1,3,3-TETRA*ISO*PROPYLDISILOXANE-1,3-DIYL)-6-*N*-OCTANOYL-ADENOSINE **64a**:

According to GP VIIIb, 1.36 g (5.10 mmol) adenosine were dissolved in 22 mL (15 eq.) pyridine and treated with 1.77 mL (5.50 mmol, 1.1 eq.) TIPDSCl$_2$ between -30 °C to rt over 18 h. The reaction mixture then was diluted with 22 mL tetrahydrofuran, and 0.84 mL (6.63 mmol, 1.3 eq.) TMSCl as well as 1.13 mL (6.63 mmol, 1.3 eq.) octanoyl chloride were added. After the intermediate work up, cleavage of the TMS ether was carried out in 22 mL tetrahydrofuran mixed with 21 mL (4 eq.) HCl (1 M, aq.). After work up and column chromatographic purification, the desired product was obtained as colorless resin.

*Yield*: 1.82 g (2.86 mmol, 56%).

*Formula*: C$_{30}$H$_{53}$N$_5$O$_6$Si$_2$.

*Molecular weight*: 635.953.

*1H-NMR (500 MHz, chloroform-d)*: δ [ppm] = 8.79 (bs, 1 H, N*H*R), 8.66 (s, 1 H, H2), 8.17 (s, 1 H, H8), 6.03 (d, $^3J_{H,H}$ = 1.2 Hz, 1 H, H1'), 5.07 (dd, $^3J_{H,H}$ = 7.9 Hz, $^3J_{H,H}$ = 5.4 Hz, 1 H, H3'), 4.20 – 4.09 (m, 2 H, H4' & H5a'), 4.09 – 3.99 (m, 1 H, H5b'), 3.20 (bs, 1 H, -O*H*), 2.86 (t, $^{2,3}J_{H,H}$ = 7.5 Hz, 2 H, C*H$_2$*C(O)NR), 1.77 (p, $^{2,3}J_{H,H}$ = 7.5 Hz, 2 H, C*H$_2$*CH$_2$C(O)NR), 1.48 – 1.21 (m, 8 H, C*H$_2$*(alkyl)), 1.13 (s, 4 H, C*H*(iPr)), 1.12 – 0.98 (m, 24 H, C*H$_3$*(iPr)), 0.88 (t, $^{2,3}J_{H,H}$ = 6.8 Hz, 3 H, C*H$_3$*(alkyl)).

*13C-NMR (126 MHz, chloroform-d)*: δ [ppm] = 172.9 (*C*(O)NR), 152.6 (C2), 150.5 (C6), 149.4 (C4), 141.4 (C8), 122.2 (C5), 90.0 (C1'), 82.5 (C4'), 75.2 (C2'), 70.8 (C3'), 61.8 (C5'), 38.1 (*C*H$_2$C(O)NR), 31.8, 29.3, 29.2, 25.0, 22.8 (*C*H$_2$(alkyl)), 17.6, 17.5, 17.5, 17.4, 17.3, 17.2, 17.1, 17.1 (*C*H$_3$(iPr)), 14.2 (*C*H$_3$(alkyl)), 13.5, 13.2, 12.9, 12.8 (*C*H(iPr)).

*IR (ATR)*: ṽ in [cm$^{-1}$] = 3266.2, 3124.9, 2928.9, 2867.5, 1688.3, 1608.5, 1584.5, 1519.0, 1464.6, 1381.5, 1351.5, 1328.3, 1294.7, 1227.8, 1194.4, 1122.8, 1089.6, 1037.6, 993.7, 906.1, 885.0, 862.7, 824.3, 777.9, 696.9, 645.5, 601.8, 556.6, 489.2, 466.2.

*MS (ESI-HR)*: m/z [M+H]$^+$ calc. for C$_{30}$H$_{54}$N$_5$O$_6$Si$_2$$^+$: 636.3613, found: 636.3616.

SYNTHESIS OF 3',5'-*O*-DI-*TERT*-BUTYLSILYL ADENOSINE-2'-BIS(4-OCTANOYLOXYBENZY)-PHOSPHATE **69**:

According to GP IX, 400 mg (0.98 mmol) 3',5'-*O*-di-*tert*-butylsilyl adenosine **62** were dissolved in 7.5 mL DMF and reacted with a solution of 753 mg (1.23 mmol, 1.3 eq.) (OB)$_2$PA **68** in 2.7 mL DMF, 6.87 mL (1.72 mmol, 1.8 eq.) DCI and 0.24 mL (1.33 mmol, 1.4 eq.) *t*BuOOH. After work up (washed with sat. NaHCO$_3$ sol.) and purification, the desired product was obtained as colorless syrup.

*Yield*: 404 mg (0.42 mmol, 43%).

*Formula*: C$_{48}$H$_{70}$N$_5$O$_{11}$PSi.

*Molecular weight*: 952.171.
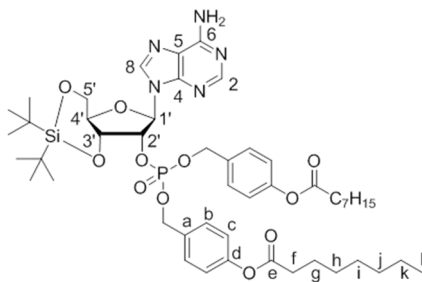


*$^1$H-NMR (400 MHz, chloroform-d)*: δ [ppm] = 8.22 (s, 1 H, H2), 7.85 (s, 1 H, H8), 7.43 – 7.35 (m, 2 H, Hb), 7.30 (d, $^3J_{H,H}$ = 8.4 Hz, 2 H, Hb), 7.13 – 6.97 (m, 4 H, Hc), 5.94 (s, 1 H, H1'), 5.29 (dd, $^3J_{H,P}$ = 8.3 Hz, $^3J_{H,H}$ = 4.9 Hz, 1H, H2'), 5.15 – 5.01 (m, 5 H, H2' & C*H*$_2$(benzylic)), 4.80 (ddd, $^3J_{H,H}$ = 8.3 Hz, $^3J_{H,H}$ = 5.1 Hz, $^3J_{H,H}$ =2.5 Hz, 1 H, H3'), 4.44 (dd, $^2J_{H,H}$ = 8.3 Hz, $^3J_{H,H}$ = 4.1 Hz, 1 H, H5a'), 4-13 – 3.95 (m, 2 H, H4' & H5b'), 2.56 (2x t, $^{2,3}J_{H,H}$ = 7.5 Hz, 4 H, Hf), 1.75 (2x p, $^{2,3}J_{H,H}$ = 7.5 Hz, 4 H, Hg), 1.47 – 1.22 (m, 16 H. Hh – k), 1.10 (s, 9 H, C*H*$_3$(*t*Bu)), 1.03 (s, 9 H, C*H*$_3$(*t*Bu)), 0.94 – 0.78 (m, , 6 H, Hl).

*$^{13}$C-NMR (126 MHz, chloroform-d)*: δ [ppm] = 172.5 (C$_q$e), 151.8 (C2), 151.1 (C$_q$d), 147.9 (C4), 143.9 (C8), 132.6 (C$_q$a), 129.6 (Cc), 122.2, 122.1 (Cb), 119.5 (C5), 90.3 (C1'), 78.1 (C2'), 75.1 (C4'), 74.5 (C3'), 69.5 (C*H*$_2$(benzylic)), 66.7 (C5'), 34.5 (Cf), 31.8, 29.2, 29.1 (Ch – j), 27.4, 27.2 (C*H*$_3$(*t*Bu)), 25.0 (Cg), 22.9 (C*H*(*t*Bu)), 22.7 (Ck), 20.5 (C*H*(*t*Bu)), 14.21 (Cl).

*$^{31}$P-NMR (162 MHz, chloroform-d)*: δ [ppm] = -1.41.

*MS (ESI-HR)*: m/z [M+H]$^+$ calc. for C$_{48}$H$_{71}$N$_5$O$_{11}$PSi$^+$: 952.4658, found: 952.3844.

SYNTHESIS OF 3',5'-*O*-(1,1,3,3-TETRA*ISO*PROPYLDISILOXANE-1,3-DIYL)-ADENOSINE-2'-BIS(4-OCTANOYL-OXYBENZY)-PHOSPHATE **70**:

According to GP IX, 275 mg (0.54 mmol) 3',5'-*O*-(1,1,3,3-tetra*iso*propyldisiloxane-1,3-diyl)-adenosine **63** were dissolved in 4.0 mL DMF and reacted with a solution of 402 mg (0.66 mmol, 1.2 eq.) (OB)$_2$PA **68** in 1.5 mL DMF, 3.78 mL (0.94 mmol, 1.8 eq.) DCI and 0.15 mL (0.82 mmol, 1.5 eq.) *t*BuOOH. After work up (washed with sat. NaHCO$_3$ sol.) and purification, the desired product was obtained as a colorless syrup.

*Yield*: 340 mg (0.32 mmol, 60%).

*Formula*: C$_{52}$H$_{80}$N$_5$O$_{12}$PSi$_2$.

*Molecular weight*: 1054.388.
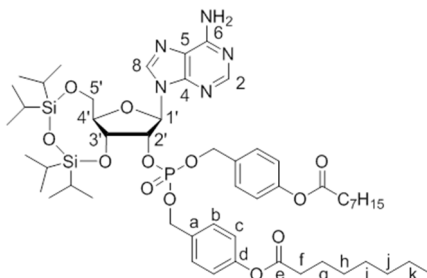


*$^1$H-NMR (500 MHz, chloroform-d)*: δ [ppm] = 8.19 (s, 1 H, H2), 8.00 (s, 1 H, H8), 7.37 (d, $^3J_{H,H}$ = 8.6 Hz, 2 H, Hb), 7.31 (d, $^3J_{H,H}$ = 8.5 Hz, 2 H, Hb), 7.07 – 7.02 (m, 4 H, Hc), 6.53 (bs, 2 H, -N*H*$_2$), 6.01 (s, 1 H, H1'), 5.29 (dd, $^3J_{H,P}$ = 8.3 Hz, $^3J_{H,H}$ = 4.9 Hz, 1H, H2'), 5.17 – 5.02 (m, 4 H, C*H*$_2$(benzylic)), 4.95 (ddd, $^3J_{H,H}$ = 9.3 Hz, $^3J_{H,H}$ = 4.9 Hz, $^3J_{H,H}$ =2.0 Hz, 1 H, H3'), 4.19 (dd, $^2J_{H,H}$ = 13.3 Hz, $^3J_{H,H}$ = 1.9 Hz, 1 H, H5$_a$'), 4.07 (dt, $^3J_{H,H}$ = 9.2 Hz, $^3J_{H,H}$ = 2.3 Hz, 1 H, H4'), 4.01 (dd, $^2J_{H,H}$ = 13.3 Hz, $^3J_{H,H}$ = 2.7 Hz, 1 H, H5$_b$'), 2.56 (2x t, $^{2,3}J_{H,H}$ = 7.5 Hz, 4 H, Hf), 1.75 (2x p, $^{2,3}J_{H,H}$ = 7.5 Hz, 4 H, Hg), 1.50 – 1.22 (m, 16 H. Hh – k), 1.16 – 0.96 (m, 28 H, C*H*$_3$(*i*Pr), C*H*(*i*Pr)), 0.89 (2x t, $^{2,3}J_{H,H}$ = 6.9 Hz, 6 H, Hl).

*$^{13}$C-NMR (126 MHz, chloroform-d)*: δ [ppm] = 172.3, 172.2 (C$_q$e), 154.2 (C6), 151.2 (C$_q$d), 150.2 (C2), 148.8 (C4), 140.4 (C8), 133.1, 133.0 (C$_q$a), 129.3, 129.2 (Cc), 122.1, 122.0 (Cb), 120.2 (C5), 88.7 (C1'), 81.6 (C4'), 79.8 (C2'), 69.3, 69.2 (C*H*$_2$(benzylic)), 68.5 (C3'), 59.9 (C5'), 34.5 (Cf), 31.8, 29.2, 29.1 (Ch – j), 25.1 (Cg), 22.7 (Ck), 17.6, 17.4, 17.4, 17.3, 17.1, 17.1, 17.0, 16.9, (C*H*$_3$(*i*Pr)), 14.2 (Cl), 13.5, 13.1, 12.9, 12.7 (C*H*(*i*Pr)).

*$^{31}$P-NMR (162 MHz, chloroform-d)*: δ [ppm] = -1.45.

*MS (ESI-HR)*: m/z [M+H]$^+$ calc. for C$_{52}$H$_{81}$N$_5$O$_{12}$PSi$_2^+$: 1054.5150, found: 1054.5337.

SYNTHESIS OF 3',5'-*O*-(1,1,3,3-TETRA*ISO*PROPYLDISILOXANE-1,3-DIYL)-6-*N*-BUTANOYL-ADENOSINE-2'-BIS(4-OCTANOYLOXYBENZYL)-PHOSPHATE **71b**:

According to GP IX, 327 mg (0.56 mmol) 3',5'-*O*-(1,1,3,3-tetra*iso*propyldisiloxane-1,3-diyl)-6-*N*-butanoyl-adenosine **64b** were converted in 6.0 mL dichloromethane with a solution of 346 mg (0.56 mmol, 1 eq.) (OB)$_2$PA **68** in 4 mL dichloromethane, 2.7 mL (0.68 mmol, 1.2 eq.) DCI and 0.13 mL (0.70 mmol, 1.3 eq.) *t*BuOOH, and gave the desired product as colorless syrup after work up (washed with aq. NH$_4$OAc (1 M)) and purification.

*Yield*: 496 g (0.44 mmol, 78%).
*Formula*: C$_{56}$H$_{86}$N$_5$O$_{13}$PSi$_2$.
*Molecular weight*: 1124.453.
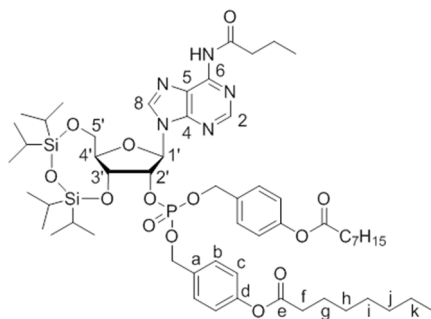


*$^1$H-NMR (400 MHz, chloroform-d)*: δ [ppm] = 8.97 (bs, 1 H, N*H*R), 8.59 (s, 1 H, H2), 8.14 (s, 1 H, H8), 7.49 – 7.35 (m, 2 H, Hb), 7.35 – 7.29 (m, 2 H, Hb), 7.14 – 6.94 (m, 4 H, Hc), 6.00 (s, 1 H, H1'), 5.32 (dd, $^3J_{H,P}$ = 8.3 Hz, $^3J_{H,H}$ = 4.8 Hz, 1 H, H2'), 5.19 – 5.01 (m, 4 H, C*H*$_2$(benzylic)), 4.95 (ddd, $^4J_{H,H}$ = 9.3 Hz, $^3J_{H,H}$ = 4.8 Hz, $^3J_{H,H}$ = 2.0 Hz, 1 H, H3'), 4.19 (dd, $^2J_{H,H}$ = 13.4 Hz, $^3J_{H,H}$ = 1.9 Hz, 1 H, H5$_a$'), 4.08 (dt, $^3J_{H,H}$ = 9.3 Hz, $^3J_{H,H}$ = 2.2 Hz, 1 H, H4'), 4.01 (dd, $^2J_{H,H}$ = 13.3, $^3J_{H,H}$ = 2.7 Hz, 1 H, H5$_b$'), 2.86 (t, $^{2,3}J_{H,H}$ = 7.4 Hz, 2 H, C*H*$_2$C(O)NR), 2.55 (2 x t, $^{2,3}J_{H,H}$ = 7.5 Hz, 4 H, Hf), 1.82 (p, $^{2,3}J_{H,H}$ = 7.4 Hz, 2 H, C*H*$_2$CH$_2$C(O)NR), 1.78 – 1.67 (m, 4 H, Hg), 1.46 – 1.23 (m, 16 H, Hh – k), 1.12 – 0.97 (m, 31 H, C*H*$_3$(*i*Pr), C*H*(*i*Pr) & C*H*$_3$(alkyl)), 0.93 – 0.84 (m, 6 H,

HI).

*$^{13}$C-NMR (121 MHz, chloroform-d)*: δ [ppm] = 172.4, 172.3 (C$_q$e ), 172.1 (*C*(O)NR), 152.7 (C2), 151.1 (C$_q$d), 150.2 (C6), 149.2 (C4), 141.3 (C8), 133.2, 133.1 (C$_q$a), 129.4, 129.3 (Cc), 122.1, 122.0 (Cb), 120.8 (C5), 88.8 (C1'), 81.7 (C4'), 80.4 (C2') 69.3, 69.2 (*C*H$_2$(benzylic)), 68.5 (C3'), 59.8 (C5'), 39.9 (*C*H$_2$C(O)NR), 34.5 (Cf), 31.8, 29.2, 29.1, 25.0, 22.8, 18.5, (Cg – k & *C*H$_2$(alkyl)), 17.6, 17.5, 17.4, 17.3, 17.1, 17.0, 16.9 (*C*H$_3$(*i*Pr)), 14.2 (Cl), 13.9 (*C*H$_3$(alkyl)), 13.5, 13.1, 12.9, 12.7 (*C*H(*i*Pr)).

*$^{31}$P-NMR (162 MHz, chloroform-d)*: δ [ppm] = -1.44.

*MS (ESI-HR)*: m/z [M+H]$^+$ calc. for C$_{56}$H$_{87}$N$_5$O$_{13}$PSi$_2^+$: 1124.5571, found: 1124.5569.

S$_{YNTHESIS}$ $_{OF}$  3',5'-*O*-(1,1,3,3-T$_{ETRA}$*$_{ISO}$*$_{PROPYLDISILOXANE}$-1,3-$_{DIYL}$)-6-*N*-$_{OCTANOYL-ADENOSINE}$-2'-$_{BIS}$(4-$_{OCTANOYLOXYBENZYL}$)-$_{PHOSPHATE}$ **71a**:

According to GP IX, 788 mg (1.24 mmol) 3',5'-*O*-(1,1,3,3-tetra*iso*propyldisiloxane-1,3-diyl)-6-*N*-octanoyl-adenosine **64a** were dissolved in 6.2 mL DMF and reacted with a solution of 950 mg (1.55 mmol, 1.3 eq.) (OB)$_2$PA **68** in 3.1 mL DMF, 6.2 mL (1.55 mmol, 1.3 eq.) DCI and 0.28 mL (1.55 mmol, 1.3 eq.) *t*BuOOH. After work up (washed with aq. NH$_4$OAc (1 M)) and purification, the desired product was obtained as colorless syrup.

*Yield*: 1.34 g (1.14 mmol, 92%).

*Formula*: $C_{60}H_{94}N_5O_{13}PSi_2$.

*Molecular weight*: 1180.578.
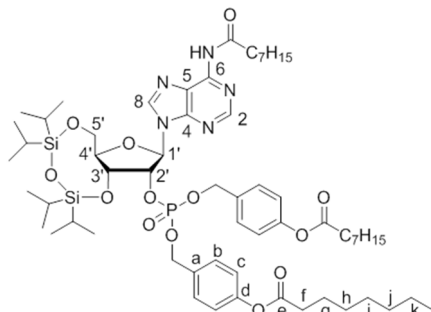
*^{1}H-NMR (500 MHz, chloroform-d)*: δ [ppm] = 8.58 (s, 1 H, H2), 8.49 (bs, 1 H,N*H*R), 8.06 (s, 1 H, H8), 7.41 – 7.34 (m, 2 H, Hb), 7.34 – 7.28 (m, 2 H, Hb), 7.13 – 6.96 (m, 4 H, Hc), 6.02 (s, 1 H, H1'), 5.33 (dd, $^3J_{H,P}$ = 8.3 Hz, $^3J_{H,H}$ = 4.9 Hz, 1 H, H2'), 5.21 – 5.04 (m, 4 H, C*H*$_2$(benzylic)), 5.00 (ddd, $^4J_{H,H}$ = 9.3 Hz, $^3J_{H,H}$ = 4.9 Hz, $^3J_{H,H}$ =2.0 Hz, 1 H, H3'), 4.19 (dd, $^2J_{H,H}$ = 13.3 Hz, $^3J_{H,H}$ = 1.9 Hz, 1 H, H5$_a$'), 4.08 (dt, $^3J_{H,H}$ = 9.3 Hz, $^3J_{H,H}$ = 2.2 Hz, 1 H, H4'), 4.01 (dd, $^2J_{H,H}$ = 13.3 Hz, $^3J_{H,H}$ = 2.7 Hz, 1 H, H5$_b$'), 2.86 (t, $^{2,3}J_{H,H}$ = 7.5 Hz, 2 H, C*H*$_2$C(O)NR), 2.68 – 2.46 (m, 4 H, Hf), 1.93 – 1.58 (m, 6 H, Hg & C*H*$_2$CH$_2$C(O)NR), 1.52 – 1.20 (m, 24 H. Hh – k, C*H*$_2$(alkyl)), 1.17 – 0.96 (m, 28 H, C*H*$_3$(*i*Pr), C*H*(*i*Pr)), 0.89 (3x t, $^{2,3}J_{H,H}$ = 7.0 Hz, 9 H, Hl & C*H*$_3$(alkyl)).

*^{13}C-NMR (126 MHz, chloroform-d)*: δ [ppm] = 172.9 (*C*(O)NR), 172.4, 172.3 (C$_q$e ), 152.6 (C2), 151.2 (C$_q$d), 150.2 (C6), 149.2 (C4), 141.3 (C8), 133.1, 133.0 (C$_q$a), 129.4, 129.3 (Cc), 122.8 (C5), 122.1, 122.0 (Cb), 88.9 (C1'), 81.7 (C4'), 79.6 (C2'), 69.3, 69.2 (C*H*$_2$(benzylic)), 68.5 (C3'), 59.8 (C5'), 38.0 (C*H*$_2$C(O)NR), 34.5 (Cf), 31.9, 31.8, 29.3, 29.2, 29.1, 25.1, 25.0, 22.8, 22.7 (Cg – k & C*H*$_2$(alkyl)), 17.6, 17.4, 17.4, 17.1, 17.1, 16.9, (C*H*$_3$(*i*Pr)), 14.2 (Cl, C*H*$_3$(alkyl)), 13.5, 13.1, 12.9, 12.7 (*C*H(*i*Pr)).

*^{31}P-NMR (162 MHz, chloroform-d)*: δ [ppm] = -0.20.

*MS (ESI-HR)*: m/z [M+H]$^+$ calc. for $C_{60}H_{94}N_5O_{13}PSi_2$: 1180.6230, found: 1180.6262.

SYNTHESIS OF 6-*N*-BUTANOYL-ADENOSINE-2'-BIS(4-OCTANOYLOXYBENZYL)-PHOSPHATE **74**:

Under anhydrous conditions, 299 mg (0.26 mmol) 3',5'-*O*-(1,1,3,3-tetra*iso*propyldisil-ox-ane-1,3-diyl)-6-*N*-butanoyl-adenosine-2'-bis(4-octanoyloxybenzyl)-phosphate **71b** were dissolved in 10 mL acetonitrile and treated with 0.52 mL (3.19 mmol, 12 eq.) TEA x 3 HF (37 wt.%) at rt for 3 -5 h. Then, the reaction was terminated by removal of all volatile compo-nents in vacuum. The crude residue was resolved in acetonitrile and dichloromethane and concentrated to dryness again, then taken up in acetonitrile and purified by automated RP flash column chromatography on $C_{18}$ modified silica gel with an acetonitrile gradient in wa-ter (50% to 100%, then 100% isocratic). The desired product was obtained as colorless resin and a mixture of two regioisomers with the 6-*N*-butanoyl-adenosine-3'-bis(4-oc-tanoyloxybenzyl)-phosphate. Since the reaction was terminated prior to full conversion, starting material was re-isolated from column chromatography. The recovered starting material was converted again, until no more starting material could be isolated from RP chromatography.

*Yield*: 148 g (0.17 mmol, 65%, as a mixture of regio isomers (1:0.85))

*Formula*: $C_{44}H_{60}N_5O_{12}P$.

*Molecular weight*: 881.961.
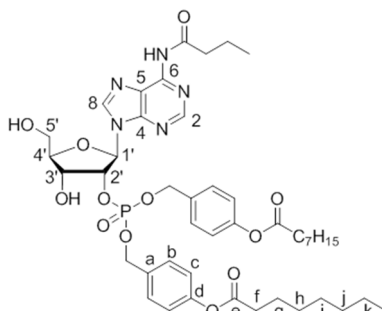
and 6-*N*(Bu)-Ado-3'-bis(OB)-phosphate

*¹H-NMR (400 MHz, chloroform-d)*: δ [ppm] = 8.73 (s, 2 H, 2 x N*H*R(2'/3'P)), 8.60 (s, 1 H, H2(3'P)), 8.59 (s, 1 H, H2(2'P)), 8.08 (s, 1 H, H8(3'P)), 7.94 (s, 1 H H8(2'P)), 7.47 – 7.37 (m, 4 H, Hb(2'P)), 7.26 – 7.22 (m, 2 H, Hb(3'P)), 7.18 – 7.13 (m, 2 H, Hb(3'P)), 7.12 – 7.07 (m, 4 H, Hb(3'P)), 7.05 – 6.95 (m, 4 H, Hc(2'P)), 5.94 (d, $^3J_{H,H}$ = 7.4 Hz, 1 H, H1'(2'P)), 5.38 (dt, $^3J_{H,H}$ = 7.5 Hz, $^3J_{H,P}$ = 5.2 Hz, 1 H, H2'(2'P)), 5.17 – 4.96 (m, 6 H, H2'(2'P), H3'(2'P),

C$H_2$(benzylic 3'P)), 4.95 – 4.85 (m, 2 H, C$H_2$(benzylic 2'P)), 4.81 (d, $^2J_{H,H}$ = 9.9 Hz, 2 H, C$H_2$(benzylic 2'P)), 4.41 (d, $^3J_{H,H}$ = 4.6 Hz, 1 H, H3'(2'P)), 4.30 (s, 1 H, H4'(2'P)), 4.24 (s, 1 H, H4'(3'P)), 3.90 (dd, $^2J_{H,H}$ = 13.0 Hz, $^3J_{H,H}$ = 1.7 Hz, 1 H, H5$_a$'(2'P)), 3.84 (dd, $^2J_{H,H}$ = 13.0 Hz, $^3J_{H,H}$ = 1.7 Hz, 1 H, H5$_a$'(3'P)), 3.70 (d, $^3J_{H,H}$ = 12.9 Hz, 1 H, H5$_b$'(2'P)), 3.58 (d, $^3J_{H,H}$ = 12.9 Hz, 1 H, H5$_b$'(3'P)) 2.84 (2 x t, $^{2,3}J_{H,H}$ = 7.6 Hz, 4 H, C$H_2$C(O)NR(2'/3'P)), 2.55 (2 x t, $^{2,3}J_{H,H}$ = 7.6 Hz, 8 H, Hf(2'/3'P)), 1.95 – 1.64 (m, 12 H, C$H_2$CH$_2$C(O)NR(2'/3'P), Hg(2'/3'P)), 1.49 – 1.20 (m, 32 H, Hh – k(2'/3'P)), 1.03 (2 x t, $^{2,3}J_{H,H}$ = 7.4 Hz, 6 H, C$H_3$(alkyl 2'/3'P)), 0.95 – 0.82 (m, 12 H, Hl(2'/3'P)).

$^{13}$C-NMR (101 MHz, chloroform-d): δ [ppm] = 172.4, 172.3 (C$_q$e(2'/3'P)), 172.2 (C(O)NR(2'/3'P)), 152.8 (C2(2'/3'P)), 151.2, 151.1 (C$_q$d(2'/3'P)), 150.0 (C6(2'P)), 149.9 (C6(3'P)), 149.8 (C4(3'P), 149.7 (C4(2'P)), 143.1 (C8(3'P)), 143.0 (C8(2'P)), 132.8, 132.7, 132.2, 132.1 (C$_q$a(2'/3'P)), 129.5, 129.4, 129.2 (Cc(2'/3'P)), 123.5 (C5(2'/3'P)), 122.1, 122.0, 121.9 (Cb(2'/3'P)), 90.7 (C1'(3'P), 87.6 (C1'(2'P)), 87.4 (C4'(2'P)), 86.2 (C4'(3'P)), 79.2 (C3'(3'P)), 78.1 (C2'(2'P)), 73.1 (C2'(3'P)), 71.7 (C3'(2'P)), 69.7, 69.6, 69.5, 69.4 (CH$_2$(benzylic 2'/3'P)), 62.8 (C5'(2'P)), 62.5 (C5'(3'P)), 39.8 (CH$_2$C(O)NR (2'/3'P)), 34.4 (Cf(2'/3'P)), 31.7, 29.1, 28.9, 24.9, 24.8, 22.6, 18.3, (Cg – k(2'/3'P) & CH$_2$(alkyl 2'/3'P)), 14.1 (Cl(2'/3'P)), 13.8, 13.7 (CH$_3$(alkyl (2'/3'P)).

$^{31}$P-NMR (162 MHz, chloroform-d): δ [ppm] = -0.31 (3'P), -1.59 (2'P).

MS (ESI-HR): m/z [M+H]$^+$ calc. for C$_{44}$H$_{61}$N$_5$O$_{12}$P$^+$: 882.4049, found: 882.4042.

Synthesis of 6-N-Butanoyl-adenosine- bis(2'-bis(4-octanoyloxybenzyl)-5')-phosphate **79**:

According to GP XII, 110 mg (0.13 mmol) 6-N-butanoyl-adenosine-2'/3'-bis(4-octanoyl-oxybenzyl)-phosphate **74/75** were dissolved in 2.6 mL acetonitrile and treated with 80 mg (0.15 mmol, 1.2 eq.) (OFm)$_2$PA **84** in 3.1 mL acetonitrile, 0.77 mL (0.18 mmol, 1.5 eq.) DCI (0.25 M in acetonitrile) and, after stirring 30 min at rt, 34 μL (0.19 mmol, 1.5 eq.) tBuOOH (5.5 M in n-decane). After another 15 min at rt, all volatile components were removed, and the crude product was separated from by-products by a first automated RP flash column chromatography on C$_{18}$ modified silica gel with an acetonitrile gradient in water (0% to 100%). The product fractions were concentrated to dryness and the residue re-dissolved in 3 mL acetonitrile to which 10 vol% (0.30 mL) triethylamine were added. After 24 h at rt, the reaction mixture was concentrated to a volume of approximately 0.5 mL, and the crude
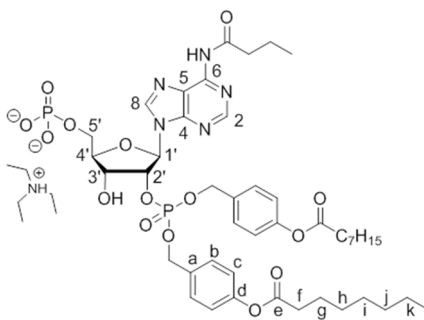
mixture was purified again by automated RP flash column chromatography on $C_{18}$ modified silica gel with an acetonitrile gradient in water (0% to 100%). The desired product was afforded as a colorless resin, a single regioisomer and its triethylammonium salt (0.67 TEAH$^+$ counter ions).

*Yield*: 24 mg (0.02 mmol, 18%, two stages)

*Formula*: $C_{44}H_{59}N_5O_{15}P_2^{2-}$.

*Molecular weight*: 959.925.



$^1$*H-NMR (600 MHz, acetonitrile-d$_3$)*: δ [ppm] = 8.59 (s, 1 H, H2), 8.43 (s, 1 H, H8), 7.51 – 7.37 (m, 4 H, Hb), 7.10 – 7.02 (m, 4 H, Hc), 6.10 (d, $^3J_{H,H}$ = 7.6 Hz, 1 H, H1'), 5.43 – 5.32 (m, 1 H, H2'), 5.21 (d, $^2J_{H,H}$ = 8.5 Hz, 2 H, C*H$_2$*(benzylic)), 5.16 (dd, $^3J_{H,H}$ = 7.8 Hz, $^3J_{H,H}$ = 4.7 Hz, 1 H, H3'), 5.11 ( 2x d, $^3J_{H,H}$ = 8.9 Hz, 2 H, C*H$_2$*(benzylic)), 4.25 (s, 1 H, H4'), 3.74 (dd, $^2J_{H,H}$ = 13.0 Hz, $^3J_{H,H}$ = 2.8 Hz, 1 H, H5$_a$'), 3.66 (dd, $^2J_{H,H}$ = 13.0, $^3J_{H,H}$ = 2.4 Hz, 1 H, H5$_b$'), 2.60 (t, $^3J_{H,H}$ = 7.4 Hz, 2 H, C*H$_2$*C(O)NR), 2.54 (2 x t, $^3J_{H,H}$ = 6.4 Hz, 4 H, Hf) 1.79 – 1.61 (m, 6 H, C*H$_2$*CH$_2$C(O)NR, Hg), 1.43 – 1.23 (m, 20 H, Hh – k), 0.97 (t, *J* = 7.4 Hz, 3 H, C*H$_3$*(alkyl)), 0.92 – 0.70 (m, 6 H, Hl).

$^{13}$*C-NMR (151 MHz, acetonitrile-d$_3$)*: δ [ppm] = 172.8 (C$_q$e), 171.5 (*C*(O)NR), 151.7 (C2), 151.2 (C6), 151.0 (C$_q$d), 149.9 (C4), 143.5 (C8), 133.6 (C$_q$a), 129.7 (cc), 123.0 (C5), 121.9 (Cb), 87.2 (C1'), 85.4 (C4'), 78.0 (C3'), 74.4 (C2'), 69.6, 69.3 (*C*H$_2$(benzylic)), 61. 6 (C5'), 38.8 (*C*H$_2$C(O)NR), 34.3 (Cf), 31.9, 29.2, 27.6, 25.1, 18.8 (Cg – h), 14.0 (Cl), 13.9 (*C*H$_3$(alkyl).

$^{31}$*P-NMR (162 MHz, chloroform-d)*: δ [ppm] = -0.00 (5'P), -1.99 (2'P).

*MS (ESI-HR)*: m/z [M+H]$^+$ calc. for $C_{44}H_{62}N_5O_{15}P_2^+$: 962.3712, found: 962.3701.

SYNTHESES OF NICOTINIC ACID BUILDING BLOCKS FOR NAADP AB DERIVATIVES

SYNTHESIS OF NICOTINIC ACID-(2,3-DI-*O*-ACETYL)-β-D-RIBOSE-5'-BIS(9*H*-FLUOREN-9-YLMETHYL)-MONO-PHOSPHATE **86**:

Under an atmosphere of nitrogen, 58 mg (0.47 mmol, 1.4 eq.) nicotinic acid and 1.2 mL 1,1,1,3,3,3-hexamethyldisilazan (HMDS, 2.5 mL/mmol) were heated to reflux until a clear solution resulted. All volatiles were removed successively. The crude residue was dried in vacuum for 2 h and then re-dissolved in 5 mL acetonitrile. To this, a solution of 240 mg (0.34 mmol) 1,2,3-tri-*O*-acetyl-D-ribose-5-bis(9*H*-fluoren-9-ylmethyl)-phosphate **84** in 1.7 mL acetonitrile was added as well as 0.47 mL (0.47 mmol, 1.4 eq.) SnCl$_4$ (1 M in di-chloromethane). The reaction mixture was stirred at rt for 18 h, then quenched with sat. NaHCO$_3$ sol., diluted and extracted with dichloromethane and lastly washed with water. The concentrated crude residue was purified by automated RP flash chromatography using a C$_{18}$ modified silica gel based stationary phase and an acetonitrile gradient in water (0% to 100%). The product was obtained as tan yellow resin and mixture of anomers α/β 1:9).

*Yield*: 71 mg (0.09 mmol, 27%).

*Formula*: C$_{43}$H$_{39}$NO$_{11}$P$^+$.

*Molecular weight*: 776.754.
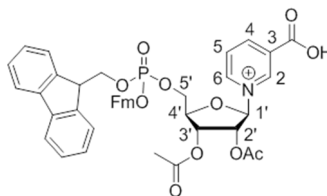


$[\alpha]^{23}_{589\,nm}$ = +52.0 (c = 0.20, MeOH/H$_2$O)

*$^1$H-NMR (500 MHz, methanol-d$_3$)*: δ [ppm] = 9.33 (s, 1 H, H2), 8.92 (d, $^3J_{H,H}$ = 7.9 Hz, 1 H, H 4), 8.54 (d, $^3J_{H,H}$ = 6.3 Hz, 1 H, H6), 7.91 − 7.18 (m, 17 H, H5 & C*H*(aromatic)), 6.46 (d, $^3J_{H,H}$ = 4.4 Hz, 1 H, H1'), 5.33 (dt, $^3J_{H,H}$ = 10.2 Hz, $^3J_{H,H}$ = 4.9 Hz, 2 H, H2', H3'), 4.55 – 4.46 (m, 2 H, H4' & C*H*$_2$(benzylic)), 4.39 (tt, $^2J_{H,H}$ = 10.6 Hz, $^3J_{H,H}$ 4.9 Hz, 3 H, C*H*$_2$(benzylic)), 4.19 - 4.06 (m, 2 H, C*H*CH$_2$(OFm)), 4.03 - 3.93 (m, 1 H, H5$_a$'), 3.84 (dd, $^2J_{H,H}$ = 12.4 Hz, $^3J_{H,H}$ = 6.0 Hz, 1 H, H5$_b$'), 2.05 (s, 3 H, C*H*$_3$(OAc)), 2.03 (s, 3 H, C*H*$_3$(OAc)).

*¹³C-NMR (151 MHz, chloroform-d)*: δ [ppm] = 172.0, 171.1 ($C_q$(OAc)), 160.5 ($C_q$(O)OR), 148.5 (C6), 144.4 (C4), 143.4 (C2), 143.0, 142.9, 142.8 ($C_q$(aromatic)), 140.5 (C3), 129.9, 129.1, 129.0, 128.9 (*C*H(aromatic)), 128.7 (C5), 128.4, 128.3, 126.1, 126.0, 125.9, 125.8, 124.8, 121.2, 121.1, 121.0, 120.7 (*C*H(aromatic)), 98.4 (C1'), 84.7 (C4'), 77.3 (C2'), 70.7 (C3'), 70.6, 70.5 (*C*H₂(benzylic)), 66.5 (C5'), 49.6 (*C*HCH₂(OFm)), 20.3, 20.2 (*C*H₃(OAc)).

*³¹P-NMR (162 MHz, D₂O)*: δ [ppm] = -2.51.

*MS (ESI-HR)*: m/z [M]⁺ calc. for $C_{43}H_{39}NO_{11}P^+$: 776.2255, found: 776.2256.

Synthesis of Nicotinic acid benzyl ester-(2,3-di-*O*-acetyl)-β-D-ribose-5'-bis(9*H*-fluoren-9-ylmethyl)-monophosphate **85**:

Under an atmosphere of nitrogen, 139 mg (0.65 mmol, 1.4 eq.) nicotinic acid benzyl ester **83** and 345 mg (0.48 mmol) 1,2,3-tri-*O*-acetyl-D-ribose-5-bis(9*H*-fluoren-9-ylmethyl)-phosphate **84** were dissolved in 10 mL acetonitrile. To the solution, 0.11 mL (0.58 mmol, 1.2 eq.) trimethylsilyl trifluoromethanesulfonate were added dropwise. After completed addition, the reaction mixture was stirred at rt for 3 h. The reaction was terminated by the addition of 1.2 mL (1.2 mmol, 2.4 eq.) aq. NH₄OAc (1 M). The mixture was further diluted with dichloromethane, the layers were then separated and the organic layer was washed with demin. water, dried over Na₂SO₄, filtered and the filtrate concentrated to dryness. The crude product was purified by automated NP flash column chromatography on silica gel with a methanol gradient dichloromethane (0% to 10%). The desired product was obtained as tan yellowish syrup and single anomer.

*Yield*: 0.93 g (2.2 mmol, 76%).
*Formula*: $C_{50}H_{45}NO_{11}P^+$.
*Molecular weight*: 866.866.
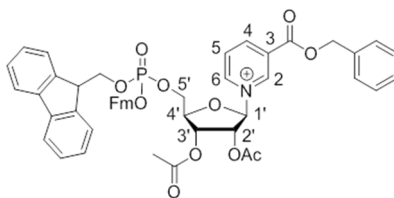
$[\alpha]^{23}_{589\,nm}$ = -9.23 (c = 0.13, MeOH)

*¹H-NMR (400 MHz, chloroform-d)*: δ [ppm] = 9.22 (s, 1 H, H2), 8.86 (d, $^3J_{H,H}$ = 6.1 Hz, 1 H, H6), 8.54 (d, $^3J_{H,H}$ = 7.9 Hz, 1 H, H 4), 7.68 – 6.83 (m, 22 H, H5 & C*H*(aromatic(OFm & OBn))), 6.47 (d, $^3J_{H,H}$ = 5.0 Hz, 1 H, H1'), 5.13 (d, $^3J_{H,H}$ = 11.9 Hz, 1 H, (C*H*₂(benzylic OBn)), 5.08 (d, $^3J_{H,H}$ = 12.0 Hz, 1 H, (C*H*₂(benzylic OBn)), 5.00 (dd, $^3J_{H,H}$ = 5.7 Hz, $^3J_{H,H}$ = 3.9 Hz, 1 H, H3'), 4.91 (t, $^3J_{H,H}$ = 5.3 Hz, 1 H, H2'), 4.21 (dt, $^2J_{H,H}$ = 10.0 Hz, $^3J_{H,H}$ = 5.9 Hz, 1 H, C*H*₂(benzylic OFm)), 4.16 – 4.04 (m, 4 H, H4' & C*H*₂(benzylic OFm)), 3.83 (d, $^3J_{H,H}$ = 4.8 Hz, 2 H, C*H*CH₂(OFm)), 3.54 (ddd, $^2J_{H,H}$ = 12.0 Hz, $^3J_{H,H}$ = 5.5 Hz, $^3J_{H,H}$ = 1.8 Hz, 1 H, H5ₐ'), 3.34 (ddd, $^2J_{H,H}$ = 12.0 Hz, $^3J_{H,H}$ = 6.2 Hz, $^3J_{H,H}$ = 1.6 Hz, 1 H, H5ᵦ'), 1.94 (s, 3 H, C*H*₃(OAc)), 1.91 (s, 3 H, C*H*₃(OAc)).

*¹³C-NMR (151 MHz, chloroform-d)*: δ [ppm] = 170.2, 169.9 (*C*q(OAc)), 160.5 (Cq(O)OR), 146.9 (C6), 144.3 (C4), 143.0 (C2), 142.7, 142.3, 141.7, 141.6 (*C*q(aromatic)), 134.4, 131.2, 129.2, 129.1, 129.0, 128.9 (*C*H(aromatic OBn & OFm)), 128.3 (C5), 128.2, 128.1, 127.5, 127.4, 127.3, 127.2, 124.9, 124.8, 124.7, 120.5, 120.4, 120.3, 120.2 (*C*H(aromatic OBn & OFm)), 97.4 (C1'), 83.7 (C4'), 75.9 (C2'), 69.6 (C3'), 69.4, 69.3 (*C*H₂(benzylic OFm)), 69.2 (*C*H₂(benzylic OBn)), 65.0 (C5'), 48.0, 47.9 (*C*HCH₂(OFm)), 20.5, 20.4 (*C*H₃(OAc)).

*³¹P-NMR (162 MHz, D₂O)*: δ [ppm] = -0.74.

*MS (ESI-HR)*: m/z [M]⁺ calc. for C₅₀H₄₅NO₁₁P⁺: 866.2725, found: 866.2748.

SYNTHESIS OF NICOTINIC ACID BENZYL ESTER-(2,3-DI-*O*-ACETYL)-β-D-RIBOSE-5'-MONOPHOSPHATE **88**:

380 mg (0.44 mmol) nicotinic acid benzyl ester-(2,3-di-*O*-acetyl)-β-D-ribose-5'-bis(9*H*-fluoren-9-ylmethyl)-monophosphate **85** were dissolved in 8.8 mL acetonitrile and mixed with 2.2 mL (25 vol.%) triethylamine. After stirring the reaction mixture at rt for 5 h, all volatile components were removed under vacuum, and the crude residue was resolved in demin. water/dichloromethane 1:1. The layers were separated, the organic layer extracted once more with demin. water, and the aqueous layers were finally unified and lyophilized. The crude freeze-dried product was purified by RP flash column chromatography using and automated chromatography system, C₁₈ modified silica gel as stationary phase and an acetonitrile gradient in water (0% to 100%). The product was obtained as yellowish cotton and

its tetra-*n*-butylammonium salt. Due to the lability of the nucleotide, the product con-
tained impurities from the cleaved nucleobase despite repeated purification.

*Yield*: 91 mg (0.10 mmol, 22%).

*Formula*: $C_{22}H_{23}NO_{11}P$.

*Molecular weight*: 509.404.
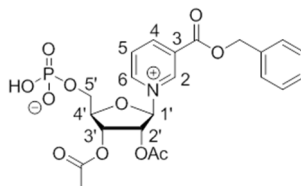


*$^1$H-NMR (400 MHz, D$_2$O)*: δ [ppm] = 9.57 (d, $^3J_{H,H}$ = 6.4 Hz, 1 H, H6), 9.37 (s, 1 H, H2), 8.98 (d, $^3J_{H,H}$ = 8.1 Hz, 1 H, H4), 8.26 (dd, $^3J_{H,H}$ = 8.1 Hz, $^3J_{H,H}$ = 6.4 Hz, 1 H, H5), 7.51 – 7.25 (m, 5 H, C*H*(aromatic)), 6.40 (d, $^3J_{H,H}$ = 4.9 Hz, 1 H, H1'), 5.52 (dd, $^3J_{H,H}$ = 9.8 Hz, $^3J_{H,H}$ = 4.7 Hz, 1 H, H3'), 5.46 (dd, $^3J_{H,H}$ = 5.4 Hz, $^3J_{H,H}$ = 3.5 Hz, 1 H, H2'), 5.39 (d, $^2J_{H,H}$ = 12.1 Hz, 1 H, C*H*$_2$(benzylic)), 5.35 (d, $^2J_{H,H}$ = 12.1 Hz, 1 H, C*H*$_2$(benzylic)), 4.77 – 4.66 (m, 1 H, H4'), 4.21 – 4.03 (m, 1 H, H5$_a$'), 3.96 – 3.87 (m, 1 H, H5$_b$'), 2.05 (s, 3 H, C*H*$_3$(OAc)), 1.96 (s, 3 H, C*H*$_3$(OAc)).

*$^{13}$C-NMR (151 MHz, D$_2$O)*: δ [ppm] = 172.5, 172.3 (*C*$_q$(OAc)), 147.5 (C6), 142.0 (C4), 141.2 (C3), 140.2 (C2), 137.2 (*C*$_q$(aromatic)), 128.7 (*C*H(aromatic)), 128.4 (C5), 127.5 (*C*H(aromatic)), 97.4 (C1'), 84.6 (C4'), 73.5 (C2'), 70.8 (C3'), 63.9 (*C*H$_2$(benzylic)), 63.6 (C5), 19.9, 19.8 (*C*H$_3$(OAc)).

*$^{31}$P-NMR (162 MHz, D$_2$O)*: δ [ppm] = 3.08.

*MS (ESI-HR)*: m/z [M]$^+$ calc. for $C_{22}H_{24}NO_{11}P$: 510.1160, found: 510.1161.

A<small>TTEMPT OF THE</small> S<small>YNTHESIS OF</small> N<small>ICOTINIC ACID</small>-(4-<small>OCTANOYLOXYBENZYL</small>) <small>ESTER</small>-2,3-<small>DI</small>-*O*-*TERT*<small>BUTYLDI</small>-<small>METHYLSILYL</small>-β-<small>D</small>-<small>RIBOSE</small> **92a**:
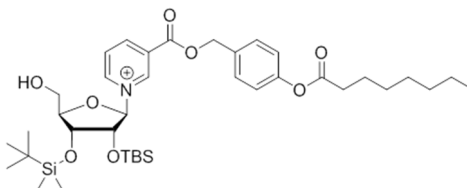
According to GP VI, 275 mg (0.45 mmol) 1,2,3,5-tetra-*O*-*tert*butyldimethylsilyl-β-D-ribose **89** were dissolved in 11.3 mL dichloromethane, cooled to -50 °C and converted with 0.50 mL (0.50 mmol, 1.1 eq.) TMSI (1 M in dichloromethane), 0.15 mL (1.08 mmol, 2.4 eq.) triethylamine and 190 mg (0.53 mmol, 1.2 eq.) nicotinic acid-(4-octanoyloxybenzyl) ester **90** dissolved in 6.7 mL dichloromethane. The reaction was terminated after 2 h, and the fully protected nicotinic acid ester riboside was obtained as yellowish syrup after purification by means of NP column chromatography.

Successively, it was attempted to 5'-desilylate in accordance with GP VIIb. The riboside was dissolved in 12.5 mL acetonitrile and treated with 0.30 mL (1.81 mmol, 4 eq.) TEA x 3 HF (37 wt.%). After stirring at rt for 5 h, the reaction was terminated and the crude product purified via automated NP flash chromatography on silica gel with an ethyl acetate gradient in petroleum ether (0% to 100%). The formed product however decomposed while purification and concentration of the product-containing fractions so that the 5'-desilylated nicotinic acid ester riboside could not be isolated.

*Yield*: - .
*Formula*: $C_{38}H_{62}NO_8Si_2^+$.
*Molecular weight*: 717.085.



S<small>YNTHESIS OF</small> N<small>ICOTINIC ACID</small>-(4-<small>OCTANOYLOXYBENZYL</small>) <small>ESTER</small>-β-<small>D</small>-<small>RIBOSE</small> **92b**:

Following GP VI for the glycosylation and GP VIIb for the desilylation, 119 mg (0.19 mmol) 1,2,3,5-tetra-*O*-*tert*butyldimethylsilyl-β-D-ribose **89** were dissolved in 4.9 mL dichloromethane, cooled to -50 °C and converted with 0.21 mL (0.21 mmol, 1.1 eq.) TMSI (1 M in dichloromethane). After 30 min, 0.07 mL (0.47 mmol, 2.4 eq.) triethylamine and 87 mg

(0.24 mmol, 1.2 eq.) nicotinic acid-(4-octanoyloxybenzyl) ester **90** were added to the cooled solution. The reaction was allowed to warm up slowly and was terminated after further 2 h. The desired product was obtained as yellowish syrup in 97% yield (159 mg, 0.19 mmol) after purification by means of NP column chromatography. Successively, the fully protected riboside was desilylated by treatment with 0.56 mL (3.43 mmol, 18 eq.) TEA x 3 HF (37 wt.%). After 4 d at rt, the reaction was terminated and the crude product purified via automated RP flash column chromatography with an acetonitrile gradient in water (0% to 100%). The desired product was obtained as colorless cotton after freeze-drying and a single anomer.

*Yield*: 46 g (0.09 mmol, 47% over two steps).

*Formula*: $C_{26}H_{34}NO_8^+$.

*Molecular weight*: 488.558.
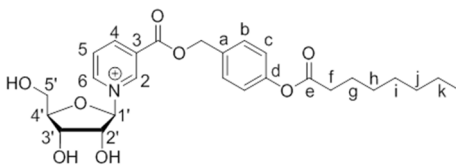


$[\alpha]^{23}_{589\,nm}$ = +95.5 (c = 0.11, $H_2O$)

*$^1$H-NMR (400 MHz, methanol-$d_4$)*: δ [ppm] = 9.45 (s, 1 H, H2), 9.30 (d, $^3J_{H,H}$ = 6.2 Hz, 1 H, H6), 9.04 (dt, $^3J_{H,H}$ = 8.1 Hz, $^3J_{H,H}$ = 1.5 Hz, 1 H, H4), 8.21 (dd, $^3J_{H,H}$ = 8.0 Hz, $^3J_{H,H}$ = 6.2 Hz, 1 H, H5), 7.65 – 7.46 (m, 2 H, Hb), 7.26 – 7.07 (m, 2 H, Hc), 6.57 (d, $^3J_{H,H}$ = 5.6 Hz, 1 H, H1'), 5.50 (s, 2 H, C$H_2$(benzylic)), 4.92 (t, $^3J_{H,H}$ = 5.2 Hz, 1 H, H2'), 4.68 (td, $^3J_{H,H}$ = 3.7 Hz, $^3J_{H,H}$ = 1.8 Hz, 1 H, H4'), 4.26 (dd, $^3J_{H,H}$ = 4.8 Hz, $^3J_{H,H}$ = 1.9 Hz, 1 H, H3'), 3.81 (dd, $^2J_{H,H}$ = 12.4 Hz, $^3J_{H,H}$ = 3.6 Hz, 1 H, H5$_a$'), 3.73 (dd, $^2J_{H,H}$ = 12.4 Hz, $^3J_{H,H}$ = 3.8 Hz, 1 H, H5$_b$'), 2.60 (t, $^{2,3}J_{H,H}$ = 7.4 Hz, 2 H, Hf), 1.74 (p, $^{2,3}J_{H,H}$ = 7.4 Hz, 2 H, Hg), 1.60 – 1.20 (m, 8H,Hh – k), 1.05 – 0.76 (m, 3 H, Hl). *$^{13}$C-NMR (101 MHz, methanol-$d_4$)*: δ [ppm] = 173.7 ($C_q$e), 163.0 (C(O)OR$_{OB\ ester}$), 152.5 ($C_q$a), 147.4 (C4), 146.8 (C6), 143.7 (C2), 134.0 ($C_q$d), 131.1 (Cb), 130.4 (C3), 128.9 (C5), 123.1 (Cb), 98.6 (C1'), 91.5 (C4'), 73.9 (C2'), 72.6 (C3'), 68.7 (C$H_2$(benzylic)), 62.9 (C5'), 34.9 (Cf), 32.8, 30.2, 30.0, 25.9, 23.6 (Cg – k), 14.3 (Cl).

*IR (ATR)*: ṽ in [cm⁻¹] = 3384.9, 3092.3, 2954.6, 2927.1, 2856.2, 2063.5, 1992.6, 1734.2, 1637.6, 1608.9, 1508.3, 1452.9, 1418.2, 1378.1, 1292.7, 1199.2, 1135.3, 1100.6, 1018.4, 976.5, 918.2, 836.4, 721.6, 677.1, 577.3, 495.8, 474.6.

*MS (ESI-HR)*: m/z [M]⁺ calc. for $C_{26}H_{34}NO_8^+$: 488.2279, found: 488.2314.

ATTEMPT OF THE SYNTHESIS OF 5-CHLORO-*CYCLOSAL*-(NICOTINIC ACID-(4-OCTANOYLOXYBENZYL) ESTER-β-D-RIBOSE-5')-PHOSPHATE **95a**:

Under anhydrous conditions, 45 mg (0.09 mmol) nicotinic acid-(4-octanoyloxybenzyl) ester-β-D-ribose **92b** were dissolved in 4.6 mL DMF and cooled to -25 °C. To the cooled solution, 16 µL (0.11 mmol, 1.2 eq) TEA, 9.5 µL (0.12 mmol, 1.3 eq.) 1-methylimidazole were added as well as 120 µL of a solution of 5-chloro-*cyclo*Saligenylchlorophosphate (0.12 mmol, 1.3 eq, 1 M in THF) in portions of 24 µL over 1 h. The reaction mixture was allowed to warm to 0 °C and stirred for further 2 h. The reaction was terminated by removal of all volatile components in vacuum, and a crude NMR was recorded indicating the formation of the desired product. Accordingly, the crude mixture was intended to be purified by automated NP flash column chromatography on silica gel and with an ethyl acetate gradient in petroleum ether (+ 2% AcOH) as eluents. The product, however, could not be isolated due to decomposition while column chromatography and only traces of the nucleobase and excess reagent were collected.

*Yield*: - .

*Formula*: $C_{33}H_{38}ClNO_{11}P^+$.

*Molecular weight*: 691.086.
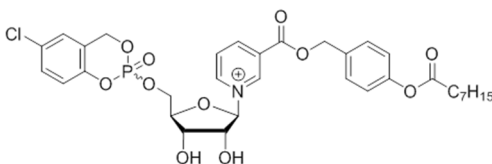
SYNTHESIS OF 1-*O*-(4-OCTANOYLOXYBENZYL)-2,3,-DI-*O*-*TERT*BUTYLDIMETHYLSILYL-β-D-RIBOSE **97**:

According to GP VI, 220 mg (0.36 mmol) 1,2,3,5-tetra-*O*-*tert*butyldimethylsilyl-β-D-ribose **89** were dissolved in 5.4 mL dichloromethane and converted with 0.39 mL (0.39 mmol, 1.1 eq.) TMSI (1 M in dichloromethane), 0.12 mL (0.87 mmol, 2.4 eq.) triethylamine and 109 mg (0.43 mmol, 1.2 eq.) 4-(hydroxymethyl)-phenyloctanoate **58**. The reaction was terminated after 2 h, and the fully protected riboside obtained as a yellowish syrup in 80 % yield (210 mg, 0.29 mmol) after purification by means of automated NP flash column chromatography.

Successively, the fully protected riboside was 5'-desilylated in accordance with GP VIIb. Therefore, 210 mg (0.29 mmol) of the riboside were treated with 0.16 mL (0.95 mmol, 3.3 eq.) TEA x 3 HF (37 wt.%). After 18 h at rt, the reaction was terminated and the crude product purified via automated NP flash column chromatography on silica gel with an ethyl acetate gradient in petroleum ether (0% to 100%). The desired product was obtained as colorless syrup and a single anomer.

*Yield*: 142 mg (0.23 mmol, 64% over two steps).

*Formula*: C$_{32}$H$_{58}$O$_7$Si$_2$.

*Molecular weight*: 610.979.
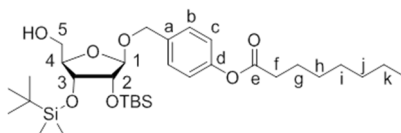


$[\alpha]^{23}_{589\,nm}$ = +62,5 (c = 0.12, CHCl$_3$)

*$^1$H-NMR (500 MHz, chloroform-d)*: δ [ppm] = 7.45 – 7.32 (m, 2 H, Hb), 7.03 – 6.93 (m, 2 H, Hc), 5.00 (d, $^3J_{H,H}$ = 3.8 Hz, 1 H, H1), 4.81 (d, $^2J_{H,H}$ = 12.2 Hz, 1 H, C*H*$_2$(benzylic)), 4.54 (d, $^3J_{H,H}$ = 12.3 Hz, 1 H, C*H*$_2$(benzylic)), 4.14 – 4.06 (m, 1 H, H4), 4.03 (dd, $^3J_{H,H}$ = 5.5 Hz, $^3J_{H,H}$ = 4.5 Hz, 1 H, H3), 3.95 (dd, $^3J_{H,H}$ = 5.5 Hz, $^3J_{H,H}$ = 3.8 Hz, 1 H, H2), 3.80 (dd, $^2J_{H,H}$ = 12.1 Hz, $^3J_{H,H}$ = 3.0 Hz, 1 H, H5$_a$), 3.60 (dd, $^2J_{H,H}$ = 12.0 Hz, $^3J_{H,H}$ = 3.7 Hz, 1 H, H5$_b$), 2.55 (t, $^{2,3}J_{H,H}$ = 7.6

Hz,2 H, Hf), 1.75 (p, $^3J_{H,H}$ = 7.5 Hz, 2 H, Hg), 1.49 – 1.22 (m, 6 H, Hh – k), 0.99 – 0.69 (m, 21 H, Hl & C$H_3$(tBu)), 0.16 – -0.04 (m, 12 H, C$H_3$Si).

*$^{13}$C-NMR (126 MHz, chloroform-d)*: δ [ppm] = 172.6 (C$_q$e), 150.0 (C$_q$d), 136.1 (C$_q$a), 128.6 (Cb), 121.3 (Cc), 101.9 (C1), 84.6 (C4), 74.2 (C2), 71.4 (C3), 68.6 (C$H_2$(benzylic)), 62.4 (C5), 34.6 (Cf), 31.8, 29.2, 29.1 (Hh – j), 26.1, 26.0 (C$H_3$(tBu)), 25.1, 22.7 (Hg & Hk), 18.6, 18.3 (C$_q$(tBu)), 14.2 (Cl), -4.1, -4.2, -4.4, -4.8 (C$H_3$Si).

*IR (ATR)*: ṽ in [cm$^{-1}$] = 3471.9, 2953.9, 2925.6, 2854.6, 2329.5, 2225.1, 2203.4, 2156.0, 2109.2, 2029.6, 1984.8, 1949.9, 1761.1, 1608.4, 1508.1, 1462.8, 1377.6, 1361.4, 1251.5, 195.2, 1165.6, 1118.2, 1015.8, 919.9, 894.4, 836.3, 776.3, 738.3, 704.8, 670.3, 569.5.

*MS (ESI-HR)*: m/z [M+NH$_4$]$^+$ calc. for C$_{32}$H$_{62}$NO$_7$Si$_2^+$: 628.4059, found: 628.4055.

SYNTHESIS OF 1-*O*-(4-OCTANOYLOXYBENZYL)-β-D-RIBOSE **98**:

Following GP VI and GP VIIb, 219 mg (0.36 mmol) 1,2,3,5-tetra-*O-tert*butyldimethylsilyl-β-D-ribose **89** were dissolved in 5.4 mL dichloromethane and converted with 0.40 mL (0.40 mmol, 1.1 eq.) TMSI (1 M in dichloromethane), 0.12 mL (0.87 mmol, 2.4 eq.) triethylamine and 108 mg (0.43 mmol, 1.2 eq.) 4-(hydroxymethyl)-phenyloctanoate **58**. The reaction was terminated after 1 h, and the fully protected riboside obtained as yellowish syrup in 72% yield (189 mg, 0.26 mmol) after purification by means of NP column chromatography. Successively, the fully protected riboside was desilylated completely by treatment with 1.14 mL (7.02 mmol, 27 eq.) TEA x 3 HF (37 wt.%). After 4 d at rt, the reaction was terminated and the crude product purified via automated RP flash column chromatography with an acetonitrile gradient in water (0% to 100%). The desired product was obtained as a colorless resin and a single anomer.
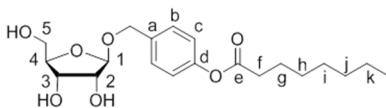
*Yield*: 78 mg (0.20 mmol,

56% over two steps).

*Formula*: $C_{20}H_{30}O_7$.

*Molecular weight*: 382.453.



$[\alpha]_{589\,nm}^{23}$ = +92.7 (c = 0.11, $H_2O$)

*$^1$H-NMR (400 MHz, chloroform-d)*: δ [ppm] = 7.49 – 7.28 (m, 2 H, Hb), 7.15 – 6.93 (m, 2 H, Hc), 5.12 (d, $^3J_{H,H}$ = 4.4 Hz, 1 H, H1), 4.82 (d, $^2J_{H,H}$ = 11.9 Hz, 1 H, C$H_2$(benzylic)), 4.58 (d, $^2J_{H,H}$ = 11.9 Hz, 1 H, C$H_2$(benzylic)), 4.06 (q, $^3J_{H,H}$ = 3.7 Hz, 2 H, H2 & H4), 3.96 (dd, $^3J_{H,H}$ = 6.5 Hz, $^3J_{H,H}$ = 3.6 Hz, 1 H, H3), 3.80 (dd, $^2J_{H,H}$ = 12.0 Hz, 3.3 Hz, 1 H, H5$_a$'), 3.68 (dd, $^2J_{H,H}$ = 12.0 Hz, $^3J_{H,H}$ = 4.2 Hz, 1 H, H5$_b$'), 2.55 (t, $^3J_{H,H}$ = 7.5 Hz, 2 H, Hf), 1.83 – 1.65 (m, 2 H, Hg), 1.58 – 1.16 (m, 8 H, Hh – k), 0.98 – 0.78 (m, 3 H, ).

*$^{13}$C-NMR (101 MHz, chloroform-d)*: δ [ppm] = 172.5 ($C_q$e), 150.6 ($C_q$d), 134.6 ($C_q$a), 129.3 (Cb), 121.87 (Cc), 100.8 (C1), 85.1 (C4), 71.9 (C2), 70.7 (C3), 69.2 (C$H_2$(benzylic)), 62.7 (C5), 34.5 (Cf), 31.7, 29.2, 29.0, 25.0, 22.7 (Cg – k), 14.2 (Cl).

*IR (ATR)*: ṽ in [$cm^{-1}$] = 3379.8, 2925.7, 2855.9, 2120.9, 1756.0, 1604.8, 15507.5, 1458.7, 1416.5, 1353.9, 1197.6, 1165.4, 1138.6, 1087.0, 1013.9, 916.7, 852.6, 766.8, 721.6, 609.8, 563.1, 502.6.

*MS (ESI-HR)*: m/z [M+Na]$^+$ calc. for $C_{20}H_{30}NaO_7^+$: 405.1884, found: 405.1885.

SYNTHESIS OF 1-*O*-(4-OCTANOYLOXYBENZYL)-β-D-RIBOSE MONOPHOSPHATE **99**:

Following GP XII, 78 mg (0.20 mmol) 1-*O*-(4-octanoyloxybenzyl)-β-D-ribose **98** were dis-solved in 2.0 mL acetonitrile and reacted with 0.77 mL (0.24 mmol, 1.2 eq.) of a (OFm)$_2$PA **84** solution (0.3 M in acetonitrile), 0.98 mL DCI (0.25 M in acetonitrile, 0.24 mmol, 1.2 eq.) and 0.05 mL (0.25 mmol, 1.3 eq.) *t*BuOOH (5.5 M in *n*-decane). After removal of all volatile components in vacuum, the crude residue was resolved in 2.8 mL acetonitrile to which

0.28 mL (10 vol.%) triethylamine were added. After 12 h, 3 mL demin water were added to the reaction mixture. After further 5 h, the reaction mixture was concentrated to an approximate volume of 1 mL and the mixture was purified by automated RP flash column chromatography on $C_{18}$ modified silica gel with an acetonitrile gradient in water (0% to 100%). The desired product was obtained as a colorless resin and triethylammonium salt (1.3 counter ions, calculated from $^1$H-NMR spectrum).

*Yield*: 40 mg (0.07 mmol, 33%).

*Formula*: $C_{20}H_{29}O_{10}P^{2-}$.

*Molecular weight*: 460.417.
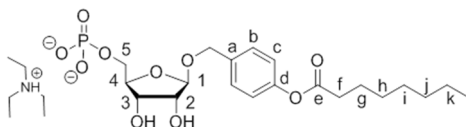


*$^1$H-NMR (400 MHz, D$_2$O)*: δ [ppm] = 7.44 (d, $J_{H,H}$ = 8.3 Hz, 2 H, Hb), 7.04 (d, $^3J_{H,H}$ = 8.4 Hz, 2 H, Hc), 5.15 (d, $J_{H,H}$ = 2.6 Hz, 1 H, H1), 4.76 (d, $^3J_{H,H}$ = 12.3 Hz, 1 H, C$H_2$(benzylic)), 4.60 (d, $^3J_{H,H}$ = 12.3 Hz, 1 H, C$H_2$(benzylic)), 4.25 (s, 1 H, H4), 4.20 – 4.10 (m, 2 H, H2 & H3), 4.06 – 3.94 (m, 2 H, H5$_a$ & H5$_b$), 2.53 (t, $^3J_{H,H}$ = 7.4 Hz, 2 H, Hf), 1.67 (q, $^3J_{H,H}$ = 7.3 Hz, 2 H, Hg), 1.55 – 1.27 (m, 8 H, Hh – k), 0.91 (t, $^3J_{H,H}$ = 6.5 Hz, 3 H, Hl).

*$^{13}$C-NMR (101 MHz, D$_2$O)*: δ [ppm] = 174.1 (C$_q$e), 149.8 (C$_q$d), 135.6 (C$_q$a), 129.3 (Cb), 121.4 (Cc), 101.3 (C1), 83.3 (C4), 71.0 (C2), 69.6 (C3), 68.9 (C$H_2$(benzylic)), 64.9 (C5), 33.9 (Cg), 31.4, 28.6, 28.6, 24.5, 22.3 (Cg – k), 13.6 (Cl).

*$^{31}$P-NMR (162 MHz, D$_2$O)*: δ [ppm] = 0.22.

*MS (ESI-HR)*: m/z [M-H]$^-$ calc. for $C_{20}H_{30}O_{10}P^-$: 461.1582, found: 461.1585.

SYNTHESIS OF (4-OCTANOYLOXYBENZYL)-(1-*O*-(4-OCTANOYLOXYBENZYL)-2,3,-DI-*O*-*TERT*BUTYLDI-ME-THYLSILYL-β-D-RIBOSE-5)-PHOSPHONAT **106**:

Under anhydrous conditions, 60 mg (0.24 mmol, 1 eq.) 4-(hydroxymethyl)-phenyloctanoate **58** were co-evaporated with pyridine and then dissolved in 1.2 mL pyridine. At -30 °C,

54 μL (0.28 mmol, 1.2 eq.) diphenyl phosphine were added to the solution. The reaction mixture was allowed to warm to rt and stirred for 18 h before cooling down to -30 °C again. To the cooled solution, 143 mg (0.23 mmol, 1 eq.) 1-*O*-(4-octanoyloxybenzyl)-2,3,-di-*O*-*tert*butyldimethylsilyl-β-D-ribose **97**, dissolved in 1.2 mL pyridine, were added, and the mixture brought to rt again and stirred for another 18 h. Successively, all volatile components were removed under high vacuum and the residue was co-evaporated with toluene and dichloromethane several times. The crude product was purified finally by automated NP flash column chromatography on silica gel with an ethyl acetate gradient in petroleum ether (0% to 100%, + 2% AcOH) to afford the desired product as a colorless resin and mixture of two diastereomers.

*Yield*: 102 mg (0.11 mmol, 48%).

*Formula*: $C_{47}H_{79}O_{11}PSi_2$.

*Molecular weight*: 907.282.
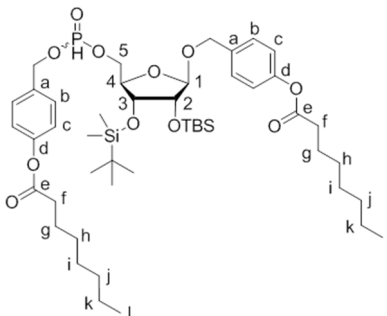


*¹H-NMR (400 MHz, chloroform-d)*: δ [ppm] = 7.50 – 7.31 (m, 2 x 4 H, H*b*), 7.16 – 7.05 (m, 2 x 2 H, H*c*), 7.05 – 6.96 (m, 2 x 2 H, H*c*), 6.95 (d, $^1J_{H,P}$ = 711.4 Hz, 1 H, P*H*), 6.92 (d, $^1J_{H,P}$ = 712.4 Hz, 1 H, P*H*), 5.18 – 5.03 (m, 2 x 2 H, C*H₂*(benzylic)), 4.98 (t, $^3J_{H,H}$ = 3.6 Hz, 2 x 1 H, H1), 4.78 (2 x d, $^2J_{H,H}$ = 12.2 Hz, 1 H, C*H₂*(benzylic)), 4.50 (2 x d, $^2J_{H,H}$ = 12.2 Hz, 1 H, C*H₂*(benzylic)), 4.27 (ddd, $^2J_{H,H}$ = 11.5 Hz, $^3J_{H,H}$ = 8.6 Hz, $^3J_{H,H}$ = 3.0 Hz, 2 x 1 H, H5*a*′), 4.15 (dd, $^3J_{H,H}$ = 6.5 Hz, $^3J_{H,H}$ = 2.9 Hz, 2 x 1 H, H4), 4.05 (ddd, $^2J_{H,H}$ = 13.3 Hz, $^3J_{H,H}$ = 9.0 Hz, $^3J_{H,H}$ = 4.9 Hz, 2 x 1 H, H5*b*′), 4.03 – 3.97 (m, 1 H, 2 x H2), 3.95 (dd, $^3J_{H,H}$ = 5.4 Hz, $^3J_{H,H}$ = 4.0 Hz, 2 x 1 H, H3), 2.54 (2 x t, $^3J_{H,H}$ = 7.3 Hz, 2 x 4 H, H*f*), 1.75 (p, $^3J_{H,H}$ = 7.5 Hz, 2 x 4 H, H*g*), 1.51 – 1.17 (m, 2 x 16 H, H*h* – *k*), 0.98 – 0.75 (m, 2 x 21 H, H*l* & C*H₃*(*t*Bu)), 0.38 – -0.22 (m, 2 x 12 H, C*H₃*Si).

*$^{13}$C-NMR (126 MHz, chloroform-d)*: δ [ppm] = 172.5, 172.3 ($C_q$e), 151.2, 151.1, 150.1, 150.0 ($C_q$d), 135.9, 135.8, 133.2, 133.1 ($C_q$a), 129.4, 129.3, 128.6, 128.5 ($C_q$d), 122.1, 121.3 (Cc), 101.8, 101.6 (C1), 82.4, 82.3 (C4), 73.8 (C2), 71.4, 71.3 (C3), 68.9, 68.8, 66.7, 66.6 ($CH_2$(ben-zylic)), 65.5, 65.3 (C5), 34.6, 34.5 (Cf), 31.8, 29.2, 29.1, 29.0 (Ch – j), 26.1, 25.9 ($CH_3$(*t*Bu)), 25.1, 25.0, 22.7 (Hg & Hk), 18.6, 18.2 ($C_q$(*t*Bu)), 14.2 (Cl), -4.1, -4.2, -4.5, -4.8 ($CH_3$Si).
*$^{31}$P-NMR (162 MHz, chloroform-d):* δ [ppm] = 8.94, 8.40.

*IR (ATR)*: ṽ in [cm$^{-1}$] = 2953.5, 2927.7, 2856.0, 2447.9, 1759.3, 1678.5, 1608.8, 1508.6, 1463.1, 1416.9, 1377.8, 1360.7, 1252.5, 1197.2, 1166.0, 1139.6, 1105.1, 1005.3, 963.5, 920.2, 836.7, 777.1, 725.1, 671.2, 507.0.

*MS (ESI-HR)*: m/z [M+NH$_4$]$^+$ calc. for C$_{47}$H$_{83}$NO$_{11}$PSi$_2$$^+$: 924.5237, found: 924.5239.

SYNTHESIS OF 6-*N*-BUTANOYL-ADENOSINE MONOPHOSPHATE **104**:

Following GP XII, 100 mg (0.30 mmol) 6-*N*-butanoyl-adenosine **102** were dissolved in 3 mL DMF and reacted with 1.1 mL (0.33 mmol, 1.1 eq.) of a 0.3 M solution of (OFm)$_2$PA **84** in acetonitrile, and 1.5 mL (0.39 mmol, 1.3 eq.) DCI (0.25 M in acetonitrile) as well as 0.07 mL (0.37 mmol, 1.3 eq.) *t*BuOOH (5.5 M in *n*-decane). Successively, all volatile components were removed in vacuum, and the crude residue was resolved in 4 mL acetonitrile to which 0.42 mL (10 vol.%) triethylamine were added. After 12 h, 4 mL demin water were added to the reaction mixture. After further 5 h, the reaction mixture was concentrated to an ap-proximate volume of 1 mL and the mixture was purified by automated RP flash column chromatography on C$_{18}$ modified silica gel with an acetonitrile gradient in water (0% to 100%). The desired product was obtained as colorless resin and triethylammonium salt (1.3 counter ions).

*Yield*: 43 mg (0.08 mmol, 26%).

*Formula*: $C_{14}H_{18}N_5O_8P^{2-}$.

*Molecular weight*: 415.299.



*$^1$H-NMR (400 MHz, D$_2$O)*: δ [ppm] 8.72 (s, 1 H, H2), 8.69 (s, 1 H, H8), 6.26 (d, $^3J_{H,H}$ = 5.5 Hz, 1 H, H1'), 4.85 – 4.81 (m, 1 H, H2'), 4.54 (t, $^3J_{H,H}$ = 4.5 Hz, 1 H, H3'), 4.42 (p, $^3J_{H,H}$ = 3.1 Hz, 1 H, H4'), 4.27 – 4.04 (m, 2 H, H5$_a$' & H5$_b$'), 2.61 (t, $^{2,3}J_{H,H}$ = 7.4 Hz, 2 H, C$H_2$C(O)NR), 1.78 (h, $^{2,3}J_{H,H}$ = 7.4 Hz, 2 H, C$H_2$CH$_2$C(O)NR), 1.03 (t, $^{2,3}J_{H,H}$ = 7.4 Hz, 3 H, C$H_3$(alkyl)).

*$^{13}$C-NMR (151 MHz, acetonitrile-d$_3$)*: δ [ppm] = 175.8 (*C*(O)NR), 152.0 (C2), 151.8 (C6) 148.6 (C4), 142.9 (C8), 123.2 (C5), 87.4 (C1'), 84.1 (C4'), 74.5 (C2'), 70.4 (C3'), 64.4 (C5'), 38.7, 18.6 (*C*H$_2$(alkyl)), 12.8 (*C*H$_3$(alkyl)).

*$^{31}$P-NMR (162 MHz, D$_2$O):* δ [ppm] = -0.31.

*MS (ESI-HR)*: m/z [M+H]$^+$ calc. $C_{14}H_{21}N_5O_8P^+$: 418.1122, found: 418.1168.

SYNTHESIS OF 6-*N*-BUTANOYL-2'-DEOXYADENOSINE MONOPHOSPHATE **110**:

In accordance with GP XII, 104 mg (0.31 mmol) 6-*N*-butanoyl-2'-deoxyadenosine **109** were dissolved in 3.2 mL DMF and reacted with 387 mg (0.74 mmol, 2.3 eq.) (OFm)$_2$PA, **84** dissolved in 3.7 mL acetonitrile, and 1.4 mL (0.36 mmol, 1.1 eq.) DCI (0.25 M in acetonitrile) as well as 0.13 mL (0.71 mmol, 2.2 eq.) *t*BuOOH (5.5 M in *n*-decane). Successively, all volatile components were removed in vacuum, and the crude residue was resolved in 4.4 mL acetonitrile to which 0.45 mL (10 vol.%) triethylamine were added. After 12 h, 4 mL demin water were added to the reaction mixture. After further 5 h, the reaction mixture was concentrated to an approximate volume of 1 mL and the mixture was purified by automated RP flash column chromatography on C$_{18}$ modified silica gel with an acetonitrile gradient in
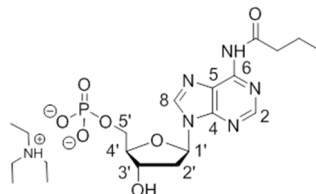
water (0% to 100%). The desired product was obtained as colorless resin and tri-
ethylammonium salt (1.3 counter ions).

*Yield*: 54 mg (0.10 mmol, 31%).

*Formula*: $C_{14}H_{18}N_5O_7P^{2-}$.

*Molecular weight*: 399.301.



$^1$*H-NMR (400 MHz, D$_2$O)*: δ [ppm] 8.64 (s, 1 H, H2), 8.61 (s, 1 H, H8), 6.57 (t, $^3J_{H,H}$ = 6.7 Hz, 1 H, H1'), 4.73 (dt, $^3J_{H,H}$ = 6.3 Hz, $^3J_{H,H}$ = 3.3 Hz, 1 H, H3'), 4.29 (qd, $^3J_{H,H}$ = 3.6 Hz, $^3J_{H,H}$ = 1.7 Hz, 1 H, H4'), 4.07 (d, $^3J_{H,H}$ = 3.7 Hz, 1 H, H5$_a$'), 4.06 (d, $^3J_{H,H}$ = 3.6 Hz, 1 H, H5$_b$'), 2.84 (ddd, $^2J_{H,H}$ = 13.6 Hz, $^3J_{H,H}$ = 7.2 Hz, $^3J_{H,H}$ = 6.0 Hz, 1 H, H2$_a$'), 2.70 – 2.60 (m, 1 H, H2$_b$'), 2.57 (t, $^{2,3}J_{H,H}$ = 7.4 Hz, 2 H, C$H_2$C(O)NR), 1.75 (h, $^{2,3}J_{H,H}$ = 7.4 Hz, 2 H, C$H_2$CH$_2$C(O)NR), 0.99 (t, $^{2,3}J_{H,H}$ = 7.4 Hz, 3 H, C$H_3$(alkyl)).

$^{13}$*C-NMR (151 MHz, acetonitrile-d$_3$)*: δ [ppm] = 175.7 (*C*(O)NR), 151.7 (C2), 151.3 (C6) 148.4 (C4), 143.0 (C8), 123.0 (C5), 86.1 (C1'), 84.1 (C4'), 71.3 (C3'), 64.6 (C5'), 39.2 (C2'), 38.7, 18.2 (*C*H$_2$(alkyl)), 12.8 (*C*H$_3$(alkyl)).

$^{31}$*P-NMR (162 MHz, D$_2$O):* δ [ppm] = -0.35.

*MS (ESI-HR)*: m/z [M-H]$^-$ calc. for $C_{14}H_{19}N_5O_7P^-$: 400.1028, found: 440.0985.

SYNTHESIS OF 6-*N*-BUTANOYL-2'-DEOXYADENOSINE-(4-OCTANOYLOXYBENZYL)-DIPHOSPHO-(1-*O*-(4-OC-
TANOYLOXYBENZYL)-2,3,-DI-*O-TERT*BUTYLDI-METHYLSILYL)-β-D-RIBOSE **111**:

According to GP XIII, 32 mg (35 μmol) (4-octanoyloxybenzyl)-(1-*O*-(4-octanoyloxybenzyl)-
2,3,-di-*O-tert*butyldimethylsilyl-β-D-ribose-5)-phosphonat **106** were dissolved in 1.8 mL ac-
etonitrile and reacted with 9 mg (71 μmol, 2 eq.) NCS. After stirring at rt for 18 h, 38 mg
(71 μmol, 2 eq.) 6-*N*-butanoyl-2'-deoxyadenosine monophosphate **110** were dissolved in
1 mL acetonitrile and added to the reaction. After 6 h, all volatile components were

removed and the crude residue was purified by automated RP flash column chromatography on $C_{18}$ modified silica gel with an acetonitrile gradient in water (0% to 100%). The desired product was obtained as colorless resin and mixture of two diastereomers.
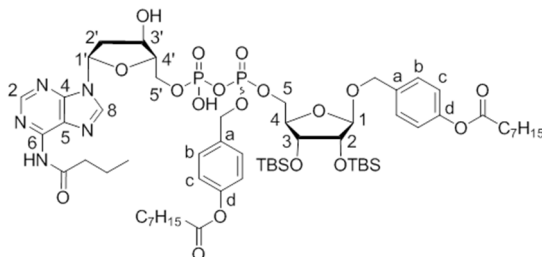
*Yield*: 12 mg
(9.3 µmol, 26%).
*Formula*:
$C_{61}H_{97}N_5O_{18}P_2Si_2$.
*Molecular weight*:
1306.582.



*$^1H$-NMR (600 MHz, acetonitrile-$d_3$)*: δ [ppm] = 8.87 (bs, 2 H, 2 x N$H$), 8.63 (2 x s, 2 H, H2), 8.56 (2 x s, 2 H. H8), 7.60 – 7.32 (m, 8 H, 4 x Hb), 7.13 – 6.91 (m, 8 H, 4 x Hc), 6.45 (t, $^3J_{H,H}$ = 6.1 Hz, 2 H, 2 x H1'), 5.16 – 5.08 (m, 2 H, C$H_2$(benzylic)), 5.02 – 4.98 (m, 4 H, 2 x H1$_{rib}$, C$H_2$(benzylic)), 4.89 (d, $^2J_{H,H}$ = 6.7 Hz, 2 H, C$H_2$(benzylic)), 4.75 – 4.62 (m, 4 H, 2 x H3$_{rib}$, C$H_2$(benzylic)), 4.50 – 4.41 (m, 2 H, C$H_2$(benzylic)), 4.18 – 4.02 (12 H, 2 x H3', 2 x H2', 2 x H2$_{rib}$, 2 x H4', 4 x H5') 3.92 (dt, $^2J_{H,H}$ = 9.3 Hz, $^2J_{H,H}$ = 4.5 Hz, 2 H, 2 x H5$_{a\ rib}$), 3.88 – 3.83 (m, 2 H, 2 x H5$_{b\ rib}$), 2.72 (t, $^3J_{H,H}$ = 7.2 Hz, 4 H, 2 x C$H_2$C(O)NR), 2.57 – 2.49 (m, 8 H, 4 x Hf), 1.76 – 1.65 (m, 12 H, C$H_2$(alkyl)), 1.63 – 1.55 (m, 12 H, C$H_2$(alkyl)), 1.42 – 1.25 (m, 36 H, C$H_2$(alkyl)), 0.98 – 0.94 (m, 18 H, C$H_3$(alkyl)), 0.93 – 0.78 (m, 36H, 12 x C$H_3$(*t*Bu)), 0.10 - -0.04 (m, 24 H, 8 x C$H_3$Si).

*$^{13}C$-NMR (151 MHz, acetonitrile-$d_3$)*: δ [ppm] = 173.3, 173.2, 173.1, 170.4, 170.3 (C$_q$(C(O)), 152.7 (C2), 151.3 (C6), 151.0, 150.1 (C$_q$d), 148.6 (C4), 143.1 (C8), 137.5, 135.9 (C$_q$a), 130.9, 130.1, 129.5, 129.4 (C$_q$d), 123.2, 122.8, 122.5, 122.3 (Cc), 102.8, 102.7 (C1$_{rib}$), 87.1 (C1'), 85.2, 84.5, 84.3, 84.2 (C4' & C4$_{rib}$), 74.5, 74.4 (C2'), 72.5, 72.3, 71.3, 71.0 (C3' & C3$_{rib}$), 69.2, 69.1, 67.4, 66.6 (C$H_2$(benzylic)), 66.0, 65.8, (C5' & C5$_{rib}$), 40.8, 40.7 (C2$_{rib}$), 39.9, 34.7, 32.4, 29.7, 29.6 (C$H_2$(alkyl)), 26.4, 26.3, 26.2 (C$H_3$(*t*Bu)), 25.6, 25.5, 24.3, 23.3, 20.3, 19.1 (C$H_2$(alkyl)), 18.9, 18.8, 18.7 (C$_q$(*t*Bu)), 14.3 , 13.7(C$H_3$(alkyl)), -4.0, -4.3, -4.4, -4.5 (C$H_3$Si).

*$^{31}P$-NMR (162 MHz, $D_2O$):* δ [ppm] = -11.5, -12.0.

*MS (ESI-HR)*: m/z [M-H] calc. for $C_{61}H_{96}N_5O_{18}P_2Si_2^-$: 1304.5770, found: 1304.5755.

SYNTHESIS OF 6-*N*-BUTANOYL-ADENOSINE-(4-OCTANOYLOXYBENZYL)-DIPHOSPHO-(1-*O*-(4-OCTANOYL-OXYBENZYL)-2,3,-DI-*O*-*TERT*BUTYLDI-METHYLSILYL)-β-D-RIBOSE **107**:

Following GP XIII, 40 mg (45 µmol) (4-octanoyloxybenzyl)-(1-*O*-(4-octanoyloxybenzyl)-2,3,-di-*O*-*tert*butyldimethylsilyl-β-D-ribose-5)-phosphonat **106** were dissolved in 2.2 mL acetonitrile and reacted with 18 mg (134 µmol, 3 eq.) NCS. After stirring at 50 °C to rt for 32 h, 32 mg (51 µmol, 1.2 eq.) 6-*N*-butanoyl-adenosine monophosphate **104** were dissolved in 1 mL DMF and added to the reaction. After 2 h, all volatile components were removed and the crude residue was attempted to purify by automated RP flash column chromatography on $C_{18}$ modified silica gel with an acetonitrile gradient in water as well as an THF gradient in water (each 0% to 100%). The product could not be separated entirely from monophosphate **104** and was thus obtained as a compound mixture and as colorless resin. The product was used directly in the next step for desilylation.

*Yield*: 11 mg (crude, [18%]).
*Formula*: $C_{61}H_{97}N_5O_{19}P_2Si_2$.
*Molecular weight*: 1322.581.



$^{31}$*P-NMR (162 MHz, D$_2$O):* δ [ppm] = -11.2, -11.3.

Experimental Part

S<small>YNTHESIS</small> <small>OF</small> 6-*N*-B<small>UTANOYL</small>-2'-<small>DESOXYADENOSINE</small>-(4-O<small>CTANOYLOXYBENZYL</small>)-<small>DIPHOSPHO</small>-(1-*O*-(4-O<small>CTANOYLOXYBENZYL</small>)-β-<small>D</small>-<small>RIBOSE</small> **113**:

12 mg (9.3μmol) 6-*N*-butanoyl-2'-desoxyadenosine-(4-Octanoyloxybenzyl)-diphospho-(1-*O*-(4-Octanoyloxybenzyl)-2,3,-di-*O*-*tert*butyldi-methylsilyl)-β-<small>D</small>-ribose **111** was dissolved in anhydrous acetonitrile and treated with 12 μL (74 μmol, 12 eq.) TEA · 3 HF (37 wt% in TEA) at rt for 20 h. Successively, all volatile components were removed and the crude residue was purified by automated RP flash column chromatography on $C_{18}$ modified silica gel with an acetonitrile gradient in water (0% to 100%). The desired product could not be separated entirely from formed monophosphate by-products and was obtained as yellowish resin.

*Yield*: 3 mg
([2.3 μmol, 25%]).
*Formula*:
$C_{49}H_{69}N_5O_{18}P_2$.
*Molecular weight*:
1078.056.



*$^{31}P$-NMR (162 MHz, $D_2O$):* δ [ppm] = -11.7, -12.0.

*MS (ESI-HR)*: m/z [M-H] calc. for $C_{49}H_{68}N_5O_{18}P_2^-$: 1076.4040, found: 1076.4180.

SYNTHESES OF CYCLIC NUCLEOTIDE MONOPHOSPHATE AB DERIVATIVES

SYNTHESIS OF 6-*N*-BUTANOYL-ADENOSINE **102**:
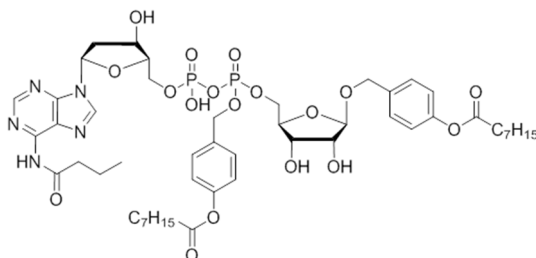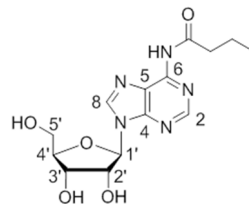
In accordance with GP X, 1.40 g (5.26 mmol) adenosine were dissolve in 34 mL pyridine/tetrahydrofuran 1:1 and converted with 2.11 mL (16.5 mmol, 3.2 eq.) TMSCl and 0.60 mL (5.78 mmol, 1.1 eq.) butyryl chloride. After 6 h of stirring at rt, 2.5 mL 1 M HCl (aq.) were added, and after 5 min more, all volatile components were removed under vacuum. Upon final purification of the crude product via automated RP flash column chromatography on $C_{18}$ modified silica gel with an acetonitrile gradient in water (0% to 100%), the product was obtained as colorless powder.

*Yield*: 1.09 g (3.22 mmol, 61%).

*Formula*: $C_{14}H_{19}N_5O_5$.

*Molecular weight*: 337.336.



*$^1$H-NMR (500 MHz, DMSO-$d_6$)*: δ [ppm] = 10.63 (s, 1 H, N*H*R), 8.69 (s, 1 H, H2), 8.65 (s, 1 H, H8), 6.01 (d, $^3J_{H,H}$ = 5.8 Hz, 1 H, H1'), 5.53 (d, $^3J_{H,H}$ = 5.8 Hz, 1 H, O*H*(H2')), 5.23 (d, $^3J_{H,H}$ = 4.8 Hz, 1 H, O*H*(H3')), 5.12 (t, $^3J_{H,H}$ = 5.6 Hz, 1 H, O*H*(H5')), 4.63 (q, $^3J_{H,H}$ = 5.4 Hz, 1 H, H2'), 4.19 (q, $^3J_{H,H}$ = 4.3 Hz, 1 H, H3'), 3.98 (q, $^3J_{H,H}$ = 3.9 Hz, 1 H, H4'), 3.76 – 3.64 (m, 1 H, H5$_a$'), 3.58 (ddd, $^2J_{H,H}$ = 11.9 Hz, $^3J_{H,H}$ = 6.1 Hz, $^3J_{H,H}$ = 4.0 Hz, 1 H, H5$_b$'), 2.55 (t, $^{2,3}J_{H,H}$ = 7.3 Hz, 2 H, C*H*$_2$C(O)NR), 1.63 (h, $^{2,3}J_{H,H}$ = 7.4 Hz, 2 H, C*H*$_2$CH$_2$C(O)NR), 0.94 (t, $^{2,3}J_{H,H}$ = 7.4 Hz, 3 H, C*H*$_3$(alkyl)).

*$^{13}$C-NMR (126 MHz, DMSO-$d_6$)*: δ [ppm] = 171.5 (*C*(O)NR), 151.7 (C6), 151.6 (C2), 149.7 (C4), 142.7 (C8), 123.9 (C5), 87.6 (C1'), 85.7 (C4'), 73.7 (C2'), 70.3 (C3'), 61.3 (C5'), 38.0, 18.2 (*C*H$_2$(alkyl)), 13.5 (*C*H$_3$(alkyl)).

*IR (ATR)*: ṽ in [cm$^{-1}$] = 3273.2, 2963.3, 2934.0, 2875.0, 1716.3, 1685.0, 1613.3, 1587.0, 1521.9, 1460.3, 1409.0, 1356.6, 1327.0, 1224.3, 1124.1, 1082.2, 1056.7, 984.6, 902.4, 866.3, 799.6, 745.0, 704.7, 643.7, 547.3.

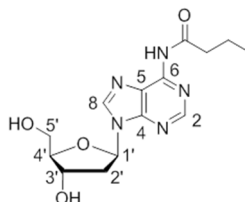*MS (ESI-HR)*: m/z [M+H]$^+$ calc. for $C_{14}H_{20}N_5O_5^+$: 338.1459, found: 338.1469.

SYNTHESIS OF 6-*N*-BUTANOYL-2'-DEOXYADENOSINE **109**:

Following GP X, 1.14 g (4.24 mmol) 2'-deoxyadenosine were dissolve in 24 mL pyridine/dichloromethane 1:2. At 0 °C, 1.13 mL (8.91 mmol, 2.1 eq.) TMSCl were added, and the reaction mixture was stirred at rt for 18 h. Successively, 0.48 mL (4.67 mmol, 1.1 eq.) butyryl chloride were added. After further 3 h of stirring at rt, TMS ethers were removed by addition of 8 mL methanol at 0 °C. After further 5 h at rt, the reaction was terminated by removing all volatile components under vacuum. The crude product was taken up in water containing little acetonitrile and purified via automated RP flash column chromatography on $C_{18}$ modified silica gel with an acetonitrile gradient in water (0% to 100%) to afford the desired product as colorless powder.

*Yield*: 0.43 g (1.35 mmol, 32%).

*Formula*: $C_{14}H_{19}N_5O_4$.

*Molecular weight*: 321.337.



$^1$*H-NMR (400 MHz, methanol-d$_4$)*: δ [ppm] = 8.66 (s, 1 H, H2), 8.62 (s, 1 H, H8), 6.61 – 6.52 (m, 1 H, H1'), 4.64 (dt, $^3J_{H,H}$ = 6.1 Hz, $^3J_{H,H}$ = 3.1 Hz, 1 H, H3'), 4.10 (q, $^3J_{H,H}$ = 3.4 Hz, 1 H, H4'), 3.88 (dd, $^2J_{H,H}$ = 12.2 Hz, $^3J_{H,H}$ = 3.4 Hz, 1 H, H5$_a$'), 3.79 (dd, $^2J_{H,H}$ = 12.2 Hz, $^3J_{H,H}$ = 3.9 Hz, 1 H, H5$_b$'), 2.88 (ddd, $^2J_{H,H}$ = 13.4 Hz, $^3J_{H,H}$ = 7.4 Hz, $^3J_{H,H}$ = 6.0 Hz, 1 H, H2$_a$'), 2.67 (t, $^{2,3}J_{H,H}$ = 7.4 Hz, 2 H, C*H*$_2$C(O)NR), 2.51 (ddd, $^2J_{H,H}$ = 13.5 Hz, $^3J_{H,H}$ = 6.2 Hz, $^3J_{H,H}$ = 3.3 Hz, 1 H, H2$_b$'), 1.82 (h, $^{2,3}J_{H,H}$ = 7.4 Hz, 2 H, C*H*$_2$CH$_2$C(O)NR), 1.08 (t, $^{2,3}J_{H,H}$ = 7.4 Hz, 3 H, C*H*$_3$(alkyl)). $^{13}$*C-NMR (101 MHz, methanol-d$_4$)*: δ [ppm] = 174.4 (*C*(O)NR), 152.9 (C2), 150.7 (C4), 144.3 (C8), 123.2 (C5), 89.7 (C1'), 86.7 (C4'), 72.7 (C3'), 63.4 (C5'), 41.5 (C2'), 39.9, 19.6 (*C*H$_2$(alkyl)), 14.0 (*C*H$_3$(alkyl)).

*IR (ATR)*: ṽ in [cm$^{-1}$] = 3336.8, 2964.6, 2933.1, 2875.3, 2592.1, 2330.9, 1682.2, 1612.5.1585.9, 1522.5, 1459.6, 1402.8, 1354.8, 1329.2, 1223.8, 1093.3, 1058.5, 993.8, 941.1, 867.1, 799.6, 749.6, 984.8, 644.4, 585.3, 561.2, 542.4, 527.4, 509.6, 464.7.

*MS (ESI-HR)*: m/z [M+H]$^+$ calc. for $C_{14}H_{20}N_5O_4^+$: 322.1510, found: 322.1521.

SYNTHESIS OF 2-*N*-BUTANOYL-GUANOSINE **117**:

According to GP X, 1.55 g (5.48 mmol) guanosine were co-evaporated with pyridine three times and then dissolved in 81 mL pyridine/dichloromethane 1:2. At 0 °C, 6.28 mL (49.4 mmol, 9 eq.) TMSCl were added, and the reaction mixture was stirred at rt for 4 h. Successively, 0.62 mL (6.03 mmol, 1.1 eq.) butyryl chloride were added. After 3 h stirring at rt, the cleavage of TMS ethers was induced by addition of 27 mL MeOH, and after further 12 h at rt, the reaction was terminated and all volatile components were removed under vacuum. The crude residue was taken up in water containing little acetonitrile and purified via automated RP flash column chromatography on $C_{18}$ modified silica gel with an acetonitrile gradient in water (0% to 100%) to afford the desired product as colorless powder.

*Yield*: 0.92 g (2.61 mmol, 48%).

*Formula*: $C_{14}H_{19}N_5O_6$.

*Molecular weight*: 353.335.



*$^1$H-NMR (400 MHz, DMSO-d$_6$)*: δ [ppm] = 12.07 (bs, 1 H, N*H*R), 11.71 (bs, 1 H, N*H*), 8.26 (s, 1 H, H8), 5.80 (d, *J* = 5.7 Hz, 1 H, H1'), 5.47 (d, $^3J_{H,H}$ = 5.7 Hz, 1 H, O*H*(H2')), 5.17 (d, $^3J_{H,H}$ = 4.5 Hz, 1 H, O*H*(H3')), 5.03 (t, $^3J_{H,H}$ = 5.4 Hz, 1 H, O*H*(H5')), 4.43 (d, $^3J_{H,H}$ = 5.2 Hz, 1 H, H2'), 4.20 − 4.05 (m, 1 H, H3'), 3.90 (q, *J* = 3.9 Hz, 1 H, H4'), 3.64 (dt, $^2J_{H,H}$ = 11.9 Hz, $^3J_{H,H}$ = 4.8 Hz, 1 H, H5$_a$'), 3.55 (dt, $^2J_{H,H}$ = 11.9 Hz, $^3J_{H,H}$ = 4.7 Hz, 1 H, H5$_b$'), 2.45 (t, $^{2,3}J_{H,H}$ = 7.3 Hz, 2 H, C*H$_2$*C(O)NR), 1.62 (h, $^{2,3}J_{H,H}$ = 7.4 Hz, 2 H, C*H$_2$*CH$_2$C(O)NR), 0.92 (t,

$^{2,3}J_{H,H}$ = 7.5 Hz, 3 H, C$H_3$(alkyl)).

$^{13}$*C-NMR (101 MHz, DMSO-d$_6$)*: δ [ppm] = 176.2 (*C*(O)NR), 154.8 (C6), 148.8 (C4), 148.0 (C2), 137.6 (C8), 120.1 (C5), 86.6 (C1'), 85.3 (C4'), 73.9 (C2'), 70.2 (C3'), 61.1 (C5'), 37.8, 17.9 (*C*H$_2$(alkyl)), 13.4 (*C*H$_3$(alkyl)).

*IR (ATR)*: ṽ in [cm$^{-1}$] = 3364.4, 3279.5, 2968.3, 2941.1, 1680.2, 1608.8, 1564.3, 1554.1, 1536.0, 1481.4, 1469.2, 1449.9, 1402.5, 1251.7, 1204.2, 1179.4, 1127.9, 1089.0, 1060.2, 993.3, 976.4, 901.1, 863.3, 818.6, 801.0, 762.7, 737.4, 717.0, 680.4, 643.7, 607.0, 589.1, 562.3, 510.2, 484.2.

*MS (ESI-HR)*: m/z [M+H]$^+$ calc. for C$_{14}$H$_{19}$N$_5$O$_6$$^+$: 354.1408, found: 354.1400.
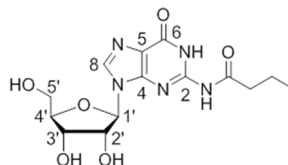
SYNTHESIS OF URIDINE-3',5'-(4-OCTANOYLOXYBENZYL)-CYCLOPHOSPHATE **115**:

According to GP XI, 26 mg (0.11 mmol) uridine were dissolved in 2 mL DMF and reacted with 57 mg (0.12 mmol, 1.1 eq.) (OB)PA$_2$ **101**, dissolved in 2.5 mL acetonitrile, in the presence of 0.54 mL (0.13 mmol, 1.3 eq.) DCI (0.25 M in acetonitrile) and 0.45 mL (0.13 mmol, 1.3 eq.) BTT (0.3 M in acetonitrile). The addition of 32 µL (0.16 mmol, 1.5 eq.) *t*BuOOH (5.5 M in *n*-decane) followed successively. After purification by automated RP flash column chromatography on C$_{18}$ modified silica gel with an acetonitrile gradient in water (0% to 100%) and lyophilization, the product was obtained as colorless cotton and in two fractions containing each of the stereoisomers.

*Yield*: 11 mg (0.02 mmol, 19%).

*Formula*: $C_{24}H_{31}N_2O_{10}P$.

*Molecular weight*: 538.490.
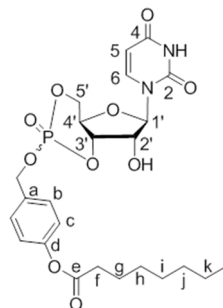
$^1$*H-NMR (400 MHz, methanol-d$_4$)*: δ [ppm] = 7.66 – 7.51 (m, 2 H, Hb), 7.47 (d, $^3J_{H,H}$ = 8.1 Hz, 1 H, H5), 7.22 – 7.08 (m, 2 H, Hb), 5.69 (d, $^3J_{H,H}$ = 8.0 Hz, 1 H, H6), 5.64 (d, $^3J_{H,H}$ = 0.9 Hz, 1 H, H1'), 5.24 – 5.14 (m, 2 H, C*H*$_2$(benzylic)), 4.64 (ddd, $^3J_{H,P}$ = 22.5 Hz, $^2J_{H,H}$ = 9.3 Hz, $^3J_{H,H}$ = 4.6 Hz, 1 H, H5$_a$'), 4.39 (ddd, $^3J_{H,H}$ = 10.2, $^2J_{H,H}$ = 9.4, $^3J_{H,H}$ = 0.8 Hz, 1 H, H5$_b$'), 4.35 – 4.25 (m, 2 H, H2' & H3'), 4.25 – 4.10 (m, 1 H, H4'), 2.58 (t, $^{2,3}J_{H,H}$ = 7.4 Hz, 2 H, Hf), 1.73 (p, $^{2,3}J_{H,H}$ = 7.4 Hz, 2 H, Hg), 1.53 – 1.22 (m, 8 H, Hh - Hk), 1.05 – 0.82 (m, 3 H, Hl)

and

7.63 (d, $^3J_{H,H}$ = 8.1 Hz, 1 H, H5), 7.53 – 7.47 (m, 2 H, Hb), 7.19 – 7.10 (m, 2 H, Hc), 5.73 (d, $^3J_{H,H}$ = 1.2 Hz, 1 H, H1'), 5.71 (d, $^3J_{H,H}$ = 8.1 Hz, 1 H, H6), 5.19 (d, $^2J_{H,H}$ = 8.7 Hz, 2 H, C*H*$_2$(benzylic)), 4.81 (ddd, $^3J_{H,P}$ = 9.8 Hz, $^3J_{H,H}$ = 5.1 Hz, $^3J_{H,H}$ = 1.0 Hz, 1 H, H3'), 4.67 (ddd, $^3J_{H,P}$ = 14.2 Hz, $^2J_{H,H}$ = 9.2 Hz, $^3J_{H,H}$ = 5.5 Hz, 1 H, H5$_a$'), 4.62 – 4.47 (m, 2 H, H2' & H4'), 4.42 (td, $^2J_{H,H}$ = 10.1, $^3J_{H,H}$ = 5.5 Hz, 1 H, H5$_b$'), 2.60 (t, $^{2,3}J_{H,H}$ 7.4 Hz, 2 H, Hf), 1.74 (p, $^{2,3}J_{H,H}$ 7.4 Hz, 2 H, Hg), 1.50 – 1.26 (m, 8 H, Hh – Hk), 1.02 – 0.84 (m, 3 H, Hl).

$^{13}$*C-NMR (101 MHz, methanol-d$_4$)*: δ [ppm] = 173.8 (C$_q$e), 165.9 (C4), 151.5 (C$_q$d), 150.1 (C2) 143.7 (C5), 134.3 (C$_q$a), 131.2 (Cb), 123.3 (Cc), 103.0 (C6), 97.5 (C1'), 80.1 (C3'), 72.4 (C2'), 71.5 (C4'), 71.2(C5'), 70.3 (C*H*$_2$(benzylic)), 35.0 (Cf), 32.9, 30.2, 30.1, 25.0, 23.7 (Cg – k), 14.4 (Cl).

and

172.8 (C$_q$e), 164.9 (C4), 151.7 (C$_q$d), 150.5 (C2 ), 143.5 (C5), 133.0 (C$_q$a), 130.2 (Cb), 122.8 (Cc), 103.1 (C6), 97.7 (C1'), 79.3 (C3'), 72.4 (C2'), 71.2 (C4'), 71.1 (C*H*$_2$(benzylic)), 70.6 (C5'),

35.0 (Cf), 32.8, 30.2, 30.1, 26.0, 23.7 (Cg – k), 14.4 (Cl).

$^{31}P$-NMR (162 MHz, methanol-$d_4$): δ [ppm] = --3.93, -5.01.

MS (ESI-HR): m/z [M+Na]$^+$ calc. for $C_{24}H_{31}N_2O_{10}PNa^+$: 561.1609, found: 561.1445.

SYNTHESIS OF ADENOSINE-3′,5′-(4-OCTANOYLOXYBENZYL)-CYCLOPHOSPHATE **118**:

Following GP XI, 21 mg (78 μmol) adenosine were dissolved in 2 mL DMF and treated with a solution of 41 mg (85 μmol, 1.1 eq.) (OB)PA$_2$ **101** in 2 mL acetonitrile as well as 0.74 mL (0.19 mmol, 2.4 eq.) DCI (0.25 M in acetonitrile). Lastly, 23 μL (0.12 mmol, 1.5 eq.) $t$BuOOH (5.5 M in $n$-decane) were added for oxidation.

After purification by automated RP flash column chromatography on $C_{18}$ modified silica gel with an acetonitrile gradient in water (0% to 100%) and lyophilization, the product was obtained as a colorless cotton and mixture of two diastereomers.

Yield: 5 mg (10 μmol, 12%).

Formula: $C_{25}H_{32}N_5O_8P$.

Molecular weight: 561.5318.
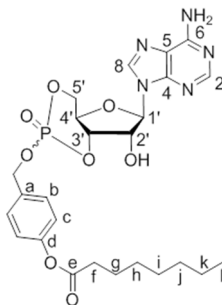


$^1H$-NMR (400 MHz, acetonitrile-$d_3$): δ [ppm] = 8.19, 8.09 (2 x s, 1 H, H2), 7.93, 7.88 ( 2x s, 1 H, H8), 7.55 – 7.46, 7.45 – 7.41 (2 x m, 2 H, Hb), 7.12 – 7.02 (m, 4 H, 2 x Hc), 5.99 (bs, 4 H, 2 x N$H_2$), 5.98, 5.93 (2 x s, 1 H, H1′), 5.47 (dd, $^3J_{H,P}$ = 9.1 Hz, $^3J_{H,H}$ = 5.1 Hz, 1 H, H3′), 5.27 (ddd, $^3J_{H,P}$ = 9.4 Hz, $^3J_{H,H}$ = 4.9 Hz, $^3J_{H,H}$ = 1.0 Hz, 1 H, H3′), 5.19 (ddd, $^3J_{H,P}$ = 9.3 Hz, $^3J_{H,H}$ = 5.0 Hz, $^3J_{H,H}$ = 1.6 Hz, 1 H, H3′), 5.14 – 5.06 (m, 4 H, 2 x C$H_2$(benzylic)), 4.72 (d, $^3J_{H,H}$ = 4.9 Hz, 1

H, H4'), 4.60 (d, $^3J_{H,H}$ = 5.1 Hz, 1 H, H4'), 4.58 – 4.14 (m, 6 H, 2 x H2', 2 x H5$_a$', 2 x H5$_b$'), 2.50 (2 x t, $^3J_{H,H}$ = 7.5 Hz, 4 H, Hf), 1.64 (h, $^3J_{H,H}$ = 7.6 Hz, 4 H, 2 x Hg), 1.47 – 1.14 (m, 16 H, Hh-k), 0.89 – 0.78 (m, 6 H, 2x Hl).

$^{13}$C-NMR (151 MHz, acetonitrile-$d_3$): δ [ppm] = 173.3 (C$_q$e), 156.9 (C6), 153.9 (C2), 151.3 (C$_q$d), 149.4 (C4), 140.9 (C8), 133.3 (2 x C$_q$a), 130.6, 130.7 (Cc), 123.1 (Cb), 119.8 (C5), 93.6 (C1'), 81.0 (C3'), 72.7 (C4'), 71.5 (C5'), 69.4 (CH$_2$(benzylic)), 34.7 (Cf), 32.4, 29.6, 25.5, 23.3, 20.1 (Cg – k), 14.3 (Cl).

$^{31}$P-NMR (162 MHz, acetonitrile-$d_3$): δ [ppm] = -4.37, -6.03.

MS (ESI-HR): m/z [M+H]$^+$ calc. for C$_{25}$H$_{33}$N$_5$O$_8$P$^+$: 562.2061, found: 562.2068.

SYNTHESIS OF 6-N-BUTANOYL-ADENOSINE-3',5'-(4-OCTANOYLOXYBENZYL)-CYCLOPHOSPHATE **119**:

According to GP XI, 48 mg (0.14 mmol) 6-N-butanoyl-adenosine **102** were dissolved in 4 mL DMF and treated with a solution of 76 mg (0.16 mmol, 1.1 eq.) (OB)PA$_2$ **101** in 4 mL acetonitrile and 0.97 mL (0.24 mmol, 1.7 eq.) DCI (0.25 M in acetonitrile) as well as 0.62 mL (0.19 mmol, 1.3 eq.) BTT (0.3 M in acetonitrile). Then, 43 μL (0.21 mmol, 1.5 eq.) tBuOOH (5.5 M in n-decane) were added. After purification by automated RP flash chromatography on C$_{18}$ modified silica gel with an acetonitrile gradient in water (0% to 100%), the product was obtained as colorless cotton and mixture of two diastereomers.

Yield: 13 g (0.02 mmol, 14%).
Formula: C$_{29}$H$_{38}$N$_5$O$_9$P.
Molecular weight: 631.623.
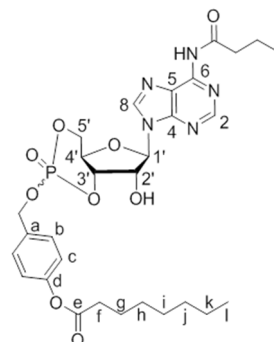
*1H-NMR (400 MHz, methanol-d4)*: δ [ppm] = 8.68, 8.58 (2 x s, 1 H, H2), 8.49, 8.38 ( 2x s, 1 H, H8), 7.62 – 7.56, 7.55 – 7.49 (2 x m, 2 H, Hb), 7.17 – 7.12, 7.13 – 7.06 (2 x m, 2 H, Hc), 6.20, 6.12 (2 x s, 1 H, H1'), 5.47 (dd, $^3J_{H,P}$ = 9.1 Hz, $^3J_{H,H}$ = 5.1 Hz, 1 H, H3') 5.23 (2 x d, $^2J_{H,H}$ = 10.4 Hz & 8.1 Hz, 2 H, C$H_2$(benzylic)), 5.05 (ddd, $^3J_{H,P}$ = 9.6 Hz, $^3J_{H,H}$ = 5.1 Hz, $^3J_{H,H}$ = 1.6 Hz, 1 H, H3'), 4.89 – 4.86 (m, 1 H, H2'), 4.73 – 4.34 (m, 7 H, H2', 2 x H4', 2 x H5a', 2 x H5b'), 2.71 – 2.55 (m, 6 H, 2 x C$H_2$C(O)NR & Hf), 2.51 (t, $^{2,3}J_{H,H}$ = 7.4 Hz, 2 H, Hf), 1.86 – 1.70 (m, 6 H, 2 x C$H_2$CH2C(O)NR, 2 x Hg), 1.68 – 1.57 (m, 2 H, Hg), 1.53 – 1.25 (m, 16 H, 2 x Hh – k), 1.05 (2 x t, $^{2,3}J_{H,H}$ = 7.4 Hz, 6 H, C$H_3$(alkyl)), 0.98 – 0.95 (m, 6 H, 2x Hl).

*13C-NMR (151 MHz, methanol-d4)*: δ [ppm] = 173.8 (*C*(O)NR), 173.6 (Cqe), 152.8 (Cqd), 152.4 (C2), 150.8 (C6), 143.1 (C8), 133.3, 133.2 (2 x Cqa), 130.7, 130.6 (Cc), 124.5 (C5), 123.1, 123.0 (Cb), 88.8 (C1'), 81.7 (C4'), 80.4 (C2'), 69.3, 69.2 (*C*H2(benzylic)), 68.5 (C3'), 59.8 (C5'), 39.9 (*C*H2C(O)NR), 34.5 (Cf), 31.8, 29.2, 29.1, 25.0, 22.8, 18.5 (Cg – k & *C*H2(alkyl)),14.2 (Cl), 13.9 (*C*H3(alkyl)).

*31P-NMR (162 MHz, methanol-d4)*: δ [ppm] = -3.80, -4.90.

MS (ESI-HR): m/z [M+H]+ calc. for C29H39N5O9P+: 632.2848, found: 632.2848.

SYNTHESIS OF 6-*N*-BUTANOYL-2'-DEOXYADENOSINE-3',5'-(4-OCTANOYLOXYBENZYL)-CYCLOPHOSPHATE **120**:

According to GP XI, 50 mg (0.15 mmol) 6-*N*-butanoyl-2'deoxyadenosine **109** were dissolved in 4 mL DMF and reacted with 82 mg (0.17 mmol, 1.1 eq.) (OB)PA2 **101**, dissolved in 4.3 mL acetonitrile, in the presence of 1.60 mL (0.40 mmol, 2.6 eq.) DCI (0.25 M in acetonitrile) in total and 50 µL (0.25 mmol, 1.6 eq.) *t*BuOOH (5.5 M in *n*-decane). After purification by automated RP flash column chromatography on C18 modified silica gel with an acetonitrile gradient in water (0% to 100%) and lyophilization, the product was obtained as colorless cotton and mixture of two diastereomers.

*Yield*: 12 mg (0.02 mmol, 13%).

*Formula*: $C_{29}H_{38}N_5O_8P$.

*Molecular weight*: 615.624.
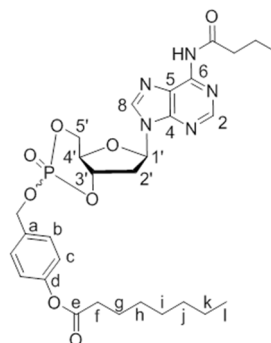
*¹H-NMR (400 MHz, methanol-d₄)*: δ [ppm] = 8.69 (s, 1 H, H2), 8.61 (s, 1 H, H8), 8.47 (s, 1 H, H2), 8.37 (s, 1 H, H8), 7.65 – 7.57, 7.55 – 7.48 (2 x m, 2 H, Hb), 7.19 – 7.10 (m, 4 H, Hc), 6.59 (dd, $^3J_{H,H}$ = 9.0 Hz, $^3J_{H,H}$ = 2.0 Hz, 1 H, H1'), 6.55 (dd, $^3J_{H,H}$ = 6.7 Hz, $^3J_{H,H}$ = 4.0 Hz, 1 H, H1'), 5.64 (q, $^3J_{H,H/P}$ = 9.2 Hz, 1 H, H3'), 5.33 (q, $^3J_{H,H/P}$ = 9.2 Hz, 1 H, H3'), 5.23 (2 x d, $^2J_{H,H}$ = 13.1 Hz & $^3J_{H,H}$ = 12.9 Hz, 4 H, C*H₂*(benzylic)), 4.70 – 4.40 (m, 4 H, 2 x H5$_{a,b}$'), 4.22 (td, $^3J_{H,H}$ = 9.9 Hz, $^3J_{H,H}$ = 5.6 Hz, 1 H, H4'), 4.08 (td, $^3J_{H,H}$ = 9.9 Hz, $^3J_{H,H}$ = 4.7 Hz, 1 H, H4'), 2.98 (ddd, $^2J_{H,H}$ = 13.1 Hz, $^3J_{H,H}$ = 7.7 Hz, $^3J_{H,H}$ = 1.9 Hz, 1 H, H2$_a$'), 2.83 – 2.70 (m, 3 H, H2$_{a,b}$'), 2.69 – 2.57 (m, 6 H, 2 x C*H₂*C(O)NR & Hf), 2.54 (t, $^{2,3}J_{H,H}$ = 7.4 Hz, 2 H, Hf), 1.90 – 1.70 (m, 6 H, C*H₂*CH₂C(O)NR, 2 x Hg), 1.66 (q, $^{2,3}J_{H,H}$ = 7.3 Hz, 2 H, C*H₂*CH₂C(O)NR), 1.51 – 1.26 (m, 16 H, Hh - k), 1.06 (2 x t, $^{2,3}J_{H,H}$ = 7.4, 6 H, C*H₃*(alkyl)), 0.98 – 0.86 (m, 6 H, 2 x Hl).

*¹³C-NMR (101 MHz, methanol-d₄)*: δ [ppm] = 174.5, 174.4 (2 x *C*(O)NR), 173.8, 173.6 (2 x C$_q$e), 153.4, 153.2 (2 x C2), 152.8, 152.7(2 x C$_q$d), 152.4, 152.3 (2 x C6), 150.8, 150.7 (2 x C4), 144.6, 144.5 (2 x C8), 134.4, 134.3 (2 x C$_q$a), 131.1, 130.7 (2 x Cc), 123.2, 123.1 (2 x Cb), 122.6 (C5), 85.8, 85.6 (2 x C1'), 79.3, 79.2 (2 x C3'), 75.7, 75.6 (2 x C4'), 71.7, 71.6 (2 x C5'), 71.4, 71.3 (2 x C*H₂*(benzylic)), 40.0, 39.9 (2 x C*H₂*C(O)NR), 35.0 (C2'), 34.9 (Cf), 32.8, 30.1, 30.0, 25.9, 25.9, 23.7, 19.7, 19.6 (Cg – k & C*H₂*(alkyl)), 14.4, 14.1, 14.0 (Cl, C*H₃*(alkyl)).

*³¹P-NMR (162 MHz, methanol-d₄)*: δ [ppm] = -4.14, -5.50.

*MS (ESI-HR)*: m/z [M+H]⁺ calc. for $C_{29}H_{39}N_5O_8P^+$: 616.2531, found: 616.2534.

SYNTHESIS OF 2-*N*-BUTANOYL-GUANOSINE-3',5'-(4-OCTANOYLOXYBENZYL)-CYCLOPHOSPHATE **121**:

In accordance with GP XI, 52 mg (0.15 mmol) 6-*N*-butanoyl-guanosine **117** were dissolved in 4 mL DMF and treated with a solution of 77 mg (0.16 mmol, 1.1 eq.) (OB)PA$_2$ **101** in 4 mL acetonitrile, 1.75 mL (0.44 mmol, 3 eq.) DCI (0.25 M in acetonitrile) in total and finally, 44 µL (0.21 mmol, 1.5 eq.) *t*BuOOH (5.5 M in *n*-decane). After purification by automated RP flash column chromatography on C$_{18}$ modified silica gel with an acetonitrile gradient in water (0% to 100%) and lyophilization, the product was obtained as colorless cotton and a single diastereomer.
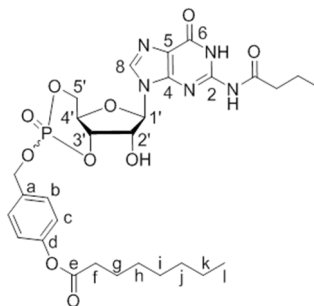
*Yield*: 4 mg (5.6 µmol, 4%).

*Formula*: C$_{29}$H$_{38}$N$_5$O$_{10}$P.

*Molecular weight*: 647.622.

*$^1$H-NMR (400 MHz, methanol-d$_4$)*: δ [ppm] = 7.92 (s, 1 H, H8), 7.56 (d, $^3J_{H,H}$ = 8.2 Hz, 2 H, Hb), 7.07 (d, $^3J_{H,H}$ = 8.3 Hz, 2 H, Hc), 6.01 (s, 1 H, H1'), 5.23 (d, $^2J_{H,H}$ = 11.6 Hz, 2 H, C$H_2$(benzylic)), 4.69 (ddd, $^3J_{H,H}$ = 22.2 Hz, $^3J_{H,P}$ = 9.4 Hz, $^3J_{H,H}$ = 4.8 Hz, 1 H, H5'$_b$), 4.55 (t, $^3J_{H,H}$ = 10.0 Hz, 1 H, H5'$_a$), 4.35 (dd, $^3J_{H,H}$ = 10.0 Hz, $^3J_{H,H}$ = 4.8 Hz, 1 H, H4'), 4.32 (d, $^3J_{H,H}$ = 4.7 Hz, 1 H, H2'), 4.18 (dd, $^3J_{H,P}$ = 9.9 Hz, $^3J_{H,H}$ = 4.7 Hz, 1 H, H3'), 2.51 (t, $^{2,3}J_{H,H}$ = 7.4 Hz, 2 H, C$H_2$C(O)NR), 2.46 (t, $^{2,3}J_{H,H}$ = 7.1 Hz, 2 H, Hf), 1.74 (h, $^{2,3}J_{H,H}$ = 7.4 Hz, 2 H, C$H_2$CH$_2$C(O)NR), 1.62 (t, $^{2,3}J_{H,H}$ = 7.1 Hz, 2 H, Hg), 1.49 – 1.25 (m, 8 H, Hh – k), 1.02 (t, $^{2,3}J_{H,H}$ = 7.4 Hz, 3 H, C$H_3$(alkyl)), 0.98 – 0.86 (m, 3 H, Hl).

*$^{13}$C-NMR (101 MHz, methanol-d$_4$)*: δ [ppm] = 177.7 (*C*(O)NR), 173.6 (C$_q$e ), 152.2 (C$_q$d), 150.0 (C4), 149.8 (C2), 137.5 (C8), 134.4 (C$_q$a), 131.4 (Cc), 123.3 (Cb), 120.2 (C5), 93.4 (C1'), 80.3 (C3'), 73.3 (C2'), 71.6 (C5'), 71.5 (C4'), 70.5 (*C*H$_2$(benzylic)), 39.4 (*C*H$_2$C(O)NR), 34.8 (Cf), 32.9, 30.1, 25.8, 23.7, 19.3 (Cg – k & *C*H$_2$(alkyl)), 14.4 (Cl), 13.9 (*C*H$_3$(alkyl)).

*31P-NMR (162 MHz, methanol-d4)*: δ [ppm] = --4.93.

*MS (ESI-HR)*: m/z [M+H]+ calc. for $C_{29}H_{39}N_5O_{10}P^+$: 648.2429, found: 648.2720.

## 9.3. Compound evaluation methods

FE(III) COORDINATION CAS ASSAY:

Preparation of the CAS assay solutions was performed as reported by Schwyn and Neilands.[73] The CAS solution (115 µL, 15 µM Fe(III), 150 µM Chromeazurol S) was mixed with 115 µL of a solution containing the potential siderophore (the siderophore-type pro-drugs or reference compounds) (150 µM, DMSO/Water 0.02:1)). This solution was immediately transferred to a cuvette and the absorption at 630 nm measured at several time points.

ANTIBACTERIAL ACTIVITY ASSAYS:

Evaluation of the antibacterial activity of the compounds using Staphylococcus aureus subsp. aureus (Newman strain), Bacillus subtilis subsp. subtilis, Pseudomonas aeruginosa PAO1, Escherichia coli K12, E. coli TolC, and E. coli D22 strains was performed as described in the literature.[38,40] Iron-deficient and iron-rich conditions were attained by the addition of either 2,2'-bipyridine (100 µM) or FeCl3 (100 µM) respectively to Luria Broth (LB) growth medium.[57] Given percent of growth inhibition or minimal inhibitory concentrations (MICs) are means of two independent determinations.

PREPARATION OF ESCHERICHIA COLI LYSATE:

A fresh E. coli K12 culture with an OD600 of 0.8 was prepared and centrifuged. The pellet was washed twice with PBS followed by resuspension with two weight volumes of PBS. Bacterial cells were broken on ice by ultrasonication (6 x 10 s cycles with 5 s breaks). Either this crude lysate was used directly for incubations or, in parallel, the supernatant of centrifuged lysate. Tubes with lysate were always kept on ice. Before storage at -80 °C tubes were shock frozen in liquid nitrogen. The presence of esterase activity in the lysate was confirmed by demonstrating the concentration dependent hydrolyzation of β-naphthyl acetate to β-naphthol. Fluorescence intensities were measured in a CLARIOstar platereader (BMG LABTECH GmbH, Ortenberg, Germany) with excitation at 320 nm and an emission wavelength of 410 nm.

LC-MS/MS BASED STABILITY DETERMINATIONS:

Solutions of of the siderophore prodrugs (20 μM) were incubated in E. coli K12 lysate for different periods of time (0 min, 15 min, 2 h and 5 h) at 37 °C. Reactions were stopped by using acetonitrile. Two volumes of ethyl acetate (+ 0.1 % formic acid) were used to extract the compounds. As internal standard we used an in house compound with structural similarity to compounds **5** and **6**. Measurements were performed employing an UHPLC (Ultimate 3000)-MS/MS (TSQ Quantum Access Max) system (Thermo Scientific, Waltham, MA, USA) using Gravity and Accucore columns. Calibration curves were produced for the parent compounds **5** and **6** (lowest calibrator at 200 nM) and used for quantification of hydrolyzed prodrugs.

FRET-SENSOR BASED LIVE CELL IMAGING ASSAYS:

Primary mouse ventricular cardiomyocytes were isolated from Epac1-camps biosensor expressing transgenic mice and plated onto laminin coated glass cover slides. Measurements were performed 1 – 2 h after plating using a Nikon Ti microscope based FRET imaging system containing pE-100 440 nm light source (CoolLED), DV2 Dual View and ORCA-03G charge-coupled device camera (Hamamatsu), and analyzed. Cells were kept in a buffer containing 144 mM NaCl, 5.4 mM KCl, 1 mM $MgSO_4$, 1 mM $CaCl_2$, 10 mM Hepes (pH 7.3) and stimulated with OB-cNMPs dissolved 1:1000 in the same buffer from a freshly made 20 mM DMSO stock solution.

cNMP-DRIVEN $Ca^{2+}$ MOBILIZATION ASSAYS:

Jurkat T cells were incubated with the membrane-permeable AM ester of the $Ca^{2+}$ dye Fura-2 (4 μM, Calbiochem). Therefore, about $2 \times 10^6$ cells were centrifuged at 500 g for 5 min and resuspended in 1 mL of freshly supplemented RPMI medium containing Fura-2 AM. Cells were incubated for 30 min at 37 °C. After centrifugation, cells were washed and resuspended in $Ca^{2+}$ buffer [140 mM NaCl, 5 mM KCl, 1 mM $MgSO_4$, 1 mM $CaCl_2$, 20 mM Hepes (pH 7.4), 1 mM $NaH_2PO_4$, 5 mM glucose] and kept for 20 min at room-temperature (RT) for deesterification. Cells were added on prepared coverslips and allowed to adhere before measurement. Slides were mounted onto a Leica IRBE microscope (100-fold

magnification) and after 120s the respective OB-cNMPs (20 μM) or DMSO (as control) were added. As positive control, Thapsigagarin (1.67 μM, Calbiochem) was added after 900 s. A Sutter DG-4 was used as a light source, and frames were acquired with an electron-multiplying charge-coupled device camera (C9100-13, Hamamatsu). Images (512 × 512 pixels) were acquired in 16-bit mode with the following filter sets (AHF Analysentechnik) [excitation (ex), beam splitter (bs), and emission (em), all in nanometers]: Fura-2 (ex, HC 340/26, HC 387/11; bs, 400DCLP; em, 510/84).

## 10. Bibliography

(1)     World Economic Forum. *Global Risks 2013 Eighth Edition*; 2013.

(2)     World Health Organization. *Antimicrobial Resistance Global Report on Surveillance*; 2014.

(3)     World Economic Forum. *Global Risks 2015 10th Edition*; 2015.

(4)     Smith, R. D.; Coast, J. Antimicrobial Resistance: A Global Response. *Bull. World Health Organ.* **2002**, *80* (2), 126–133.

(5)     Blair, J. M. A.; Webber, M. A.; Baylay, A. J.; Ogbolu, D. O.; Piddock, L. J. V. Molecular Mechanisms of Antibiotic Resistance. *Nat. Rev.* **2014**, *13* (1), 42–51.

(6)     World Health Organization. Worldwide Country Situation Analysis: Response to Antimicrobial Resistance. **2015**.

(7)     Levy, S. B.; Marshall, B. Antibacterial Resistance Worldwide: Causes , Challenges and Responses. *Nat. Med.* **2004**, *10* (12), 122–129.

(8)     Coast, J.; Smith, R. D.; Millar, M. R. Superbugs: Should Antimicrobial Resistance Be Included as a Cost in Economic Evaluation? *Health Econ.* **1996**, *5*, 217–226.

(9)     Brown, E. D.; Wright, G. D. Antibacterial Drug Discovery in the Resistance Era. *Nature* **2016**, *529*, 336–343.

(10)    Costa, V. M. D.; King, C. E.; Kalan, L.; Morar, M.; Sung, W. W. L.; Schwarz, C.; Froese, D.; Zazula, G.; Calmels, F.; Debruyne, R.; et al. Antibiotic Resistance Is Ancient. *Nature* **2011**, *477*, 457–461.

(11)    Forsberg, K. J.; Reyes, A.; Wang, B.; Selleck, E. M.; Sommer, M. O. A.; Dantas, G. The Shared Antibiotic Resistome of Soil Bacteria and Human Pathogen. *Science (80-. ).* **2012**, *337*, 1107–1112.

Bibliography

(12)     Perry, J. A.; Westman, E. L.; Wright, G. D. The Antibiotic Resistome: What' s New? *Curr. Opin. Microbiol.* **2014**, *21*, 45–50.

(13)     CDC. *Antibiotic Resistance Threats in the United States, 2013*; 2013.

(14)     Silver, L. L. Challenges of Antibacterial Discovery. *Clin. Microbiol. Rev.* **2011**, *24* (1), 71–109.

(15)     Lewis, K. Platforms for Antibiotic Discovery. *Nat. Rev. Drug Discov.* **2013**, *12*, 371–387.

(16)     Levy, S. B. Microbial Resistance to Antibiotic: An Evolving and Persistent Problem. *Lancet* **1982**, 83–88.

(17)     Barber, M.; Rozwadowska-dowzenko, M. Infection by Penicillin-Resistant Staphylococci. *Lancet* **1948**, *2*, 641–644.

(18)     Watanabe, T. Infective Heredity of Multiple Drug Resistance in Bacteria. *Baceriology Rev.* **1963**, *27*, 87–115.

(19)     Amábile-Cuevas, C. F. Regional Review Antibiotic Resistance in Mexico: A Brief Overview of the Current Status and Its Causes. *J. Infect. Dev. Ctries.* **2010**, *4* (3), 126–131.

(20)     Elwell, L. P.; Roberts, M.; Mayer, L. W.; Falkow, S. Plasmid-Mediated Beta-Lactamase Production in Neisseria Gonorrhoeae. *Antimicrob. Agents Chemother.* **1977**, *11* (3), 528–533.

(21)     Graaff, J. D. E.; Elwell, L. P.; Falkow, S. Molecular Nature of Two Beta-Lactamase-Specifying Plasmids Isolated from Haemophilus Influenzae Type B. *J. Bacteriol.* **1976**, *126* (1), 439–446.

(22)     Boucher, H. W.; Talbot, G. H.; Bradley, J. S.; Edwards, J. E.; Gilbert, D.; Rice, L. B.; Scheld, M.; Spellberg, B.; Bartlett, J. Bad Bugs , No Drugs: No ESKAPE! An Update from the Infectious Diseases Society of America. *Clin. Infect. Dis.* **2009**, *48*, 1–12.

251

Bibliography

(23)     Weinstein, R. A. Controlling Antimicrobial Resistance in Hospitals: Infection Control and Use of Antibiotics. *Emerg. Infect. Dis.* **2001**, *7* (2), 188–192.

(24)     Johnson, A. P.; Woodford, N. Global Spread of Antibiotic Resistance: The Example of New Delhi Metallo-Beta-Lactamase (NDM)-Mediated Carbapenem Resistance. *J. Med. Microbiol.* **2013**, *62*, 499–513.

(25)     Kumarasamy, K. K.; Toleman, M. A.; Walsh, T. R.; Bagaria, J.; Butt, F.; Balakrishnan, R.; Chaudhary, U.; Paterson, D. L.; Pearson, A.; Perry, C.; et al. Emergence of a New Antibiotic Resistance Mechanism in India, Pakistan, and the UK: A Molecular, Biological, and Epidemiological Study. *Lancet Infect. Dis.* **2010**, *10* (9), 597–602.

(26)     Queenan, A. M.; Bush, K. Carbapenemases: The Versatile Beta-Lactamases. *Clin. Microbiol. Rev.* **2007**, *20* (3), 440–458.

(27)     Ebright, R. H. RNA Polymerase: Structural Similarities Between Bacterial RNA Polymerase and Eukaryotic RNA Polymerase II. *J. Mol. Biol.* **2000**, *304*, 687–698.

(28)     Darst, S. A. New Inhibitors Targeting Bacterial RNA Polymerase. *TRENDS Biochem. Sci.* **2004**, *29* (4), 159–162.

(29)     Sensi, P. History of the Development of Rifampin. *Rev. Infect. Dis.* **1983**, *5*, 402–406.

(30)     Campbell, E. A.; Korzheva, N.; Mustaev, A.; Murakami, K.; Nair, S.; Goldfarb, A.; Darst, S. A. Structural Mechanism for Rifampicin Inhibition of Bacterial RNA Polymerase. *Cell* **2001**, *104*, 901–912.

(31)     Mukhopadhyay, J.; Das, K.; Ismail, S.; Koppstein, D.; Jang, M.; Hudson, B.; Sarafianos, S.; Tuske, S.; Patel, J.; Jansen, R.; et al. The RNA Polymerase '"Switch Region"' Is a Target for Inhibitors. *Cell* **2008**, *135*, 295–307.

(32)     Borukhov, S.; Nudler, E. RNA Polymerase: The Vehicle of Transcription. *Trends Microbiol.* **2008**, *16* (3), 126–134.

(33)     Darst, S. A. Bacterial RNA Polymerase. *Curr. Opin. Struct. Biol.* **2001**, *11*, 155–162.

(34)     Mooney, R. A.; Landick, R. RNA Polymerase Unveiled. *Cell* **1999**, *98*, 687–690.

(35)     Haebich, D.; Nussbaum, F. Von. Lost in Transcription — Inhibition of RNA Polymerase. *Angew. Chemie Int. Ed* **2009**, *48*, 3397–3400.

(36)     Irschik, H.; Gerth, K.; Hofle, G.; Kohl, W.; Reichenbach, H.; Mikrobiologie, A.; Naturstoffchemie, A. The Myxopyronins, New Inhibitors of Bacterial RNA Synthesis from Myxococcus Fulvus. *J. Antibiot. (Tokyo).* **1983**, *XXXVI* (12), 1651–1657.

(37)     Srivastava, A.; Talaue, M.; Liu, S.; Degen, D.; Ebright, R. Y.; Sineva, E.; Chakraborty, A.; Druzhinin, S. Y.; Chatterjee, S.; Mukhopadhyay, J.; et al. New Target for Inhibition of Bacterial RNA Polymerase: 'Switch Region.' *Curr. Opin. Microbiol.* **2011**, *14*, 532–543.

(38)     Sahner, J. H.; Groh, M.; Negri, M.; Haupenthal, J.; Hartmann, R. W. Novel Small Molecule Inhibitors Targeting the "Switch Region" of Bacterial RNAP: Structure-Based Optimization of a Virtual Screening Hit. *Eur. J. Med. Chem.* **2013**, *65*, 223–231.

(39)     Hinsberger, S.; Hüsecken, K.; Groh, M.; Negri, M.; Haupenthal, J.; Hartmann, R. W. Discovery of Novel Bacterial RNA Polymerase Inhibitors: Pharmacophore Based Virtual Screening and Hit Optimization. *J. Medicianal Chem.* **2013**, *56* (21), 8332–8338.

(40)     Elgaher, W. A. M.; Furth, M.; Groh, M.; Haupenthal, J.; Hartmann, R. W. Expanding the Scaffold for Bacterial RNA Polymerase Inhibitors: Design, Synthesis and Structure–activity Relationships of Ureido- Heterocyclic-Carboxylic Acids. *RSC Adv.* **2014**, *4*, 2177–2194.

(41)     Silver, L. L. A Gestalt Approach to Gram-Negative Entry. *Bioorg. Med. Chem.* **2016**, *24*, 6379–6389.

Bibliography

(42)     Shea, R. O.; Moser, H. E. Physicochemical Properties of Antibacterial Compounds:
         Implications for Drug Discovery. *J. Med. Chem.* **2008**, *51* (10), 2871–2878.

(43)     Pagès, J.; James, C. E.; Winterhalter, M. The Porin and the Permeating Antibiotic:
         A Selective Diffusion Barrier in Gram-Negative Bacteria. *Nat. Rev. Microbiol.*
         **2008**, *6*, 893–903.

(44)     Nikaido, H. Molecular Basis of Bacterial Outer Membrane Permeability Revisited.
         *Microbiol. Mol. Biol. Rev.* **2003**, *67* (4), 593–656.

(45)     Rautio, J.; Kumpulainen, H.; Heimbach, T.; Oliyai, R. Prodrugs: Design and Clinical
         Applications. *Nat. Rev. Drug Discov.* **2008**, *7*, 255–270.

(46)     Huttunen, K. M.; Raunio, H.; Rautio, J. Prodrugs — from Serendipity to Rational
         Design. *Pharmacol. Revoews* **2011**, *63* (3), 750–771.

(47)     Ruthenbeck, A.; Elgaher, W. A. M.; Haupenthal, J.; Hartmann, R. W.; Meier, C.
         Bacterial RNAP Inhibitors: Synthesis and Evaluation of Prodrugs of Aryl-
         Ureidothiophene-Carboxylic Acids. *ChemistrySelect* **2017**, *2*, 11899–11905.

(48)     Junge, W.; Heymann, E. Characterization of the Isoenzymes of Pig-Liver Esterase.
         *Eur. J. Biochem.* **1979**, *95*, 519–525.

(49)     Hakamata, W.; Machida, A.; Oku, T.; Nishio, T. Design and Synthesis of an ER-
         Specific Fluorescent Probe Based on Carboxylesterase Activity with Quinone
         Methide Cleavage Process. *Bioorg. Med. Chem. Lett.* **2011**, *21*, 3206–3209.

(50)     Hider, R. C.; Kong, X. Chemistry and Biology of Siderophores. *Nat. Prod. Rep.*
         **2010**, *27*, 637–657.

(51)     Möllmann, U.; Heinisch, L.; Bauernfeind, A.; Köhler, T.; Ankel-Fuchs, D.
         Siderophores as Drug Delivery Agents: Application of the "Trojan Horse"
         Strategy. *BioMetals* **2009**, *22* (4), 615–624.

(52)     Mislin, L. A.; Schalk, I. J. Siderophore-Dependent Iron Uptake Systems as Gates

for Antibiotic Trojan Horse Strategies against Pseudomonas Aeruginosa. *Metallomics* **2014**, *6*, 408–420.

(53)     Neilands, J. B. Siderophores: Structure and Function of Microbial Iron Transport Compounds. *J. Biol. Chem.* **1995**, *270* (45), 26723–26726.

(54)     Möllmann, U.; Heinisch, L.; Bauernfeind, A.; Köhler, T.; Ankel-Fuchs, D. Siderophores as Drug Delivery Agents: Application of the '"Trojan Horse"' Strategy. *Biometals* **2009**, *22*, 615–624.

(55)     Ji, C.; Miller, M. J. Chemical Syntheses and in Vitro Antibacterial Activity of Two Desferrioxamine B-Ciprofloxacin Conjugates with Potential Esterase and Phosphatase Triggered Drug Release Linkers. *Bioorganic Med. Chem.* **2012**, *20* (12), 3828–3836.

(56)     Souto, A.; Montaos, M. A.; Balado, M.; Osorio, C. R.; Rodríguez, J.; Lemos, M. L.; Jiménez, C. Synthesis and Antibacterial Activity of Conjugates between Norfloxacin and Analogues of the Siderophore Vanchrobactin. *Bioorganic Med. Chem.* **2013**, *21* (1), 295–302.

(57)     Ji, C.; Miller, P. A.; Miller, M. J. Iron Transport-Mediated Drug Delivery: Practical Syntheses and In Vitro Antibacterial Studies of Tris-Catecholate Siderophore − Aminopenicillin Conjugates Reveals Selectively Potent Antipseudomonal Activity. *J. Am. Chem. Soc.* **2012**, *134*, 9898–9901.

(58)     Brown, M. F.; Mitton-Fry, M. J.; Arcari, J. T.; Barham, R.; Casavant, J.; Gerstenberger, B. S.; Han, S.; Hardink, J. R.; Harris, T. M.; Hoang, T.; et al. Pyridone-Conjugated Monobactam Antibiotics with Gram-Negative Activity. *J. Med. Chem.* **2013**, *56* (13), 5541–5552.

(59)     Arnould, J. C.; Boutron, P.; Pasquet, M. J. Synthesis and Antibacterial Activity of C4 Substituted Monobactams. *Eur. J. Med. Chem.* **1992**, *27*, 131–140.

(60)     Curtis, N. A. C.; Eisenstadt, R. L.; East, S. J.; Cornford, R. J.; Walker, L. A.; White,

Bibliography

A. J.; Al, C. E. T. Iron-Regulated Outer Membrane Proteins of Escherichia Coli K-12 and Mechanism of Action of Catechol-Substituted Cephalosporins. *Antimicrob. Agents Chemother.* **1988**, *32* (12), 1879–1886.

(61)  Sloderbach, A.; Marszałł, M. P. Siderophore – Drug Complexes: Potential Medicinal Applications of the ' Trojan Horse ' Strategy. *Trends Pharmacol. Sci.* **2014**, *35* (9).

(62)  Braun, V.; Braun, M. Active Transport of Iron and Siderophore Antibiotics. *Curr. Opin. Microbiol.* **2002**, *5*, 194–201.

(63)  Greene, T. W.; Wuts, P. G. M. *Protective Groups in Organic Synthesis*, Third Edit.; John Wiley & Son, Inc., 1999.

(64)  Higgins, G.; Slassi, A.; Isaac, M. Use of D-Serin Derivatives for the Treatnemt of Anxiety Disorders, 2008.

(65)  Yoon, N. M.; Pak, C. S.; Brown Herbert, C.; Krishnamurthy, S.; Stocky, T. P. Selective Reductions. XIX. Rapid Reaction of Carboxylic Acids with Borane-Tetrahydrofuran. Remarkably Convenient Procedure for the Selective Conversion of Carboxylic Acids to the Corresponding Alcohols in the Presence of Other Functional Groups. *J. Org. Chem.* **1973**, *38* (16), 2786–2792.

(66)  Dugar, S.; Mahajan, D.; Hollinger Peter, F. Substituted Methyl Formyl Reagents for Modification of Physiochemical Pharmacokinetic Properties, 2012.

(67)  Mitton-Fry, M. J.; Arcari, J. T.; Brown, M. F.; Casavant, J. M.; Finegan, S. M.; Flanagan, M. E.; Gao, H.; George, D. M.; Gerstenberger, B. S.; Han, S.; et al. Novel Monobactams Utilizing a Siderophore Uptake Mechanism for the Treatment of Gram-Negative Infections. *Bioorganic Med. Chem. Lett.* **2012**, *22* (18), 5989–5994.

(68)  Brickner, S. J.; Flanagan, M. E.; Lall, M. S. Monocarbams, 2010.

(69)  Brückner, R.; Harmate, M. *Organic Mechanisms*; Springer-Verlag Berlin, 2010.

(70)  Mitsunobu, O. The Use of Diethyl Azodicarboxylate and Triphenylphosphine in Synthesis and Transformation of Natural Products. *Synthesis (Stuttg).* **1981**, 1–28.

(71)  Ahn, C.; Correia, R.; Deshong, P. Mechanistic Study of the Mitsunobu Reaction. *J. Org. Chem.* **2002**, *20742* (18), 1751–1753.

(72)  Yuen, T.; But, S.; Toy, P. H. The Mitsunobu Reaction: Origin, Mechanism, Improvements, and Applications. *Chem. An Asian J.* **2007**, *2*, 1340–1355.

(73)  Neilands, J. B.; Schwyn, B. Universal Chemical Assay for the Detection Determination of Siderophores. *Anal. Biochem.* **1987**, *56* (160), 47–56.

(74)  Iglesias, E.; Brandariz, I.; Jiménez, C.; Soengas, R. G. Iron(III) Complexation by Vanchrobactin, a Siderophore of the Bacterial Fish Pathogen Vibrio Anguillarum W. *Metallomics* **2011**, *3*, 521–528.

(75)  Faraldo-Gómez, J. D.; Sansom, M. S. P. Acquisition of Siderophores in Gram-Negative Bacteria. *Nat. Rev. Mol. Cell Biol.* **2003**, *4* (2), 105–116.

(76)  Ji, C.; Miller, M. J. Exploiting Bacterial Iron Acquisition: Siderophore Conjugates. *Future Med. Chem.* **2012**, *4* (3), 297–313.

(77)  Nikaido, H. Preventing Drug Access to Targets: Cell Surface Permeability Barriers and Active Efflux in Bacteria. *Cell Dev. Biol.* **2001**, *12*, 215–223.

(78)  Krewulak, K. D.; Vogel, H. J. Structural Biology of Bacterial Iron Uptake. *Biochim. Biophys. Acta* **2008**, *1778*, 1781–1804.

(79)  Chakraborty, R.; Storey, Æ. E. Molecular Mechanism of Ferricsiderophore Passage through the Outer Membrane Receptor Proteins of Escherichia Coli. *Biometals* **2007**, *20*, 263–274.

(80)  Berg, J.; Tymoczko, J.; Stryer, L. *Biochemistry 5th Edition*; W. H. Freeman and Company, 2002.

Bibliography

(81)     Heinrich, P. C.; Müller, M.; Graeve, L. *Löffler / Petrides Biochemie Und Pathobiochemie*; 2014.

(82)     Alberts, B.; Johnson, A.; Lewis, J.; Raff, M.; Roberts, K.; Walter, P. *Molecular Biology of the Cell*, 4th ed.; Garland Science, New York, 2002.

(83)     Schulz von Thun, F. *Miteinander Reden 1. Störungen Und Klärungen. Allgemeine Psychologie Der Kommunikation.*; Rowohlt: Reinbek, 1981.

(84)     Junger, W. G. Immune Cell Regulation by Autocrine Purinergic Signalling. *Nat. Rev. Immunol.* **2011**, *11* (3), 201–212.

(85)     Idzko, M.; Ferrari, D.; Eltzschig, H. K. Nucleotide Signalling during Inflammation. *Nature* **2014**, *509* (7500), 310–317.

(86)     Eltzschig, H. K.; Sitkovsky, M. V.; Robson, S. C. Purinergic Signaling during Inflammation. *N. Engl. J. Med.* **2012**, *367* (24), 2322–2333.

(87)     Färber, K.; Kettenmann, H. Purinergic Signaling and Microglia. *Pflugers Arch. - Eur. J. Physiol.* **2006**, *452* (5), 615–621.

(88)     Clapham, D. E. Calcium Signaling. *Cell* **2007**, *131* (6), 1047–1058.

(89)     Alexander, S. P. H.; Mathie, A.; Peters, J. A. Guide to Receptors and Channels (GRAC), 5th Edition. *Br. J. Pharmacol.* **2009**, *164*, 1–324.

(90)     Tovar, K. R.; Westbrook, G. L. *Ligand-Gated Ion Channels*, Fourth Edi.; Elsevier Inc., 2012.

(91)     Barker, B. S.; Young, G. T.; Soubrane, C. H.; Stephens, G. J.; Stevens, E. B.; Patel, M. K. *Ion Channels*; Elsevier Inc., 2016.

(92)     Pankratov, Y. V; Lalo, U. V; Krishtal, O. a. Role for P2X Receptors in Long-Term Potentiation. *J. Neurosci.* **2002**, *22* (19), 8363–8369.

(93)     Elliott, M. R.; Chekeni, F. B.; Trampont, P. C.; Lazarowski, E. R.; Kadl, A.; Walk, S.

F.; Park, D.; Woodson, R. I.; Ostankovich, M.; Sharma, P.; et al. Nucleotides Released by Apoptotic Cells Act as a Find-Me Signal to Promote Phagocytic Clearance. *Nature* **2009**, *461* (7261), 282–286.

(94)     Vivanco-Cid, H.; Mellado-Sánchez, G.; Sumoza-Toledo, A. Transient Receptor Potential Melastatin-2 Channel and Inflammation. *OA Inflamm.* **2013**, *1* (2), 12–16.

(95)     Melzer, N.; Hicking, G.; Göbel, K.; Wiendl, H. TRPM2 Cation Channels Modulate T Cell Effector Functions and Contribute to Autoimmune CNS Inflammation. *PLoS One* **2012**, *7* (10), 1–6.

(96)     Patel, S. Function and Dysfunction of Two-Pore Channels. *Sci. Signal.* **2015**, *8* (384), 1–7.

(97)     Guse, A. H.; Wolf, I. M. A. Ca2+ Microdomains, NAADP and Type 1 Ryanodine Receptor in Cell Activation. *Biochim. Biophys. Acta - Mol. Cell Res.* **2016**, *1863* (6), 1379–1384.

(98)     Wolf, I. M. A.; Diercks, B. P.; Gattkowski, E.; Czarniak, F.; Kempski, J.; Werner, R.; Schetelig, D.; Mittrücker, H. W.; Schumacher, V.; Von Osten, M.; et al. Frontrunners of T Cell Activation: Initial, Localized Ca2+ Signals Mediated by NAADP and the Type 1 Ryanodine Receptor. *Sci. Signal.* **2015**, *8* (398), 1–13.

(99)     Wolf, I. M. A.; Guse, A. H. Ca2+ Microdomains in T-Lymphocytes. *Front. Oncol.* **2017**, *7*, 1–11.

(100)    Churchill, G. C.; Galione, A. Spatial Control of Ca2+ Signaling by Nicotinic Acid Adenine Dinucleotide Phosphate Diffusion and Gradients. *J. Biol. Chem.* **2000**, *275* (49), 38687–38692.

(101)    Brailoiu, E.; Hooper, R.; Cai, X.; Cristina Brailoiu, G.; Keebler, M. V.; Dun, N. J.; Marchant, J. S.; Patel, S. An Ancestral Deuterostome Family of Two-Pore Channels Mediates Nicotinic Acid Adenine Dinucleotide Phosphate-Dependent

Calcium Release from Acidic Organelles. *J. Biol. Chem.* **2010**, *285* (5), 2897–2901.

(102)   Churchill, G. C.; Okada, Y.; Thomas, J. M.; Genazzani, A. A.; Patel, S.; Galione, A. NAADP Mobilizes Ca 2+ from Reserve Granules, Lysosome-Related Organelles, in Sea Urchin Eggs. *Cell Press* **2002**, *111*, 703–708.

(103)   Wilson, H. L.; Galione, A. Differential Regulation of Nicotinic Acid-Adenine Dinucleotide Phosphate and CADP-Ribose Production by CAMP and CGMP. *Biochem. J.* **1998**, *331 ( Pt 3*, 837–843.

(104)   Churchill, G. C.; O'Neill, J. S.; Masgrau, R.; Patel, S.; Thomas, J. M.; Genazzani, A. A.; Galione, A. Sperm Deliver a New Second Messenger: NAADP. *Curr. Biol.* **2003**, *13* (2), 125–128.

(105)   Lee, H. C.; Aarhus, R. A Derivative of NADP Mobilizes Calcium Stores Insensitive to Inositol Trisphosphate and Cyclic ADP-Ribose. *Journal of Biological Chemistry*. 1995, pp 2152–2157.

(106)   Bjarnadóttir, T. K.; Gloriam, D. E.; Hellstrand, S. H.; Kristiansson, H.; Fredriksson, R.; Schiöth, H. B. Comprehensive Repertoire and Phylogenetic Analysis of the G Protein-Coupled Receptors in Human and Mouse. *Genomics* **2006**, *88* (3), 263–273.

(107)   Hilger, D.; Masureel, M.; Kobilka, B. K. Structure and Dynamics of GPCR Signaling Complexes. *Nat. Struct. Mol. Biol.* **2018**, *25* (1), 4–12.

(108)   Barnard, E. a; Kennedy, C.; Knight, G. E.; Fumagalli, M.; Gachet, C.; Jacobson, K. a; Weisman, G. a. International Union of Pharmacology LVIII: Update on the P2Y G Protein-Coupled Nucleotide Receptors: From Molecular Mechanisms and Pathophysiology to Therapy. *Pharmacol. Rev.* **2006**, *58* (3), 281–341.

(109)   Zimmerman, A. L. *Cyclic Nucleotide-Gated Ion Channels*, Fourth Edi.; Elsevier Inc., 2012.

(110)   Biel, M. *Cyclic Nucleotide-Regulated Cation Channels*, Second Edi.; Elsevier Inc.,

2010; Vol. 2.

(111)   Walsh, D. A.; van Patten, S. M. Multiple Pathways Signal Transduction by the CAMP-Dependent Protein Kinase. *FASEB J.* **1994**, *8* (15), 1227–1236.

(112)   Bopp, T.; Becker, C.; Klein, M.; Klein-Heßling, S.; Palmetshofer, A.; Serfling, E.; Heib, V.; Becker, M.; Kubach, J.; Schmitt, S.; et al. Cyclic Adenosine Monophosphate Is a Key Component of Regulatory T Cell–mediated Suppression. *J. Exp. Med.* **2007**, *204* (6), 1303–1310.

(113)   Bodor, J.; Bopp, T.; Vaeth, M.; Klein, M.; Serfling, E.; Hünig, T.; Becker, C.; Schild, H.; Schmitt, E. Cyclic AMP Underpins Suppression by Regulatory T Cells. *Eur. J. Immunol.* **2012**, *42* (6), 1375–1384.

(114)   Gasser, A.; Glassmeier, G.; Fliegert, R.; Langhorst, M. F.; Meinke, S.; Hein, D.; Krüger, S.; Weber, K.; Heiner, I.; Oppenheimer, N.; et al. Activation of T Cell Calcium Influx by the Second Messenger ADP-Ribose. *J. Biol. Chem.* **2006**, *281* (5), 2489–2496.

(115)   Knowles, H.; Li, Y.; Perraud, A. L. The TRPM2 Ion Channel, an Oxidative Stress and Metabolic Sensor Regulating Innate Immunity and Inflammation. *Immunol. Res.* **2013**, *55* (1–3), 241–248.

(116)   Adriouch, S.; Haag, F.; Boyer, O.; Seman, M.; Koch-Nolte, F. Extracellular NAD+: A Danger Signal Hindering Regulatory T Cells. *Microbes Infect.* **2012**, *14* (14), 1284–1292.

(117)   Guse, A.; Haag, F.; Koch-Nolte, F.; Lund, F.; Ziegler, M. Emerging Roles of NAD and NAD-Metabolites in Cell Signalling. *Nad2008* **2008**, *2* (57).

(118)   Partida-Sanchez, S.; Gasser, A.; Fliegert, R.; Siebrands, C. C.; Dammermann, W.; Shi, G.; Mousseau, B. J.; Sumoza-Toledo, A.; Bhagat, H.; Walseth, T. F.; et al. Chemotaxis of Mouse Bone Marrow Neutrophils and Dendritic Cells Is Controlled by ADP-Ribose, the Major Product Generated by the CD38 Enzyme Reaction. *J.*

*Immunol.* **2007**, *179* (11), 7827–7839.

(119) Schuber, F.; Lund, F. E. Structure and Enzymology of ADP-Ribosyl Cyclases: Conserved Enzymes That Produce Multiple Calcium Mobilizing Metabolites. *Curr. Mol. Med.* **2004**, *4* (3), 249–261.

(120) Isabelle, M.; Moreel, X.; Gagné, J. P.; Rouleau, M.; Ethier, C.; Gagné, P.; Hendzel, M. J.; Poirier, G. G. Investigation of PARP-1, PARP-2, and PARG Interactomes by Affinity-Purification Mass Spectrometry. *Proteome Sci.* **2010**, *8*, 1–11.

(121) Fonfria, E.; Marshall, I. C. B.; Benham, C. D.; Boyfield, I.; Brown, J. D.; Hill, K.; Hughes, J. P.; Skaper, S. D.; McNulty, S. TRPM2 Channel Opening in Response to Oxidative Stress Is Dependent on Activation of Poly(ADP-Ribose) Polymerase. *Br. J. Pharmacol.* **2004**, *143* (1), 186–192.

(122) Buelow, B.; Song, Y.; Scharenberg, A. M. The Poly(ADP-Ribose) Polymerase PARP-1 Is Required for Oxidative Stress-Induced TRPM2 Activation in Lymphocytes. *J. Biol. Chem.* **2008**, *283* (36), 24571–24583.

(123) Fliegert, R.; Bauche, A.; Wolf Pérez, A.-M.; Watt, J. M.; Rozewitz, M. D.; Winzer, R.; Janus, M.; Gu, F.; Rosche, A.; Harneit, A.; et al. 2'-Deoxyadenosine 5'-Diphosphoribose Is an Endogenous TRPM2 Superagonist. *Nat. Chem. Biol.* **2017**, *13*, 1036.

(124) Clapper, D. L.; Walseth, T. F.; Dargie, P. J.; Hon Cheung Lee. Pyridine Nucleotide Metabolites Stimulate Calcium Release from Sea Urchin Egg Microsomes Desensitized to Inositol Trisphosphate. *J. Biol. Chem.* **1987**, *262* (20), 9561–9568.

(125) Aarhus, R.; Graeff, R. M.; Dickey, D. M.; Walseth, T. F.; Lee, H. C. ADP-Ribosyl Cyclase and CD38 Catalyze the Synthesis of a Calcium-Mobilizing Metabolite from NADP. *J. Biol. Chem.* **1995**, *270* (51), 30327–30333.

(126) Corey, E. J.; Kang, M.; Desai, M. C.; Ghosh, A. K.; Houpis, I. N. Total Synthesis of (+/-)-Ginkgolide B. *J. Am. Chem. Soc.* **1988**, *10* (3), 649–651.

(127)    Zhang, B.; Wagner, G. K.; Weber, K.; Garnham, C.; Morgan, A. J.; Galione, A.; Guse, A. H.; Potter, B. V. L. 2'-Deoxy Cyclic Adenosine 5'-Diphosphate Ribose Derivatives: Importance of the 2'-Hydroxyl Motif for the Antagonistic Activity of 8-Substituted CADPR Derivatives. *J. Med. Chem.* **2008**, *51*, 1623–1636.

(128)    Palade, P. The Hunt for an Alternate Way to Generate NAADP. Focus on "NAADP as a Second Messenger: Neither CD38 nor Base-Exchange Reaction Are Necessary for in Vivo Generation of NAADP in Myometrial Cells ." *Am J Physiol Cell Physiol* **2007**, No. 29, 4–7.

(129)    Mojžišová, A.; Križanová, O.; Žáčiková, Ľ.; Komínková, V.; Ondriaš, K. Effect of Nicotinic Acid Adenine Dinucleotide Phosphate on Ryanodine Calcium Release Channel in Heart. *Pflugers Arch. Eur. J. Physiol.* **2001**, *441* (5), 674–677.

(130)    Guse, A. H.; M A Ernst, I.; Fliegert, R. NAADP Signaling Revisited. *Curr. Top. Med. Chem.* **2013**, 2978–2990.

(131)    Calcraft, P. J.; Ruas, M.; Pan, Z.; Cheng, X.; Arredouani, A.; Hao, X.; Tang, J.; Rietdorf, K.; Teboul, L.; Chuang, K. T.; et al. NAADP Mobilizes Calcium from Acidic Organelles through Two-Pore Channels. *Nature* **2009**, *459* (7246), 596–600.

(132)    Brailoiu, E.; Churamani, D.; Cai, X.; Schrlau, M. G.; Brailoiu, G. C.; Gao, X.; Hooper, R.; Boulware, M. J.; Dun, N. J.; Marchant, J. S.; et al. Essential Requirement for Two-Pore Channel 1 in NAADP-Mediated Calcium Signaling. *J. Cell Biol.* **2009**, *186* (2), 201–209.

(133)    Zong, X.; Schieder, M.; Cuny, H.; Fenske, S.; Gruner, C.; Rötzer, K.; Griesbeck, O.; Harz, H.; Biel, M.; Wahl-Schott, C. The Two-Pore Channel TPCN2 Mediates NAADP-Dependent Ca2+-Release from Lysosomal Stores. *Pflugers Arch. Eur. J. Physiol.* **2009**, *458* (5), 891–899.

(134)    Lin-Moshier, Y.; Walseth, T. F.; Churamani, D.; Davidson, S. M.; Slama, J. T.; Hooper, R.; Brailoiu, E.; Patel, S.; Marchant, J. S. Photoaffinity Labeling of Nicotinic Acid Adenine Dinucleotide Phosphate (NAADP) Targets in Mammalian

Cells. *J. Biol. Chem.* **2012**, *287* (4), 2296–2307.

(135)   Cordiglieri, C.; Odoardi, F.; Zhang, B.; Nebel, M.; Kawakami, N.; Klinkert, W. E. F.; Lodygin, D.; Lühder, F.; Breunig, E.; Schild, D.; et al. Nicotinic Acid Adenine Dinucleotide Phosphate-Mediated Calcium Signalling in Effector T Cells Regulates Autoimmunity of the Central Nervous System. *Brain* **2010**, *133* (7), 1930–1943.

(136)   Bartholomäus, I.; Kawakami, N.; Odoardi, F.; Schläger, C.; Miljkovic, D.; Ellwart, J. W.; Klinkert, W. E. F.; Flügel-Koch, C.; Issekutz, T. B.; Wekerle, H.; et al. Effector T Cell Interactions with Meningeal Vascular Structures in Nascent Autoimmune CNS Lesions. *Nature* **2009**, *462* (7269), 94–98.

(137)   Peterson, L. W.; McKenna, C. E. Prodrug Approaches to Improving the Oral Absorption of Antiviral Nucleotide Analogues. *Expert Opin. Drug Deliv.* **2009**, *6* (4), 405–420.

(138)   Zhang, Y.; Gao, Y.; Wen, X.; Ma, H. Current Prodrug Strategies for Improving Oral Absorption of Nucleoside Analogues. *Asian J. Pharm. Sci.* **2014**, *9* (2), 65–74.

(139)   Schultz, C. Prodrugs of Biologically Active Phosphate Esters. *Bioorganic Med. Chem.* **2003**, *11* (6), 885–898.

(140)   Engels, J.; Schlaeger, E. J. Synthesis, Structure, and Reactivity of Adenosine Cyclic 3',5'-Phosphate-Benzyltriesters. *J. Med. Chem.* **1977**, *20* (7), 907–911.

(141)   Korth, M.; Engels, J. The Effects of Adenosine- and Guanosine 3',5'-Phosphoric Acid Benzyl Esters on Guinea-Pig Ventricular Myocardium. *Naunyn-Schmiedberg's Arch. Pharmacol.* **1979**, *314*, 103–111.

(142)   Schultz, C.; Vajanaphanich, M.; Harootunian, A. T.; Sammak, P. J.; Barrett, K. E.; Tsien, R. Y. Acetoxymethyl Esters of Phosphates, Enhancement of the Permeability and Potency of CAMP. *J. Biol. Chem.* **1993**, *268* (9), 6316–6322.

(143)   Pahnke, K.; Meier, C. Synthesis of a Bioreversibly Masked Lipophilic Adenosine Diphosphate Ribose Derivative. *ChemBioChem* **2017**, *18* (16), 1616–1626.

Bibliography

(144)    Rosen, D.; Bloor-Young, D.; Squires, J.; Parkesh, R.; Waters, G.; Vasudevan, S. R.; Lewis, A. M.; Churchill, G. C. Synthesis and Use of Cell-Permeant Cyclic ADP-Ribose. *Biochem. Biophys. Res. Commun.* **2012**, *418* (2), 353–358.

(145)    Schultz, C.; Vajanaphanich, M.; Genieser, H. G.; Jastorff, B.; Barrett, K. E.; Tsien, R. Y. Membrane-Permeant Derivatives of Cyclic AMP Optimized for High Potency, Prolonged Activity, or Rapid Reversibility. *Mol. Pharmacol.* **1994**, *46* (4), 702–8.

(146)    Galione, A.; Chuang, K.; Funnell, T. M.; Davis, L. C.; Morgan, A. J.; Parrington, J.; Churchill, G. C. Synthesis of NAADP-AM as a Membrane-Permeant NAADP Analog. *Cold Spring Harb Protoc* **2014**, 1097–1100.

(147)    Parkesh, R.; Lewis, A. M.; Aley, P. K.; Arredouani, A.; Rossi, S.; Tavares, R.; Vasudevan, S. R.; Rosen, D.; Galione, A.; Dowden, J.; et al. Cell-Permeant NAADP: A Novel Chemical Tool Enabling the Study of Ca 2 + Signalling in Intact Cells. *Cell Calcium* **2008**, *43*, 531–538.

(148)    Bartsch, M.; Zorn-Kruppa, M.; Kühl, N.; Genieser, H. G.; Schwede, F.; Jastorff, B. Bioactivatable, Membrane-Permeant Analogs of Cyclic Nucleotides as Biological Tools for Growth Control of C6 Glioma Cells. *Biol. Chem.* **2003**, *384* (9), 1321–1326.

(149)    Lee, H. C.; Aarhus, R.; Gee, K.; Kestner, T. Caged Nicotinic Acid Adenine Dinucleotide Phosphate. *J.Biol.Chem.* **1997**, *272* (7), 4172–4178.

(150)    Aarhus, R.; Gee, K.; Lee, H. C. Caged Cyclic ADP Ribose - Synthesis and Use. *J. Biol. Chem.* **1995**, *270* (13), 7745–7749.

(151)    Guse, A. Personal Communication.

(152)    Mitchell, A. G.; Thornson, W.; Nicholls, D.; Irwin, W. J.; Freeman, S. Bioreversible Protection for the Phospho Group: Bioactivation of the Di (4-Acyloxybenzyl) and Mono(4-Acyloxybenryl) P Hosp Hoesters of Methyl Phosphonate and Phosphonoacetate. *J. Chem. Soc. Perkin Trans. 1* **1992**, *3*, 2345–2353.

(153)    Freeman, S.; Irwin, W. J.; Mitchell, A. G.; Nicholls, D.; Thomson, W. Bioreversible Protection for the Phospho Group: Chemical Stability and Bioactivation of Di(4-Acetoxybenzyl) Methylphosphonate with Carboxyesterase. *J. Chem. Soc.* **1991**, *01*, 875–877.

(154)    Carl, P. L.; Chakravarty, P. K.; Katzenellenbogen, J. A. A Novel Connector Linkage Applicable in Prodrug Design. *J. Med. Chem.* **1981**, *24* (5), 479–480.

(155)    Thomson, W.; Nicholls, D.; Irwin, W. J.; Al-Mushadani, J. S.; Freeman, S.; Karpas, A.; Petrik, J.; Mahmood, N.; Hay, A. J. Synthesis, Bioactivation and Anti-HIV Activity of the Bis(4-Acyloxybenzyl) and Mono(4-Acyloxybenzyl) Esters of the 5'-Monophosphate of AZT. *J. Chem. Soc. Perkin Trans. 1* **1993**, No. 11, 1239–1245.

(156)    Gollnest, T.; De Oliveira, T. D.; Schols, D.; Balzarini, J.; Meier, C. Lipophilic Prodrugs of Nucleoside Triphosphates as Biochemical Probes and Potential Antivirals. *Nat. Commun.* **2015**, *6*, 1–15.

(157)    Gollnest, T.; De Oliveira, T. D.; Rath, A.; Hauber, I.; Schols, D.; Balzarini, J.; Meier, C. Membrane-Permeable Triphosphate Prodrugs of Nucleoside Analogues. *Angew. Chemie - Int. Ed.* **2016**, *55* (17), 5255–5258.

(158)    Jessen, H. J.; Schulz, T.; Balzarini, J.; Meier, C. Bioreversible Protection of Nucleoside Diphosphates. *Angew. Chemie - Int. Ed.* **2008**, *47* (45), 8719–8722.

(159)    Schulz, T.; Balzarini, J.; Meier, C. The DiPPro Approach: Synthesis, Hydrolysis, and Antiviral Activity of Lipophilic D4T Diphosphate Prodrugs. *ChemMedChem* **2014**, *9* (4), 762–775.

(160)    Meier, C.; Jessen, H. J.; Schulz, T.; Weinschenk, L.; Pertenbreiter, F.; Balzarini, J. Rational Development of Nucleoside Diphosphate Prodrugs: DiPPro-Compounds. *Curr. Med. Chem.* **2015**, *22* (34), 3933–3950.

(161)    Meier, C. Nucleoside Diphosphate and Triphosphate Prodrugs – An Unsolvable Task? *Antivir. Chem. Chemother.* **2017**, *25* (3), 69–82.

(162)    Weinschenk, L.; Schols, D.; Balzarini, J.; Meier, C. Nucleoside Diphosphate Prodrugs: Nonsymmetric DiPPro-Nucleotides. *J. Med. Chem.* **2015**, *58* (15), 6114–6130.

(163)    Reimer, I. S. *3′- S-Phosphorthiolatverbrückte Oligonucleotide Und Fluoreszierende Nucleotid-Prodrugs Für Zellaufnahmestudien*; 2017.

(164)    Gollnest, T. Das Tri PPPro-Konzept: Entwicklung Und Charakterisierung von Antiviralen Nukleosidtriphosphat-Prodrugs. *Dissertation* **2015**.

(165)    Yu, P.; Wang, Q.; Zhang, L.; Lee, H.; Zhang, L.; Yue, J. A Cell Permeable NPE Caged ADP-Ribose for Studying TRPM2. *PLoS One* **2012**, *7* (12), e51028.

(166)    Besada, P.; Gachet, C.; Gao, Z.; Jacobson, K. A. Caged Agonist of P2Y1 and P2Y12 Receptors for Light-Directed Facilitation of Platelet Aggregation. *Biochem. Pharmacol.* **2008**, *75*, 1341–1347.

(167)    Poh, J. S.; Tran, D. N.; Battilocchio, C.; Hawkins, J. M.; Ley, S. V. A Versatile Room-Temperature Route to Di- and Trisubstituted Allenes Using Flow-Generated Diazo Compounds. *Angew. Chemie - Int. Ed.* **2015**, *54* (27), 7920–7923.

(168)    Huchting, J.; Ruthenbeck, A.; Meier, C. Synthesis of *Cyclo* Sal-(Glycopyranosyl-6)-Phosphates as Activated Sugar Phosphates. *European J. Org. Chem.* **2013**, *2013* (30), 6907–6916.

(169)    Warnecke, S.; Meier, C. Synthesis of Nucleoside Di- and Triphosphates and Dinucleoside Polyphosphates with Cyclosal-Nucleotides. *J. Org. Chem.* **2009**, *74* (8), 3024–3030.

(170)    Zhu, X.; Williams, H. J.; Scott, A. I. Aqueous Trifluoroacetic Acid — an Efficient Reagent for Exclusively Cleaving the 5′-End of 3′, 5′-TIPDS Protected Ribonucleosides. *Tetrahedron Lett.* **2000**, *41*, 9541–9545.

(171)    Higashibayashi, S.; Shinko, K.; Ishizu, T.; Hashimoto, K.; Shirahama, H. Selective Deprotection of t -Butyldiphenylsilyl Ethers in the Presence of t -

Butyldimethylsilyl Ethers by Tetrabutylammonium Fluoride , Acetic Acid , and Water. *Synlett* **2000**, *9*, 1306–1308.

(172) Ruda, G. F.; Alibu, V. P.; Mitsos, C.; Bidet, O.; Kaiser, M.; Brun, R.; Barrett, M. P.; Gilbert, I. H. Synthesis and Biological Evaluation of Phosphate Prodrugs of 4-Phospho- d -Erythronohydroxamic Acid , an Inhibitor of 6-Phosphogluconate Dehydrogenase. **2007**, 1169–1180.

(173) Crouch, R. D. Selective Deprotection of Silyl Ethers. *Tetrahedron* **2013**, *69*, 2383–2417.

(174) Karimi, B.; Zamani, A.; Zareyee, D. N-Iodosuccinimide (NIS) as a Mild and Highly Chemoselective Catalyst for Deprotection of Tert -Butyldimethylsilyl Ethers. *Tetrahedron Lett.* **2004**, *45*, 9139–9141.

(175) Hunter, R.; Hinz, W.; Richards, P. On the Chemoselectivity and Mechanism of Desilylation Of. *Tetrahedron Lett.* **1999**, *40*, 3643–3646.

(176) Westmanu, E.; Stromberg, R. Removal of F-Butyldimethylsilyl Protection in RNA-Synthesis. Triethylamine Trihydrofluoride (TEA, 3HF) Is a More Reliable Alternative to Tetrabutylammonium Fluoride (TBAF). *Nucleic Acids Res.* **1994**, *22* (12), 2430–2431.

(177) Meier, C.; Balzarini, J. Application of the CycloSal-Prodrug Approach for Improving the Biological Potential of Phosphorylated Biomolecules. *Antiviral Res.* **2006**, *71* (2–3 SPEC. ISS.), 282–292.

(178) Sowa, T.; Ouchi, S. The Facile Synthesis of 5'-Nucleotides by the Selective Phosphorylation of a Primary Hydroxyl Group of Nucleosides with Phosphoryl Chloride. *Bull. Chem. Soc. Jpn.* **1975**, *48* (7), 2084–2090.

(179) Cremosnik, G. S.; Hofer, A.; Jessen, H. J. Iterative Synthesis of Nucleoside Oligophosphates with Phosphoramidites. *Angew. Chemie - Int. Ed.* **2013**, *53* (1), 286–289.

(180)    Huchting, J.; Vanderlinden, E.; Winkler, M.; Nasser, H.; Naesens, L.; Meier, C. Prodrugs of the Phosphoribosylated Forms of Hydroxypyrazinecarboxamide Pseudobase T-705 and Its De-Fluoro-Analogue T-1105 as Potent Influenza Virus Inhibitors. *J. Med. Chem.* **2018**, acs.jmedchem.8b00617.

(181)    Liu, H.; Yan, X.; Li, W.; Huang, C. A Mild and Selective Method for Cleavage of O - Acetyl Groups with Dibutyltin Oxide. **2002**, *337*, 1763–1767.

(182)    Huchting, J.; Winkler, M.; Nasser, H.; Meier, C. Synthesis of T-705-Ribonucleoside and T-705-Ribonucleotide and Studies of Chemical Stability. *ChemMedChem* **2017**, *12* (9), 652–659.

(183)    Baldoni, L.; Marino, C.; Glycobiology, W. Facile Synthesis of Per-O-Tert - Butyldimethylsilyl-b-D-Galactofuranose and Efficient Glycosylation via the Galactofuranosyl Iodide. *J. Org. Chem.* **2009**, *74*, 1994–2003.

(184)    Dureau, R.; Legentil, L.; Caniellou, R.; Ferrieres, V. Two-Step Synthesis of Per-O-Acetylfuranoses: Optimization and Rationalization. *J. Org. Chem.* **2012**, *77*, 1301–1307.

(185)    Schmidt, R. R.; Michel, J. Direct O-Glycosyl Trichloroacetimidate Formation, Nucleophilicity of the Anomeric Oxygen Atom. *Tetrahedron Lett.* **1984**, *25* (8), 821–824.

(186)    Meier, C. CycloSal Phosphates as Chemical Trojan Horses for Intracellular Nucleotide and Glycosylmonophosphate Delivery - Chemistry Meets Biology. *European J. Org. Chem.* **2006**, No. 5, 1081–1102.

(187)    Meier, C. CycloSal-Pronucleotides - Design of Chemical Trojan Horses. *Mini-Reviews Med. Chem.* **2002**, *2* (3), 219–234.

(188)    Fan, Y.; Gaffney, B. L.; Jones, R. A. Transient Silylation of the Guanosine O6 and Amino Groups Facilitates N-Acylation. *Org. Lett.* **2004**, *6* (15), 2555–2557.

(189)    Dahl, B. H.; Nielsen, J.; Dahl, O. Mechanistic Studies on the Phosphoramidite

Coupling Reaction in Oligonucleotide Synthesis. I. Evidence for Nudeophilic Catalysis by Tetrazole and Rate Variations with the Phosphorus Substituents. *Nucleic Acids Res.* **1987**, *15* (4), 1729–1743.

(190)   Russell, M. A.; Laws, A. P.; Atherton, J. H.; Page, M. I. The Mechanism of the Phosphoramidite Synthesis of Polynucleotides. *Org. Biomol. Chem.* **2008**, *6* (18), 3270–3275.

(191)   Börner, S.; Schwede, F.; Schlipp, A.; Berisha, F.; Calebiro, D.; Lohse, M. J.; Nikolaev, V. O. FRET Measurements of Intracellular CAMP Concentrations and CAMP Analog Permeability in Intact Cells. *Nat. Protoc.* **2011**, *6* (4), 427–438.

(192)   Seifert, R. Distinct Signaling Roles of CIMP, CCMP, and CUMP. *Structure* **2016**, *24* (10), 1627–1628.

# 11. Appendix

| Compound | GHS-code | H-statement | P-statement |
|---|---|---|---|
| Acetic acid | 02, 05 | 226, 314 | 280, 305+351+338, 310 |
| Acetic anhydride | 02, 05, 06 | 226, 302, 314, 330 | 210, 260, 280, 304+340+310, 305+351+338, 370+378 |
| Acetone | 02, 07 | 225, 319, 336 | 210, 280, 304+340+312, 305+351+338, 337+313, 403+235 |
| Acetonitrile | 02, 07 | 225, 302+312+332, 319 | 210, 261, 280, 305+351+338, 370+378, 403+235 |
| Acetonitrile-*d3* | 02, 07 | 225, 302+312+332, 319 | 210, 261, 280, 305+351+338, 370+378, 403+235 |
| Adenosine | No hazardous substance according to regulation (EC) 1272/2008 | | |
| Ammonium acetate | No hazardous substance according to regulation (EC) 1272/2008 | | |
| Ammonium chloride | 07 | 302, 319 | 301+312+330, 305+351+338 |
| Benzoic acid | 08, 05 | 315, 318, 372 | 260, 280, 305+351+338+310 |
| Benzyl bromide | 08 | 315, 319, 335 | 261, 305+351+338 |

| | | | |
|---|---|---|---|
| Bis(*N,N*-di*iso*propylamino)-chlorophosphine | 05 | 314, 318 | 280, 305+351+338, 310 |
| Borane-THF complex (1 M THF) | 02, 05, 07 | 225, 260, 302, 315, 318, 335, EUH019 | 210, 223, 231+232, 261, 370+378, 422 |
| Boron trichloride (1 M in $CH_2Cl_2$) | 05, 06, 08 | 301+331, 314, 335, 336, 351, 373, EUH014 | 261, 280, 301+310, 305+351+338, 310 |
| Boron tribromide (1 M in $CH_2Cl_2$) | 05, 06, 08 | 300+330, 314, 335, 336, 351, 373 | 260, 280, 301+310+330, 303+361+353, 304+340+310, 305+351+338, 403+233 |
| Bromotrimethylsilane | 02, 05 | 226, 314 | 280, 305+351+338, 310 |
| *tert*Butanol | 02, 07 | 225, 319, 332, 335, 336 | 210, 261, 305+351+338, 370+378, 403+235 |
| *tert*Butylhydroperoxide (5.5 M in *n*-decane) | 02, 05, 06, 08, 09 | 226, 302, 304, 311+331, 314, 317, 341, 411 | 210, 280, 301+310, 303+361+353, 304+340+310, 305+351+338, 331, 403+233 |
| Butyryl chloride | 02, 05 | 225, 314 | 210, 280, 305+351+338, 310 |
| Celite® | 07, 08 | 319, 335, 373 | 261, 305+351+338 |
| Chloroform | 06, 08 | 302, 315, 319, 331, 336, 351, 361d, 372 | 261, 281, 305+351+338, 311 |

| | | | |
|---|---|---|---|
| Chloroform-*d* | 06, 08 | 302, 315, 319, 331, 351, 361d, 372 | 260, 280, 301+312+330, 304+340+311, 305+351+338, 403+233 |
| Chloromethyl chloroformate | 05, 06 | 314, 331 | 261, 280, 305+351+338, 310 |
| Chloromethyl chlorosulfate | 05, 06, 08 | 302, 314, 330, 350 | 201, 260, 280, 304+340+310, 305+351+338, 308+313 |
| *N*-Chlorosuccinimide | 05, 07 | 302, 314 | 280, 305+351+338, 310 |
| 2'-Deoxyadenosine | No hazardous substance according to regulation (EC) 1272/2008 | | |
| Dess-Martin periodinane | 03, 07 | 272, 315, 319, 335 | 210, 220, 221, 305+351+338, 370+378 |
| Deuterium oxide-*d2* | No hazardous substance according to regulation (EC) 1272/2008 | | |
| 4,5-Dicyanoimidazole (0.25 M in MeCN) | 02, 05, 07 | 225, 302, 312, 315, 318, 332, 335 | 210, 261, 280, 305+351+338 |
| Dichloromethane | 07, 08 | 315, 319, 335, 336, 351, 371 | 260, 280, 305+351+338 |
| 1,3-Dichlor-1,1,3,3-tetra-*iso*propyldisiloxane | 05 | 314 | 280, 305+351+338, 310 |
| 3-(3,4-Dihydroxyphenyl)-propionic acid | 07 | 315, 319, 335 | 261, 305+351+338 |
| Di*iso*propyl azodicarbox-ylate | 07, 08, 09 | 315, 319, 335, 351, 373, 411 | 261, 273, 281, 305+351+338 |

| | | | |
|---|---|---|---|
| 4-(Dimethylamino)-pyridine | 06 | 301, 310, 315, 319, 335 | 280, 301+310+330, 302+352+310, 304+340+312, 305+351+338, 337+313 |
| *N,N*-Dimethylformamide | 02, 07, 08 | 226, 312+332, 319, 360 | 201, 280, 305+351+338, 308+313 |
| Dimethylsulfoxide-*d6* | No hazardous substance according to regulation (EC) 1272/2008 | | |
| Diphenyl phosphine | 05, 07 | 302, 315, 318, 335 | 261, 280, 305+351+338 |
| Di-*tert*butylsilyl bis(trifluo-romethane-sulfonate) | 05 | 314 | 280, 305+351+338, 310 |
| Dowex 50WX8 hydrogen form | 07 | 319 | 305+351+338 |
| Ethanol | 02, 07 | 225, 319 | 210, 280, 305+351+338, 337+313, 403+23 |
| Ethylacetate | 02, 07 | 225, 319, 336 | 210, 305+351+338, 370+378, 403+235 |
| Guanosine | 06 | 301 | 301+310 |
| 1,1,1,3,3,3-Hexamethyldisi-lazan | 02, 05, 06 | 225, 302, 311+331, 314 | 210, 280, 301+330+331, 302+352, 304+340, 305+351+338, 308+310, 403+235 |
| Hydrochloric acid | 05, 07 | 290, 314, 335 | 261, 280, 305+351+338, 310 |

| | | | |
|---|---|---|---|
| Hydrochloric acid (1 M, aq.) | 05 | 290 | |
| 4-Hydroxybenzylalcohl | 07 | 319 | 305+351+338 |
| Hydroxylamine hydrochloride | 05, 07, 08, 09 | 302+312, 351, 315, 319, 317, 373, 400, 290 | 273, 281, 302+352, 305+351+338, 308+313 |
| Hydrazine monohydrate (80%) | 05, 06, 08, 09 | 301, 312, 314, 317, 330, 350, 410 | 201, 260, 273, 280, 284, 301+310 |
| Imidazole | 05, 07, 08 | 302, 314, 360d | 201, 260, 280, 303+361+353, 305+351+338, 308+313 |
| Iodotrimethylsilane | 02, 05 | 225, 314 | 210, 280, 305+351+338, 310 |
| Kojic acid | No hazardous substance according to regulation (EC) 1272/2008 | | |
| Methanesulfonyl chloride | 05, 06 | 301+311, 314, 317, 330, 335 | 260, 280, 301+330+331+310, 303+361+353, 304+340+310, 305+351+338 |
| Methanol | 02, 06, 08 | 225, 301+311+331, 370 | 210, 260, 280, 301+310, 311 |
| Methanole-*d4* | 02, 06, 08 | 225, 301+311+331, 370 | 210, 280, 302+352+312, 304+340+311, 370+378, 403+235 |
| 1-Methylimidazole | 05, 06 | 302, 311, 314 | 280, 301+312+330, 303+361+353, |

| | | | |
|---|---|---|---|
| | | | 304+340+310, 305+351+338 |
| *N*-Methyl-2-pyrrolidone | 07, 08 | 315, 319, 335, 360d | 201, 280, 305+351+338, 308+313 |
| Nicotinic acid | 07 | 319 | 280, 305+351+338, 337+313 |
| Nicotinic acid chloride (hydrochloride) | 05 | 314 | 280, 305+351+338, 310 |
| Octanoyl chloride | 05, 06 | 280, 315, 317, 318, 330 | 280, 302+352, 305+351+338, 310, 402+404 |
| Petroleum ether | 02, 07, 08, 09 | 224, 304, 336, 411 | 210, 261, 273, 301+310, 331 |
| Potassium carbonate | 07 | 315, 319, 335 | 305+351+338 |
| *iso*Propanol | 02, 07 | 225, 319, 336 | 210, 305+351+338, 370+378, 403+235 |
| Pyridine | 02, 07 | 225, 302+312+332, 315, 319 | 210, 261, 280, 305+351+338, 370+378, 403+235 |
| Hydrogen fluoride pyridine | 05, 06 | 300+310+330, 314 | 260, 280, 303+361+353, 304+310, 305+351+338 |
| Silica gel | No hazardous substance according to regulation (EC) 1272/2008 | | |
| Sodium bicarbonate | No hazardous substance according to regulation (EC) 1272/2008 | | |
| Sodium hydroxide | 05 | 290, 314 | 280, 305+351+338, 310 |

Appendix

| | | | |
|---|---|---|---|
| Sodium sulfate | No hazardous substance according to regulation (EC) 1272/2008 | | |
| Sodium thiosulfate | No hazardous substance according to regulation (EC) 1272/2008 | | |
| Tetra-*n*-butylammonium hydrogensulfate | 07 | 315, 319 | 302+352, 305+351+338 |
| Tetra-*n*-butylammonium hydroxide (10%, aq. sol.) | 05 | 314 | 260, 264, 280, 304+340, 301+330+331, 305+351+338, 303+361+353, 363, 310, 405, 501 |
| Tetra-*n*-butylammonium iodide | 07 | 302 | 301+312+330 |
| Tetrahydrofuran | 02, 07, 08 | 225, 302, 319, 335, 351 | 210, 280, 301+312+330, 305+351+338, 370+378, 403+235 |
| *tert*Butyldimethylsilyl chloride | 02, 05 | 228, 314 | 210, 260, 280, 303+361+353, 305+351+338 |
| Toluene | 02, 07, 08 | 225, 304, 315, 336, 361d, 373 | 210, 260, 280, 301+310, 370+378, 403+235 |
| Trimethylsilyl trifluoromethanesulfonate | 02, 05 | 226, 314 | 280, 305+351+338, 310 |
| Triethylamine | 02, 05, 06 | 225, 302, 311+331, 314, 335 | 210, 280, 303+361+353, 304+340+310, 305+351+338, 403+233 |

278

Appendix

| | | | |
|---|---|---|---|
| Triethylamine trihydrofluoride (37 wt%, TEA) | 05, 06 | 300+310+330, 314 | 260, 280, 303+361+353, 304+340+310, 305+351+338 |
| Triflouroacetic acid | 05, 07 | 314, 332, 412 | 273, 280, 305+351+338, 310 |
| Uridine | No hazardous substance according to regulation (EC) 1272/2008 | | |

LEGEND:

| GHS 01 | 02 | 03 | 04 | 05 | 06 | 07 | 08 | 09 |
|---|---|---|---|---|---|---|---|---|
| | | | | | | | | |

## 12. Acknowledgement

## 13.  Declaration on Oath

I hereby declare on oath, that I have written the present dissertation by my own and have not used other than the acknowledged resources and aids. The submitted written version corresponds to the version on the electronic storage medium. I hereby declare that I have not previously applied or pursued for a doctorate (Ph.D. studies).

_____                              _____

Place, Date                                                    Alexandra Ruthenbeck, M.Sc.